UAB
Universitat Autònoma de Barcelona

Optimal control of an integrating system consisting of a sewer network and a wastewater treatment plant

Iulian VASILIEV

ADVERTIMENT. L'accés als continguts d'aquesta tesi queda condicionat a l'acceptació de les condicions d'ús establertes per la següent llicència Creative Commons: https://creativecommons.org/licenses/?lang=ca

ADVERTENCIA. El acceso a los contenidos de esta tesis queda condicionado a la aceptación de las condiciones de uso establecidas por la siguiente licencia Creative Commons: https://creativecommons.org/licenses/?lang=es

WARNING. The access to the contents of this doctoral thesis it is limited to the acceptance of the use conditions set by the following Creative Commons license: https://creativecommons.org/licenses/?lang=en

„Dunărea de Jos" University of Galați – Doctoral School of Fundamental and Engineering Sciences

Autonomous University of Barcelona – Doctoral Program in Electronic and Telecommunication Engineering

PhD Thesis

Optimal control of an integrating system consisting of a sewer network and a wastewater treatment plant

PhD Student,

Iulian VASILIEV

PhD supervisors,

Prof. Sergiu CARAMAN, PhD

Prof. Ramon VILANOVA ARBOS, PhD

Series: I8: System Engineering No. 12

GALAŢI

2024

„Dunărea de Jos” University of Galați – Doctoral School of Fundamental and Engineering Sciences

Autonomous University of Barcelona – Doctoral Program in Electronic and Telecommunication Engineering

PhD Thesis

OPTIMAL CONTROL OF AN INTEGRATING SYSTEM CONSISTING OF A SEWER NETWORK AND A WASTEWATER TREATMENT PLANT

PhD Student,

Iulian VASILIEV

President,	**Prof. Marian BARBU, PhD** Universitatea „Dunărea de Jos” din Galați, România
PhD Supervisors,	**Prof. Sergiu CARAMAN, PhD** Universitatea „Dunărea de Jos” din Galați, România
	Prof. Ramon VILANOVA ARBOS, PhD Universitat Autònoma de Barcelona, Spania
Scientific referees,	**Prof. Harsha RATNAWEERA, PhD** Norwegian University of Life Sciences, Norvegia
	Prof. Manuel BESCHI, PhD Università degli Studi di Brescia, Italia
	Prof. Radu-Emil PRECUP, PhD Universitatea Politehnica Timișoara. România
	Prof. Dan SELIȘTEANU, PhD Universitatea din Craiova, România

Series: I8: System Engineering No. 12

GALAŢI

2024

The series of doctoral theses publicly defended in UDJG starting from October 1, 2013, are:

The fundamental field ENGINEERING SCIENCES

Series I 1**:** **Biotechnology**
Series I 2**:** **Computers and Information Technology**
Series I 3: **Electrical Engineering**
Series I 4**:** **Industrial Engineering**
Series I 5: **Materials Engineering**
Series I 6**:** **Mechanical Engineering**
Series I 7**:** **Food Engineering**
Series I 8: **System Engineering**
Series I 9**:** **Engineering and Management in Agriculture and Rural Development**

The fundamental field SOCIAL SCIENCES

Series E 1: **Economy**
Series E 2: **Management**
Series E 3: **Marketing**
Series SSEF: **Science of Sport and Physical Education**
Series SJ: **Law**

The fundamental field HUMANITIES

Series U 1: **Philology - English**
Series U 2: **Philology - Romanian**
Series U 3**:** **History**
Series U 4: **Philology - French**

The fundamental field MATHEMATICS AND NATURAL SCIENCES

Series C: **Chemistry**

The fundamental field BIOMEDICAL SCIENCES

Series M: **Medicine**
Series F: **Farmaceutical**

Acknowledgements

This thesis is the result of a challenging academic journey that would not have been possible without the constant support, guidance, and encouragement of those around me. For this reason, I would like to sincerely thank all those who contributed to this journey. Thank you all for your invaluable contribution to my success.

Firstly, I would like to thank my PhD supervisors, professors Sergiu Caraman and Ramon Vilanova for their invaluable guidance and support. Their expertise and advice were essential to the success of this thesis. I greatly appreciate their patience and willingness to guide me throughout every step of the research.

I would like to thank the members of the guidance committee, professors Montserrat Meneses Benitez, Marian Barbu and Laurențiu Luca, for their constant support throughout the entire period of doctoral studies. They were always available to guide me, giving me valuable feedback and encouraging me to overcome any obstacle I encountered. Their input was crucial in maintaining the quality of my research.

Special thanks to my colleagues, Larisa Diaconu and Liliana Ghinea, who provided me with their valuable help.

This project would not have been possible without the support of the two institutions, “Dunărea de Jos” University of Galați and Universitat Autònoma de Barcelona, whose resources were fundamental to the conduct of my research. The facilities, access to resources, and the financial support were essential to the progress and completion of my thesis.

Finally, I want to thank my family and friends for their patience, understanding and unconditional support, which have been of great help throughout this academic journey. Their presence and encouragement motivated me to continue and achieve my goals. Without their love and support, this project would not have been possible.

Iulian Vasiliev,

September 2024, Galați

Table of Contents

Introduction ..... **V**

Introducere ..... **IX**

Acronyms ..... **XIII**

List of Figures ..... **XV**

List of Tables ..... **XIX**

Chapter 1. Background **1**

1.1. Introduction 1

1.1.1. A brief history of wastewater management 2

1.1.2. Impact of water quality on the environment and the human health 3

1.1.3. Water quality 4

1.1.4. Factors impacting the wastewater 5

1.1.5. Law regulations on wastewater 6

1.2. State of the art in modelling and control of Sewer Networks 7

1.2.1. Sewer Network modelling 9

1.2.2. Sewer Network control strategies 14

1.3. State of the art in modelling and control of Wastewater Treatment Plants 20

1.3.1. Wastewater Treatment Plants modelling 22

1.3.2. Wastewater Treatment Plants control strategies 28

1.4. State of the art in modelling and control of Integrated Urban Wastewater Systems 35

1.5. Chapter conclusions 37

Chapter 2. Modelling of Wastewater Collecting and Treatment Systems **39**

2.1. Introduction 39

2.2. Sewer Network modelling 39

2.2.1. The collecting areas 40

2.2.2. The Sewer Network characteristics 41

2.2.3. The influent of the Sewer Network 42

2.2.4. The model simulation 47

2.2.5. The simplified model 51
2.3. Wastewater Treatment Plant modelling 53
2.3.1. Neural Network modelling 53
2.3.2. Estimating process values using Neural Networks 60
2.3.3. Estimating effluent quality using Neural Networks 64
2.4. Integrated Urban Wastewater System modelling 66
2.4.1. BSMSewer – ASM2d 67
2.4.2. BSMSewer – BSM2G 71
2.5. Chapter conclusions 74

Chapter 3. Optimal Control of Wastewater Collecting and Treatment Systems 77
3.1. Introduction 77
3.2. Sewer Network optimal control 78
3.2.1. Offline optimal control 79
3.2.2. Online optimal control 94
3.3. Wastewater Treatment Plant optimal control 101
3.3.1. Model Predictive Control strategy based on Neural Network model 101
3.3.2. Fuzzy-Optimal control strategy 107
3.3.3. Optimal-Setpoint-Based control strategy 113
3.4. Integrated Urban Wastewater System optimal control 120
3.4.1. Controlling Sewer Network outlet valve 120
3.4.2. Model Predictive Control for the Sewer Network 124
3.5. Chapter conclusions 129

Chapter 4. Final Conclusions and Future Work 133
4.1. Original contributions 135
4.2. Future work 136
4.3. Results dissemination 137

References 141

Cuprins

Introducere ..... **IX**

Acronime ..... **XIII**

Listă Figuri ..... **XV**

Listă Tabele ..... **XIX**

Capitolul 1. Context **1**

1.1. Introducere 1
1.1.1. O scurtă istorie a managementului apei uzate 2
1.1.2. Impactul calității apei asupra mediului și a sănătății umane 3
1.1.3. Calitatea apei 4
1.1.4. Factori care influențează apele uzate 5
1.1.5. Reglementări legale privind apele uzate 6
1.2. Stadiul actual în modelarea și controlul rețelelor de canalizare 7
1.2.1. Modelarea rețelelor de canalizare 9
1.2.2. Strategii de control a rețelelor de canalizare 14
1.3. Stadiul actual în modelarea și controlul stațiilor de tratare a apelor uzate 20
1.3.1. Modelarea stațiilor de tratare a apelor uzate 22
1.3.2. Strategii de control a stațiilor de tratare a apelor uzate 28
1.4. Stadiul actual în modelarea și controlul sistemelor integrate de ape uzate urbane 35
1.5. Concluziile capitolului 37

Capitolul 2. Modelarea sistemelor de colectare si tratare a apelor uzate **39**

2.1. Introducere 39
2.2. Modelarea unei rețele de canalizare 39
2.2.1. Suprafețele de colectare 40
2.2.2. Caracteristicile rețelei de canalizare 41
2.2.3. Influentul rețelei de canalizare 42
2.2.4. Simularea modelului 47
2.2.5. Modelul simplificat 51
2.3. Modelarea stațiilor de tratare a apelor uzate 53

2.3.1. Modelarea utilizând rețele neuronale 53
2.3.2. Estimarea valorilor din proces utilizând rețele neuronale 60
2.3.3. Estimarea calității efluentului utilizând rețele neuronale 64
2.4. Modelarea sistemelor integrate de ape uzate urbane....66
2.4.1. BSMSewer – ASM2d 67
2.4.2. BSMSewer – BSM2G 71
2.5. Concluziile capitolului....74

Capitolul 3. Controlul optimal al sistemelor de colectare si tratare a apelor uzate....77

3.1. Introducere 77
3.2. Controlul optimal al rețelelor de canalizare 78
3.2.1. Control optimal offline 79
3.2.2. Control optimal online 94
3.3. Controlul optimal al stațiilor de tratare a apelor uzate....101
3.3.1. Model Predictive Control utilizând model neuronal....101
3.3.2. Strategie de control optimal bazată pe tehnici fuzzy 107
3.3.3. Strategie de control la referințe optimale....113
3.4. Controlul optimal al sistemelor integrate de ape uzate urbane....120
3.4.1. Controlul valvei de ieșire a rețelei de canalizare 120
3.4.2. Model Predictive Control aplicat rețelei de canalizare 124
3.5. Concluziile capitolului....129

Capitolul 4. Concluzii finale și direcții viitoare....133

4.1. Contribuții originale 135
4.2. Direcții viitoare de cercetare....136
4.3. Diseminarea rezultatelor 137

Bibliografie 141

Introduction

Since the Industrial Revolution, humanity faced unprecedented development which enabled the human population to grow from hundreds of millions to billions. In 2022, the total world population reached 8 billion and the United Nations predictions [1] say that, by the end of the century, it will reach 10 billion. The quick population growth, combined with the accelerated technological development and the intense urbanization led to a series of environmental crises on a global scale: pollution, climate change and biodiversity loss [2]. A significant part of the pollution disaster, in addition to air and land pollution, is represented by the growing quantity of pollutants in our water sources. As life would not be possible on Earth without water, its quality has a major impact on the environment, but also on the public health, making this topic one of great importance. Human activities are the main driver of the water pollution as during these activities large quantities of wastewater are produced. Knowing the potential of this heavily polluted water to compromise our water sources, it can be stated that wastewater management is a very important topic. For this reason, it is included in the most important global organisations' agenda. One example is the United Nations 2030 Agenda for Sustainable Development [3] that includes wastewater management as an important part of its Sustainable Development Goal 6 (SDG6). Even if SDG6 was established in 2015, today, in the middle of the period allocated for this goal, the 2023 SDG6 Synthesis Report on Water and Sanitation [4] shows that humanity is not on track to reach it, water quality is suffering, and climate change is putting additional stress on this topic. The Synthesis Report concludes that, if we want to achieve SDG6 before 2030, we need to accelerate our effort.

Due to the growing awareness of the importance of water quality, national and international governments imply regulations limiting the quantity of pollutants present in the wastewater that is discharged in natural receptors. Because the legislation is stricter and stricter regarding these limits, the governments created frameworks in which these limits should be respected. For example, in the European Union, the Water Framework Directive [5] is establishing a common approach to be used in the state members legislation in order to protect the environment, but also to restore the water quality of all water sources across Europe. Respecting these regulations in the continuously evolving civilization is challenging and requires researching for new wastewater management technologies, but also improving the already existing infrastructure by increasing its operational efficiency.

Moreover, as the world is of high complexity, the topic of wastewater management extends its influence in various challenges of the current world, be they of environmental, social, or political nature. For example, wastewater transport and treatment systems, like any other industrial facilities, are a source of greenhouse gases [6], that are contributing to another one of the planetary scale crises: the climate change. In this context, as international organisations state that it is imperative to reduce these emissions [7], [8], wastewater management should take them into consideration.

Besides environmental aspects related to wastewater management, this topic has high political importance, especially in the context of the nowadays tensions. The United Nations World Water Development Report 2024 [9] highlights that maintaining a good quality of our water source and an equitable access to water services, including wastewater management, is an important factor in maintaining peace and assuring prosperity for all human beings.

For this reason, this thesis is delving into advanced topics related to wastewater management. More specific, into optimal control Sewer Networks (SNs) and Wastewater Treatment Plants (WWTPs). The main goal is to apply a series of control actions to both systems (SN and WWTP) in order to reduce their environmental impact by discharging a quantity as little as possible of pollutants into natural receptors, while, at the same time, using as little energy as possible, without releasing too much greenhouse gases into the atmosphere. The literature abounds with optimal control strategies that are developed for each system and that are used to reduce the environmental impact of the system in terms of one or more of the above mentioned subgoals. However, it is important to be aware of the interconnectivity of these two systems. Applying control strategies to one of the two systems might produce unwanted effects on the other one, thus it is imperious to consider both systems when developing optimal control strategies. Consequently, the way that this thesis approaches the optimal control of SNs and WWTPs is in an integrated way, paving the for reducing further the environmental impact of such systems, by studying the topic of optimal control of integrated urban wastewater systems.

The first goal of this thesis is to develop and apply online and optimal control algorithms on the SN to reduce its environmental impact in terms of quantity of wastewater that is not properly directed to the treatment facility, but also in terms of quantity of pollutants in that wastewater. However, for such control to be applied, there is a need for digital tools for simulating such SNs. Thus, developing a SN model is imposed as a first step of this goal. The second goal is to develop and apply various optimal control algorithms on the WWTP to reduce its environmental impact in terms of quantity of pollutants in the plant effluent. Of course, reaching this goal also requires simulation tools for WWTPs. For this reason, as a first step, a series of WWTP models will be developed by implying Machine Learning techniques. The third and final objective of this work represents the study of the interconnectivity of the two systems. Thus, models for the integrated system are created and used for studying how applying control actions to the SN affects the performances of both subsystems and how the overall efficiency of the integrated system can be improved.

This PhD thesis is structured in four chapters, as presented in the following.

Chapter 1, named “Background” presents a series of introductive aspects related to wastewater collecting and treatment, such as a short history of wastewater management, the impact that water quality has on both the environment and public health, how water quality is measured, how various factors are impacting the wastewater and how governments are trying to deal with this topic throughout legislation.

This is followed by the main part of this chapter, dedicated to a state of the art in modelling and control of SN, WWTP and integrated systems. The literature reports for SN and WWTP modelling, a various number of models, ranging from simplified ones to complex ones that can model most processes taking place in these facilities, but require more computational effort. Recent research is avoiding the complexity of the mathematical models and uses data-driven models. The literature presents various strategies, structures, and methods to control the SNs and the WWTPs. However, when it comes to integrated wastewater systems (SN + WWTP), the

literature shows only a few papers, most of them focusing only on modelling the integrated system. This chapter shows that wastewater management is an important field and there is a place for lots of improvements that could help to reduce its effects on public health and the environment. Based on this, research gaps and future research directions that could improve the effectiveness of our wastewater collecting and treatment facilities are identified.

Chapter 2, named “Modelling of Wastewater Collecting and Treatment Systems” presents the development of models for both subsystems (SN and WWTP), but also for the integrated system. It is shown that the model complexity is important if the model will be used in optimal control strategies, consequently, the integration time is an important aspect when developing models. For this reason, after developing a full SN quality model deserving a city of about 250.000 inhabitants, and defining a test influent for that model, a simplified flow model is proposed to reduce the integration time and to be used in online optimal control strategies. On the other hand, as the literature abounds of complex WWTP models, this chapter deals with developing models with reduced simulation time, based on already existing benchmark models. This is achieved by implying a series of machine learning techniques to capture the complex dynamics of the WWTPs.

The end of this chapter is dedicated to developing integrated system models. It is shown that usually, SN model effluent variables are different than WWTP influent variables, thus a conversion block is needed in the process of developing such integrated models. This chapter provides a series of tools for digital simulation and analysis of these systems, that will be useful in the next chapter.

Chapter 3, named “Optimal Control of Wastewater Collecting and Treatment Systems” presents the development of optimal control strategies for both subsystems (SN and WWTP), but also for the integrated system.

Firstly, offline and online optimal control for SN is presented. The offline control part deals with testing and comparing five optimal control strategies, four optimization algorithms and makes an analysis regarding quantity vs. quality of overflowed wastewater before integrating everything in a sliding-window technique. On the other hand, online optimal control of SN is achieved using Model Predictive Control (MPC) technique. Because this is an online method, the integration time of the model used by the algorithm must be as low as possible. For this reason, a computational effort analysis is made.

Secondly, a series of optimal control strategies for WWTP are presented. Two of them are based on a MPC approach that makes use of simplified neural network models of the WWTP, while the other two are based on offline optimization.

The last part of the chapter deals with the integrated system composed of SN and WWTP. More specific, it studies of interconnectivity of the two systems by showing how applying control actions to the SN affects the performances of both subsystems. The proposed methodology shows that it is possible, when implying optimal control for the SN, to use a set of control actions for the SN that does not provide the best performances of the SN, but the best performances of the integrated system, minimizing its environmental impact in terms of quantity of pollutants discharged, costs involved and greenhouse gases emissions.

Chapter 4, named “Final Conclusions and Future Work” shows the conclusions drawn from this thesis, alongside the original scientific contributions of the author and the consequent research directions.

Introducere

De la Revoluția Industrială, omenirea s-a confruntat cu o dezvoltare fără precedent, care a permis populației umane să crească de la sute de milioane la miliarde. În 2022, populația totală a lumii a ajuns la 8 miliarde, iar previziunile ONU [1] spun că, până la sfârșitul secolului, va ajunge la 10 miliarde. Creșterea rapidă a populației, combinată cu dezvoltarea tehnologică accelerată și urbanizarea intensă a dus la o serie de crize de mediu la scară globală: poluare, schimbări climatice și pierderea biodiversității [2]. O parte semnificativă a crizei poluării, pe lângă poluarea aerului și a solului, este reprezentată de cantitatea tot mai mare de poluanți din sursele noastre de apă. Întrucât viața pe Pământ nu ar fi posibilă fără apă, calitatea acesteia are un impact major asupra mediului, dar și asupra sănătății publice, făcând acest subiect unul de mare importanță. Activitățile umane sunt principala cauză a poluării apei, deoarece în timpul acestor activități sunt produse cantități mari de apă uzată. Cunoscând potențialul acestei ape puternic poluate de a compromite sursele noastre de apă, se poate afirma că gestionarea apelor uzate este un subiect foarte important. Din acest motiv, este inclusă în agenda celor mai importante organizații globale. Un exemplu este Agenda 2030 pentru Dezvoltare Durabilă a Națiunilor Unite [3], care include gestionarea apelor uzate ca parte importantă a Obiectivului său de Dezvoltare Durabilă 6 (ODD6). Chiar dacă ODD6 a fost definit în 2015, astăzi, la jumătatea perioadei alocate acestui obiectiv, un raport de sinteză din 2023 referitor la acest obiectiv [4] arată că omenirea nu este pe cale să-l atingă, calitatea apei suferă, iar schimbările climatice pun un stres suplimentar. Raportul de sinteză concluzionează că, dacă dorim să atingem ODD6 înainte de 2030, trebuie să ne accelerăm eforturile.

Datorită conștientizării tot mai mari a importanței calității apei, guvernele naționale și internaționale impun reglementări care limitează cantitatea de poluanți prezenți în apele uzate care sunt deversate în receptorii naturali. Pentru că legislația este din ce în ce mai strictă în ceea ce privește aceste limite, guvernele au creat cadre legale în care aceste limite ar trebui respectate. De exemplu, în Uniunea Europeană, Directiva-cadru privind apa [5] stabilește o abordare comună care să fie utilizată în legislația statelor membre pentru a proteja mediul înconjurător, dar și pentru a restabili calitatea apei din toate sursele de apă din Europa. Respectarea acestor reglementări în civilizația noastră în continuă evoluție este o provocare și necesită dezvoltarea de noi tehnologii de management a apelor uzate, dar și îmbunătățirea infrastructurii deja existente prin creșterea eficienței operaționale a acesteia.

Mai mult, întrucât lumea este de o complexitate crescută, tema managementului apelor uzate își extinde influența în diverse provocări ale lumii actuale, fie ele de natură ecologică, socială sau politică. De exemplu, sistemele de transport și tratare a apelor uzate, ca orice alte instalații industriale, sunt o sursă de gaze cu efect de seră [6], care contribuie la o altă criză la scară planetară: schimbările climatice. În acest context, întrucât organizațiile internaționale afirmă că este imperativă reducerea acestor emisii [7], [8], managementul apelor uzate ar trebui să le ia în considerare.

Pe lângă aspectele de mediu legate de managementul apelor uzate, acest subiect are o importanță politică ridicată, mai ales în contextul tensiunilor din zilele noastre. Raportul Națiunilor Unite privind dezvoltarea apei din 2024 [9] subliniază că menținerea unei bune calități a surselor noastre de apă și a unui acces echitabil la serviciile de apă, inclusiv gestionarea apelor uzate, este un factor important în menținerea păcii și asigurarea prosperității pentru toate ființele umane.

Din acest motiv, această teză aprofundează subiecte avansate legate de managementul apelor uzate. Mai specific, controlul optimal al Rețelelor de Canalizare (SN – Sewer Network) și al Stațiile de Tratare a Apelor Uzate (WWTP – Wastewater Treatment Plant). Scopul principal este aplicarea unor acțiuni de control asupra ambelor sisteme (SN și WWTP) pentru a reduce impactul acestora asupra mediului prin deversarea unei cantități cât mai mici de poluanți în receptorii naturali, în timp ce, se utilizează cât mai puțină energie, fără a elibera prea multe gaze cu efect de seră în atmosferă. Literatura de specialitate abundă de strategii de control optimal care sunt dezvoltate pentru fiecare sistem și care sunt utilizate pentru a reduce impactul asupra mediului al sistemului în ceea ce privește unul sau mai multe dintre obiectivele menționate mai sus. Cu toate acestea, este important să fim conștienți de interconectivitatea acestor două sisteme. Aplicarea strategiilor de control unuia dintre cele două sisteme poate produce efecte nedorite asupra celuilalt, de aceea este imperios să se ia în considerare ambele sisteme atunci când se dezvoltă strategii de control optimal. În consecință, modul în care această teză abordează controlul optimal al SN și al WWTP este într-o manieră integrată, pregătind calea spre o reducere adițională a impactului unor astfel de sisteme asupra mediului, prin studierea controlului optimal al sistemelor integrate de ape uzate urbane.

Primul obiectiv al acestei teze este dezvoltarea și aplicarea unor algoritmi de control optimal offline și online asupra rețelei de canalizare pentru a reduce impactul acesteia asupra mediului în ceea ce privește cantitatea de apă uzată care nu este dirijată corespunzător către instalația de tratare, dar și în ceea ce privește cantitatea de poluanți din această apă. Cu toate acestea, pentru ca un astfel de control să poată fi aplicat, este nevoie de instrumente digitale pentru simularea unor astfel de sisteme. Astfel, dezvoltarea unui model de rețea de canalizare se impune ca prim pas al acestui obiectiv. Al doilea obiectiv este dezvoltarea și aplicarea a diverși algoritmi de control optimal asupra stațiilor de tratare pentru a reduce impactul acestora asupra mediului în ceea ce privește cantitatea de poluanți din efluentul instalației. Desigur, și atingerea acestui obiectiv necesită instrumente de simulare pentru stațiile de tratare. Din acest motiv, ca prim pas, vor fi dezvoltate o serie de modele WWTP prin implicarea tehnicilor de Machine Learning. Al treilea și ultimul obiectiv al acestei lucrări reprezintă studiul interconectivității celor două sisteme. Astfel, sunt create modele pentru sistemul integrat. Acestea sunt apoi utilizate pentru a studia modul în care aplicarea acțiunilor de control asupra rețelelor de canalizare afectează performanțele ambelor subsisteme și cum poate fi îmbunătățită eficiența generală a sistemului integrat.

Această teză de doctorat este structurată în patru capitole, după cum este prezentat în cele ce urmează.

Capitolul 1, denumit „Context” prezintă o serie de aspecte introductive legate de colectarea și tratarea apelor uzate, cum ar fi o scurtă istorie a managementului apelor uzate, impactul pe care calitatea apei îl are atât asupra mediului, cât și asupra sănătății publice, modul în care este măsurată calitatea apei, felul in care diverși factori influențează apele uzate și modul în care guvernele încearcă să abordeze acest subiect cu ajutorul legislației.

Acestea sunt urmate de partea principală a acestui capitol, dedicată unui stadiu al literaturii de specialitate ce tratează modelarea și controlul SN, WWTP și a sistemelor integrate. În ceea

ce privește modelarea SN și WWTP, în literatură se găsesc un număr variat de modele, variind de la cele mai simple la cele mai complexe care pot modela majoritatea proceselor care au loc în aceste instalații, dar necesită mai mult efort de calcul. Cercetările recente evită complexitatea modelelor matematice și utilizează modele bazate pe date. În literatura de specialitate se prezintă diverse strategii, structuri și metode de control a SN și WWTP. Cu toate acestea, când vine vorba de sisteme integrate de apă uzată (SN + WWTP), se pot găsi doar câteva lucrări, majoritatea concentrându-se doar pe modelarea sistemelor integrate. Acest capitol arată că managementul apelor uzate este un domeniu important și că există loc pentru o mulțime de îmbunătățiri care ar putea contribui la reducerea efectelor apelor uzate asupra sănătății publice și asupra mediului. Pe baza acestui fapt, sunt identificate lacunele de cercetare și direcțiile viitoare de cercetare care ar putea îmbunătăți eficacitatea instalațiilor noastre de colectare și tratare a apelor uzate.

Capitolul 2, denumit „Modelarea sistemelor de colectare și tratare a apelor uzate” prezintă dezvoltarea modelelor pentru ambele subsisteme (SN și WWTP), dar și pentru sistemul integrat. Se arată că complexitatea modelului este importantă dacă modelul va fi utilizat în strategii de control optimal, în consecință, timpul de integrare este un aspect important în dezvoltarea modelelor. Din acest motiv, după elaborarea unui model complet de rețea de canalizare care deservește un oraș de aproximativ 250.000 de locuitori și după definirea unui influent ce va fi folosit pentru a testa strategii de control asupra acestui model, se propune un model hidrologic simplificat ce reduce timpul de integrare și care poate fi utilizat în strategiile de control optimal online. Pe de altă parte, deoarece literatura de specialitate abundă de modele complexe de WWTP, acest capitol se ocupă de dezvoltarea unor modele cu timp de simulare redus, bazate pe modelele de tip benchmark deja existente. Acest lucru se realizează prin utilizarea tehnicilor de Machine Learning pentru a capta dinamica complexă a stațiilor de tratare.

Sfârșitul acestui capitol este dedicat dezvoltării modelelor de sisteme integrate. Se arată că, de obicei, variabilele efluentului modelului SN sunt diferite de variabilele influentului stației de tratare, astfel încât este necesar un bloc de conversie în procesul de dezvoltare a unor astfel de modele integrate. Acest capitol oferă o serie de instrumente pentru simularea și analiza digitală a acestor sisteme, care vor fi utile în capitolul următor.

Capitolul 3, intitulat „Controlul optimal al sistemelor de colectare și tratare a apelor uzate” prezintă dezvoltarea strategiilor de control optimal a ambelor subsisteme (SN și WWTP), dar și a sistemului integrat.

În primul rând, este prezentat controlul optimal offline și online pentru SN. Partea de control offline prezintă testarea și compararea a cinci strategii de control optimal, patru algoritmi de optimizare și face o analiză privind cantitatea vs. calitatea apei uzate revărsate înainte de a integra totul într-o tehnică de tip „fereastră alunecătoare”. Pe de altă parte, controlul optimal online al SN este realizat folosind tehnica Model Predictive Control (MPC). Deoarece aceasta este o metodă online, timpul de integrare a modelului utilizat de algoritm trebuie să fie cât mai mic posibil. Din acest motiv, se face o analiză a efortului computațional.

În al doilea rând, sunt prezentate o serie de strategii de control optimal pentru WWTP. Două dintre ele se bazează pe o abordare MPC care utilizează modele simplificate de rețele neuronale ale WWTP, în timp ce celelalte două se bazează pe optimizarea offline.

Ultima parte a capitolului tratează sistemul integrat compus din SN și WWTP. Mai specific, se prezintă interconectivitatea celor două sisteme, arătând modul în care aplicarea acțiunilor de control asupra SN afectează performanțele ambelor subsisteme. Metodologia propusă arată că

este posibil ca, atunci când utilizăm un control optimal pentru SN, să se utilizeze un set de acțiuni de control pentru SN care nu oferă cele mai bune performanțe ale rețelei, ci cele mai bune performanțe ale sistemului integrat, minimizând astfel impactul asupra mediului în ceea ce privește cantitatea de poluanți evacuați, costurile implicate și emisiile de gaze cu efect de seră.

Capitolul 4, intitulat „Concluzii finale și direcții viitoare” prezintă concluziile desprinse din această teză, alături de contribuțiile științifice originale ale autorului și direcțiile de cercetare viitoare.

Acronyms

ADM	Anaerobic Digestion Model
AMOEA/D	Adaptive Multi-Objective Evolutionary Algorithm based on Decomposition
ANN	Artificial Neural Network
ASM	Activated Sludge Model
AOB	Ammonia-Oxidizing Bacteria
BHTPSO	Binary Hybrid Topology Particle Swarm Optimisation
BOD	Biochemical Oxygen Demand
BSM	Benchmark Simulation Model
CBR	Case-Based Reasoning
CH_4	Methane
CO_2	Carbon Dioxide
COD	Chemical Oxygen Deman
COD_{part}	Particulate Chemical Oxygen Deman
COD_{sol}	Soluble Chemical Oxygen Deman
CSO	Combined Sewer Overflow
DO	Dissolved Oxygen
DQI	Discharge Quality Index
EBPR	Enhanced Biological Phosphorus Removal
EQI	Effluent Quality Index
ENN	Elman Neural Network
ESN	Echo State Network
EU	European Union
FIFO	First-In First-Out
GA	Genetic Algorithm
GD-MOEA/D	Grid-based Dynamic Multi-Objective Evolutionary Decomposition algorithm
GHG	Greenhouse Gases
GPRFNN	Growing and Pruning Recurrent Fuzzy Neural Network
GRU	Gated Recurrent Unit
FFC	Feed-Forward Controller
IAWQ	International Association on Water Quality
IOCS-FOF	Intelligent Optimal Control System with Flexible Objective Functions
IoT	Internet of Things
IPCC	Intergovernmental Panel on Climate Change
IUWS	Integrated Urban Wastewater System
IWA	International Water Association
LDDA	Local Descent Deterministic Algorithm
LSTM	Long Short-Term Memory
MAPE	Mean Absolute Percentage Error
MLP	Multi-Layer Perceptron

MPC	Model Predictive Control
MSE	Mean Square Error
NO	Nitric Oxide
NSGA-II	Non-dominated Sorting Genetic Algorithm
N_2O	Nitrous Oxide
OQI	Overflow Quality Index
PAO	Phosphate Accumulating Organisms
p.e.	Population Equivalent
PHA	Polyhydroxyalkanoates
PI	Proportional Integral controller
PO_4^{3-}	Phosphate
PP	Polyphosphates
PSO	Particle Swarm Optimisation
R^2	Coefficient of Determination
ReLU	Rectifier Linear Unit
RFNN	Recurrent Fuzzy Neural Network
RMSE	Root Mean Square Error
RNN	Recurrent Neural Network
RTC	Real-Time Control
RWQM1	River Water Quality Model no. 1
SBR	Sequencing Batch Reactor
SN	Sewer Network
SOO	Single-Objective Optimization
SSC	Supervisory Sequential Controller
SWMM	Storm Water Management Model
TKi	Sewer Network Storage Tank no. *i*
TOC	Total Organic Carbon
TSS	Total Suspended Solids
TUDP	Technical University Delft Phosphorus
V_{ovf}	Volume of Overflow
WNN	Wavelet Neural Network
WWTP	Wastewater Treatment Plant

List of Figures

Figure 1.1 – Water cycle 1
Figure 1.2 – Organic carbon fractions 4
Figure 1.3 – Wastewater management systems interfaces 5
Figure 1.4 – Rainfall mechanism 5
Figure 1.5 – Combined sewer network 8
Figure 1.6 – Separate sewer network 8
Figure 1.7 – Classification of SN models 10
Figure 1.8 – Water flow in a channel 10
Figure 1.9 – Storage tank with overflow capability 11
Figure 1.10 – Workflow for the proposed methodology 16
Figure 1.11 – Optimal control structure 16
Figure 1.12 – Predictive control structure 17
Figure 1.13 – Example of fuzzy membership function for water level 17
Figure 1.14 – Flowchart of the multi-objective optimization algorithm 19
Figure 1.15 – WWTP inputs and outputs 21
Figure 1.16 – The growth phases of bacterial cultures 23
Figure 1.17 – The Monod dependence between substrate concentration and growth rate 24
Figure 1.18 – BSM1 structure 26
Figure 1.19 – BSM2 structure 27
Figure 1.20 – GPRFNN-based Control System 29
Figure 1.21 – Feed-forward control strategy 29
Figure 1.22 – WWTP control strategy based on RFNN 30
Figure 1.23 – Cascade control setup 31
Figure 1.24 – Supervisory control setup 31
Figure 1.25 – Hierarchical control setup 32
Figure 1.26 – Hybrid Intelligent Optimal Control System 33
Figure 1.27 – Dynamic multi-objective optimization control 34
Figure 1.28 – SYNOPSIS integrated model structure 36

Figure 2.1 – The SN structure 40
Figure 2.2 – Variation profile for the domestic and industrial components 43
Figure 2.3 – Area 1 influent evolution 44
Figure 2.4 – Area 2 influent evolution 45
Figure 2.5 – Area 3 influent evolution 45
Figure 2.6 – Area 4 influent evolution 46
Figure 2.7 – Area 5 influent evolution 46
Figure 2.8 – Wastewater volume evolution in Sewer Network tanks – “no control” 48
Figure 2.9 – Wastewater overflow from Sewer Network tanks – “no control” 48
Figure 2.10 – Water flowing in a pipe 51
Figure 2.11 – Storage tank with overflow capability 52
Figure 2.12 – The structure of the simplified 4th order WWTP model 54
Figure 2.13 – The structure used for training the NN model (1st version) 55
Figure 2.14 – The structure of the NN model (1st version) 56
Figure 2.15 – The evolution of the loss function during NN training (1st version) 56
Figure 2.16 – The NN validation – real and predicted evolutions of process states (1st version) 57
Figure 2.17 – The NN validation – prediction error (1st version) 57
Figure 2.18 – The structure used for training the NN model (2nd version) 58
Figure 2.19 – The structure of the NN model (2nd version) 58
Figure 2.20 – The evolution of the loss function during NN training (2nd version) 59
Figure 2.21 – The NN validation – real and predicted evolution of substrate concentration and the error between them (2nd version) 59
Figure 2.22 – The NN based Soft Sensor 60
Figure 2.23 – The structure of the Sliding Window algorithm 61
Figure 2.24 – The structure of the soft sensor NN 61
Figure 2.25 – The K-Fold training method 62
Figure 2.26 – The NN validation – The real and predicted evolution of $S_{NH,e}$ 63
Figure 2.27 – NN-based effluent quality prediction architecture 64
Figure 2.28 – The model validation – real and predicted evolution of SNO,e with deterministic $KLa3$ 65
Figure 2.29 – The model validation – real and predicted evolution of effluent variables with stochastic KLa 66
Figure 2.30 – The architecture of the IUWS (BSMSewer – ASM2d) 67
Figure 2.31 – The conversion from BSMSewer variables to ASM2d variables 68
Figure 2.32 – SN effluent variables 69

Figure 2.33 – WWTP effluent results 70
Figure 2.34 – The architecture of the IUWS (BSMSewer – BSM2G) 71
Figure 2.35 – The conversion from BSMSewer variables to BSM2G variables 72
Figure 3.1 – The crossover operator of the GA 80
Figure 3.2 – The chromosome structure in Strategy #1 80
Figure 3.3 – Output command depending on liquid level in tank 81
Figure 3.4 – The chromosome structure in Strategy #2 81
Figure 3.5 – The chromosome structure in Strategy #3 82
Figure 3.6 – The chromosome structure in Strategy #4 82
Figure 3.7 – The chromosome structure in Strategy #5 82
Figure 3.8 – Fitness function values evolutions 83
Figure 3.9 – The points on the Pareto Front 85
Figure 3.10 – Choosing the optimal solution using Nash Bargaining Solution 86
Figure 3.11 – The MOO in two steps algorithm 87
Figure 3.12 – The MOO in two steps algorithm – best fitness evolution during the SOO step 87
Figure 3.13 – The MOO in two steps algorithm – the optimisation results 88
Figure 3.14 – The obtained probability distribution when randomly generating solutions 90
Figure 3.15 – The Sliding-Window based algorithm 92
Figure 3.16 – The MPC structure 94
Figure 3.17 – The MPC simulation setup 96
Figure 3.18 – Example MPC simulation result 97
Figure 3.19 – The MPC control strategy 102
Figure 3.20 – The first 30 days of the generated influent 103
Figure 3.21 – Example of W and S evolution during day no. 26 (1st MPC version) 104
Figure 3.22 – Example of W and S evolution during day no. 26 (2nd MPC version) 105
Figure 3.23 – The evolution of the fitness function in the three cases 106
Figure 3.24 – The simplified scheme of the WWTP with the control strategy 107
Figure 3.25 – First 70 days of the influent used for testing the fuzzy-optimal control strategy 108
Figure 3.26 – The evolution of performance indicators as a function of $kDRY$ 109
Figure 3.27 – The evolution of performance indicators as a function of $kRAIN$ 111
Figure 3.28 – The evolution of performance indicators as a function of $kSTORM$ 112
Figure 3.29 – Membership functions of Qin to the operating regime 112
Figure 3.30 – The optimal-setpoint-based control strategy 114
Figure 3.31 – Influent flow variations corresponding to the operating regimes 115

Figure 3.32 – The chromosome structure 116
Figure 3.33 – Fitness function evolution in the three operating regimes 117
Figure 3.34 – Effluent loads in the aggregated regime 119
Figure 3.35 – Results obtained with constant outlet valve opening 121
Figure 3.36 – Results obtained with constant outlet valve opening 122
Figure 3.37 – Results obtained with limited outflow 123
Figure 3.38 – The schematic representation of the constrained MPC control structure 125
Figure 3.39 – Statistics of the resulted scaled values of the performance indicators 126
Figure 3.40 – The mean values of the integrated performance indicator with respect to $UTK7$ and λ 127
Figure 3.41 – Fuzzy block used to compute the MPC constraint 128
Figure 3.42 – The constrained MPC control structure with dynamic constraint 128
Figure 3.43 – Mean values of $I(\lambda)$ for various values of λ in both considered constrained cases 129

List of Tables

Table 1.1 – EU requirements for WWTP effluent 6
Table 1.2 – EU requirements for WWTP effluent if receiving water is identified as sensitive 6
Table 1.3 – BSMSewer performance indicators 14
Table 2.1 – The collecting areas characteristics 41
Table 2.2 – The SN tanks characteristics 42
Table 2.3 – The average loads and flow of the forecasted influent 43
Table 2.4 – The average loads concentrations of the forecasted influent 44
Table 2.5 – Performance indicators values calculated in the “no control” case 49
Table 2.6 – Performance indicators values calculated in the case $UTK3 = 0.7$ 49
Table 2.7 – Performance indicators values calculated in the case $UTK3 = 0.7$ and $UTK4 = 0.7$ 50
Table 2.8 – The process constants of the simplified 4th order WWTP model 55
Table 2.9 – The characteristics of the WWTP components 68
Table 2.10 – The operating points of the WWTP 70
Table 2.11 – WWTP quality and cost indexes 71
Table 2.12 – The values of the IUWS performance indicators in the base case 74
Table 3.1 – Solutions obtained with the five strategies 83
Table 3.2 – Performances obtained with the five strategies 84
Table 3.3 – Statistical parameters of Strategy #3 when minimizing $Vovf$ 84
Table 3.4 – Statistical parameters of MOO algorithm solutions 86
Table 3.5 – Statistical parameters of PSO algorithm solutions 90
Table 3.6 – Initial points for FminSearch 91
Table 3.7 – Statistical parameters of Sliding-Window based PSO when minimizing $Vovf$ 92
Table 3.8 – Statistical parameters of Sliding-Window based PSO with penalty term 93
Table 3.9 – Statistical parameters of MPC (1st case) 96
Table 3.10 – Quality indexes for each tank 98
Table 3.11 – Statistical parameters of MPC (2nd case) 99
Table 3.12 – Statistical parameters of MPC (3rd case) 99

Table 3.13 – MPC computational effort tests results 101
Table 3.14 – Results obtained in the DRY regime.....109
Table 3.15 – Results obtained in the RAIN regime.....110
Table 3.16 – Results obtained in the STORM regime 111
Table 3.17 – Results obtained in each regime and in the aggregate regime 113
Table 3.18 – Average concentrations of the three influent scenarios.....114
Table 3.19 – Limits of the components of the optimal setpoints vector.....116
Table 3.20 – The values of the optimal setpoints obtained for each regime 117
Table 3.21 – Results obtained in each regime 118
Table 3.22 – Results obtained in the aggregate regime 119
Table 3.23 – IUWS performance indicators when SN is controlled by unconstrained MPC.....124
Table 3.24 – IUWS performance indicators when SN is controlled by the constrained MPC with the constraint dynamically computed 129

Chapter 1. Background

1.1. Introduction

Water is one of the most important elements in the world, representing one of the basic needs for all the living organisms on Earth, including humans. 70% of our planet surface is covered with water, however, only 0.007 is available for human consumption [10]. For humans, water is not important only for drinking, but needed for many other daily activities such as cooking, maintaining hygiene, agriculture, industry, generating power, aquaculture etc., activities that are producing a lot of wastewater, usually heavily polluted, that could compromise our public health and environment. Therefore, it is very important to collect, transport and treat the water to maintain our ecosystems and protect our freshwater sources. For these purposes, humanity interfered with the natural water cycle, as presented in Figure 1.1, by creating systems for wastewater collecting (Sewer Networks – SN) and treatment (Wastewater Treatment Plants – WWTP) to maintain an equilibrium and minimize the effects of the human activities on the environment.

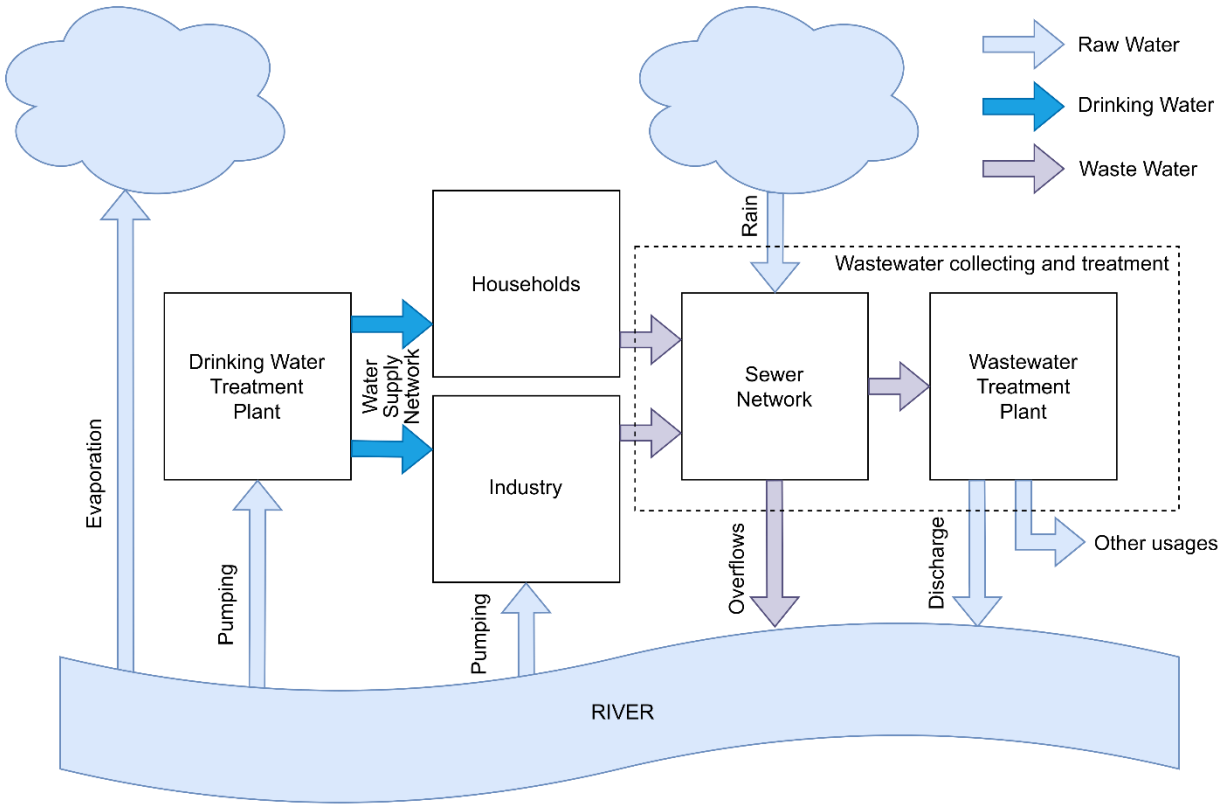


Figure 1.1 – Water cycle

Therefore, if it is desired to maintain this equilibrium and not to compromise our water resources, it is important to have the most efficient SNs and WWTPs. However, we are living in

a dynamic world, affected by a lot of phenomena like urbanization, migration, global warming etc. that could impact the operational efficiency of the wastewater systems, and, therefore, optimal control and operation strategies for these systems should be considered to overcome all the changes resulting from external factors. With this purpose in mind, developing new complex control strategies requires the knowledge of the already existing control systems to identify research gaps and future research directions that could lead to further improvements in the effectiveness of wastewater collecting and treatment systems. For developing such control strategies, tools for digital simulation of the systems and tools for analysis are required.

In consequence, the main objective of this chapter is to analyse the challenges that our society is facing regarding wastewater and to present a state of the art of current research in SNs and WWTPs modelling and control to identify which research directions should be followed to increase the effectiveness of the wastewater collecting and treatment systems so humans activities impact on the water is diminished, protecting this way the public health and the environment.

1.1.1. A brief history of wastewater management

Water is the source of life on earth, or "Hydor[1] is the beginning of everything" as stated by Thales from Miletus (ca. 636–546 BC) [11]. Humans always needed freshwater sources, but they also needed methods to safely remove the polluted water [12]. In early history, humans had very little impact on the environment, and the excess water was taken up by natural hydrological processes, while wastes were naturally "treated" [13].

The first artificial systems started to develop when humans tried to control their environment. Drainage systems were used over time to get rid of excess water, usually meteorological water. These systems were intended to prevent flooding. With the urban development, due to the increase of the population density in certain communities, the need to have sewerage systems appeared [14]. In ancient Greece, at the end of the Bronze Age, the Minoan civilization provided a major contribution to wastewater management. This civilization's palaces had sewerage and drainage systems, some of them even had toilets with flushing systems [15]. The most known ancient sewerage system is the *Cloaca Maxima* developed by the Roman Empire. This system was collecting the stormwater and the wastewater, which then reached the Tiber River [14]. With the fall of the Roman Empire, the population of the cities began to decline, which led to the abandonment of sewerage systems and, over time, their deterioration. In the Dark Ages, rainwater and wastewater resulting from craft activities were taken using ditches and dumped into natural collectors, while human waste was used in the garden or simply left on the street [16].

The increase in the rate of industrialization and urbanization led in the nineteenth century to an awareness of the importance of wastewater management [17]. The first country to take action to improve the city's environmental conditions was Britain, followed by Germany, France, and Italy [18]. The twentieth century came with a revolution in wastewater management through scientific discoveries related to this topic [19]. In 1912 [20] introduced the concept of biochemical oxygen demand (BOD) and defined standards for sewage effluent. A few years later [21] enhanced our understanding of the relationship between water pollution and toxicity. In the '60s, the discoveries in spectrography and chromatography led to a deeper understanding of pollutants

[1] Water

[22]. All these discoveries, together with the awareness of the importance of environmental protection, have eventually led to modern and advanced wastewater collecting and treatment systems.

1.1.2. Impact of water quality on the environment and the human health

Because it can dissolve various substances, water is considered a “universal solvent” and because it can carry these dissolved substances alongside other substances, some of them highly toxic, untreated wastewater represents a threat to both the environment and public health.

Water bodies (such as rivers, lakes etc.) are the most susceptible to the negative effects of wastewater. The aquatic ecosystems could be disrupted by toxic substances. If a lot of organic substances are present in the water, organisms will decompose them. In the decomposition process, a lot of the water Dissolved Oxygen (DO) is used, and the effect of oxygen depletion can appear. DO is critical for aquatic life, therefore oxygen depletion can be life-threatening to fish. The increase of the nutrient concentrations (particularly nitrogen and phosphorus) can lead to eutrophication [23], a phenomenon in which, because of the high concentration of nutrients, the plants and algae in the water start to grow excessively, setting off a chain reaction in the ecosystem. The excess plants and algae will eventually die and decompose, producing high amounts of carbon dioxide (CO_2) which can lead to oxygen depletion and fish dying. Besides this, the large amounts of CO_2 produced in the algae decomposition process can decrease the pH of seawater, contributing to the ocean acidification phenomena. Moreover, wastewater can contain oils and fats that can settle on the water surface, blocking the light that is needed for the photosynthetic aquatic plants. Wastewater usually has a higher temperature than the temperature of the receiving body, therefore it can increase the water temperature which can affect the DO concentration, but also the fish living in that water because they are relying on the water temperature to regulate their body temperature as they are cold-blooded beings.

Unproperly treated wastewater contributes to the contamination, and eventually, the destruction of the natural habitats by exposing the wildlife to harmful substances: pathogens, heavy metals, salts, oils, greases, toxic chemicals, nutrients, acids and bases, toxic compounds etc.

It is important to mention, even if it is not a direct effect of the water quality on the environment, but an effect of the wastewater treatment, that WWTPs, like other industrial facilities, can, during their operation, emit greenhouse gases (GHG) such as CO_2, methane (CH_4) and nitrous oxide (N_2O), contributing to the global warming.

Besides the threats posed to the environment, wastewater represents a threat to public health. According to a report of the World Health Organization, annually, 4 billion cases of diseases related to water are causing 3.4 million people to die worldwide [24]. Human faeces are the main vector for transmitting various diseases, therefore wastewater must be properly treated before being discharged to avoid epidemics. In tropical countries, rainwater must be collected and transported from the human communities, as, in those places, standing water represents the mosquito habitat. This can lead to the spread of malaria or other kinds of diseases [13]. In addition to this, fish is part of the human diet, and therefore contaminated water means contaminated fish, especially with heavy metals, which can affect human health.

1.1.3. Water quality

To provide the most performant and efficient wastewater collecting and treatment systems, it is necessary to measure the efficiency of these systems by quantifying the water quality at various points of the systems.

Firstly, as water contains and carries away various substances, there is a need to quantify the quantities of these substances in the water. For this, the concentration, usually expressed in mg/l is used [13]:

$$c = M/V \tag{1.1}$$

where c is the substance concentration in the water, M is the substance mass found in a volume of water equal to V. The substance flux or mass-flow, L, can be further calculated by multiplying the substance concentration, c, by the liquid flow rate, Q:

$$L = c \cdot Q = M/t \tag{1.2}$$

Having a method to measure the concentrations of various substances, a series of quality of water parameters can be defined:

1. Total Suspended Solids (TSS) – the solid mater in suspension.
2. Dissolved Oxygen (DO) – an indicator of the water "health" as all higher forms of aquatic life require it.
3. Organic Compounds – Total Organic Carbon (TOC) – the total organic carbon concentration in the water.
4. Nitrogen (N) – can exist in water in four forms: organic nitrogen, ammonia, nitrate and nitrite. Total nitrogen is the sum of all four compounds.
5. Phosphorus (P) – can be expressed as organic phosphorus, inorganic phosphorus and total phosphorus.

Because not all the Total Organic Carbon is oxidizable, in the wastewater sector there is a common practice to measure only the oxygen demand, which means the equivalent quantity of oxygen in water required to degrade the organic compounds in inorganic compounds, in the form of Chemical Oxygen Demand (COD) and Biochemical Oxygen Demand (BOD). The relationship between the organic carbon fractions in wastewater can be seen in Figure 1.2.

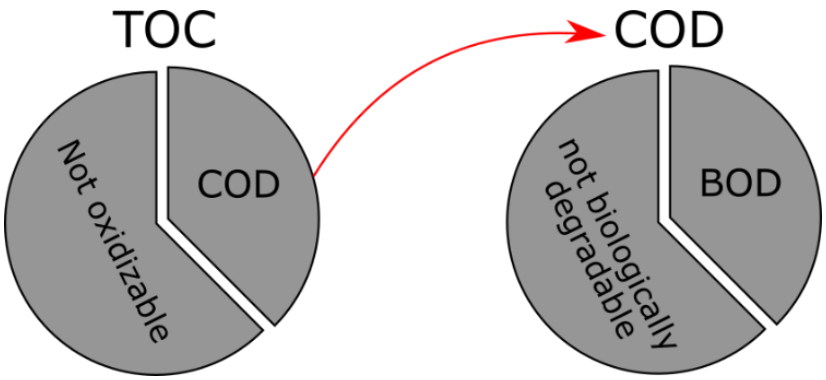


Figure 1.2 – Organic carbon fractions

1.1.4. Factors impacting the wastewater



Figure 1.3 – Wastewater management systems interfaces

The wastewater collecting and treatment systems are important as they mediate the interaction between the natural water cycle and human activities. These systems have, as stated in Figure 1.3, two interfaces: one with the public and one with the environment [13].

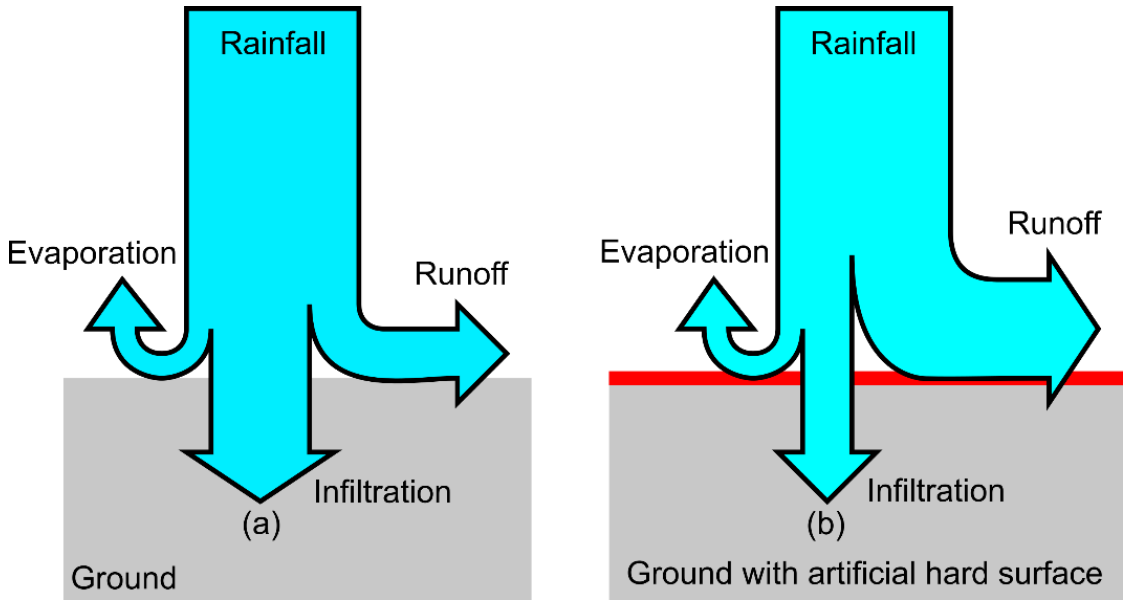


Figure 1.4 – Rainfall mechanism
(a) pre-urbanization; (b) post-urbanization

Currently, the world is in a process of accelerated urbanization [25] that is increasing the population density in urban areas putting additional stress on the existing wastewater systems, on both interfaces. The increased domestic and industrial wastewater production leads to systems overloading increasing the environmental pollution of these systems. On the other hand, urban development usually comes with covering the ground with artificial surfaces, increasing the amount of surface stormwater runoff (see Figure 1.4). This stormwater runoff is fast travelling (as the ground is covered with hard impermeable surfaces) meaning that its flow will start and end quickly, leading to a peak flow that increases the danger of floods. On top of that, this has also strong implications in terms of water quality as the fast rainwater flow is likely to wash off pollutants and sediments and might cause additional pollution to the river [13]. Thus, the stormwater runoff must be somehow collected to prevent urban floods, therefore SN must be able to take it over.

The previously mentioned factor caused by urbanization, high stormwater runoff, is getting accentuated by one of the current major challenges of humanity: global warming, as it is causing extreme rainstorms [26], [27].

1.1.5. Law regulations on wastewater

To assure that the water quality is not negatively impacting the environment and human health, governments imposed laws that regulate wastewater management and the necessary quality that wastewater must have before discharging it into the natural receptors.

At the European Union (EU) level, the most important directive regulating water management, inclusively wastewater, is the Water Framework Directive 2000/60/EC [5] which aims at creating a framework for reaching a common European goal: achieving a “good status” for all European water bodies by protecting and restoring aquatic ecosystems, reducing water pollution and guaranteeing sustainable water management by both the economic sectors and the population. The current EU’s legislation for managing urban wastewater has been adopted in 1991 as the Council Directive 91/271/EEC [28] and has been multiple times amended resulting in the actual consolidated form of the law [29]. This directive aims at protecting the European environment and public health from the negative effects of wastewater by setting up a set of rules for all stages of wastewater management: collecting, transporting, treatment and discharging. All union members must monitor both the WWTP’s performances and the natural collectors' water quality, while, at the same time, taking measures to limit the negative impact of the SN overflows during heavy rains. This directive also states that all human agglomerations which have a population equivalent (p.e.) of more than 2000 should have systems for collecting and transporting the wastewater and all wastewater from human agglomerations having more than 10000 p.e. should be subject to secondary treatment before being discharged into natural receptors. By exception, secondary treatment is mandatory for all human agglomerations having more than 2000 p.e. if the receiving collector is a source for drinking water or if it is an estuary.

The quality parameters of the water discharged from the treatment plants are also regulated by this directive as presented in Table 1.1. If the receiving water body is identified as a sensitive area susceptible to eutrophication, the additional quality parameters presented in Table 1.2 must be fulfilled.

Table 1.1 – EU requirements for WWTP effluent

Parameter	Limit	Minimum reduction through treatment
Biochemical Oxygen Demand	25 mg/l O_2	70 – 90 %
Chemical Oxygen Demand	125 mg/l O_2	75 %
Total Suspended Solids	35 mg/l (60 mg/l if p.e. between 2000 and 10000)	90 % (70 % if p.e. between 2000 and 10000)

Table 1.2 – EU requirements for WWTP effluent if receiving water is identified as sensitive

Parameter	Limit	Minimum reduction through treatment
Total Phosphorus	2 mg/l (1 mg/l if p.e. > 100000)	80 %
Total Nitrogen	15 mg/l (10 mg/l if p.e. > 100000)	70 – 80 %

An annual minimum number of samples that must be taken at regular intervals is imposed for monitoring these parameters, depending on the WWTP size:

- 2000 – 9999 p.e.: 12 samples during the first functioning year. 4 samples in the next years, only if all the first year samples met the above-mentioned requirements.
- 10000 – 49999 p.e.: 12 samples per year.
- > 50000 p.e.: 24 samples per year.

In Romania, the legislation for wastewater management is “NORME TEHNICE from 28 February 2002” [30] which has been adopted in 2002 and subsequently amended multiple times to align it with the EU legislation. This regulation defines the rules for collecting, transporting, treating and discharging wastewater. This regulation also stipulates the need for secondary treatment to keep the discharged water quality parameters below certain limits. The defined limits are the same as the ones defined by the EU regulations presented in Table 1.1 and Table 1.2.

Another Romanian legislation for wastewater management is the “NORMATIV NTPA-002 from 28 February 2002” [31] which is regulating the water entering the SN or the water sent directly to WWTPs. It provides a series of standards for the wastewater quality to meet to be allowed to send it to the public SN. On the contrary, wastewater must be subject to pre-treatment to fulfil the quality requirements. These quality requirements refer to keeping the concentration of pollutants below certain limits, but also to keep the wastewater temperature and pH in a certain interval. Also, the following are forbidden from the wastewater when entering public SNs or WWTPs: big solids, oils, fats, substances that could solidify or coagulate with other substances in the sewer, substances that are chemically aggressive, inhibitors of the biological processes that take place in the WWTP, radioactive substances, heavy metals etc.

1.2. State of the art in modelling and control of Sewer Networks

A sewer network is a system used to collect and transport rainwater and/or wastewater from the population or industrial facilities to a designated place (for example, to a WWTP). Most communities rely on artificial water draining systems consisting of a network of storage tanks connected through pipes. Of course, some isolated communities, even from developed countries, never had access to such systems, and they rely on natural draining [13].

SNs usually handle two types of water flow: rainwater (pluviometric water) and wastewater (domestic wastewater and industrial wastewater), so, in consequence, there are two constructive types of SNs [32]:

1. **Combined sewer networks** (see Figure 1.5) in which both the rainwater and wastewater are transported in the same pipes. The system transports only wastewater flow during dry weather, but during pluviometric events, the flow in the SN increases as a consequence of rainwater addition. In heavy rainfalls, it can cause overflows of SN leading to floods and environmental pollution. To avoid overflows, the SN needs to provide the capacity to store and transport the heavy rainfall flows. This is not economically feasible as the SN will collect and transport usually only wastewater flow that represents only a tiny part of heavy rainwater flows. The solution is to develop control strategies for SN to minimize overflows.

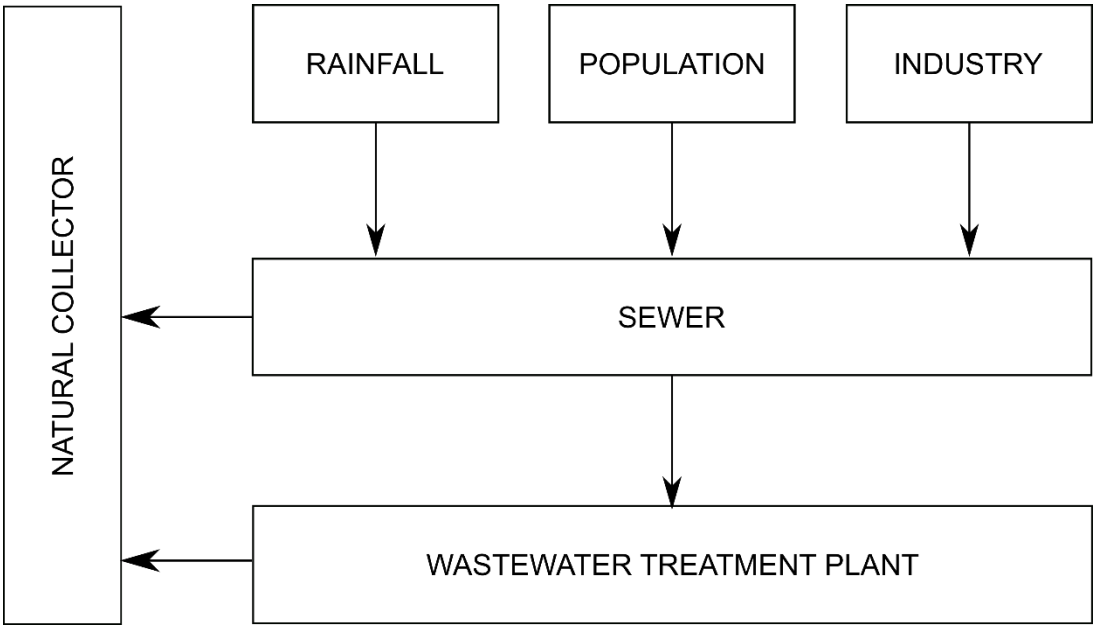


Figure 1.5 – Combined sewer network

2. **Separate sewer networks** (see Figure 1.6) in which the rainwater flows in separate pipes from the wastewater. These types of SNs have the main advantage of carrying rainwater directly to natural receptors, and because the wastewater is usually constant, no overflow occurs. However, this type of SN is more expensive than a combined SN and there is no insurance that the rainwater is not getting polluted for any reason (infiltrations from and to the wastewater piping, washing pollutants from the catchment surface etc.)

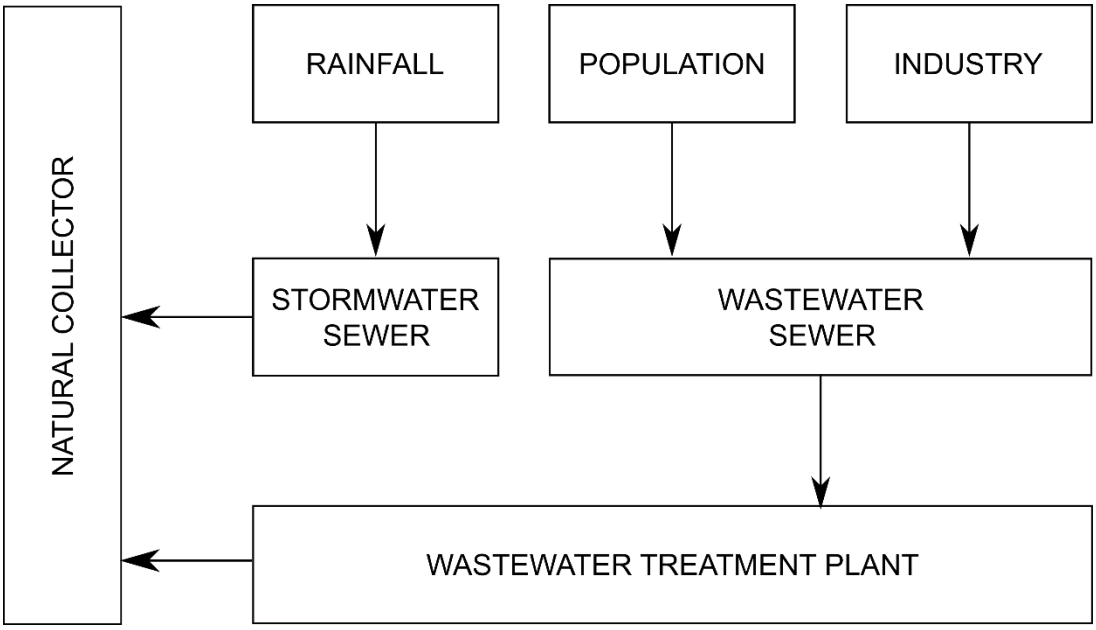


Figure 1.6 – Separate sewer network

Some communities have hybrid SNs where an important part of the rainwater flows in separate pipes from the wastewater, while some of it gets mixed with the wastewater. Usually, this is a consequence of extending the existing combined SN with a separate SN part [13].

The quick development of the cities and the high water demand, that eventually gets into the SN, led to the need for complex control of SNs. But for such control to be implemented, there is a need for digital simulation and analysis of SNs [33].

1.2.1. Sewer Network modelling

The beginning of the SN model development occurred in the early 1970s [34] with the release of the Storm Water Management Model (SWMM) by the Environmental Protection Agency in the USA. This model is used to predict flows and pollutant concentrations and can simulate both continuous and single-event [35]. The first version of SWMM was programmed in FORTRAN and was composed of 5 blocks [36]:

1. Executive Block.
2. Runoff Block – based on Horton Infiltration Model [37]:

$$f = f_0 + (f_{max} - f_0) \cdot e^{-k \cdot t} \tag{1.3}$$

   where f is the infiltration capacity in the soil $(\mathrm{mm/h})$, f_0 is the initial infiltration capacity, f_{max} is the maximum infiltration capacity $(\mathrm{mm/h})$ and k is the decay rate $(1/\mathrm{h})$ [38] and on Manning's equations for overland flow approximation:

$$Q = \frac{1}{n} \cdot R^{2/3} \cdot S^{1/2} \cdot A \tag{1.4}$$

   where Q is the flow $(\mathrm{m^3/s})$, n is the Manning's Roughness Coefficient (unitless), R is the hydraulic radius (m), S is the slope $(\mathrm{m/m})$ and A is the flow area $(\mathrm{m^2})$ [39].

3. Transport Block implemented by the usage of the kinematic wave method.
4. Storage Block.
5. Receiving Water Block.

This model has been improved over the years getting to the current version, SWMM 5.2, which includes various hydrological processes, such as time-varying rainfall, evaporation, snow accumulation, snow melting, infiltration in various types of soil, groundwater and SN interflow, the buildup of pollutants during dry weather, reduction in loads concentrations by natural processes in the sewer system etc. [40].

Some studies approached, using SWMM, the modelling and prediction of various compounds transported or generated in the sewer, such as hydrogen sulphide [41] or various drugs (amphetamine, 6-monoacetylmorphine, 6-acetylcodeine etc.) with their specific transformations [42]. In [43], a toolkit for SWMM has been developed for identifying the pollution sources in a SN using Genetic Algorithms (GA).

The specialized literature distinguishes two types of mathematical models for SNs [36]:

1. Flow models – are using scientific knowledge about water runoff, pipe flow, pipes and tanks deposits etc. to mathematically model the hydrological processes that takes place in the SN.
2. Quality models – are needed when information about the pollutants entering, moving through, or exiting the SN is required. Usually, quality models include the modelling of

pollutants entering and leaving and their transport through the SN. Other processes that could be included in this type of model are sedimentation, pollutant transformations, biochemical interactions etc.

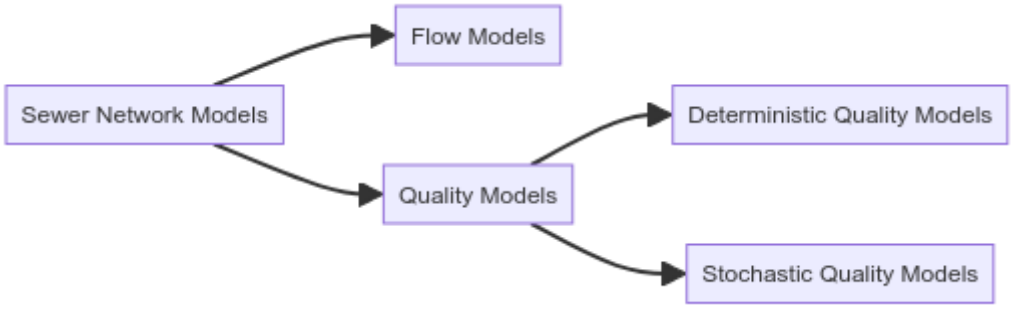


Figure 1.7 – Classification of SN models

The SN flow models are based on a set of partial differential equations describing the water flow (Saint-Venant equations) [45]. There are two equations: a continuity equation and a dynamic one [46]:

$$v \cdot \frac{\partial A}{\partial x} + A \cdot \frac{\partial v}{\partial x} + b \cdot \frac{\partial h}{\partial t} = 0 \tag{1.5}$$

$$g \cdot \frac{\partial h}{\partial x} + v \cdot \frac{\partial v}{\partial x} + \frac{\partial v}{\partial t} = g(S_0 - S_f) \tag{1.6}$$

where:

- v $[m/s]$ – the water velocity.
- x $[m]$ – the position of the measurement from the upstream end.
- A $[m^2]$ – the flow cross-section area.
- b $[m]$ – width of the section.
- h $[m]$ – depth of flow.
- g $[m/s^2]$ – gravitational acceleration.
- S_0 – the bed slope.
- S_f – the friction slope.

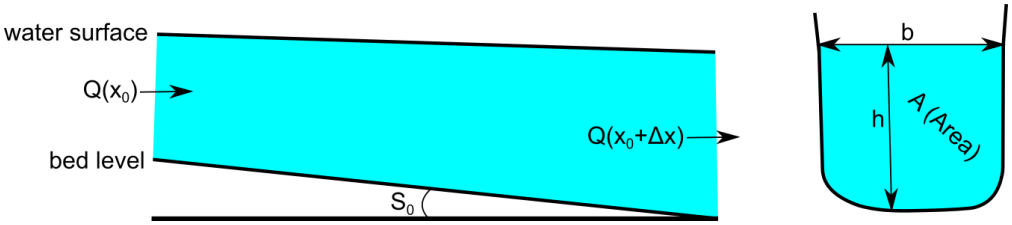


Figure 1.8 – Water flow in a channel

Knowing that the flow rate $Q = A \cdot v$ $[m^3/s]$, then:

$$\frac{\partial Q}{\partial x} = \frac{\partial (A \cdot v)}{\partial x} = v \cdot \frac{\partial A}{\partial x} + A \cdot \frac{\partial v}{\partial x} \tag{1.7}$$

$$\frac{\partial Q}{\partial t} = \frac{\partial (A \cdot v)}{\partial t} = A \cdot \frac{\partial v}{\partial t} \tag{1.8}$$

Introducing relations (2.5) and (2.6) into the partial differential equations (2.3) and (2.4), the Saint-Venant equations represented in terms of flow rate instead of velocity are obtained:

$$\frac{\partial Q}{\partial x} + b \cdot \frac{\partial h}{\partial t} = 0 \tag{1.9}$$

$$\frac{\partial Q}{\partial t} + \frac{\partial \left({}^{Q^2}/_{A} \right)}{\partial x} + g \cdot A \cdot \frac{\partial A}{\partial x} - g \cdot A \cdot \left(S_0 - S_f \right) = 0 \tag{1.10}$$

Modelling the storage component of a SN in a flow model is based on the mass conservation principle. Therefore, the accumulation (volume change) can be expressed as the difference between inflow and outflow. For the storage tank with overflow capability presented in Figure 1.9 the continuity equation is [47]:

$$\frac{dV}{dt} = Q_{in}(t) - Q_{out}(t) - Q_{over}(t) \tag{1.11}$$

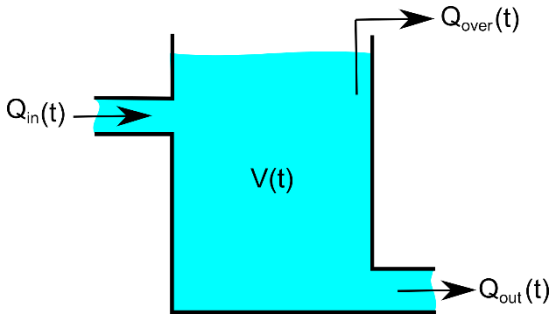


Figure 1.9 – Storage tank with overflow capability

with:

- $V(t)$ $[m^3]$ – currently stored volume of water in the tank.
- $Q_{in}(t)$ $[m^3/s]$ – tank's inflow.
- $Q_{out}(t)$ $[m^3/s]$ – tank's outflow.
- $Q_{over}(t)$ $[m^3/s]$ – tank's overflow – multiple methods and formulas, depending on the weir shape and characteristics, are used to calculate the overflow [48].

For control purposes, because complex flow models of SNs require a lot of computational effort, simplified discrete models have been proposed [27]. In these models, the transport component delay is translated into a certain amount of discretization steps, while the storage component model is obtained by discretizing equation (1.11):

$$V[k+1] = V[k] + T \cdot (Q_{in}[k] - Q_{out}[k] - Q_{over}[k]) \tag{1.12}$$

where:

- T – discrete time interval.
- k – time index.
- $V[k]$ – the stored volume of water in the tank at the moment $k \cdot T$.
- $Q_{in}[k]$ – the inflow of the tank over the period $[k \cdot T,\ (k+1) \cdot T]$.
- $Q_{out}[k]$ – the outflow of the tank over the period $[k \cdot T,\ (k+1) \cdot T]$.

- $Q_{over}[k]$ – the overflow of the tank over the period $[k \cdot T,\ (k+1) \cdot T]$. In the simplified discrete model, it is assumed that the overflow occurs when $V[k] \geq V_{max}$, with V_{max} being the tank storage capacity, therefore, the overflow can be calculated by:

$$Q_{over}[k] = \begin{cases} \frac{d_0}{T} \cdot (V[k] - V_{max}) & if\ V[k] \geq V_{max} \\ 0 & else \end{cases} \tag{1.13}$$

  with d_0 a parameter empirically estimated to best fit the real overflow.

Because the volume of water in the tank cannot exceed the tank's capacity, in [49] a modified nonlinear version of the above presented discrete model is proposed. The equation (1.12) becomes:

$$V[k+1] = \min\left(V_{max}, V[k] + T \cdot (Q_{in}[k] - Q_{out}[k] - Q_{over}[k])\right) \tag{1.14}$$

while the overflow is calculated by:

$$Q_{over}[k] = \max\left(0, V[k] + T \cdot (Q_{in}[k] - Q_{out}[k] - Q_{over}[k]) - V_{max}\right) \tag{1.15}$$

Other researchers [50] integrated the SN flow model with the topology of the urban roads to obtain a sewer-road network model in order to use it for analysing the interdependency of the two sub-systems, especially during events with high precipitations.

Besides the flow models, quality models of SNs began to be developed as a tool to be used in optimizing the pollution load caused by sewer overflows [51]. Two approaches can be distinguished: stochastic quality models which are data-driven, and deterministic quality models [52].

Various methods have been used for developing stochastic quality models, such as using multigene genetic programming [53] or evolutionary polynomial regression [54] for sediment transport modelling.

In [55] a stochastic model has been implemented in InfoWorks to predict both flow and quality profiles to analyse the effect water-saving strategies have on sewer flow and pollutants concentrations. A similar approach has been presented in [56], where the model was implemented to predict flow, nutrient and temperature changes in a sewer. The model was then used to quantify the impact of water-saving strategies: greywater recycling using smart water appliances and rainwater collecting.

More specific stochastic models were developed in [57], where a Monte Carlo simulation has been used to model the chemical oxygen demand transformations in the sewer, and in [58], where the modelling of pharmaceuticals in the SN has been done.

Other approaches are focusing on human waste modelling, such as [59] where Artificial Neural Networks (ANN) have been used to obtain a predictive model to forecast faecal indicator bacteria concentrations of a SN, and [60] where image processing techniques and particle image velocimetry were used to quantify physical disintegration (erosion and breakage) of faeces in sewers.

In parallel with data-driven stochastic models, deterministic models have been developed, where changes in water quality have been mathematically expressed based on their concentrations and decay coefficients. These models describe various processes that happen on SN loads:

1. Sediments deposition and transport: [61], [62], [63], [64], [65].
2. Chemical Oxygen Demand: [66], [67].
3. Total Suspended Solids: [67].
4. Methane: [68], [69], [70], [71].
5. Hydrogen sulphide: [68], [72], [73], [70], [71], [74].

In [75] a benchmark simulation model (BSM) for catchment and SNs is proposed, aiming to evaluate urban sewerage control strategies and to facilitate the integration with standard WWTP models. This benchmark simulation model, BSMSewer, models the wastewater flow with its loads: particulate and soluble chemical oxygen demand, ammonia and phosphate, being composed of:

1. Catchment model – inspired by BSM2 dynamic influent pollutant disturbance scenario generator [76], aims at generating the wastewater in catchment areas by combining the domestic influent, the industrial influent, the pluviometric influent and the infiltration to the SN;
2. SN model – composed of three components modelling the wastewater transport, sewer pipes flushing and sewage water storage. The model does not consider biological transformations of the loads in the SN.

The transport component models wastewater pipe flowing. The pipe is modelled as a completely mixed tank with a certain volume, so, therefore, the mathematical model is based on the mass conservation principle as seen in equation (1.11), with the remark that $Q_{over,T}(t) = 0$ as the pipes do not have overflow capabilities. The outflow of the transport component is related to the volume of wastewater in the pipe and a residence time constant (K_R):

$$Q_{out,T}(t) = \frac{V_T(t)}{K_R} \tag{1.16}$$

Similar to wastewater flow modelling, the transport component models the load transport using the same mass balance principle:

$$\frac{dM_T}{dt} = X_{in,T}(t) - X_{out,T}(t) \tag{1.17}$$

$$X_{out,T}(t) = \frac{M_T(t)}{K_R} \tag{1.18}$$

where:

- M_T $[kg]$ – the pollutant mass in the pipe.
- $X_{in,T}(t)$ $[kg/day]$ – the input load.
- $X_{out,T}(t)$ $[kg/day]$ – the output load.

The sewer pipe flushing component models the accumulation of particulates in the sewer and their flushing when the flow through the pipe reaches a threshold value:

$$\frac{dM_F}{dt} = X_{in,F}(t) \cdot \left(1 - \frac{M_F(t)}{M_{max,F}}\right) - \frac{\left(Q_{in,F}(t)\right)^{n_f}}{\left(Q_{lim,F}\right)^{n_f} + \left(Q_{in,F}(t)\right)^{n_f}} \cdot M_F(t) \cdot FF \tag{1.19}$$

with:

- M_F $[kg]$ – the pollutant (COD_{part}) mass accumulated in the system.

- $M_{max,F}$ $[kg]$ – the maximum pollutant mass that can settle.
- $X_{in,F}$ $[kg/day]$ – the pollutant influx.
- $Q_{in,F}$ $[m^3/day]$ – the inflow.
- $Q_{lim,F}$ $[m^3/day]$ – the threshold flow that triggers the pipe flushing effect.
- FF $[1/day]$ and n_f – adjustable parameters for tunning the model.

The storage component of the BSMSewer uses the same mass conservation principle to model the volume of water and the quantities of pollutants in the storage tanks. The overflow, $Q_{over}(t)$, is modelled using specific methods and equations depending on the overflow weir characteristics, while the tank's outflow, $Q_{out}(t)$, depends on the tank output type. If the tank output is equipped with a pump, then the outflow will be the pump flow. If the output tank is equipped with a valve and the wastewater flows due to gravitational effect, then the outflow will be:

$$Q_{out}(t) = \frac{Q_{max} \cdot (h(t) - h_{min})^n}{h_o^n + (h(t) - h_{min})^n} \tag{1.20}$$

where:

- Q_{max} $[m^3/day]$ – the maximum tank outflow – depending on the outlet valve opening.
- $h(t)$ $[m]$ – wastewater liquid column height in the tank.
- h_{min} $[m]$ – minimum wastewater liquid column height in the tank.
- h_o $[m]$ – wastewater liquid column height in the tank when $Q_{out}(t) = Q_{max}/2$;
- n – tunning parameter of the model.

As stated before, this model aims to be used to evaluate urban sewerage control strategies. For this purpose, a set of 10 performance indicators have been defined in [75] and presented in Table 1.3.

Table 1.3 – BSMSewer performance indicators

Indicator	Unit	Description
N_{ovf}	$events/year$	Total number of overflow events
T_{ovf}	$days/year$	Total duration of overflow events
V_{ovf}	$m^3/year$	Total volume of overflowed wastewater
OQI	$kg - polluting\ units/day$	Overflow quality index calculated similarly as the effluent quality index of BSM WWTPs gets calculated [77] after converting overflow to ASM variables using [76]
$C_{max,TSS}$	$g\ COD/m^3$	Maximum pollutants concentrations continuously overflowed for one hour (Total Suspended Solids, Nitrogen and Phosphorus)
$C_{max,TKN}$	$g\ N/m^3$	
$C_{max,PO4}$	$g\ P/m^3$	
$T_{exc,TSS}$	$days/year$	Total duration of pollutant exceeding the legal limits during a year
$T_{exc,TKN}$	$days/year$	
$T_{exc,PO4}$	$days/year$	

1.2.2. Sewer Network control strategies

Sewer network control strategies are important as they assure safe and low-cost operations of the SN. The main goal of SN control systems is to reduce the effect of overflows, by reducing

the volume of the overflow or the quantity of pollutants discharged during overflow events. Other goals include, but are not limited to enhancing sulphide mitigation [78], optimal chemical dosing and distribution in the SN to reduce corrosion and odours [79] or preventing blockages [80].

Many of the goals can be achieved during the layout design phase of the SN. In [81] SN layout and component size optimization algorithm to minimize the total cumulative flow has been developed. The implemented method is based on spanning three algorithm for selecting the layout and a modified Particle Swarm Optimization (PSO) algorithm to optimize the component sizes of the selected layout. The method has been applied to the Sudarshanpura SN, in Jaipur, India. In [82] a hybrid GA (GA combined with three growing algorithm) is used, while in [83] an adaptive GA approach is used to optimize the layout design of SNs.

Other methods have been used to optimize the layout of SNs, such as tabu search [84], PSO [85], ant colony algorithm [86], mixed-integer linear programming [87] or arc-based ant colony optimization algorithm [88].

However, even if they achieve the desired goals, these approaches can be expensive, in terms of construction materials, and are impractical for achieving the same goals on already existing SNs or when the variables that were used during the layout optimization are changing due to the city development. For the existing SNs, it is easier to develop control strategies to reach the same goals, than to resize pipes, valves and storage tanks.

The main objective of the SN control strategies is to minimize the overflow effects on the environment. However, besides this objective, SN control strategies should also consider [47]:

1. avoiding overloading the storage tanks that do not have overflow capabilities to ensure safe operation of the SN.
2. a smooth command evolution to not force the execution elements (valves and pumps).
3. maximizing the water treated by the WWTP during rain events and immediately after.
4. balanced use of the storage tanks.

In [89], the authors propose a generic methodology for optimal control of SNs. The methodology applies when a state-space model of the system is available and consists of six steps, as shown in Figure 1.10:

1. **system analysis** where the available measurements, the control variables and the disturbances (usually the pluviometric events) are identified. During this step, the objective function is also defined. Because of the difficulty of rainfall prediction, the authors define an objective function based on both the expected and the current overflow formulating the problem as a two-step optimization problem.

2. **two-stage optimization** aims to set optimal values for the control variables, in concordance with the objective function previously defined and the given rainfall prediction. The two stages of optimization are the deterministic stage and the stochastic stage.

3. **definition of operating phases and process gains** where, because the relations between system variables are highly nonlinear and lead to completely different evolutions of variables depending on the current state of the system, operating phases of the system, such as dry weather, filling or emptying phase, are defined. For each of the phases, the system is linearized.

4. **screening of measurement** that aims the reduction of the problem by discarding measured variables that are not influenced by any of the control variables during the considered time horizon.
5. **calculate control variables** by defining the controlled variables as a linear combination of the measurements. An optimization procedure for all possible measurement combinations is done, selecting the one that minimizes the loss value. This procedure is repeated for all operating phases defined within the 3rd step.
6. **closed-loop evaluation** that is needed to validate the previously obtained results.

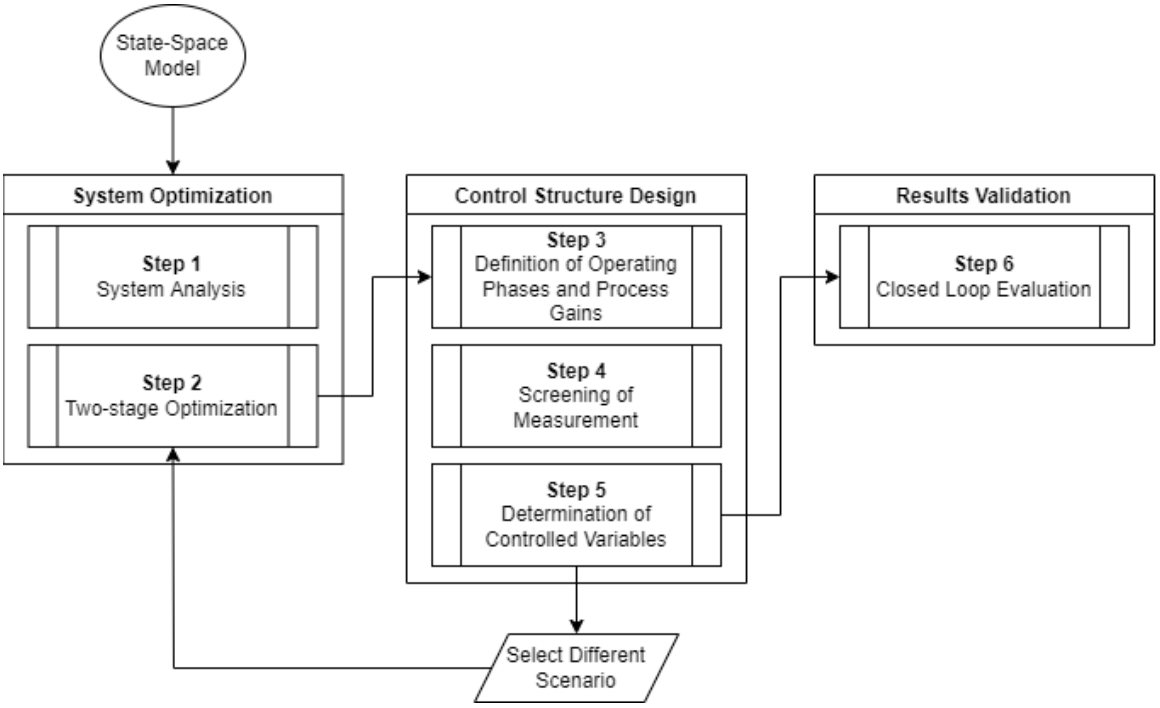


Figure 1.10 – Workflow for the proposed methodology

The methodology has been implemented in a real case study (a 135.000 inhabitants catchment area of Copenhagen) showing good results.

Other approaches are based on simplified models and consider only binary commands on the storage tanks' output valves. For example, [90] addresses the usage of Binary Hybrid Topology Particle Swarm Optimization (BHTPSO) as an optimization algorithm to solve the Sewer Network Discharge Optimization problem formulated as a Binary Optimization Problem. The control structure is presented in Figure 1.11.

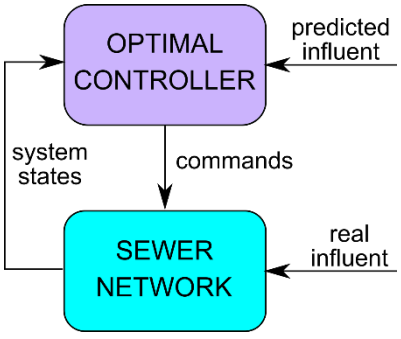


Figure 1.11 – Optimal control structure

The optimization algorithm was implemented in two versions: with and without a local deterministic descent algorithm (LDDA). At each iteration of the BHTPSO, for each of the particles in the swarm, LDDA looks for a better solution in the geographic neighbourhood of the particle. Adding the LDDA leads to better results as observed from this paper's statistical analysis section.

In [91] a predictive control structure (Figure 1.12) is defined to minimize the disturbance influence on the system by minimizing the SN overflows. The structure is proposed as an alternative to the previously described optimal control system structure and it is more suitable for larger SNs. In this paper, the control structure has been also implemented by using BHTPSO as an optimization algorithm and has been run for various SN sizes and various sizes of the sliding time horizon, with very good results.

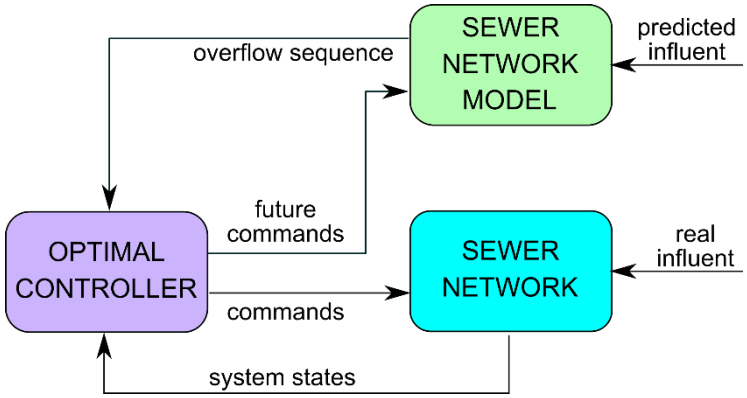


Figure 1.12 – Predictive control structure

Other researchers used fuzzy logic-based control structures to reduce the SN overflows effects. For example, in [92], for each of the storage tanks in the network, the fuzzy logic considers the levels in the storage tank and the downstream storage tank and the influent rate to control the output flow rate. The structures were implemented for the BSMSewer model, and the obtained results show improvements in the overflow in terms of pollution loads.

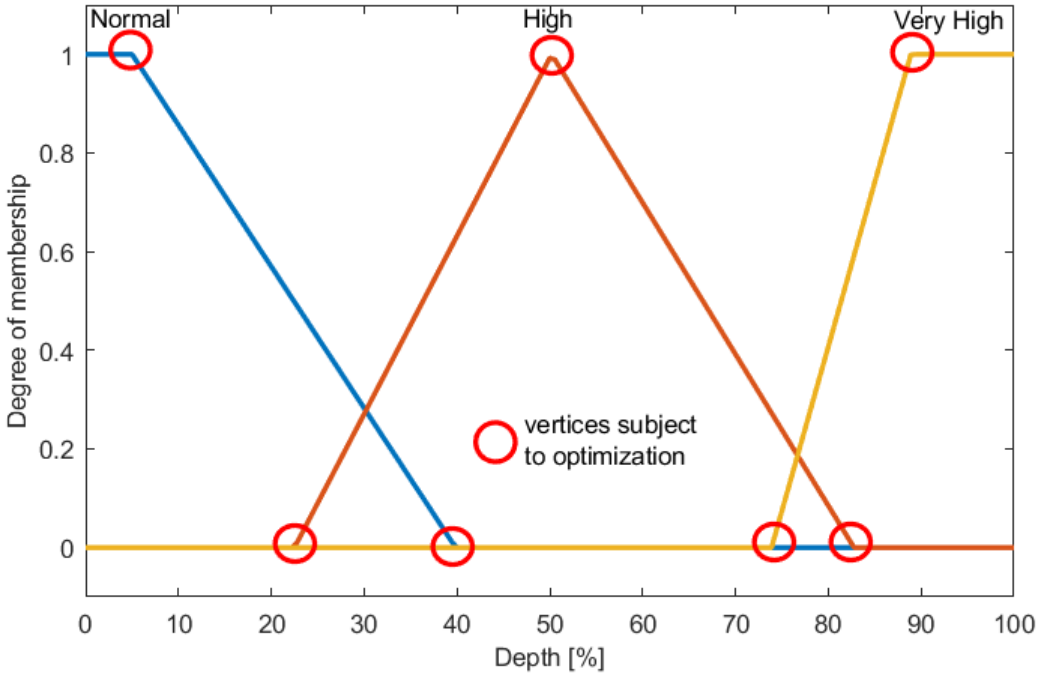


Figure 1.13 – Example of fuzzy membership function for water level

In an article published in 2019 in “Journal of Hydroinformatics”, [93], a new fuzzy logic local autonomous Real-Time Control (RTC) is introduced to minimize the overflows by using the free space in the SN. The fuzzy logic controller uses the water level before and after the control gate to control the gate opening. Its membership functions are adjusted by using a GA optimization to provide the best results (Figure 1.13) – optimized fuzzy logic membership functions led to a 25% overflow volume decrease compared to the fuzzy logic membership functions provided by human experts.

In “Output-feedback control of combined sewer networks through receding horizon control with moving horizon estimation” [94], B. Joseph-Duran, C. Ocampo-Martinez and G. Cembrano propose an output-feedback control for large scale SNs. In this approach, receding horizon control is used to solve the optimal control problem and moving horizon estimation to solve the state estimation problem.

Most of the recent papers regarding optimal control of SNs are using a Model Predictive Control (MPC) with various approaches. For example, [95] proposes and compares two types of MPC: one based on a wastewater quantity control approach and the second based on both quantity and quality approach with its uncertainty propagation, concluding that the last one provides better results because it reduces the overflow volume and pollution load without the need to add new sensors at the existing SN. For the quantity control approach, the optimization was done with a convex optimisation solver, while for the qualitative approach, due to the nonlinear model, the *fmincon* procedure [96] was used.

In [97] a MPC approach with hard constraints on the input and soft constraints on the output is proposed for the Barcelona benchmark model [45] of a SN. The paper clearly shows that it is possible to minimize the overflows by controlling the sewer wastewater flow using a prediction of the rainfall. Another approach is presented in [98] where a reduction of 17% of the volume of overflow has been obtained on InfoWorks high-fidelity simulator by using a MPC to obtain optimal solutions for multi-objective functions. A feedback simulation procedure is used to realize the communication between the optimizer and the simulator.

In a paper published in 2019 [99], the authors present a comparison of two methods regarding the overflow in SNs. The two methods, Mixed Integer MPC which is based on mixed linear dynamic formulations, and Quadratic Programming MPC, have been tested on the same Barcelona benchmark model of a SN mentioned before, showing that they provide equivalent results, but the computational costs are lower for Quadratic Programming MPC, making it more suitable for using longer prediction horizons.

In [100], A. Cembellín, M. Francisco and P. Vega propose a distributed MPC with fuzzy negotiation, the results being compared to those of a centralized and a decentralized MPC. This strategy aims at the minimization of a local objective function that depends on the evolution of the subsystem and its neighbour by using prediction models and local constraints. Then fuzzy negotiations are used to generate the final control actions. The findings of this paper are extended by the same authors in [101] where distributed MPC with fuzzy negotiations is compared to a centralized MPC including, this time, information about pollutant loads (TSS).

Recently, in 2022, the paper entitled “Model predictive control based on artificial intelligence and EPA-SWMM model to reduce CSOs impacts in sewer systems” (CSO – Combined Sewer Overflow), [102], proposes a structure that uses ANNs for predicting flows and genetic algorithms aiming to optimize the SN operation.

The paper “Balancing water quality and flows in combined sewer systems using real-time control”, [103], formulates a real-time load balancing algorithm aiming at improving flow and water quality dynamics in the SN with respect to the output to the WWTP.

In “Model-Based Sewer Network Control - Practical Experiences”, [104], the authors use model-based flow control system to minimize the overflows of a real SN in Kenten, Germany. The control system uses data from online radar and radar forecasting to model the influent of SN and it is implemented in SIWA SEWER, a SN control application developed by Siemens. Data collected for one year after the control system implementation shows that this approach led to a reduction of direct river discharges by 450000 m^3, increasing the total amount of stormwater treated by the WWTP.

U. Rathnayake and A. H. M. Faisal Anwar, in their paper “Dynamic control of urban sewer systems to reduce combined sewer overflows and their adverse impacts” [105], propose a Multi-Objective Optimization (MOO) algorithm (Figure 1.14) for a SN. The optimization algorithm (Non-dominated Sorting Genetic Algorithm II – NSGA-II) used by the authors aims at minimizing the overflow pollution load and the operating cost of the SN pumps and WWTP. Firstly, an optimization for the 0-15 minutes time window is performed resulting in a Pareto front. The extreme solutions (minimum pollution load and minimum cost) are selected for the optimization process for the 15-30 minutes time window. The procedure is then repeated for the next time windows. The algorithm provides good results, but simulation time must be improved to use it in a real-time application.

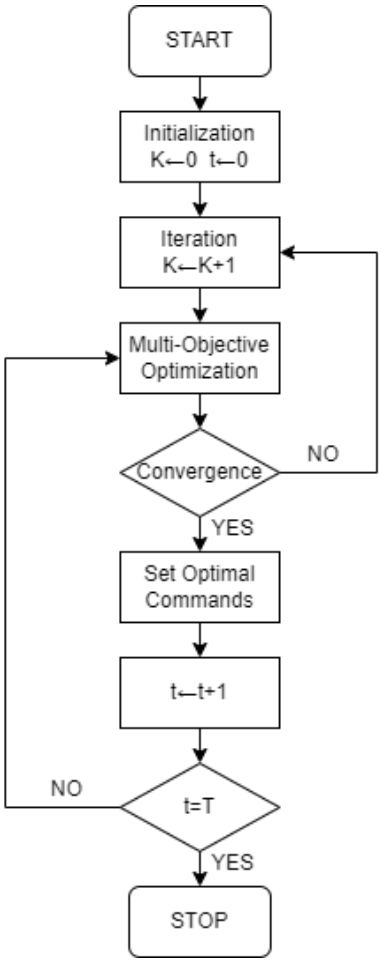


Figure 1.14 – Flowchart of the multi-objective optimization algorithm

In recent years, a new approach based on deep learning techniques can be found in the literature. For example, [106] presents a hierarchical control strategy consisting of a minimum scaled consensus control optimization algorithm that operates at the global control level and ensures optimal distribution of wastewater in the pipes and storage tanks, and a deep deterministic policy gradient algorithm that operates at the local control level and is used to handle the nonlinearities from the system. Pei et al. [107] proposes using neuro-evolution for RTC of SN by training the control policy. By having a control policy, it is possible to avoid any online optimisation procedure. Moreover, the trained policy proves its reliability and robustness by performing better than the equal filling degree strategy,

In 2018, a group of researchers from the Norwegian University of Life Sciences published a series of papers aiming at using ANNs in the control strategies defined for SNs:

1. In [108] the authors aim to use the free space in the SN piping of Drammen, Norway, to reduce the overflows. The control strategy is based on a detailed hydraulic model that is used to identify where, in the SN, there is more free space and a Recurrent Neural Network (RNN) that is used to predict the flow in the SN to obtain a good response time of the proposed control algorithm. Three architectures of the RNN have been tested and compared: Elman Neural Network (ENN), Nonlinear Autoregressive network with inputs and Long Short-Term Memory network (LSTM), showing that LSTM provides the best results in predicting the sewage flow for the next 30 minutes based on flow data of the last 30 minutes.
2. In [109], as an extension to the previous paper, the same control structure is used, but other ANN architectures are trained, tested and compared to predict the water level in the CSOs structure. The used architectures, multilayer perceptron (MLP), Wavelet Neural Network (WNN), LTSM and Gated Recurrent Unit (GRU) are trained using data collected from an Internet of Things (IoT) monitoring the SN. Results show that LTSM and GRU provide the best result, with the remark that GRU has a faster learning curve.
3. In [110] the authors propose the use of LTSM to build a model for flow-rate prediction in the sewer. This model is used in a newly proposed method for reducing overflows: Inter Catchment Wastewater Transfer which aims at redistributing the SN wastewater flow, while, at the same time, taking into account the treatment capacity of the WWTP.

1.3. State of the art in modelling and control of Wastewater Treatment Plants

A wastewater treatment plant is a system that takes the effluent provided by SN and which, by various processes, removes pollutants making its effluent suitable to be returned to the water cycle or to be used for various purposes. Depending on the local industry-specific, industrial wastewater can be discharged into the SN to be treated by the municipal WWTP or can be pretreated by the factory's WWTP.

A typical WWTP receives wastewater and produces treated water by using various processes. However, in the treatment process, there can be also other inputs and outputs [111]:

1. inputs:
   - energy
   - chemicals
2. outputs:
   - sludge
   - biogas
   - GHG

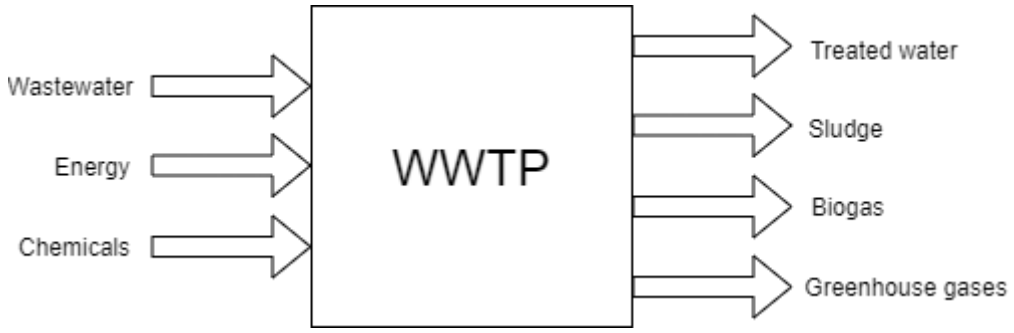


Figure 1.15 – WWTP inputs and outputs

Two of the additional WWTP outputs can find valuable usage. The biogas, obtained from the generated sludge, can be internally reused to generate energy reducing the plant's external energy requirements and being one step toward energy-neutral WWTPs [112], while the sludge, with proper treatment, can find its use in agriculture [113].

Conventional wastewater treatment usually involves three treatment stages [114]: primary, secondary and tertiary that involve various physical, chemical and biological processes.

Primary treatment aims at removing particles, oil and grease by using:

- screen – used to remove large solids to protect the mechanical integrity of the WWTP elements.
- grit chamber – used to remove sand, glass and metal fragments to protect the mechanical integrity of the WWTP pumps.
- skimming tank – used to remove floating matter: soap, wax, fat and grease that would affect the biological growth in the next treatment stage. Skimming tanks are equipped with air blowers at the bottom of the tank used to raise the floating matter.
- primary settling tank – wastewater goes through a physical/chemical precipitation process aiming at removing organic solids and fine suspended. The physical precipitation uses gravitational force to settle down heavier particles, while the chemical precipitation removes the unsettled particles by using coagulants (e.g., aluminum sulphate, ferric chloride etc.) to form floc, which will trap finer particles and will settle down at the bottom of the tank.

Secondary treatment aims at degrading biodegradable organic compounds by using specific types of microorganisms that are increasing their population by consuming the organic mass from the wastewater. Secondary treatment uses various processes [115], such as:

- aerobic digestion – the microorganisms use oxygen (provided through aeration) to oxidize the organic compounds into CO_2, water and biomass.

- anaerobic digestion – is used for treating heavily contaminated wastewater from industrial sources, it is slower than aerobic digestion as no oxygen or nitrate is present. The microorganisms convert the organic compounds into CO_2, CH_4 and water.
- anoxic digestion – the microorganisms use the oxygen from the dissolved nitrate to convert the organic compounds into CO_2, water, biomass and nitrogen, making this process suitable for nitrogen removal.

Tertiary treatment, also named advanced treatment methods, aims at removing phosphorus, nitrogen, heavy metals, viruses and pathogenic bacteria [114] by using:

- disinfection – destroying viruses and pathogenic bacteria using chemicals (usual chlorine).
- reverse osmosis – removing minerals (e.g., phosphorus, calcium, fluoride etc.) and some organic compounds including pesticides.
- electrodialysis – removing cations and anions present in wastewater.

Besides the traditional technologies used to treat wastewater, some other advanced technologies can be used:

1. activated carbon filters [116] – use the property of porous activated carbon to absorb pollutants from the wastewater.
2. magnetic nanoparticles [117] – uses their magnetic property to absorb pollutants;
3. ozonation [118] – uses the high-oxidizing property of the ozone to remove pathogens and organic and inorganic compounds from the wastewater.
4. ultraviolet radiation [119] – the UV radiation penetrates the cellular membrane of pathogenic bacteria and damages them, preventing their reproduction.

1.3.1. Wastewater Treatment Plants modelling

Biological wastewater treatment processes require bacteria to oxidize the organic compounds matter, usually referred to as a substrate, into simple compounds, and, therefore, mathematical models of WWTP must describe these biological processes.

A biological process used in wastewater treatment can be expressed by using the following reaction equation [120]:

$$v_1 \cdot S + v_2 \cdot O_2 + v_3 \cdot NH_3 + v_4 \cdot PO_4^{3-} \xrightarrow{bacteria} v_5 \cdot new\ cell + v_6 \cdot CO_2 + v_7 \cdot H_2O \quad (1.21)$$

with:

- v_1 - v_7 – stoichiometric parameters
- S – substrate concentration
- O_2 – oxygen concentration
- NH_3 – ammonia concentration
- PO_4^{3-} – phosphate concentration
- $new\ cell$ – produced biomass concentration by the bacteria multiplication
- CO_2 – carbon dioxide concentration produced
- H_2O – water produced

The first attempts to model these processes were made by Jaques Monod (1910 – 1976) in the middle of the last century. He established the growth rate of microorganisms in a bioreactor [121]. Their maximum growth rate depends on the characteristics of the microorganisms, the environmental factors and the concentration of organic compounds.

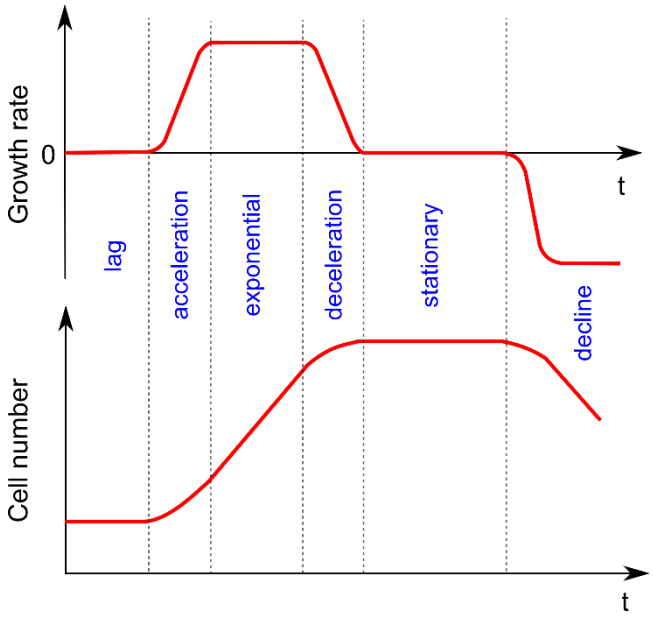


Figure 1.16 – The growth phases of bacterial cultures

Based on the cell number growth curve, Monod identified a sequence of six phases in the culture life cycle:

1. lag phase – the growth rate is null, with the microorganisms adapting to the new environment.
2. acceleration phase – the growth rate is increasing.
3. exponential phase – the growth rate remains constant, while the number of cells is exponentially increasing.
4. deceleration phase – the growth rate is decreasing.
5. stationary phase – the growth rate is null, with the number of cells remaining constant.
6. decline phase – the growth rate becomes negative thus the number of cells starts to decline.

In the exponential phase, the number of cells increases directly proportional to their mass, therefore their growth rate can be described by the first-order kinetic equation:

$$\frac{dX}{dt} = \mu \cdot X \tag{1.22}$$

where X is the biomass concentration and μ is the bacteria-specific growth rate.

Considering Y the yield coefficient, the relationship between the biomass concentration and substrate concentration is:

$$\frac{dX}{dt} = \mu \cdot X = -Y \cdot \frac{dS}{dt} \tag{1.23}$$

Therefore, because the substrate becomes a limitation factor, Monod proposes an equation for the bacteria-specific growth rate, an equation in which the specific growth rate is directly

proportional to the substrate concentration for lower substrate concentration values, but gets saturated for higher substrate concentration:

$$\mu = \frac{\mu_{max} \cdot S}{K_s + S} \tag{1.24}$$

where:

- μ_{max} – maximum specific growth rate;
- K_s – half saturation constant – numerically equal to substrate concentration when the specific growth rate is half of the maximum specific growth rate.

Therefore, for a given microorganism type and a given substrate, in the same environmental conditions, Monod considers the parameters Y, μ_{max} and K_s constants to be experimentally determined.

The equation for the bacteria-specific growth rate is based on observation, thus the Monod model is an empirical one. Also, the Monod model describes precisely only the kinetics for pure cultures with a simple certain substrate [122].

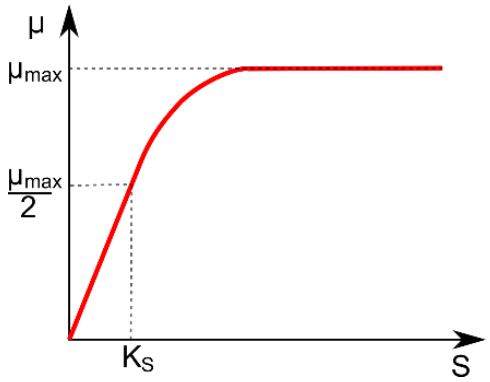


Figure 1.17 – The Monod dependence between substrate concentration and growth rate

In 1959, Contois found evidence that the specific growth rate may also depend on the biomass concentration [123]:

$$\mu = \frac{\mu_{max} \cdot S}{K_c \cdot X + S} \tag{1.25}$$

with:

$$K_c = \frac{a}{Y \cdot (a + 1)} \tag{1.26}$$

where:

- Y – the growth yield coefficient;
- $a = \frac{K_s}{S_0}$ – a constant obtained by dividing the half-saturation constant by the inflow substrate concentration.

In wastewater treatment, due to temporary high loads, periods with substrate excess can appear leading to supra saturation. During these periods, a decrease in the growth rate has been observed. For this situation, another extension of the Monod model was introduced by Haldane

[120]. The new model (Haldane model) introduces a new constant K_i to deal with the specific growth rate:

$$\mu = \frac{\mu_{max} \cdot S}{K_s + S + \frac{S^2}{K_i}} \tag{1.27}$$

The biological treatment process is a complex and nonlinear one and is composed of various stages, thus, the need for complex models that describe the process as accurately as possible arises.

At the beginning of the 1980s, the International Association on Water Quality (IAWQ), known today as the International Water Association (IWA) created the "Task Group on Mathematical Modelling for Design and Operation of Biological Wastewater Treatment" aiming to combine the most relevant biological treatment models to create a common unified model that would describe as accurately as possible the activated sludge treatment process [124].

The work of the task group led, in 1987, to the first dynamic Activated Sludge Model (ASM) – ASM1 [125], a model that is nowadays one of the most accepted and used models to describe wastewater treatment processes. This model became a reference for many pieces of research and the base for the future development of ASM-type models.

The ASM1 is a structured model that is based on Monod kinetics to predict the biological reactions that take place during the biological treatment processes, being able to model COD and nitrogen removal, sludge production and the consumption of oxygen. ASM1 models three bacterial growth processes, two biomass decay processes and another three processes related to hydrolysis. This model characterizes the wastewater in terms of [124]:

- six particulate components;
- seven dissolved components;
- DO concentration;
- alkalinity.

ASM1 models are presented as a matrix (Peterson/Gujer matrix) containing stoichiometric coefficients and a kinetic vector [126]. This representation helps at presenting the model in a condensate form, facilitating its interpretation and publication.

The necessity for the effluent to comply with the standard required quality regarding nitrogen and phosphorus led to the need to model the biological phosphorus removal, this being one of the major limitations of ASM1. Therefore, the IWA task group developed and released, in 1995, the Activated Sludge Model 2 (ASM2) [127] which modelled, besides the ASM1 processes, biological phosphorus removal processes by including Phosphate Accumulating Organisms (PAO) that only grow under aerobic conditions. ASM2, an extension of ASM1, a compromise between simplicity and complexity, includes new state variables, such as PAO, Polyhydroxyalkanoates (PHA) and Polyphosphates (PP) and includes the precipitation of phosphates with ferric hydroxide ($Fe(OH)_3$) and the redissolution of the resulting ferric phosphate ($FePO_4$) processes.

In 1999, the ASM2 model was further extended with denitrifying PAO, resulting in ASM2d [128] that includes two more processes: the anoxic growth of PAO and the storage of inorganic phosphorus as PP using the energy obtained by anoxic breathing of PHA.

In parallel with these developments, a group of researchers from Delf University of Technology, Netherlands, developed a metabolic model: TUDP (Technical University Delft Phosphorus) [129] that describes both the anaerobic and the aerobic phases of Enhanced Biological Phosphorus Removal (EBPR). This model was later integrated with ASM2, resulting in ASM2-TUDP [130].

The same Task Group that developed ASM1, ASM2 and ASM2d came in 1999 with another model, Activated Sludge Model 3 (ASM3) [131] that was aiming at solving some of the limitations of ASM1 by introduce the endogenous respiration process and the role of storage of organic substrate.

The development of control strategies for WWTP led to the need for models that include the whole wastewater treatment system and that are suitable for comparing different control strategies. In consequence, in 1988, “European Cooperation in the field of Scientific and Technical Research” (COST) groups 682 and 624 started working on a benchmark model that defines a simulation model, influent loads, a plant layout and evaluation criteria. Later, these groups, together with another Task Group from IWA released the first Benchmark Simulation Model (BSM1) [77]. Figure 1.18 shows the structure of this model.

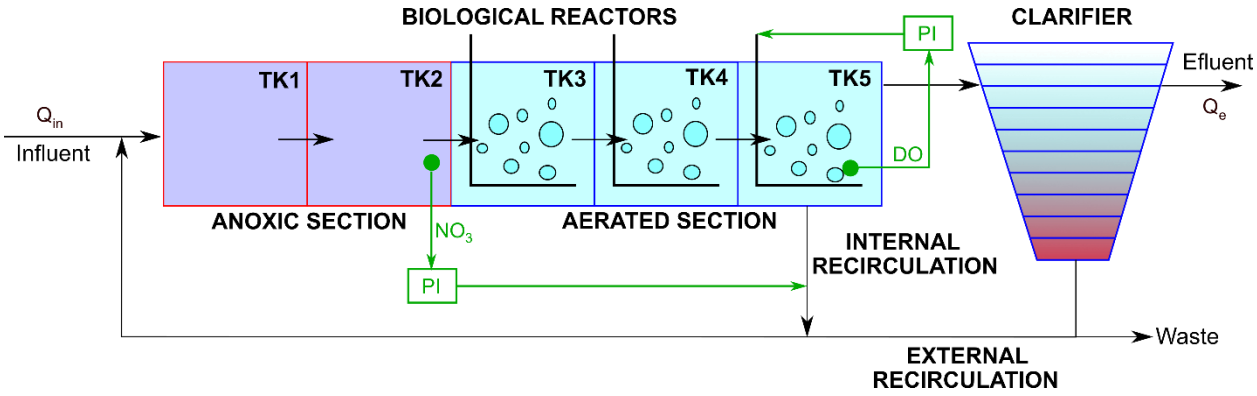


Figure 1.18 – BSM1 structure

The BSM1 plant is one of the most used layouts for nitrogen and organic compounds biological removal from municipal wastewater. The layout contains two anoxic tanks, 3 aerated ones and a secondary clarifier. The benchmark model provides three influent scenarios (dry, rain and storm), evaluating control strategies over 14 days periods.

BSM1 has further been extended into BSM1-LT [132] which allowed evaluation of the control strategies over 609 days periods. BSM1-LT also introduced the possibility to have faults and the temperature as an influent variable, with the process parameters changing with the temperature.

Significant development of the BSM1 model led to Benchmark Simulation Model 2 (BSM2) [133]. This model considers both wastewater treatment and sludge treatment. New elements have been added to the plant: a primary clarifier, a thickener for the secondary clarifier sludge, an anaerobic digestor for the sludge treatment and a dewatering unit (Figure 1.19).

The anaerobic digestor for the sludge treatment is modelled with Anaerobic Digestion Model (ADM) 1 – ADM1 [134] which was developed by the IWA Anaerobic Digestion Modelling Task Group. Anaerobic digestion implies complex molecules decomposition into simple compounds, in the absence of oxygen, by using anaerobic microorganisms. ADM1 includes 24 variables and 19 processes grouped into five steps: disintegration, hydrolysis, acidogenesis, acetogenesis and

methanogenesis. Because of the differences between variables of ASM1 and ADM1, BSM1 includes 2 conversion interfaces from ASM1 variables to ADM1 variables and vice versa.

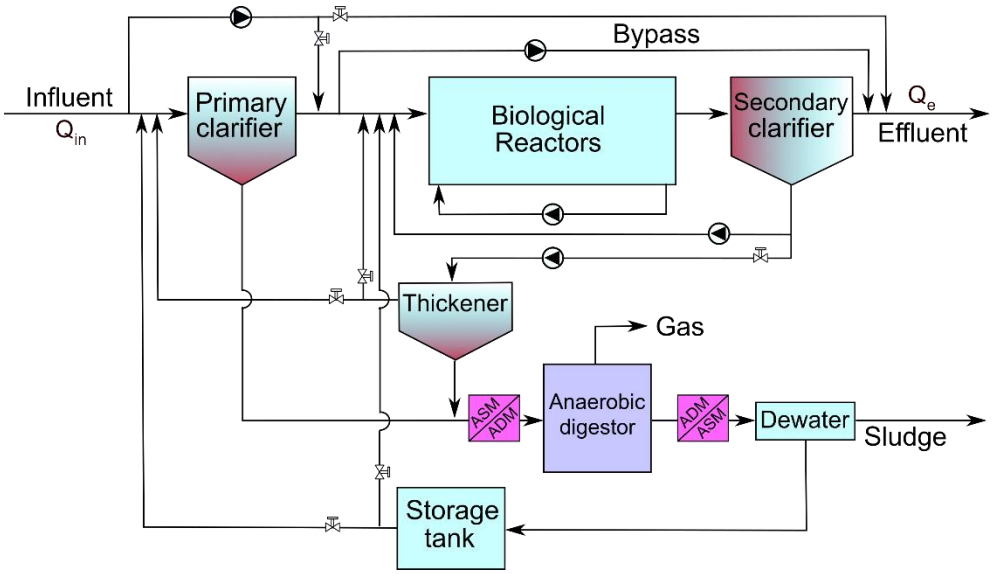


Figure 1.19 – BSM2 structure

As stated before, WWTPs are a source of GHG, that are contributing to air pollution and climate change. Therefore, for applying techniques to reduce GHG emissions, the need to integrate these emissions in WWTPs models is arising.

Estimating GHG emissions by wastewater treatment started in 2006 with the Intergovernmental Panel on Climate Change (IPCC)'s guidelines for National Greenhouse Inventory [7], guidelines that have been updated in 2019 [8].

In [135], ASM models are extended to model N_2O dynamics during nitrification and denitrification by including six new processes, while in [136] a mathematical model for Nitric Oxide (NO) and N_2O formation by Ammonia-Oxidizing Bacteria (AOB) is proposed. This latest model has been integrated with ASMN [137], a model extending ASM1 with 2-step nitrification and 4-step denitrification, resulting in a model named ASMG1 [138] that can model GHG emissions from the WWTPs. Another approach [139] extends the ASM3 model to include a pseudo-mechanistic model to describe N_2O production by both AOB nitrification and heterotrophic denitrifiers.

Flores-Alsina et al. [6] propose a benchmark simulation model named BSM2G, an extension of the BSM2 model [133], having the same structure (see Figure 1.19), but including, additionally, the dynamics of the greenhouse gases (GHG) emissions. Thus, the plant layout includes wastewater treatment (composed of five bioreactors – two anoxic and three aerated ones, with two clarifiers) and sludge treatment. All the bioreactors are modelled using an extended version of ASM1 [125] in order to, besides modelling biological pollutants removal – carbon and nitrogen, estimate the plant's GHG emissions [6]:

- from biological treatment:
  - CO_2 emissions due to BOD oxidation and biomass respiration
  - N_2O due to heterotrophic denitrification
  - CO_2 due to nitrification
- from other sources:
  - CO_2 due to sludge processing (anaerobic digestion and CH_4 combustion)

- CO_2 equivalent due to net power consumption
- GHG emissions that are associated with external carbon feeding

In a paper published in 2015, “Estimation of greenhouse gas emissions from a hybrid wastewater treatment plant” [140], the authors propose a simple comprehensive model that can estimate on-site and off-site GHG generated by the WWTP. For modelling the off-site GHG emissions, the electric energy used for plant operation and chemical production and transportation has been used to estimate CO_2 emissions, while for estimating on-site GHG emissions, the following processes have been considered:

1. for CO_2: biomass respiration, BOD oxidation and nitrification;
2. for N_2O: nitrification and denitrification processes for biological nitrogen removal;
3. for CH_4: anaerobic degradation of organic matter.

In [141], a new model that quantifies carbon and energy footprint is presented. The model estimates both on-site and off-site emissions related to both biological and physical treatment processes in a WWTP. The innovative aspects that are present in this model are: it is based on kinematic and mass balance relationships, two-step nitrification and N_2O formation during nitrification and denitrification in two forms (dissolved and gas).

In a recent paper [142], a hybrid modelling approach for N_2O emissions estimation is proposed. The approach integrates the first principal model (modified ASM1) with deep-learning techniques to predict N_2O production. This way, less calibration is required than when using a purely mechanistic model and less data is required than when using pure deep-learning techniques. For the deep-learning part of the modelling, a modified teacher-forcing LSTM has been used.

1.3.2. Wastewater Treatment Plants control strategies

Wastewater Treatment Plant control strategies are important as they ensure that the wastewater resulting from human activities does not pollute the environment and does not impact human health in any way. Therefore, the main goal of WWTP control systems is to ensure that its effluent complies with the legal standards for water to be discharged into natural receptors in terms of the different pollutants loads. Other goals include, but are not limited to, lower operational costs or lower GHG emissions.

These goals can be achieved by manipulating various control variables from the system, such as oxygen transfer coefficients from the aerated tanks, internal and external recirculation flows, or by manipulating, in the top-level control structure, the setpoints of lower-level structure such as DO concentrations in the aerated tanks or the nitrogen concentration.

[143] proposes, for DO Concentration control, a direct adaptive NN control by using a Forward NN to approximate an ideal control law. The advantages of this approach include the adaptive ability and not needing an accurate WWTP model.

One approach to WWTP control, particularly data-driven control, can be found in [144]. The authors propose a Growing and Pruning Recurrent Fuzzy Neural Network (GPRFNN)-based control system (see Figure 1.20) to control the DO concentration. The control system contains a

Recurrent Fuzzy NN (RFNN) identifier that is used to model the WWTP and RFNN controllers designed to set the control variables to ensure WWTP performances.

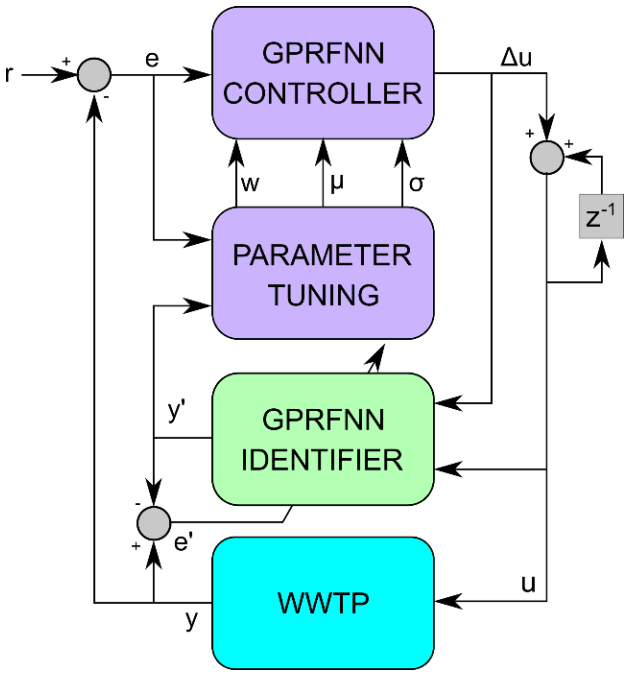


Figure 1.20 – GPRFNN-based Control System

In another approach [145], a research team, using a case study for Cluj-Napoca WWTP, proposes a control strategy for a WWTP that, in addition to the conventional NO-DO control loops, contains a Feed-Forward Controller (FFC) as presented in Figure 1.21. In this approach, the WWTP influent flow rate is considered a disturbance, and, therefore, the external recirculation flow rate is controlled to keep the COD in the effluent at the desired rate. A significant improvement in the Effluent Quality Index (EQI) has been observed, with all major nitrogen and COD overshoots being efficiently reduced.

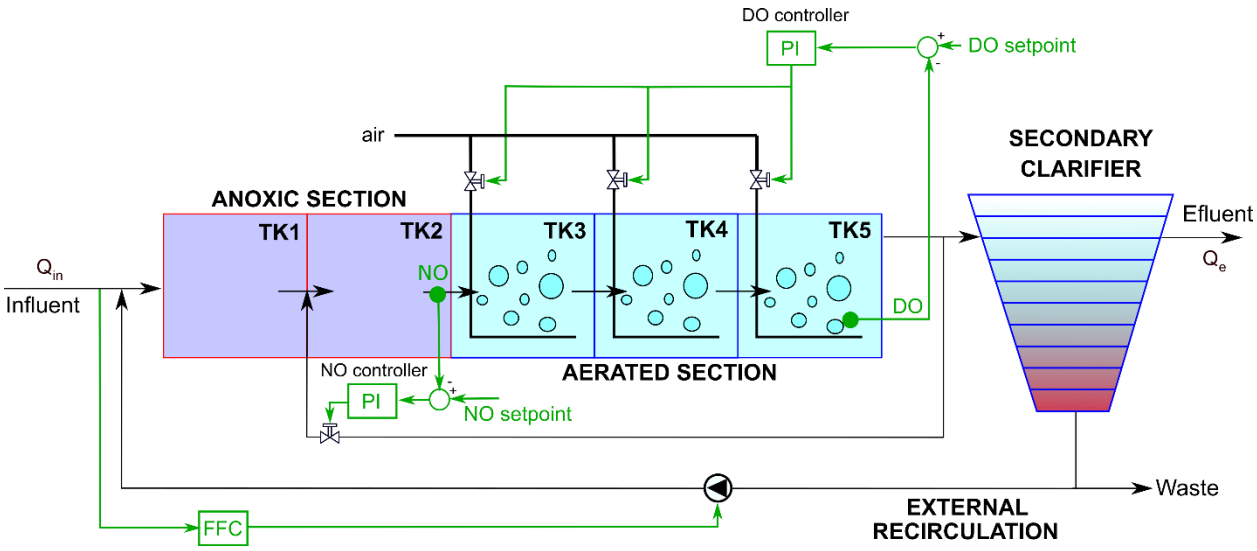


Figure 1.21 – Feed-forward control strategy

In a paper titled “ANN-based Internal Model Control strategy applied in the WWTP industry” [146] a control strategy based on Internal Model Controllers using ANNs to model the plant

behaviour without the need to perform linearization is proposed. The ANN uses an MLP architecture, and it has been trained on BSM1 influent data. In [147] a Case-Based Reasoning (CBR) system is proposed for real-time control and supervision of WWTP. Data mining methods are used to extract knowledge from historical data, knowledge that is then used to generate setpoints for the WWTP controllers. In [148] an advanced supervisory control system is implemented for a WWTP. The control system uses different optimal control strategies to improve the energy balance of a WWTP in Chorzow, Poland. Data from sensors (DO, ammonia etc.) and the mathematical model of the WWTP has been used to develop a support operator system to deal with data uncertainty.

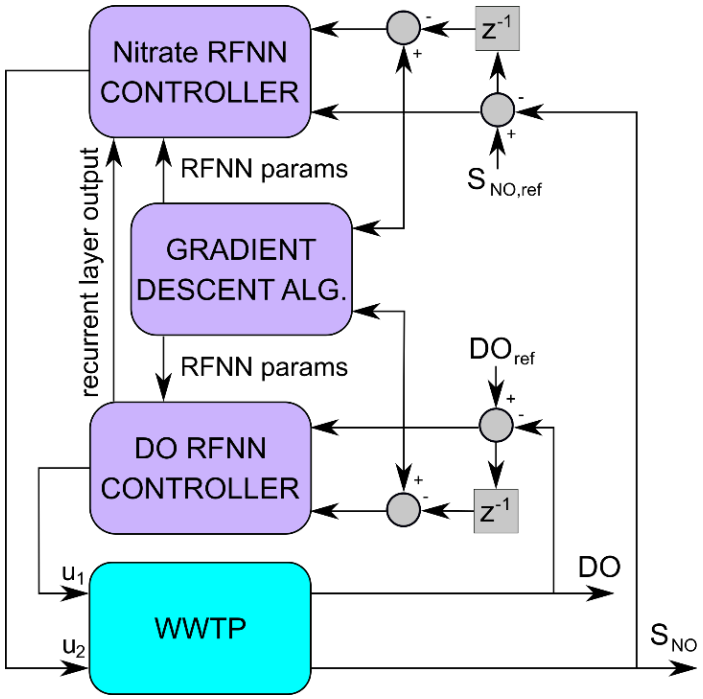


Figure 1.22 – WWTP control strategy based on RFNN

The paper [149] proposes an intelligent decoupling control strategy based on a RFNN to control the WWTP by using a decoupling strategy and a gradient descent search algorithm to decouple the nitrate and DO control loops. The control system contains two controllers, one for DO used to approximate the relationship between the DO and the oxygen transfer coefficient and one for nitrate used to approximate the relationship between the nitrate concentration and the internal recirculation flow, as shown in Figure 1.22.

In [150] a multi-variable direct self-organizing fuzzy neural network control for multi-variable control of WWTP is proposed. The control system is composed of a fuzzy NN controller used to approximate the ideal control law and a compensation controller to minimize the approximation error between the ideal control law and the neural controller.

An interesting approach can be found in the paper “Optimization and control of aeration distribution in the WWTP nitrification reactor” [151]. Here, the authors propose two control structures for ammonia-based aeration control, both of them optimized by using a GA. The first control structure is a cascade one, consisting of three DO slave Proportional Integral (PI) controllers and an ammonia master PI controller, as depicted in Figure 1.23. The optimization objective is to find the optimal air distribution along the three aerated bioreactors (parameters a, b and c).

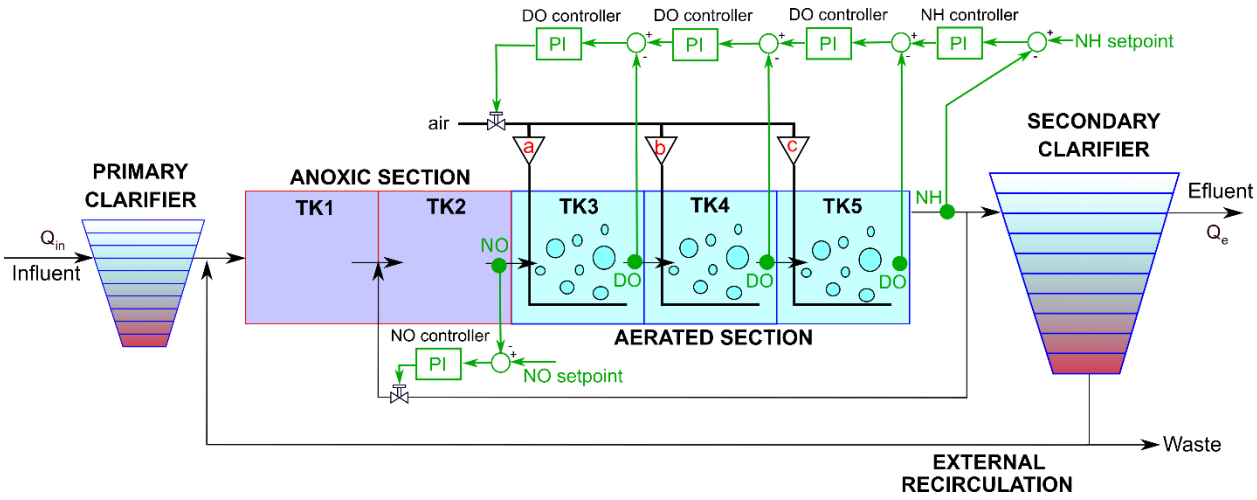


Figure 1.23 – Cascade control setup

The second proposed control structure uses a supervisory control setup (see Figure 1.24), with three DO PI controllers, whose setpoints are computed by a supervisory ammonia controller. The manipulated variable of the ammonia controller is weighted to obtain the setpoint for each of the DO controllers, with the weights being the subject of optimization.

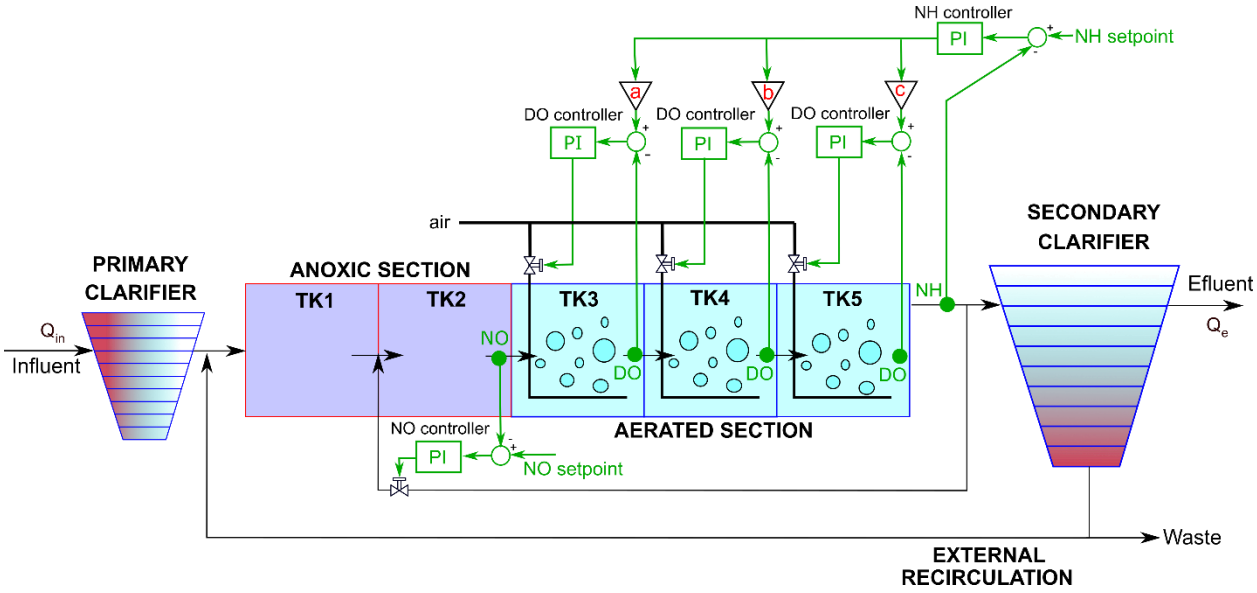


Figure 1.24 – Supervisory control setup

In [152] a hierarchical control system for a Sequencing Batch Reactor (SBR) for a real WWTP in Swarzewo, Poland is proposed. At the top level, a Supervisory Sequential Controller (SSC) is implemented to set, based on the phase of the SBR operating cycle, the DO setpoint for a nonlinear MPC that controls the DO. The SSC is based on two optimization algorithms: a deterministic one: direct search, and a stochastic one: artificial bee colony and determines the optimal trajectory for the DO setpoint. The proposed structure is presented in Figure 1.25, with the following notations: DO [gO_2/m^3] – Dissolved Oxygen; DO_{ref} [gO_2/m^3] – Dissolved Oxygen reference; $Q_{air,ref}$ [m^3/h] – Air flow setpoint; R [gO_2/m^3h] – oxygen respiration rate; V [m^3] sewage volume in the reactor; h [m] – sewage level in the reactor.

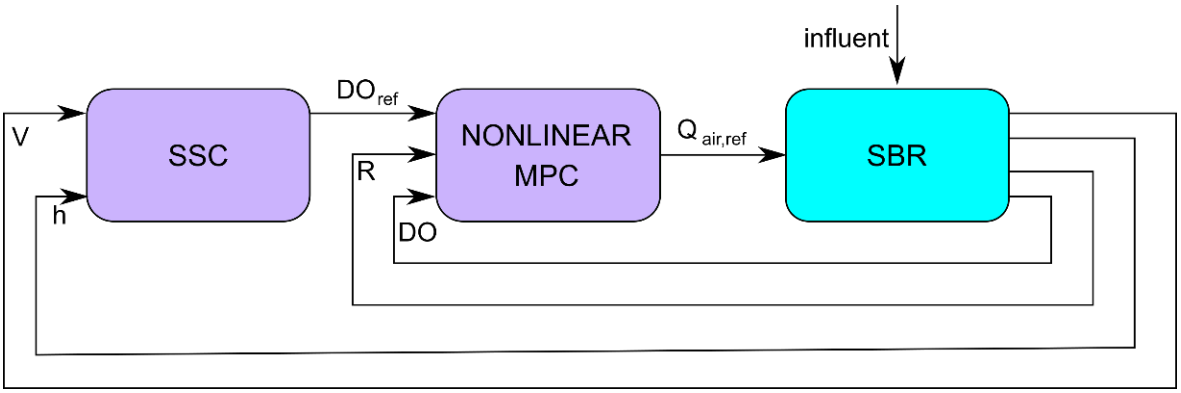


Figure 1.25 – Hierarchical control setup

The paper [153] proposes the use of direct heuristic dynamic programming-based reinforcement learning to get a desired DO concentration setpoint for the 5th aerobic reactor in a WWTP and a desired nitrate concentration in the 2nd anoxic reactor. The controlled variables are the oxygen transfer coefficient for the 5th tank and the internal recirculation flow rate. The proposed approach introduces an optimal control strategy that is entirely driven by data from the WWTP using online learning. [154] presents and compares a series of control strategies for nitrogen and phosphorus removal. The proposed control strategies are using PI control, fuzzy control and MPC.

Many research papers treat the control of the WWTP as an optimization problem. Both single-objective and multi-objective optimization algorithms are used in various control structures to minimize various fitness functions such as effluent quality, energy consumption or GHG emissions.

Single-Objective Optimization (SOO) has been used in [155] to get the best effluent quality, by using a heuristic dynamic programming scheme to control the DO concentration and nitrate level simultaneously with the optimal control values analytically calculated by the controller. The model of the WWTP and the performance index are approximated by using two Echo State Networks (ESN) trained with a gradient-based learning algorithm. In [156] a hierarchical MPC for controlling the WWTP is proposed. The MPC is added to previously developed PI controllers for DO and air pressure in the aeration pipes and it is used to compute the optimal setpoints for DO concentration to keep the output substrate below the legal limit.

The paper [157] proposes an online adaptive dynamic programming control structure based on an ESN to solve the control problem of DO concentration. The controller contains three modules of ESN to approximate the critic index, the system model and the optimal control strategy. For training the model, an online learning algorithm that is based on recursive least squares is used. Experimental results obtained on BSM1 show that this controller can achieve high performance regarding the DO level control.

In [158] a control optimization system based on hybrid intelligence to optimize the operation of a WWTP is proposed. The control system is described in Figure 1.26 and includes a feed-forward compensator designed to adjust DO and nitrate concentrations setpoints to minimize the energy consumption, a feedback supervision module, a pre-setting module and a soft-sensor module. The CBR based Pre-Setting Module is based on a simple principle: similar problems have similar solutions.

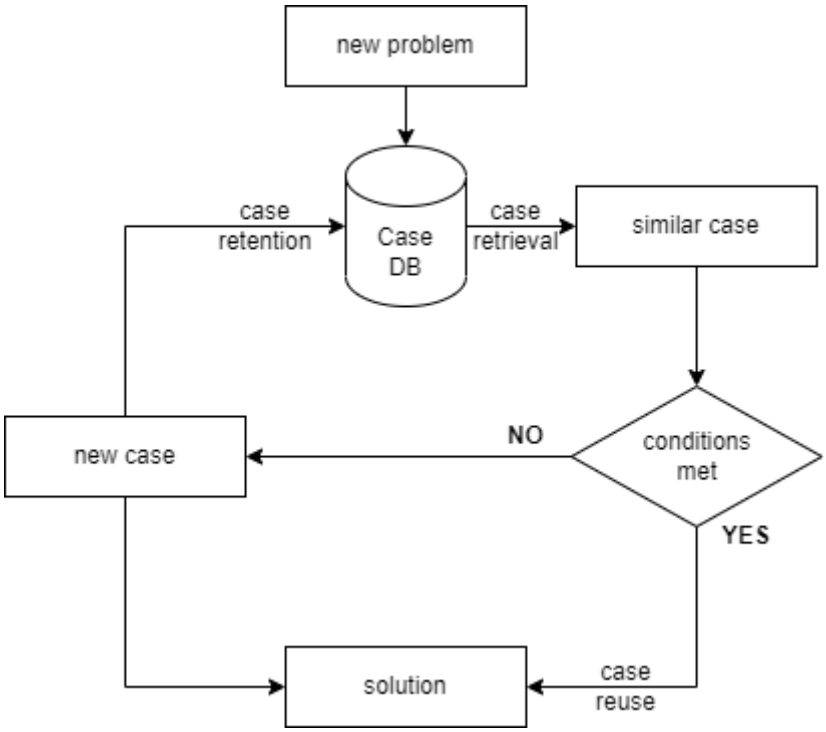


Figure 1.26 – Hybrid Intelligent Optimal Control System

In [159] a Q-learning algorithm with ASM2d-guided reward settling is combined in an integrated ASM2d-QL algorithm. The integrated algorithm is equipped with a self-learning mechanism and is used to optimize the control strategies of an anaerobic-anoxic-oxic system: hydraulic retention time and internal recirculation rate. In another approach [160], due to the nonlinear dynamics and uncertainties of the anaerobic-anoxic-oxic reactors, a robust optimal control strategy to improve the reactor's operation is proposed. To describe the changeable conditions, data-driven systematic performance criteria are developed. Further, a robust PSO algorithm is used to select the optimal solution, and then, the optimal solution is tracked in the control process by using a fuzzy NN. The proposed strategy is tested on the BSM1-P model and real reactors.

Besides SOO, MOO approaches can be found in the literature. For example, in a paper published in 2018 [161], the authors propose an adaptive fuzzy NN control system for MOO of WWTP in terms of energy consumption and effluent quality. The system consists of an optimization module algorithm for selecting the scaling factor and the crossover rate and for obtaining the optimal setpoints and a control module with the adaptive fuzzy NN to trace the setpoints for achieving the desired performances. The paper [162] introduces an improved MOO control strategy to satisfy the effluent quality and reduce the energy consumption of the WWTP. Firstly, an adaptive kernel function is used to model the complex dynamics of effluent quality and energy consumption, then an improved multi-objective PSO algorithm that uses a multi-objective gradient method, and a self-adaptive flight parameters mechanism to minimize the desired objective functions. The track control is implemented by using an adaptive fuzzy neural network controller.

Qiao and Zhang [163] propose a MOO control scheme (see Figure 1.27) to dynamically optimize the DO concentration setpoints and nitrate level setpoints with multiple performance indicators: energy consumption and EQI. The authors use an NN online modelling method to obtain a MOO model for the MOO algorithm, a model that gets solved based on the NSGA-II.

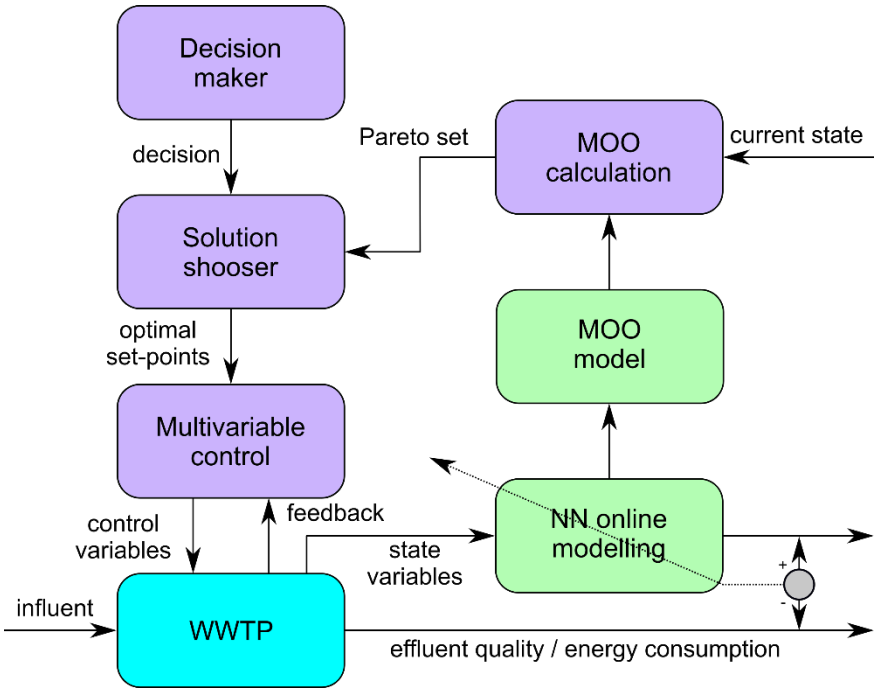


Figure 1.27 – Dynamic multi-objective optimization control

In [164] an Adaptive Multi-Objective Evolutionary Algorithm based on Decomposition (AMOEA/D) to minimize energy consumption and effluent quality of a WWTP is used. In the proposed algorithm, an auto-switching strategy using the aggregation function enhancement is implemented so the algorithm automatically switches from the 1st to the 2nd phase. The proposed solution also includes an adaptive differential evolution strategy and a self-organizing fuzzy NN approximator and controller for tracking the control setpoints of the plant. By testing the strategy on BSM1, the authors show that the AMOEA/D can reduce energy consumption, while at the same time can ensure that the effluent parameters are meeting the legal standards.

In a recent paper [165], *Hen et al.* use a data-driven multi-objective predictive control method to improve WWTP performances. The authors developed a multi-objective strategy with an adaptive fuzzy NN identifier, that, using relevant data from the process, can catch nonlinear behaviours of the WWTP. To obtain the optimal solution, a transfer MOO algorithm is proposed.

Simpler approaches can be found in [166] where GA is used to determine optimal PI controller parameters to achieve the best effluent quality with minimum energy consumption and in [167] where a dynamic multi-objective PSO algorithm concerning multiple dynamic conflicting criteria (effluent quality, energy consumption and operation stability) is proposed.

The paper [168] proposes, for computing optimal setpoints of multiple controllers, a multi-objective supervisory control strategy for WWTPs based on hybrid machine-learning algorithms. The strategy has been used to identify, using nitrogen-to-carbon ratios and fuzzy c-means algorithms, various influent scenarios. Based on the influent scenarios, the control performance was calibrated through a deep-learning-based approximation model. Then a GA was used to compute the optimal setpoints for the two PI controllers (for DO and biogas) and the nitrate cascade-PI controller.

Having in mind the changeable operational conditions of WWTP, in [169] an Intelligent Optimal Control System with Flexible Objective Functions (IOCS-FOF) is proposed. It defines an optimal control scheme and a flexible objective strategy that is used to obtain suitable objective

functions by adapting to the complex conditions in WWTP. Finally, the paper also proposes a new dynamic multi-objective optimization algorithm for flexible objectives to be used to obtain the optimal solutions for the IOCS-FOF. In [170] a Grid-based Dynamic Multi-Objective Evolutionary Decomposition algorithm (GD-MOEA/D) is proposed to minimize two objective functions for the WWTP (energy consumption and effluent quality). An intelligent optimal controller based on GD-MOEA/D is used to track control of the main WWTP variables. The proposed control strategy gets validated on the BSM1 model, resulting an important improvement of energy consumption and effluent quality.

Chen et al. [171] proposes a multi-objective integrated robust optimal control in order to solve problems related to degrading performance of MOO control under disturbances conditions. The newly proposed technique captures the nonlinear dynamics of the WWTP with an estimator and the disturbances using an observer. A prediction model is obtained from the two elements which is further used in the multi-objective integrated robust optimal control.

Even if global warming is an important concern nowadays and keeping in mind the effect of GHG emissions on global warming, only a few researchers are considering GHG emissions when developing control strategies for WWTPs. [172] uses Nelder–Mead Simplex method to perform the MOO of a WWTP in terms of effluent quality, energy consumption, but also GHG emissions, demonstrating the apparent trade-offs between the three conflicting objective functions. In [173] the GHG emissions were monitored for an industrial WWTP. By using a Monte Carlo simulation, a correlation between GHG emissions and operational parameters of the plant was defined. Then, for the designed plant conditions, minimum GHG emission has been computed, resulting in a 30% reduction of them.

1.4. State of the art in modelling and control of Integrated Urban Wastewater Systems

The two systems, SN and WWTP, are interconnected and, because the effluent of the SN represents the influent of the WWTP, it is important to also know the effects of the SN control strategies on the WWTP operation performances. A higher flow from the SN, due to control strategies avoiding overflows, could lead to WWTP overloading, with considerable environmental effects. Therefore, SN control strategies should consider their effects on the WWTP operation efficiency in terms of pollution loads and wastewater flow. On the other hand, WWTP control strategies should consider helping the SN performances when the last one is affected by considerable pluviometric events.

One of the main problems regarding the WWTP operation is the uncertainty regarding the plant's influent. Controlling and operating the SN could help in gaining control over the WWTP influent. A predictable and controlled influent for the WWTP should lead to increased plant performances. Having in mind the two above presented reasons, it is important, when developing control strategies and optimization methods for wastewater transport and treatment, to consider the integrated system consisting of the SN and the WWTP. In the scientific literature, the subject of integrated wastewater systems can be found in a few papers, most of them focusing only on modelling the integrated system.

In 2005, Butler and Schütze [174] proposed an integrated model, SYNOPSIS, consisting of both the SN and the WWTP, but also the water body receiving the WWTP effluent, as presented

in Figure 1.28. Three RTC strategies have been implemented and tested on the proposed model: a reference strategy, with fixed default setpoints, an optimized setpoint strategy and hierarchical integrated control, all of them aiming at providing the best water quality in the natural collector, with the integrated RTC providing the best results.

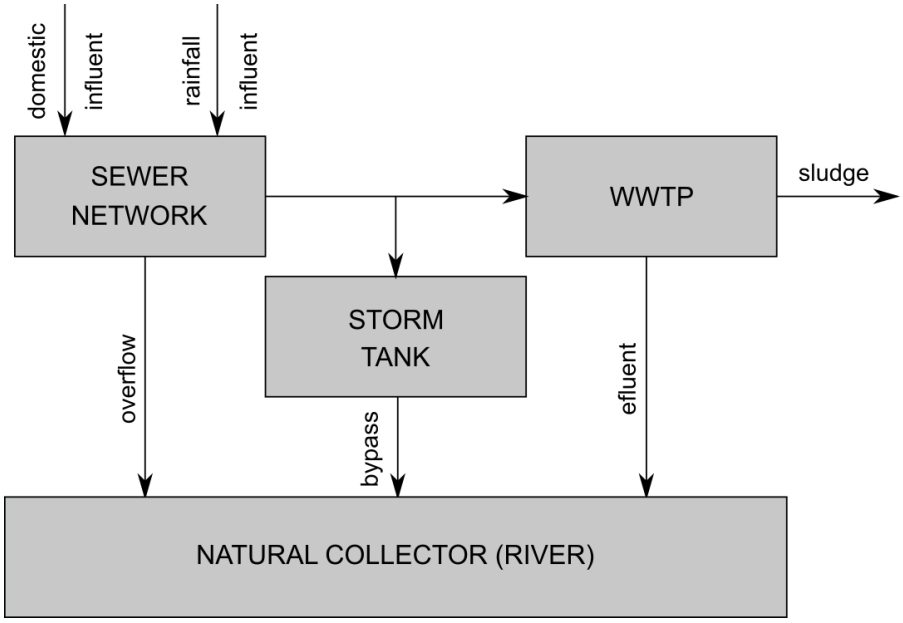


Figure 1.28 – SYNOPSIS integrated model structure

In [175] an integrated SN-WWTP model, using SeweX for the SN and ASM2d [128] for the WWTP, with the objective of being used to investigate the effects of SN chemical dosage (used to control the hydrogen sulfides in the SN) on the WWTP efficiency is proposed. In [176] two benchmark models for SNs (BSMSewer [75]) and WWTPs (BSM2 [133]) are connected in an Integrated Urban Wastewater System (IUWS), aiming at increasing the knowledge about the interaction between the two systems and at studying the influence of the sewer network control strategies on the plant's performances. [177] presents a computationally efficient SN biochemical model that can accurately capture both flow and quality dynamics of the system's effluent, to use in an integrated SN-WWTP model for evaluating optimization strategies.

One distinctive approach is made by an international research team, which proposes an IUWS benchmarking model [178]. The integrated model consists of the following components, all of them describing the flow rates and the principal pollutants (COD, TSS, nitrogen and phosphorus) dynamics:

1. Catchment model – based on BSM2 dynamic influent pollutant disturbance scenario generator [76];
2. SN – the BSMSewer model [75] previously described in section 1.2.1;
3. WWTP – described using ASM2d [128];
4. River Water System – that is using a simplified version of IWA River Water Quality Model no. 1 (RWQM1) [179].

Some scientific papers also address the control of the integrated SN-WWTP system:

1. In [180] a fuzzy-based RTC strategy for the integrated wastewater collecting and treatment system in Wilhelmshaven, Germany is presented. The main two goals of this strategy are reducing the SN overflows and avoiding unwanted situations (hydraulic overflow and

sludge drift) at the WWTP during pluvial events. The RTC system was functional for a year and proved its efficiency.

2. [181] uses a rule-based real-time control of the SN to minimize the overflow volume of the SN, while at the same time the water flow to the WWTP is limited to Q_{max}, the plant's maximum capacity, to prevent activated sludge from washing from the secondary settling tank.
3. [182] proposes, using an integrated model composed of a WWTP modelled with ASM2d [128] and a SN modelled with Infoworks, an intermittent influent control technique (an extension of the equal filling degree control algorithm) to optimize the integrated system by decreasing the SN overflows and sedimentation potential, the WWTP energy consumption and improving the effluent quality.
4. In [183] a multi-point integrated RTC method is used to stabilize the WWTP inflow and reduce SN overflows, under the conditions of SN water flow disturbances. The method is based on discrete dynamic water level variations, which does not require any model of the integrated system.
5. In [184], the problem of reducing the impact of SN overflows on the environment is addressed by using an integrated pollution-based RTC on the SN-WWTP integrated system.

1.5. Chapter conclusions

This chapter presents a state of the art of SN and WWTP modelling and control, to identify research gaps and future research directions that could reduce the effects of wastewater management on public health and the environment, by improving the effectiveness of our wastewater collecting and treatment facilities.

The literature reports for SN modelling, a various number of flow models and quality models, ranging from the discrete simplified ones to the complex ones that can model the majority of processes taking place in the SN, but require more computational effort. Recent research is avoiding the complexity of the mathematical models and uses data-driven models. This type of data-driven model presents good results. Acknowledging the accelerated urbanization and the extreme weather events produced by global warming, the need for the most efficient and performant methods for wastewater transport arises. This could be easily achieved in the design phase of the sewer networks, but for existing sewer networks, upgrading is most times impossible, therefore it is necessary to develop and implement efficient control strategies to reduce the impact on the environment and public health. The literature presents various strategies, structures, and methods to reduce the SN overflow effects by reducing either the overflow volume or the quantity of the pollutants in the overflow. However, this approach can result in heavily polluted small overflows or less pollution but heavy flows that cause floods. This way, the necessity for finding a balance between the quantity and quality of overflow by developing multi-objective optimization control strategies for the SN arises.

For the WWTP modelling, various models, most of them based on the Monod equations, can be found in the literature for modelling aerobic, anaerobic and anoxic biological digestion. Even if WWTPs are considered facilities that emit GHG, only a few papers are approaching these emissions, trying to implement either deterministic or data-driven models. The control strategies for WWTPs are important to assure that the wastewater resulting from human activities is not

negatively impacting public health or the environment. Thus, the literature reports many control strategies which, by manipulating various control variables of the system, such as oxygen transfer coefficients from the aerated tanks, internal and external recirculation flows, or by manipulating, in the top-level control structure, the setpoints of lower-level structure such as dissolved oxygen (DO) concentrations in the aerated tanks or the nitrogen concentration, have the main goal of assuring that the WWTP's effluent is complying with the legal regulations for water to be discharged into the natural receptors in terms of different pollutants loads. A part of these papers is considering, besides keeping the plant's effluent below the legal limit, minimizing the energy consumption of the plant. Even if global warming is an important concern nowadays and considering the effect of GHG emissions on global warming, only a few papers consider GHG emissions when developing control strategies for the wastewater treatment plant.

One of the most important problems related to the WWTPs operation is the uncertainty related to the plant's influent. However, the plant influent is usually the SN effluent, and, therefore, implementing SN control strategies will help on gaining control over the WWTP influent. Besides this, when implementing SN control strategies, the treatment capacity of the WWTP should be considered because an overflow reduction of the SN can be achieved by overloading the WWTP, a situation in which the pollution generated by the overloaded WWTP can overcome the decreased pollution of the SN. This leads us to the conclusion that the control of these two systems should be addressed together in an integrated way. In the literature, the subject of integrated wastewater systems (SN + WWTP) can be found only in a few papers, most of them focusing only on modelling the integrated system.

In conclusion, wastewater management is an important field and there is a place for lots of improvements that could help to reduce its effects on public health and the environment. When implementing SN and WWTP models and control strategies, the modern world problems should be considered: water quality, cost consumption, global warming, extreme pluvial events, floods, GHG emissions of WWTPs etc. Acknowledging this, the main goal of the next chapters is to develop optimal control strategies for the integrated system composed of a SN and a WWTP aiming at minimizing the overall pollution generated by the integrated system considering, at the same time, minimizing the operational cost and the GHG emissions of the WWTP.

Chapter 2. Modelling of Wastewater Collecting and Treatment Systems

2.1. Introduction

The quick development of human communities, alongside with the stress posed by the current world challenges (such as global warming, climate change, water scarcity etc.) impose the development of complex control strategies for wastewater collecting and treatment systems. However, for such control strategies to be implemented, there is a need for tools for digital simulation and analysis of these systems. In this context, this chapter of the PhD thesis presents the development of a series of models for both subsystems, SN and WWTP, but also for the whole IUWS.

Consequently, the rest of this chapter is subdivided into four more subchapters. Subchapter 2.2 presents the development of a SN model fitted for a mid-sized population city (250,000 inhabitants divided into five collecting areas) alongside the definition of an influent scenario spanning for 28 days, both of them aiming to be used for evaluating the performance of the SN control strategies that will be presented in subchapter 3.2. Moreover, to solve integration time issues when using the developed model in online control applications, a simplified version of it is developed by keeping only the flow components of the model. As one of the main challenges regarding WWTP model-based control is represented by the high complexity models that are available in the literature, leading to high numerical integration time, the subchapter 2.3 presents NN models aiming at fitting WWTP dynamics: system states, process values, but also effluent variables that are involved in calculating the EQI.

Subchapter 2.4 shows the development of IUWS models, presenting two approaches. In the first approach a simple SN model developed in BSMSewer is coupled with a previously developed WWTP model, while in the second approach, the SN model developed in the subchapter 2.2 is coupled with the BSM2G model, both of them requiring the definition of a coupling unit in order to make the variable conversion imposed by the two sub-models. The second IUWS model is intended to be used in the next chapter aiming to improve the performance of the integrated system. In this context, at the end of this subchapter, a methodology for assessing the performance of control strategies is defined in terms of both subsystems' performance indicators. The last subchapter is dedicated to the conclusions of this chapter.

2.2. Sewer Network modelling

Usually, a SN consists of storage tanks and piping connected in a given topology. Aiming at having a SN model to be used for optimal control strategies developing, testing and evaluating,

the structure presented in Figure 2.1 has been considered and implemented in BSMSewer software package [75].

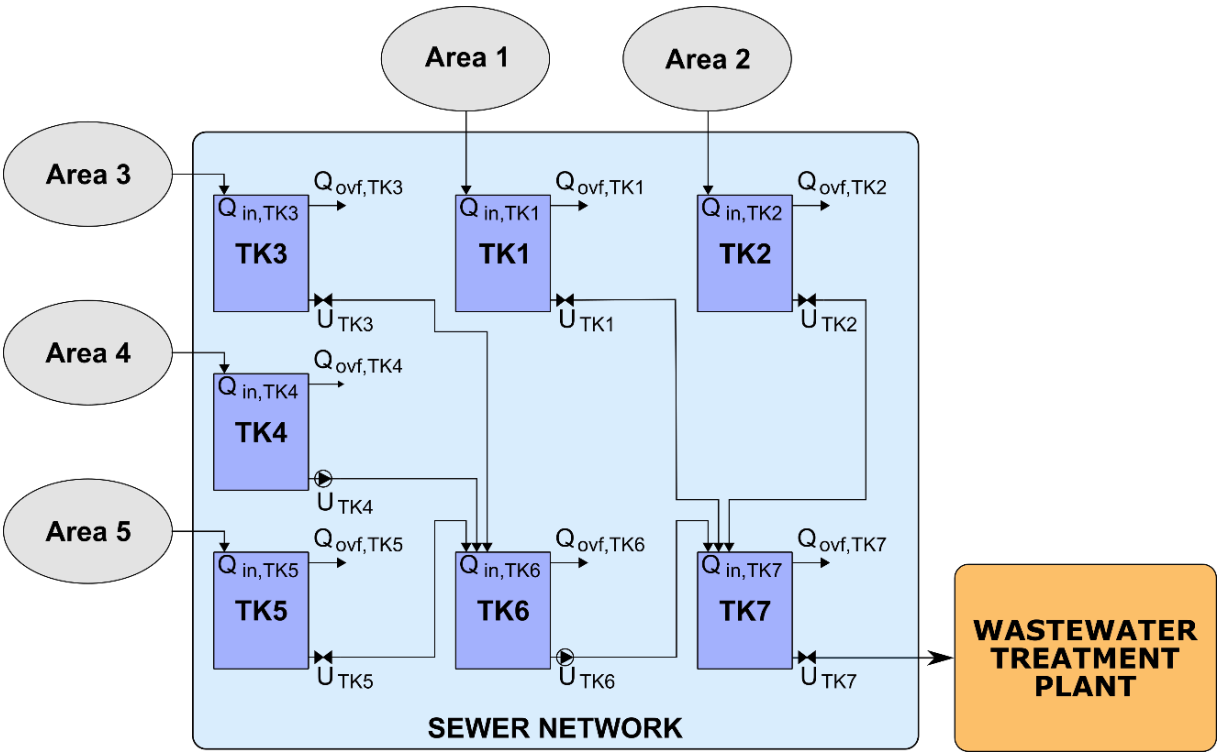


Figure 2.1 – The SN structure

The considered SN model [185] consists of 7 storage tanks that are related to 5 wastewater collecting areas, serving a medium-sized city with around 250,000 inhabitants. Each storage tank, TKi, has one input: $Q_{in,TKi}$ (the tank inflow) and two outputs: $Q_{out,TKi}$ (the tank outflow) and $Q_{ovf,TKi}$ (the tank overflow). Thus, in the considered configuration, the inflow of the first 5 storage tanks is represented by the wastewater collected from the 5 areas, the inflow of $TK6$ is the sum of the outflows of $TK3$, $TK4$ and $TK5$, while the inflow of $TK7$ is the sum of the outflows of $TK1$, $TK2$ and $TK6$. The outflow of $TK7$ is the effluent of the SN, which is in fact the influent of the WWTP.

The outflow of $TK4$ and $TK6$ is controlled by using pumps to evacuate wastewater from these storage tanks. Each of the pumps is subject to a control action $U_{TK4} \in [0,1]$ and $U_{TK6} \in [0,1]$, which are representing the pumping capacity percentage that is used from the maximum pump flow. For the other 5 tanks, the wastewater is gravitationally evacuated through an outlet valve, whose opening can be controlled by $U_{TKi} \in [0,1]$ representing its percentual opening.

2.2.1. The collecting areas

As mentioned before, the SN serves a mid-sized city that is divided in 5 wastewater collecting areas. Each of them is described by the number of inhabitants living in that area (pe_i) and the area's total surface (S_i) as presented in Table 2.1.

Table 2.1 – The collecting areas characteristics

Collecting area number	Population equivalent (pe_i) [p.e.]	Area surface (S_i) [km^2]
1	75000	25
2	50000	50
3	40000	60
4	60000	75
5	25000	35

It should be noted that area no. 5 serves the industrial part of the city, and, therefore, besides the wastewater collected from the inhabitants, it includes flow and loads that are industry specific.

2.2.2. The Sewer Network characteristics

As each of the storage tanks inflow source is different (5 of the tanks inflows are represented by the wastewater collected from the above described collecting areas which have different characteristics and the other 2 tanks inflows are represented by outflows of some other storage tanks), they should have different characteristics. Thus, for each of the storage tanks, the following characteristics have been considered:

1. The tank volume (V_i):
   a. for the tanks that are directly serving a collecting area, a volume of 0.05 m^3 for each inhabitant of that area has been considered. For the storage tank related to the 5th collecting area that includes the industrial part of the city, an additional capacity of 2500 m^3 has been added, having the same value as the average industrial wastewater production per day ($Q_{ind} = 2500\ m^3/day$).
   b. for the tanks that are not directly serving a collecting area, 0.05 m^3 for each of the average number of inhabitants served by the tanks whose outflow is included in the tank inflow has been considered.
2. The tank maximum outflow ($Q_{max,i}$):
   a. for the tanks that use pumps for evacuating wastewater, a constant value representing the maximum pump flow has been considered.
   b. for the tanks that evacuate water gravitationally, a maximum flow 3 times higher than the average wastewater production ($Q_{pe} = 0.15\ m^3/(day \cdot inhabitant)$ [75]) of the population directly or indirectly served by the tank has been considered.

Using the previously described procedure, resulted in the characteristics presented in Table 2.2.

Besides the storage tanks, the SN model accounts also for the wastewater transport through pipes. Thus, for the transport component of the model, the following assumptions have been made:

1. the wastewater reaches from one household to the corresponding storage tank in 15 minutes.
2. 25% of the TSS can accumulate in the piping, but not more than 1000 kg/km^2. The accumulated TSS will be flushed away only when the flow through the pipe exceeds a

threshold equal to 8 times the average domestic wastewater flow of the collecting area [75]. This could happen, for example, during heavy pluviometric events.

Table 2.2 – The SN tanks characteristics

Tank number	Tank volume (V_i) [m^3]	Tank maximum outflow ($Q_{max,i}$) [m^3/day]
1	3750	33750
2	2500	22500
3	2000	18000
4	3000	15000
5	3750	18750
6	2083	25000
7	2500	112500

2.2.3. The influent of the Sewer Network

As the SN serves 5 collecting areas, the influent of the SN is composed of 5 influents related to the 5 areas. Each of them is composed of two components: a domestic and a pluviometric component. In addition, the 5th collecting area includes an industrial component. Each of the components is described by the wastewater flow (m^3/day) and the pollutant loads (kg/day):

1. Particulate Chemical Oxygen Demand (COD_{part});
2. Soluble Chemical Oxygen Demand (COD_{sol});
3. Ammonia (NH_4^+);
4. Phosphate (PO_4^{3-}).

2.2.3.1. The forecasted influent

Because developing optimal control strategies requires the availability of a future influent prediction, a forecasted influent having a time span of 28 days was generated, considering the following procedure:

1. the domestic component is calculated using the average wastewater flow/loads per inhabitant multiplied by the population equivalent of the area as described in [75]. The obtained values are further adjusted with:
   a. a daily profile – accounting for daily variations related to human activities (decreased values during the night and the afternoon and increased values in the morning and in the evening) as presented in Figure 2.2 (a).
   b. a weekly profile – accounting for weekly variations related to human activities (decreased values during the weekends) as presented in Figure 2.2 (b).
   c. a yearly profile – accounting for reduced wastewater production during holydays as presented in Figure 2.2 (c).
2. the pluviometric component accounts only for flow and is calculated using a weather forecast adjusted with the collecting area surface. If Q_{event} $[m^3/day]$ represents the forecasted pluvial flow over the entire city, then the flow of the pluviometric component of the *ith* collecting area will be:

$$Q_{pluviometric,i} = Q_{event} \cdot \frac{S_i}{\sum_{k=1}^{5} S_k} \tag{2.1}$$

3. the industrial component is considered to have loads specific to a mid-sized brewery [186] and an average daily flow $Q_{ind} = 2500\, m^3/day$. These values are further adjusted with the profiles presented in Figure 2.2 (d) and (e):
   a. a weekly profile – accounting for weekly variations related to human activities (increased values on Friday afternoon – weekly cleaning and decreased values during the weekends).
   b. a yearly profile – accounting for reduced wastewater production during holidays.

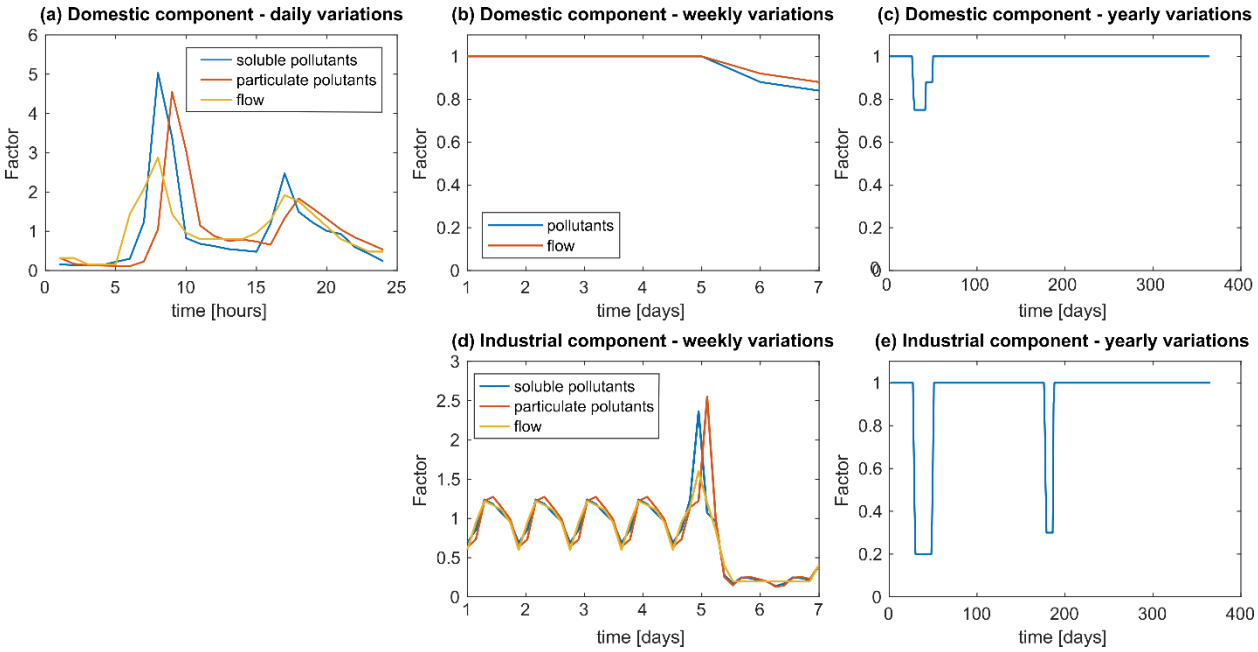


Figure 2.2 – Variation profile for the domestic and industrial components (a) daily profile of the domestic component; (b) weekly profile of the domestic component; (c) yearly profile of the domestic component – starting with the first week of July and having the same profile for pollutants and flow; (d) weekly profile of the industrial component; (e) yearly profile of the industrial component – starting with the first week of July and having the same profile for pollutants and flow

For generating the influent using the above presented procedure, two pluviometric events were considered: a rain event and a storm event. The next two tables show the average loads and flows and the average concentrations of each collecting areas influent.

Table 2.3 – The average loads and flow of the forecasted influent

Area number	COD_{part} [kg/day]	COD_{so} [kg/day]	NH_4^+ [kg/day]	PO_4^{3-} [kg/day]	Flow [m³/day]
1	5789.84	1031.10	312.72	80.10	9696.84
2	3859.89	687.40	208.48	53.40	6589.61
3	3087.91	549.92	166.78	42.72	5346.71
4	4631.87	824.88	250.18	64.08	7963.80
5	2233.68	2839.40	154.15	66.63	5282.22

Table 2.4 – The average loads concentrations of the forecasted influent

Area number	COD_{part} [g/m^3]	COD_{sol} [g/m^3]	NH_4^+ [g/m^3]	PO_4^{3-} [g/m^3]
1	597.1	106.3	32.2	8.3
2	585.8	104.3	31.6	8.1
3	577.5	102.9	31.2	8.0
4	581.6	103.6	31.4	8.0
5	422.9	537.5	29.2	12.6

The figures 2.3 – 2.7 present the evolution of the flow and loads of the generated forecasted influent for each of the five collecting areas.

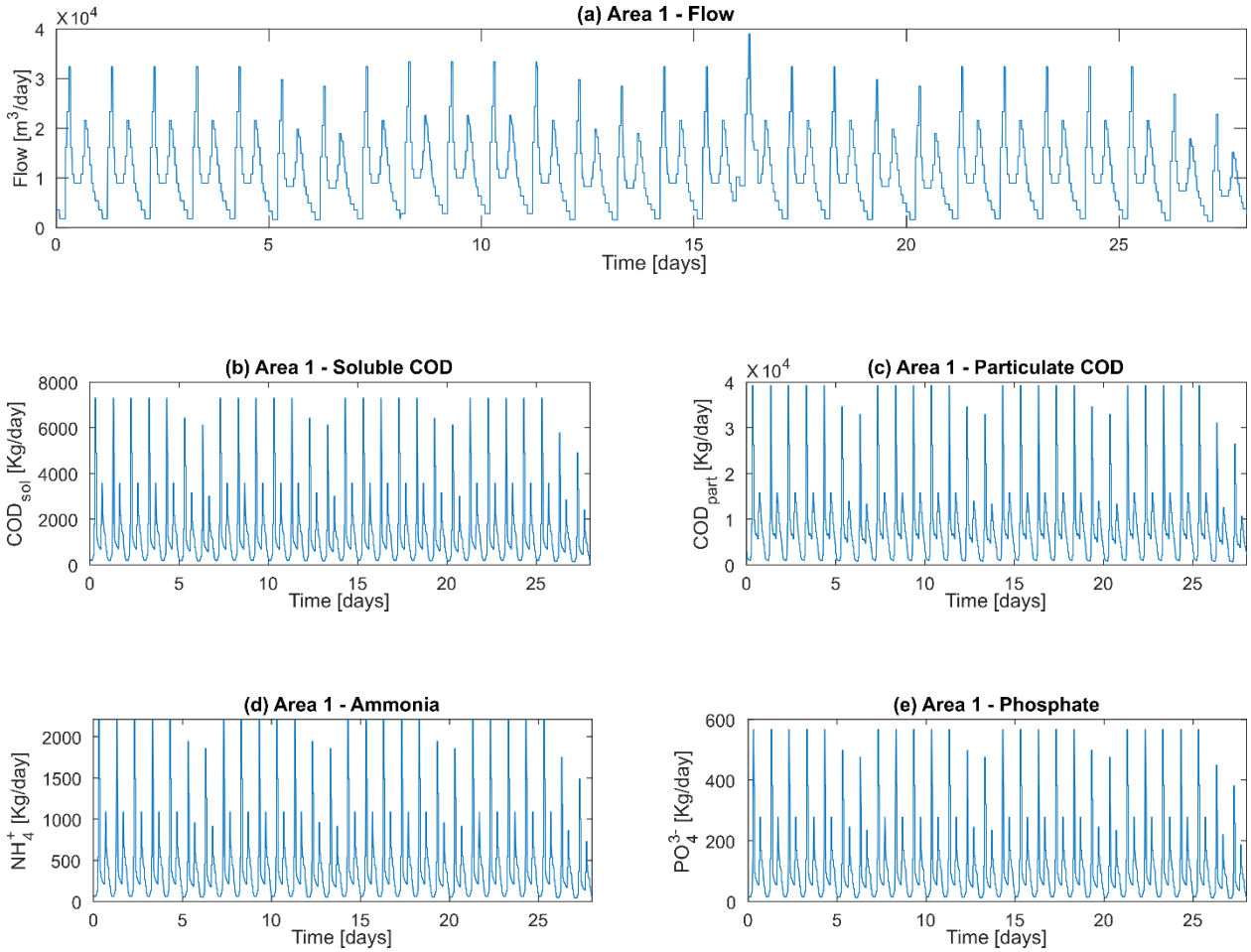


Figure 2.3 – Area 1 influent evolution
(a) Flow; (b) Soluble COD; (c) Particulate COD; (d) Ammonia; (e) Phosphate

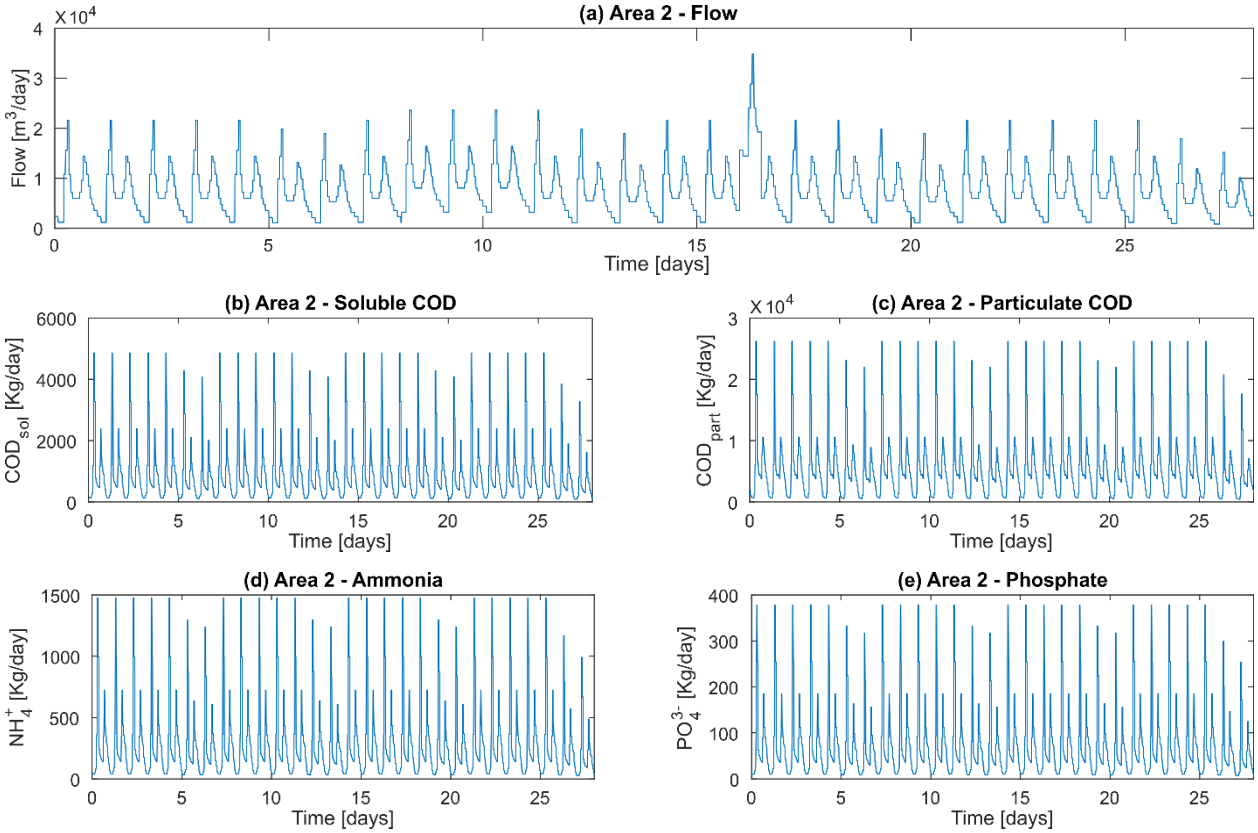


Figure 2.4 – Area 2 influent evolution
(a) Flow; (b) Soluble COD; (c) Particulate COD; (d) Ammonia; (e) Phosphate

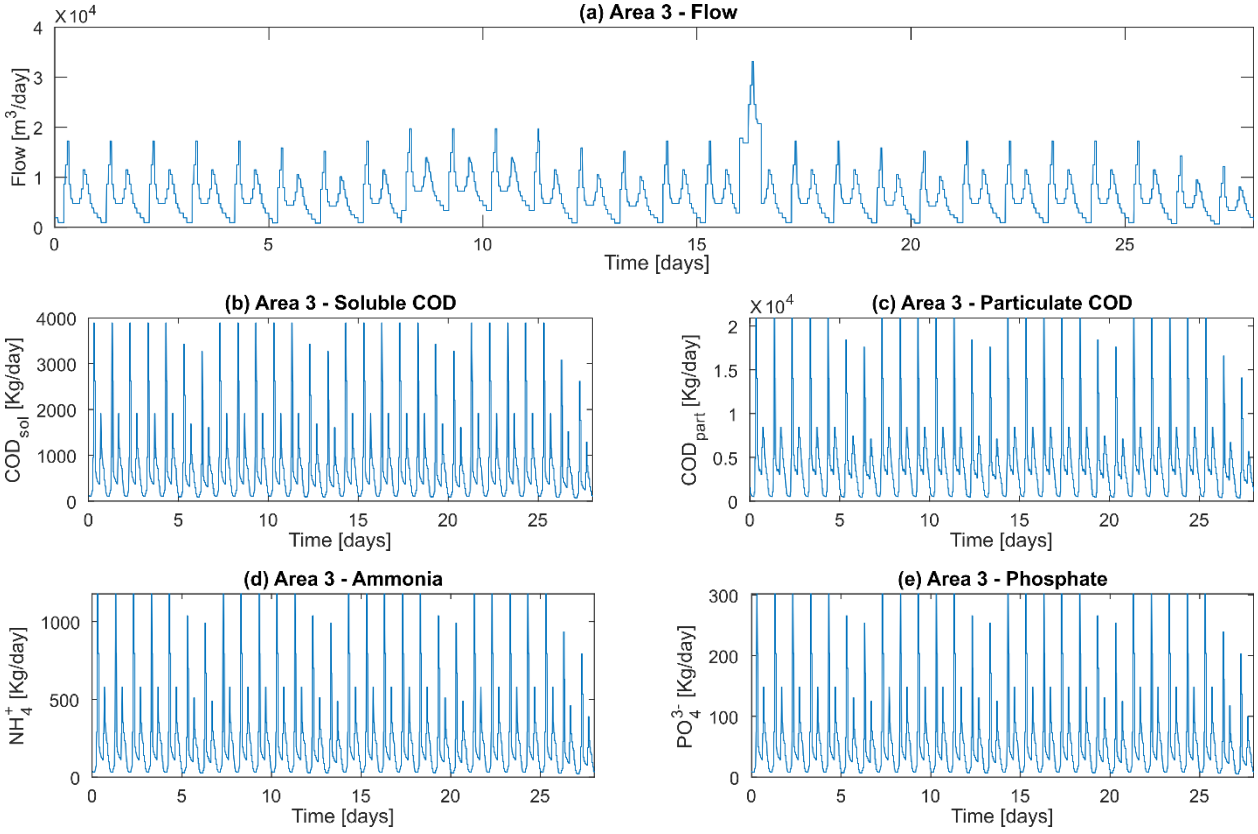


Figure 2.5 – Area 3 influent evolution
(a) Flow; (b) Soluble COD; (c) Particulate COD; (d) Ammonia; (e) Phosphate

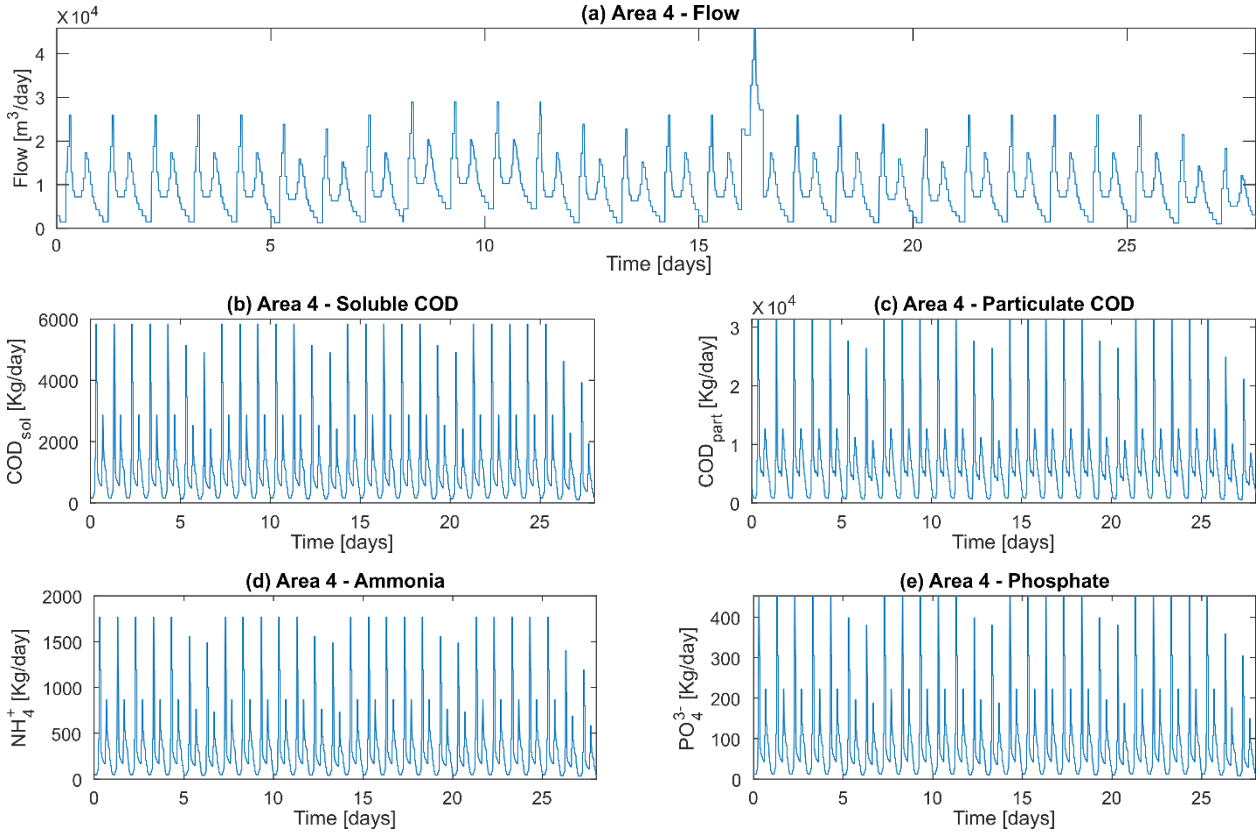


Figure 2.6 – Area 4 influent evolution
(a) Flow; (b) Soluble COD; (c) Particulate COD; (d) Ammonia; (e) Phosphate

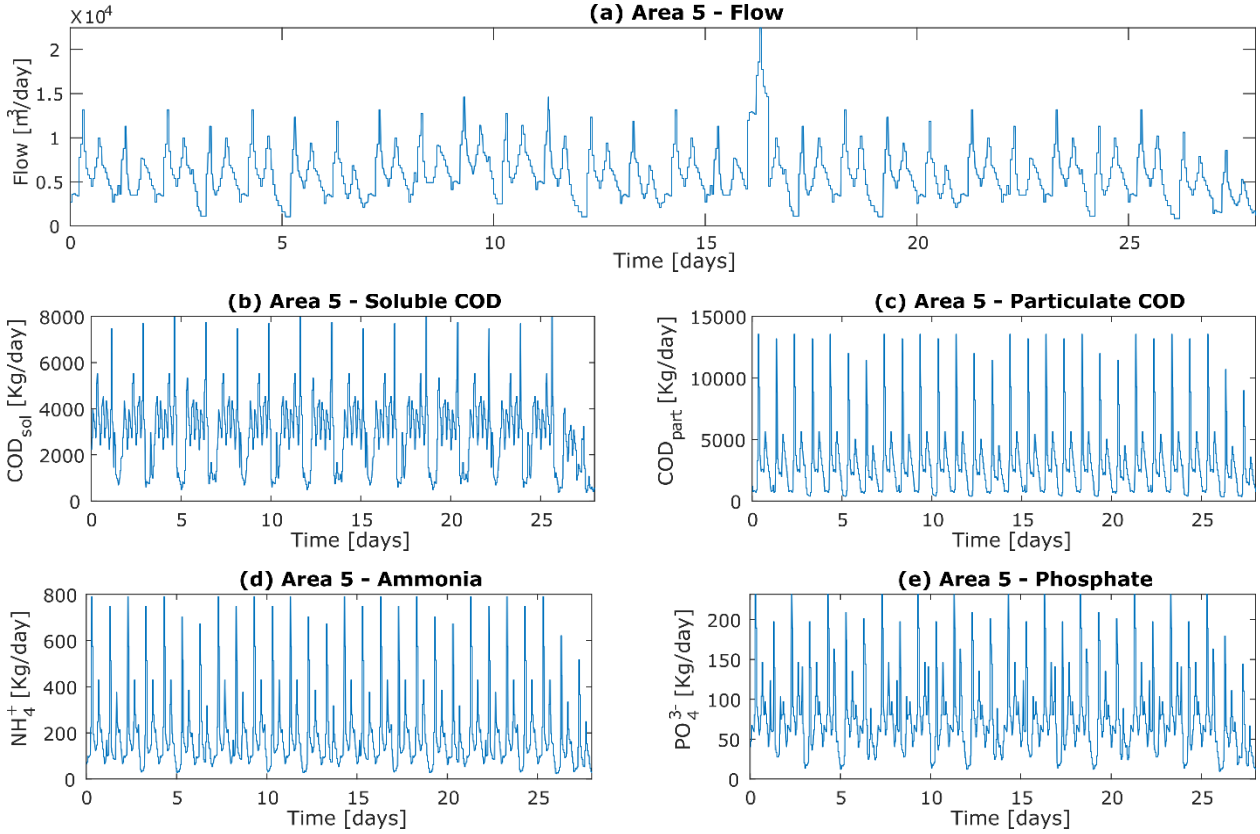


Figure 2.7 – Area 5 influent evolution
(a) Flow; (b) Soluble COD; (c) Particulate COD; (d) Ammonia; (e) Phosphate

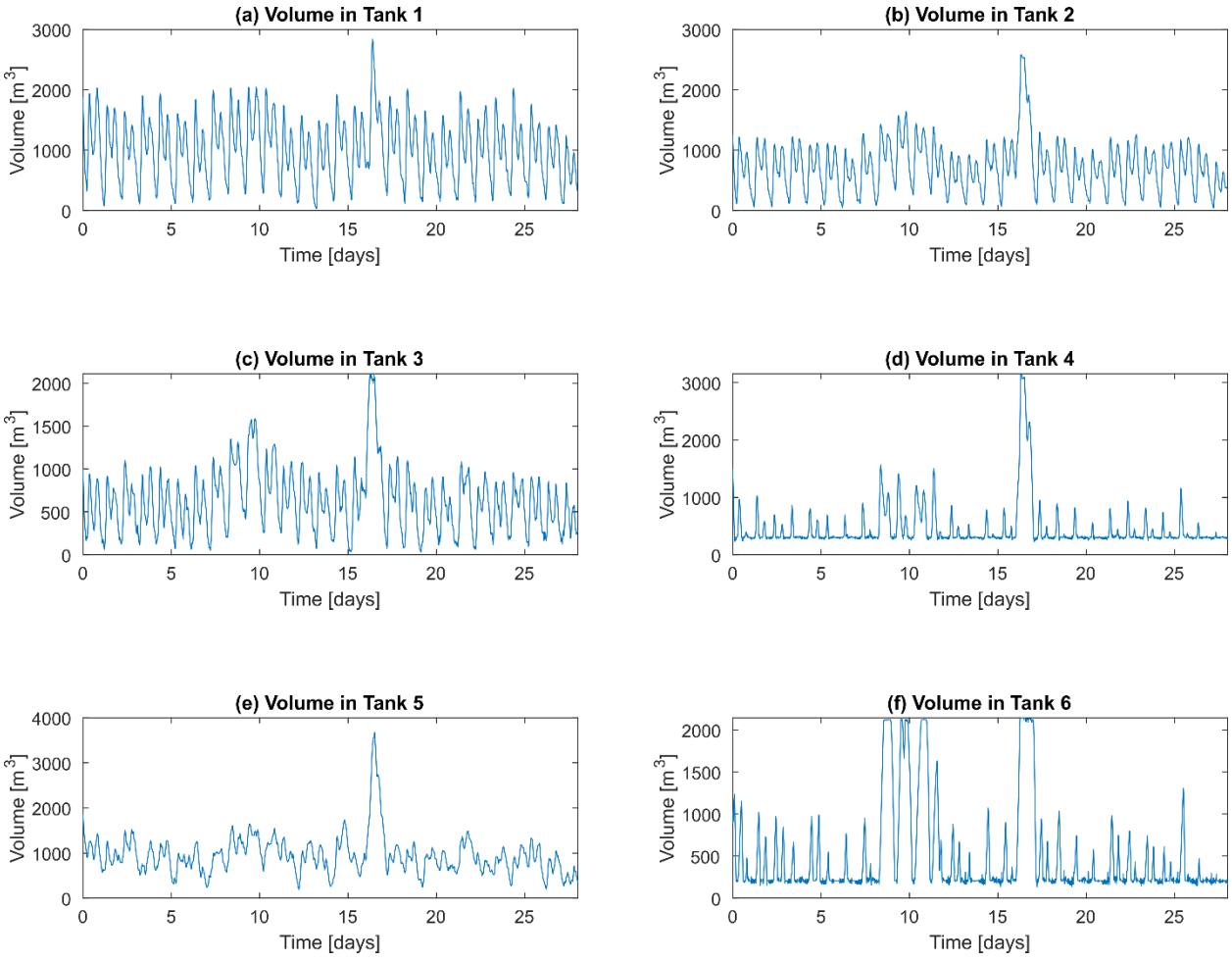
2.2.3.2. The disturbed influent

As a forecasted influent cannot be 100% accurate, deviations of each component being possible, a disturbed influent should be considered when testing optimal control strategies. For this reason, a disturbed influent scenario was generated based on the forecasted influent by adding:

1. a random number from a Gaussian distribution with 0 mean and a standard deviation equal to $0.2 \cdot pe_i \cdot Q_{pe}$ to the domestic component flow of each collecting area at each hour.
2. a random number from a Gaussian distribution with 0 mean and a standard deviation equal to $0.2 \cdot Q_{ind}$ to the industrial component flow at each hour.

2.2.4. The model simulation

The model, implemented in BSMSewer software package, has been simulated for 28 days using the disturbed influent presented in the previous section, without considering any control actions for the storage tanks output pumps / valves (all pumps running at 100% when wastewater level in the tank is above 0.5 meters and all valves fully open – base case). Figure 2.8 shows the evolution of the quantity (volume) of wastewater in each of the storage tanks, while Figure 2.9 shows the tanks overflows.



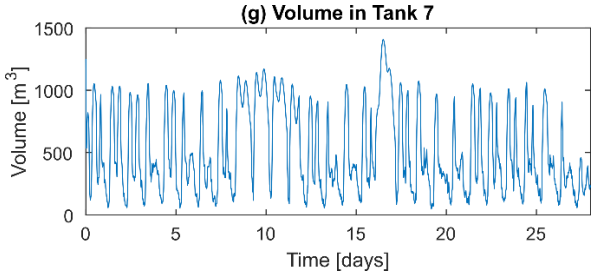


Figure 2.8 – Wastewater volume evolution in Sewer Network tanks – "no control"
(a) TK1; (b) TK2; (c) TK3; (d) TK4; (e) TK5; (f) TK6; (g) TK7

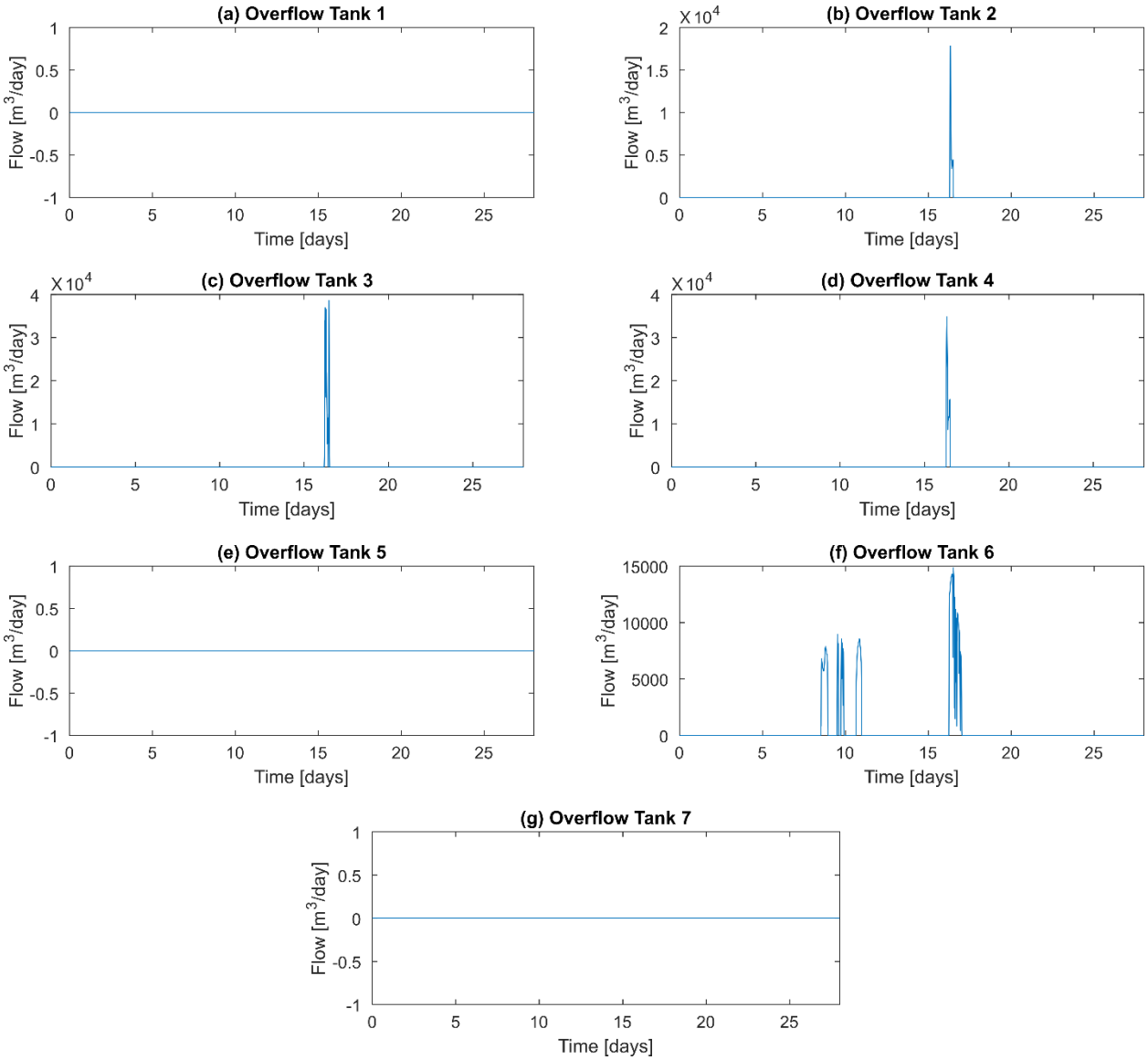


Figure 2.9 – Wastewater overflow from Sewer Network tanks – "no control"
(a) TK1; (b) TK2; (c) TK3; (d) TK4; (e) TK5; (f) TK6; (g) TK7

Figure 2.9 shows that the storage tanks 1, 5 and 7 are not overflowing, while the storage tanks 2, 3 and 4 are overflowing during the storm event. The tank 6 is overflowing during both events (rain and storm). Further, the 10 performance indicators defined by BSMSewer [75] and presented in Table 1.3 were calculated for each tank individually and globally for the whole SN, resulting the values from Table 2.5.

Table 2.5 – Performance indicators values calculated in the "no control" case

Tank number	1	2	3	4	5	6	7	global
N_{ovf} $[events/year]$	0	13	13	13	0	65	0	65
T_{ovf} $[days/year]$	0	3	4	3	0	21	0	22
V_{ovf} $[m^3/year]$	0	22735	48127	54359	0	189915	0	315137
OQI $[kg-polluting\ units/day]$	0	192	828	1185	0	3068	0	5273
$C_{max,TSS}$ $[g\ COD/m^3]$	0	402.1	1273	1245	0	1132	0	1273
$C_{max,TKN}$ $[g\ N/m^3]$	0	46.7	89.3	87.5	0	77.3	0	89.3
$C_{max,PO4}$ $[g\ P/m^3]$	0	6.7	5.9	6	0	9.7	0	9.7
$T_{exc,TSS}$ $[days/year]$	0	2.9	3.4	2.9	0	21	0	21.5
$T_{exc,TKN}$ $[days/year]$	0	3	3.8	3	0	21.5	0	21.9
$T_{exc,PO4}$ $[days/year]$	0	3	3.3	3	0	21.5	0	21.5

As observed, the tank no. 6 overflow has the biggest contribution to the SN global performance in terms of quantity of wastewater overflowed and quantity of pollutants in that wastewater. Thus, it is worth checking if keeping wastewater for a longer time in the upstream tanks has any effect on the SN performance. For this reason, a new simulation has been run in the same conditions but considering the outlet valve of $TK3$ to be only 70% open ($U_{TK3} = 0.7$). The same performance indicators were calculated obtaining the values from Table 2.6.

Table 2.6 – Performance indicators values calculated in the case $U_{TK3} = 0.7$

Tank number	1	2	3	4	5	6	7	global
N_{ovf} $[events/year]$	0	13	65	13	0	65	0	78
T_{ovf} $[days/year]$	0	3	14	3	0	17	0	25
V_{ovf} $[m^3/year]$	0	22724	96209	54423	0	125273	0	298630
OQI $[g-polluting\ units/day]$	0	192	1384	1186	0	2161	0	4923
$C_{max,TSS}$ $[g\ COD/m^3]$	0	402.1	1276	1245	0	1118	0	1276
$C_{max,TKN}$ $[g\ N/m^3]$	0	46.7	89.8	87.5	0	77	0	89.8
$C_{max,PO4}$ $[g\ P/m^3]$	0	6.7	9.3	6	0	8.8	0	9.3

$T_{exc,TSS}$ $[days/year]$	0	2.9	13.7	2.9	0	17.1	0	24.7
$T_{exc,TKN}$ $[days/year]$	0	3	14.1	3	0	17.1	0	25.1
$T_{exc,PO4}$ $[days/year]$	0	3	14.1	3	0	17.1	0	25.1

It can be observed, the global V_{ovf} and the global OQI have decreased by approximately 5–6 % when the $TK3$ outlet valve has been kept at 70% open. Further, the simulation has been repeated considering, this time, the outlet valve of $TK3$ to be only 70% open ($U_{TK3} = 0.7$) and the pump used to evacuate wastewater from $TK4$ to be running at 70% ($U_{TK4} = 0.7$), resulting in the performance indicators values presented in Table 2.7.

Table 2.7 – Performance indicators values calculated in the case $U_{TK3} = 0.7$ and $U_{TK4} = 0.7$

Tank number	1	2	3	4	5	6	7	global
N_{ovf} $[events/year]$	0	13	65	13	0	52	0	65
T_{ovf} $[days/year]$	0	3	14	3	0	15	0	24
V_{ovf} $[m^3/year]$	0	22724	96207	54581	0	103203	0	276741
OQI $[kg - polluting\ units/day]$	0	192	1383	1187	0	1854	0	4615
$C_{max,TSS}$ $[g\ COD/m^3]$	0	402.1	1276	1245	0	1123	0	1276.3
$C_{max,TKN}$ $[g\ N/m^3]$	0	46.7	89.8	87.5	0	77.2	0	89.8
$C_{max,PO4}$ $[g\ P/m^3]$	0	6.7	9.3	6	0	8.8	0	9.3
$T_{exc,TSS}$ $[days/year]$	0	2.9	13.7	2.9	0	15.1	0	23.9
$T_{exc,TKN}$ $[days/year]$	0	3	14.1	3	0	15.1	0	24.3
$T_{exc,PO4}$ $[days/year]$	0	3	14.1	3	0	15.1	0	24.3

It can be observed that this time the global V_{ovf} decreased by 13% and the global OQI decreased by 12%. On the other hand, the global duration of overflows and the global number of overflows are approximatively the same as in the “no control” case.

Concluding, the values of the performance indicators of the storage tanks whose output control was modified have been increased, while the $TK6$ indicators have been decreased, this having a positive effect on some of the global performance indicators (less volume of overflow and a smaller quantity of pollutants in the overflowed water) and a negative effect on other indicator (total time of overflow). This could be seen as a positive effect because instead of having short duration overflows with heavy flow and higher quantity of pollutants, there are longer overflow events with a lighter flow and a smaller quantity of pollutant. Consequently, it has been proven that there are storage tank outlet controls combinations that could provide a better

performance of the SN than the case when everything is running at 100% resulting the need for optimal control of the SN to find the optimal control combination.

On the other hand, implementing real-time optimal control of the SN will require numerical integration of the model multiple times in a short time interval. However, it has been observed that the integration of the implemented model over the 28 days horizon takes around 30 seconds when using a mid-range computer (Intel® Core™ i5-6200U CPU @ 2.30GHz with 8GB of RAM). This could pose a problem when the number of numerical integrations of the model is high during the optimization procedure resulting the need for a simplified model. In the following section, a simplified model has been implemented by keeping only the flow part of the model, the consequence being a decrease of the numerical integration time to 3 seconds for the same time horizon.

2.2.5. The simplified model

In BSMsewer, the mathematical model of the SN contains three components: the transport component, the flushing component and the storage component, each of them considering the wastewater flow and its loads (soluble and particulate chemical oxygen demand, ammonia and phosphate concentrations).

The transport component of BSMsewer models the flow and the pollutant transport within the SN as a completely mixed tank by using mass balance equations. In the simplified model the transport component will consider only the wastewater flow, therefore it will have only one state: the water volume in the transport component (V_T), which will change based on the inflow ($Q_{in,T}$) and outflow ($Q_{out,T}$) according to Figure 2.10 and the mass balance equation (2.2).

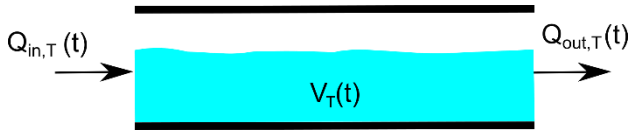


Figure 2.10 – Water flowing in a pipe

$$\frac{dV_T}{dt} = Q_{in,T} - Q_{out,T} \tag{2.2}$$

The outflow of the transport component is proportional to the water volume (V_T) scaled by a residence time constant (K_T):

$$Q_{out,T} = \frac{1}{K_T} \cdot V_T \tag{2.3}$$

The flushing component models the accumulation of the sediments in the network during the dry regime and their flushing when the influent flow exceeds a certain limit. Because it has an effect only on the pollutant's quantities, having no effect on the wastewater flow, this component has been removed in the simplified model.

The storage component models the storage tanks of the network. BSMsewer provides four different types of tank configuration: online passthrough, online bypass, offline passthrough and offline bypass [75]. As the architecture of the network contains only two of these four types (online

and offline passthrough), only these two will be integrated in the simplified model after removing all states and dynamics related to the pollutant's storage.

Thus, each storage tank will have only one state: the liquid level in it (h_{TKi}) whose dynamics will depend on the inflow ($Q_{in,TKi}$), the outflow ($Q_{out,TKi}$), the overflow ($Q_{ovf,TKi}$) according to Figure 2.11 and the mass balance equation (2.4):

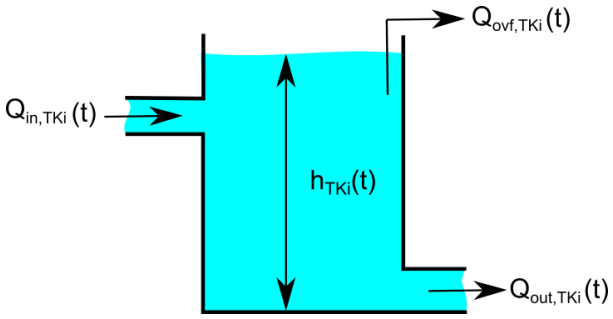


Figure 2.11 – Storage tank with overflow capability

$$\frac{dh_{TKi}}{dt} = \frac{1}{A_{TKi}}\left(Q_{in,TKi} - Q_{out,TKi} - Q_{ovf,TKi}\right) \tag{2.4}$$

The inflow of each tank is represented by the outflow of the corresponding transport component. The outflow of each tank depends on the tank type. Therefore, in the case of the offline passthrough tanks, as the wastewater is evacuated by using a pump, the outflow will be directly proportional to the pump flow ($Q_{pump,TKi}$). The command given to the tank ($U_{TKi} \in [0,1]$) satisfies the constraint that the pump will be running only if the wastewater level in tank is above a low limit (0.5 m) and with a 0.1 m hysteresis around this limit:

$$Q_{out,TKi} = U_{TKi} \cdot Q_{pump,TKi} \tag{2.5}$$

For the online passthrough tanks, the wastewater is evacuated gravitationally through a valve whose opening can be controlled ($U_{TKi} \in [0,1]$), and, consequently, the outflow depends on the maximum possible outflow of the tank ($Q_{max,TKi}$ – the outflow when the tank is full), the water level in tank ($h_{TKi} = V_{TKi}/A_{TKi}$), the minimum level in tank ($h_{min,TKi}$) and the level $h_{o,TKi}$ that determines $Q_{out,TKi} = Q_{max,TKi}/2$:

$$Q_{out,TKi} = U_{TKi} \cdot Q_{max,TKi} \cdot \frac{h_{TKi} - h_{min,TKi}}{h_{o,TKi} + h_{TKi} - h_{min,TKi}} \tag{2.6}$$

The tank overflow occurs if the wastewater level in tank exceeds a certain limit ($h_{ovf,TKi}$) and depends on the characteristics of the overflow weir (weir constant – $C_{weir,TKi}$ and weir length – $L_{weir,TKi}$) and on the wastewater level in tank:

$$Q_{ovf,TKi} = C_{weir,TKi} \cdot L_{weir,TKi} \cdot \left(h_{TKi} - h_{ovf,TKi}\right)^{1.5} \tag{2.7}$$

The implementation of the simplified model in Simulink considered the possibility to run the model multiple times in parallel. Therefore, all configuration variables, all input variables, all control inputs and all output variables have been packed in data structures that could be separately passed to each of the simulations. All the initial states can be set to any desired value

and all the input vectors containing data varying in time have been augmented with specific timestamps making possible to integrate the model for any specific interval $[t_x, t_y]$.

The possibility to run the model multiple times in parallel has a series of advantages. One of them is that the metaheuristic optimization could be solved in a reduced time, as it requires integrating the model many times, which could be made in parallel. However, the decision to use parallel computation or not should be taken after analyzing some factors regarding the used computational machine and the MATLAB Parallel Computing Toolbox. This is because the MATLAB Parallel Computing Toolbox takes some extra time to load and clean the parallel pool that must be compensated by the parallel computing time reduction. Therefore, the PC running the optimization should have enough CPU cores for parallel computing, so the reduction of the optimization time is higher than the delays added by the MATLAB Parallel Computing Toolbox.

As the simplified model accounts only the wastewater flow through the network, only three of the ten performance indicators defined for BSMsewer can be calculated for each storage tank of sewer network, but also globally for the whole network:

- N_{ovf} $[events/year]$ – yearly overflow frequency
- T_{ovf} $[days/year]$ – yearly overflow duration
- V_{ovf} $[m^3/year]$ – yearly overflow volume

2.3. Wastewater Treatment Plant modelling

As one of the current challenges related to WWTP model-based control is represented by the numerical integration time of the complex plant models that are available in literature, this subchapter aims to use NNs to model various dynamics of such facilities in three approaches: 1. using a MLP network to estimate the state variables of a simple WWTP, 2. using LSTM networks to estimate a process variable based on easily measurable values and 3. using LSTM networks to estimate WWTP effluent variables based on the influent and aeration rates.

2.3.1. Neural Network modelling

As the mathematical models of WWTPs are usually complex, their integration time is high enough to make them unfeasible to be used in real-time control of such facilities. For this reason, the current section is dedicated to developing two NN models based on data obtained with the simplified 4th order mathematical model presented in Figure 2.12 [187]. In the next chapter, these models will be used in a MPC strategy.

The considered WWTP mathematical model [188] is composed of two units: an aerated bioreactor that is used for organic carbon removal, and a clarifier that is used to separate the sludge from the effluent. It considers the following assumptions:

1. The inflow, respectively outflow dilution rates are equal (D), thus the volume of wastewater in the WWTP remains constant.
2. The dilution rate of the recirculated sludge is proportional to D with a constant value r (recirculating rate).

3. The dilution rate of the excess sludge is proportional to D with a constant value β (excess sludge rate).
4. There is no dissolved oxygen, nor substrate in the recirculated sludge flow.
5. The aerated bioreactor outflow dilution rate is equal to the sum of the dilutions of the WWTP (D) and of the recirculated sludge ($r \cdot D$).

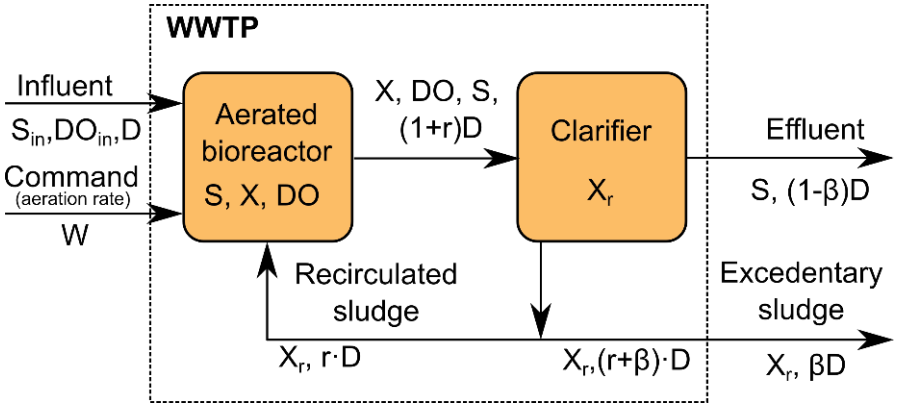


Figure 2.12 – The structure of the simplified 4th order WWTP model

Having the previously mentioned assumptions, and considering the WWTP structure presented in Figure 2.12, the process dynamics are described by the following differential equations [188]:

$$\frac{dX}{dt} = \mu(t) \cdot X(t) - D(t) \cdot (1 + r) \cdot X(t) + r \cdot D(t) \cdot X_r(t) \tag{2.8}$$

$$\frac{dS}{dt} = \frac{\mu(t)}{Y} \cdot X(t) - D(t) \cdot (1 + r) \cdot S(t) + D(t) \cdot S_{in}(t) \tag{2.9}$$

$$\frac{dDO}{dt} = -\frac{(1 - Y) \cdot \mu(t) \cdot X(t)}{Y} \cdot 10^3 - D(t) \cdot (1 + r) \cdot DO(t) + 60 \cdot \alpha \cdot W(t) \cdot \left(DO_{sat} - DO(t)\right) + D(t) \cdot DO_{in} \tag{2.10}$$

$$\frac{dX_r}{dt} = D_s(t) \cdot (1 + r) \cdot X(t) - D_s(t) \cdot (\beta + r) \cdot X_r(t) - 0.5 \cdot D_s(t) \cdot (1 + r) \cdot X_r(t) \tag{2.11}$$

where $\mu(t)$ represents the specific growth rate and is described by:

$$\mu(t) = \mu_{max} \cdot \frac{S(t)}{K_s + S(t)} \cdot \frac{DO(t)}{K_{DO} + DO(t)} \tag{2.12}$$

and:

1. The process states:
   a) $X(t)$ – the biomass concentration
   b) $S(t)$ – the substrate concentration
   c) $DO(t)$ – the dissolved oxygen concentration
   d) $X_r(t)$ – the recirculated biomass concentration
2. The influent variables:
   a) $D(t)$ – the dilution rate
   b) $S_{in}(t)$ – the substrate concentration

c) $DO_{in}(t)$ – the DO concentration – considered constant ($DO_{in}(t) = 2\ mg/l$)

3. The control variable:
   a) $W(t)$ – the aeration rate
4. The process constants – described in Table 2.8.
5. Table 2.8

Table 2.8 – The process constants of the simplified 4th order WWTP model

Constant	Description	Value	Unit
μ_{max}	the maximum specific growth rate	0.11	h^{-1}
r	the recirculating rate	1	–
Y	the yield coefficient	0.67	–
K_S	the substrate saturation constant	0.18	g/l
K_{DO}	the dissolved oxygen saturation constant	0.2	g/l
α	the oxygen transfer rate	0.0033	l^{-1}
β	the excess sludge rate	0.2	–
DO_{sat}	the saturation value of the dissolved oxygen	8	mg/l

2.3.1.1. The 1st version of the neural network model

Figure 2.13 shows the training structure that was used for obtaining the 1st version of the NN model. In this NN model version, all 4 process states are considered measurable (X, S, DO and X_r). For this reason, the NN model will estimate the dynamics of these four states ($\hat{X}$, $\hat{S}$, $\widehat{DO}$ and $\widehat{X_r}$), based on data provided at its inputs: influent data (D and S_{in}), aeration command (W) and the four output variables that were estimated in the previous time step.

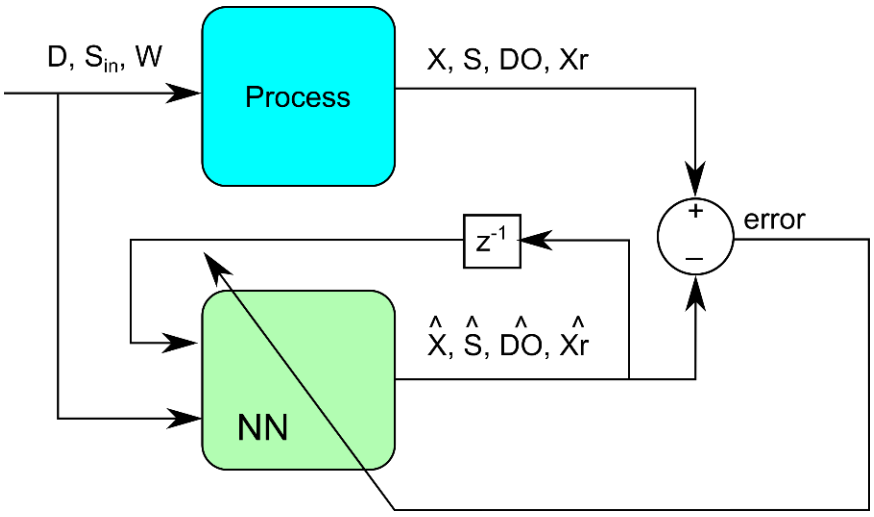


Figure 2.13 – The structure used for training the NN model (1st version)

The training has been performed using, as input data, randomly generated signals scaled to feasible values. The NN is a MLP containing one hidden layer with 10 neurons, as seen in Figure 2.14. The number of neurons in the hidden layer was experimentally determined such as the NN provides the best performances (high estimation accuracy with low training and exploitation time). The activation function used for the hidden layer is tansig, while for the output layer a linear one was considered.

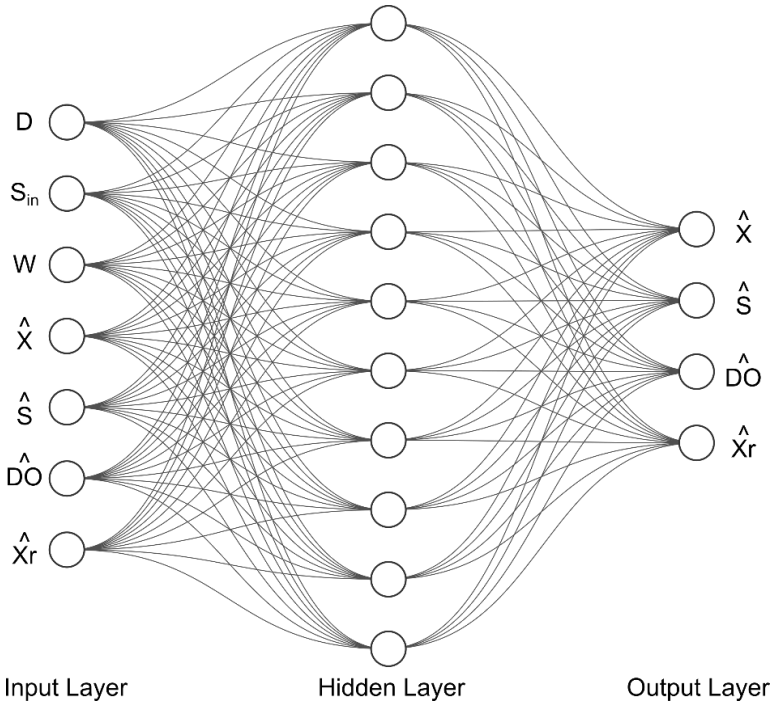


Figure 2.14 – The structure of the NN model (1st version)

Considering that the WWTP system is nonlinear, the Levenberg-Marquardt algorithm has been considered for training the NN as it is more efficient for this kind of systems [189]. Figure 2.15 shows the training performance (Mean Squared Error – MSE) evolution during the 1000 epochs of the training.

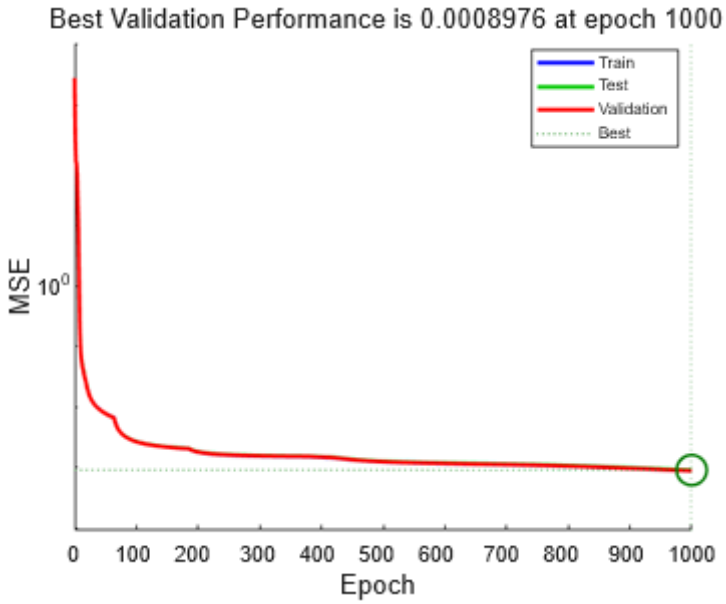


Figure 2.15 – The evolution of the loss function during NN training (1st version)

The NN model has been validated by using as input data another randomly generated signal scaled to feasible values. The values of the four process state variables estimated by the NN model were compared to the state variables of the mathematical model, proving that the NN is able to estimate the dynamics of the WWTP (see Figure 2.16) within an acceptable error (see Figure 2.17).

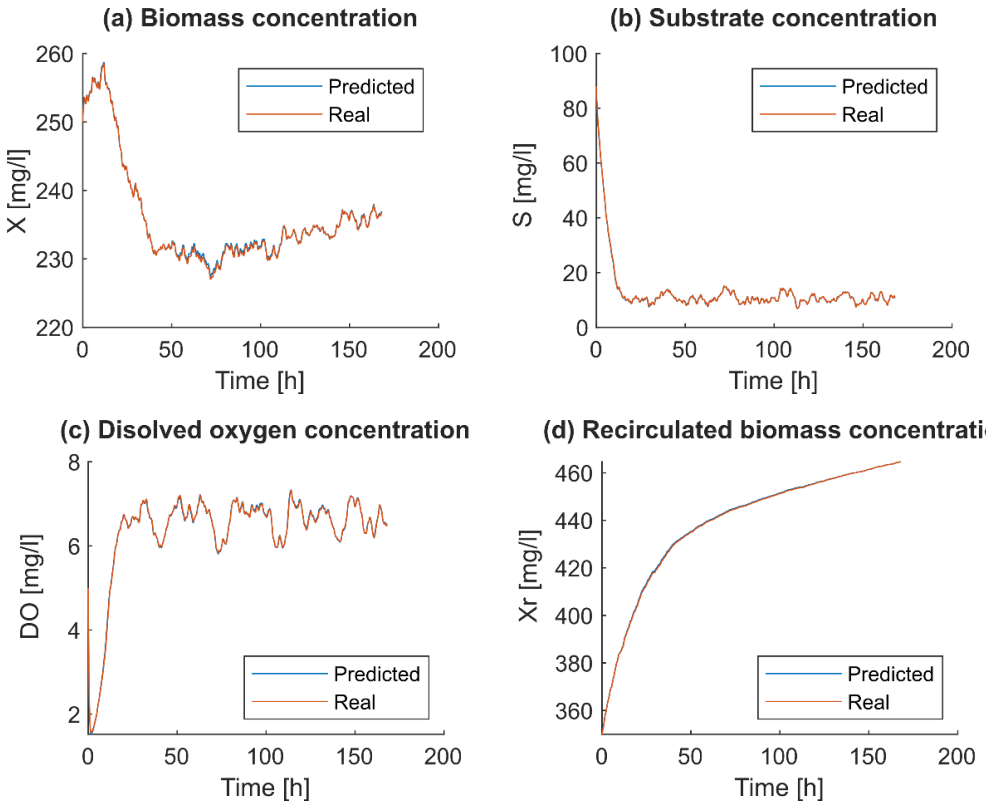


Figure 2.16 – The NN validation – real and predicted evolutions of process states (1st version) (a) biomass concentration; (b) substrate concentration; (c) dissolved oxygen concentration; (d) recirculated biomass concentration

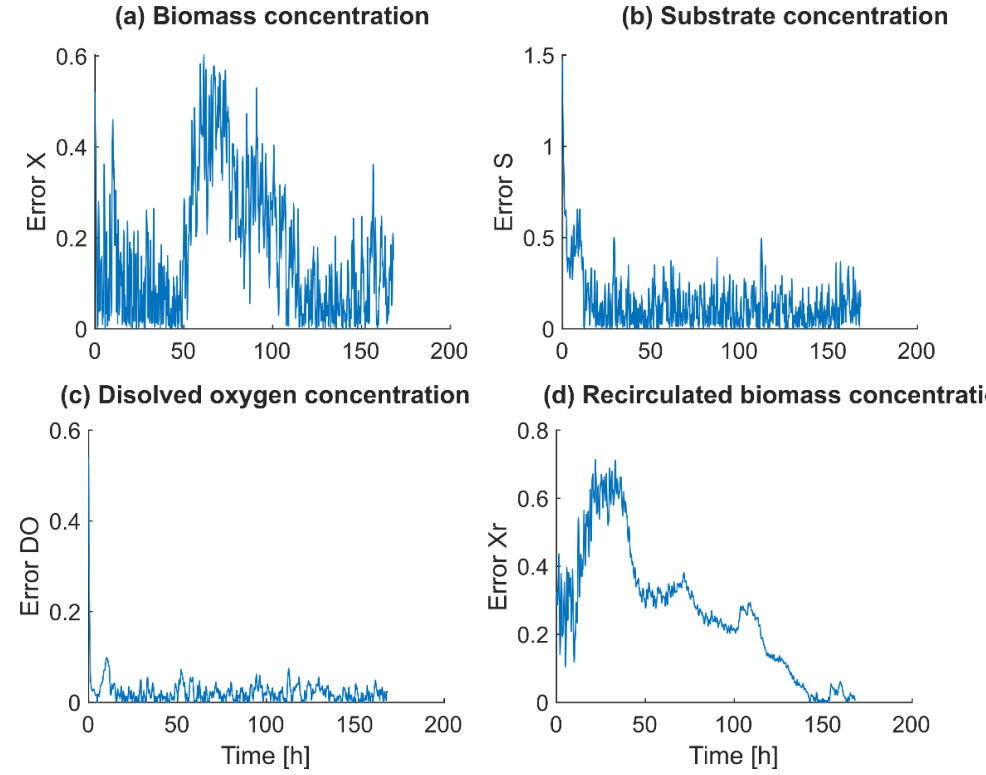


Figure 2.17 – The NN validation – prediction error (1st version) (a) biomass concentration; (b) substrate concentration; (c) dissolved oxygen concentration; (d) recirculated biomass concentration

2.3.1.2. The 2nd version of the neural network model

Figure 2.18 shows the training structure that was used for obtaining the 2nd version of the NN model. In this NN model version, only one state variable of the WWTP is considered measurable (S). For this reason, the NN model will estimate only the dynamics of this variable ($\hat{S}$), based on data provided at its inputs: influent data (D and S_{in}), aeration command (W) and the substrate concentration estimated in the previous time step.

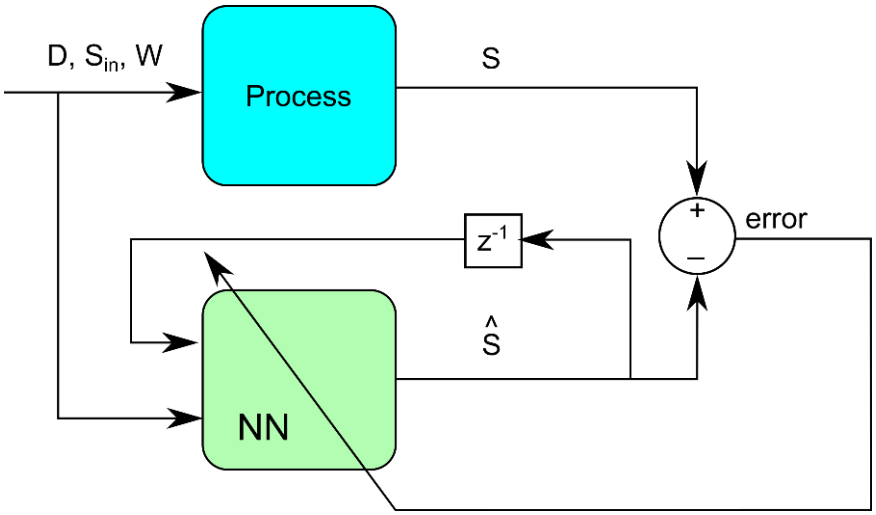


Figure 2.18 – The structure used for training the NN model (2nd version)

The training has been performed using, as input data, the same randomly generated signals scaled to feasible values that were used for training the 1st version. The NN is also an MLP containing one hidden layer, this time with 4 neurons, as seen in Figure 2.19. The number of neurons in the hidden layer was experimentally determined such as the NN provides the best performances (high estimation accuracy with low training and exploitation time). The activation function used for the hidden layer is tansig, while for the output layer, a linear one was considered.

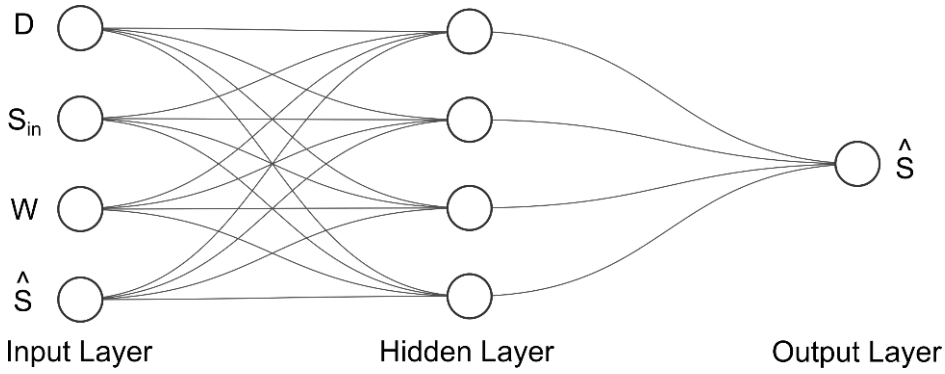


Figure 2.19 – The structure of the NN model (2nd version)

Figure 2.20 shows the training performance (MSE) evolution during the 1000 epochs of the training.

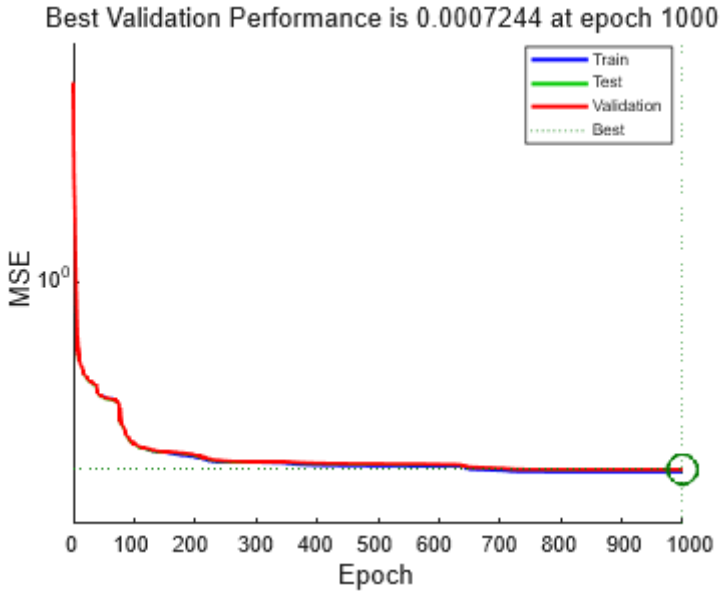


Figure 2.20 – The evolution of the loss function during NN training (2nd version)

The obtained trained NN model has been validated by using as input data another randomly generated signal scaled to feasible values. The value of the substrate concentration estimated by the NN model vas compared to the same state variable value obtained using the mathematical model, proving that the NN can estimate the dynamics of the WWTP within an acceptable error, as seen in Figure 2.21.

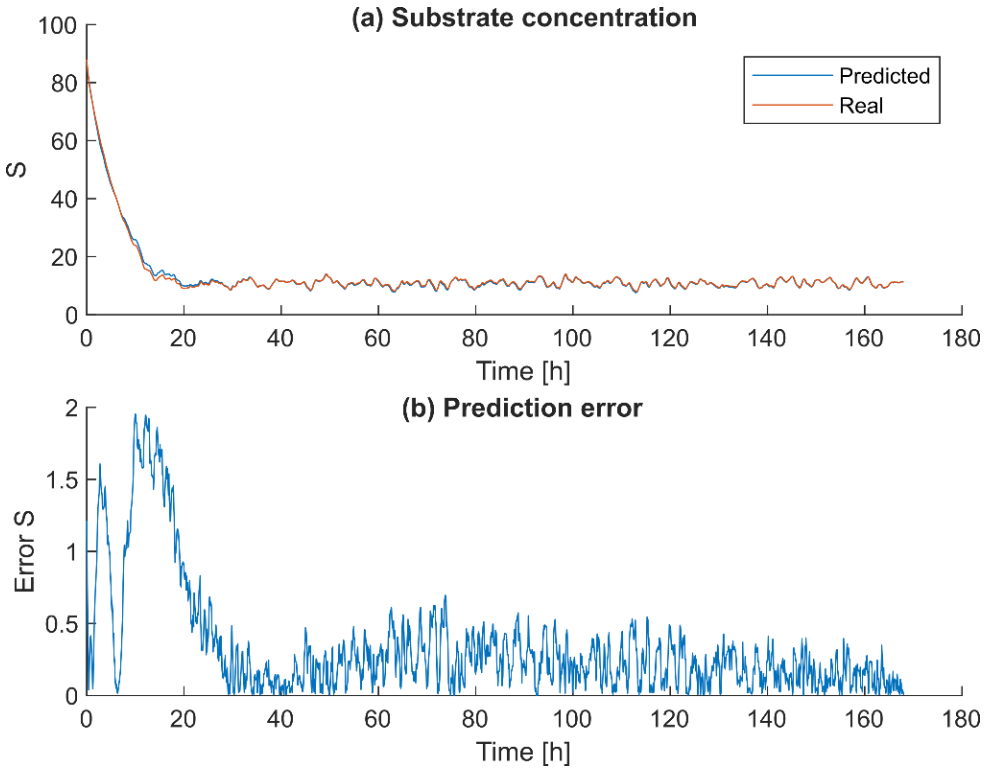


Figure 2.21 – The NN validation – real and predicted evolution of substrate concentration and the error between them (2nd version)
(a) substrate concentrations; (b) prediction error

2.3.2. Estimating process values using Neural Networks

Another issue regarding WWTP modelling and control is that many of the process variables are not easily measurable, mostly because of the expensive sensors and the high costs of technological plant upgrades. Thus, this section investigates the use of NN as virtual instrumentation tools (software estimators or soft sensors), more specific, predicting ammonium concentrations (S_{NH}) in the WWTP effluent based on easily measurable values [190].

The training and test data have been obtained by using BSM2 model, consisting of various measurements of influent, effluent and other variables collected over a period of two years with a sampling time of 15 minutes. From this dataset, the first year of data was used for training, while the other year of data was used for validating the resulted NN soft sensor.

The soft sensor provides a prediction of the effluent ammonium concentration ($\hat{S}_{NH,e}$), having the structure presented in Figure 2.22. As observed, the inputs of the soft sensor are passed through a data preprocessing stage before being fed to the NN estimator. These inputs are:

- Q_{po} – the outflow of the primary clarifier
- $S_{NH,5}$ – the ammonium concentration in the 5th bioreactor
- TSS – Total Suspended Solids in the effluent
- T_{as} – The environmental temperature

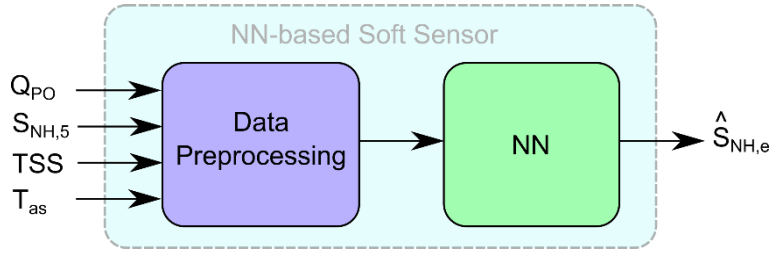


Figure 2.22 – The NN based Soft Sensor

The data preprocessing stage is important as it assures optimum performance and complexity of the NN [191] and consists of two steps:

1. Data normalisation. This step addresses the data heterogeneity issue by using the Z-score normalisation method, being computed as in (2.13). This method standardises the data and reduce the adverse effects given by extreme values in the input timeseries.

$$\tilde{x}[k] = \frac{x[k] - \bar{x}}{\sigma_x} \tag{2.13}$$

   where:
   - $x[k]$ is the original value of the k^{th} sample of the signal x
   - $\tilde{x}[k]$ is the normalized value of the k^{th} sample of the signal x
   - $\bar{x}$ is the mean value of the signal x
   - σ_x is the standard deviation of the signal x
2. Sliding window technique [192]. This step addresses the temporal coherence of the dataset, incorporating both current and past measurements, a new measurement being generated each time the sliding window moves, while the oldest measurement gets removed (basically, using the First-In First-Out (FIFO) principle). Figure 2.23 shows the

structure of the sliding window algorithm incorporating two parameters: the window length (WL) and the prediction horizon (PH). The two parameters of the algorithm have been chosen accordingly: $WL = 10\ h$ - aimed to capture a broad context of the input data and $PH = 4\ h$ - aimed at facilitating proactive decision-making.

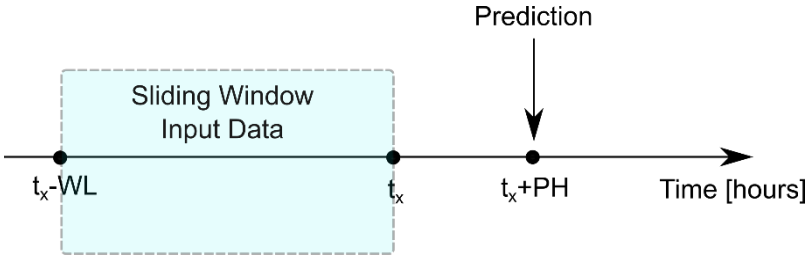


Figure 2.23 – The structure of the Sliding Window algorithm

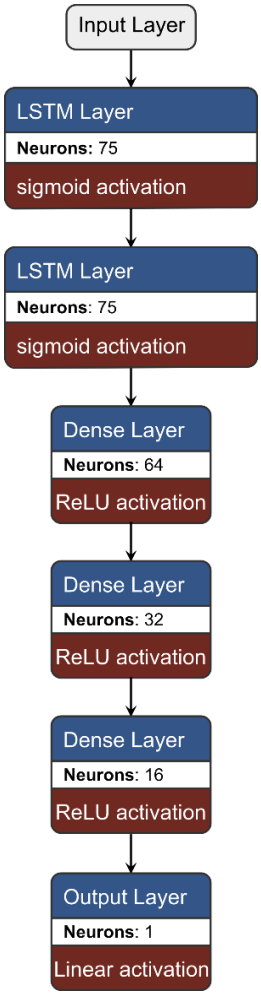


Figure 2.24 – The structure of the soft sensor NN

The NN is based on LSTM architecture [193], a type of RNN aimed at predicting time-series. An LSTM layer is composed of LSTM cells, which are characterised by their gating mechanism: each cell has an input and output gate, but also a forget gate, being able to remember their value over arbitrary time intervals. The NN is composed of two LSTM layers, 3 dense layers with a decreasing number of neurons and one output layer, as presented in Figure 2.24. Each of the LSTM layers contains 75 LSTM cells. The considered activation function of these two layers is the sigmoid function. The three dense layers contain a decreasing number of neurons, ranging

from 64 to 16, and use a Rectifier Linear Unit (ReLU) activation function. For the output layer, a linear function has been considered.

When dealing with time-series datasets, it is common to encounter imbalanced data, WWTP effluent values being one such example. Not addressing this issue while training the NN can lead to biased predictions favouring the most frequently occurring values [194]. To rectify this imbalance effects, the K-Fold technique has been used during the learning process [192]. The K-Fold technique involves splitting the training dataset into a number of K subsets. The training process will be performed K times, using each time one distinct subset for validation purposes, and the rest of $K-1$ subsets for training [195]. The model resulted in the fold that provided the highest accuracy among all folds will be selected for the final application. Figure 2.25 shows the schematic representation of the considered K-Fold mechanism for $K = 5$.

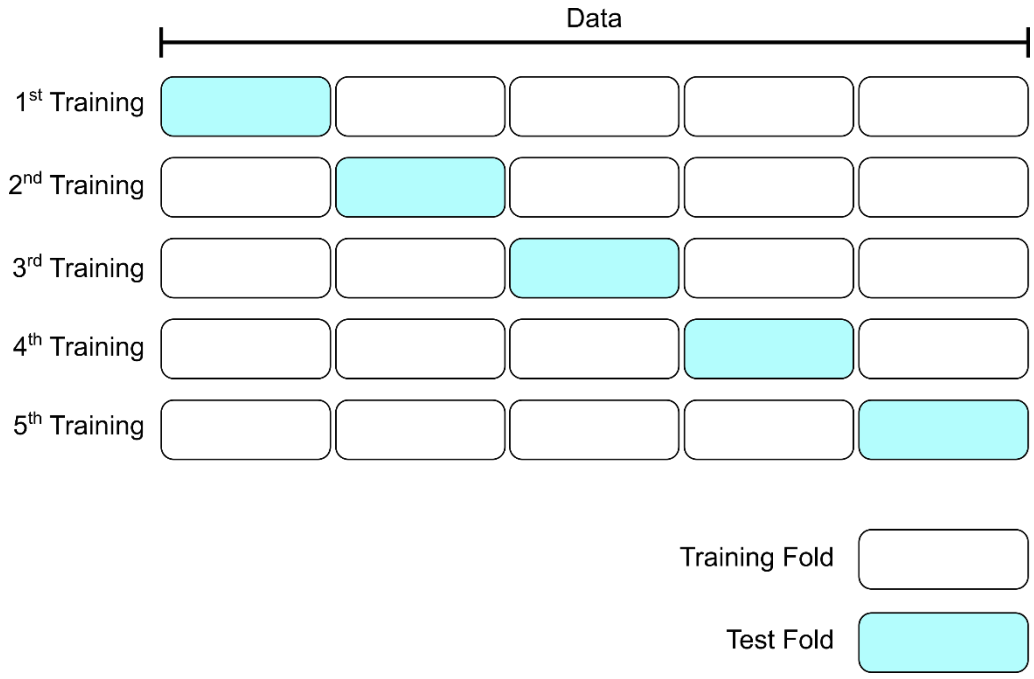


Figure 2.25 – The K-Fold training method

The assessment of the NN performances hinges on the predictions that are produced by the Soft Sensor. For this reason, three metrics has been integrated to provide a comprehensive evaluation of the performance of the Soft Sensor:

1. Root Mean Squared Error (RMSE) – it measures the difference between the actual signal (y) and the predicted one ($\hat{y}$):

$$RMSE = \sqrt{\frac{1}{N}\sum_{k=1}^{N}(y[k] - \hat{y}[k])^2} \tag{2.14}$$

   An accurate prediction implies a lower value of RMSE. In the case of the above developed Soft Sensor the obtained value ($RMSE = 0.048$) suggests the accuracy of the obtained model.

2. Mean Absolute Percentage Error (MAPE) – the average percentual error in the prediction:

$$MAPE = \frac{100}{N}\sum_{k=1}^{N}\left|\frac{y[k]-\hat{y}[k]}{y[k]}\right| \tag{2.15}$$

The obtained value for this metric ($MAPE = 3.54\%$) also suggests the reliability of the Soft Sensor

3. Coefficient of Determination (R^2) – a statistical measure assessing the ability of a NN to deal with variability in data, yielding values between 0 and 1, with 1 denoting the ideal corelation between factual and predicted values.

$$R^2 = 1 - \frac{\sum_{k=1}^{N}(y[k]-\hat{y}[k])^2}{\sum_{k=1}^{N}(y[k]-\bar{y})^2} \tag{2.16}$$

where $\bar{y}$ is the mean value of the real signal. The implemented Soft Sensor model is capable of accounting around 97% of the data variance ($R^2 = 0.97$) resulting in precise predictions.

The values of the considered metrics proved the reliability and precision of predictions of $S_{NH,e}$ using the implemented Soft Sensor, precision which is further demonstrated by using the model for predicting $S_{NH,e}$ values for inputs that were not part of the training dataset (second year of collected data). Figure 2.26 shows an example of real and predicted evolutions of $S_{NH,e}$ for 20 days, the Soft Sensor showing a high degree of accuracy in prediction.

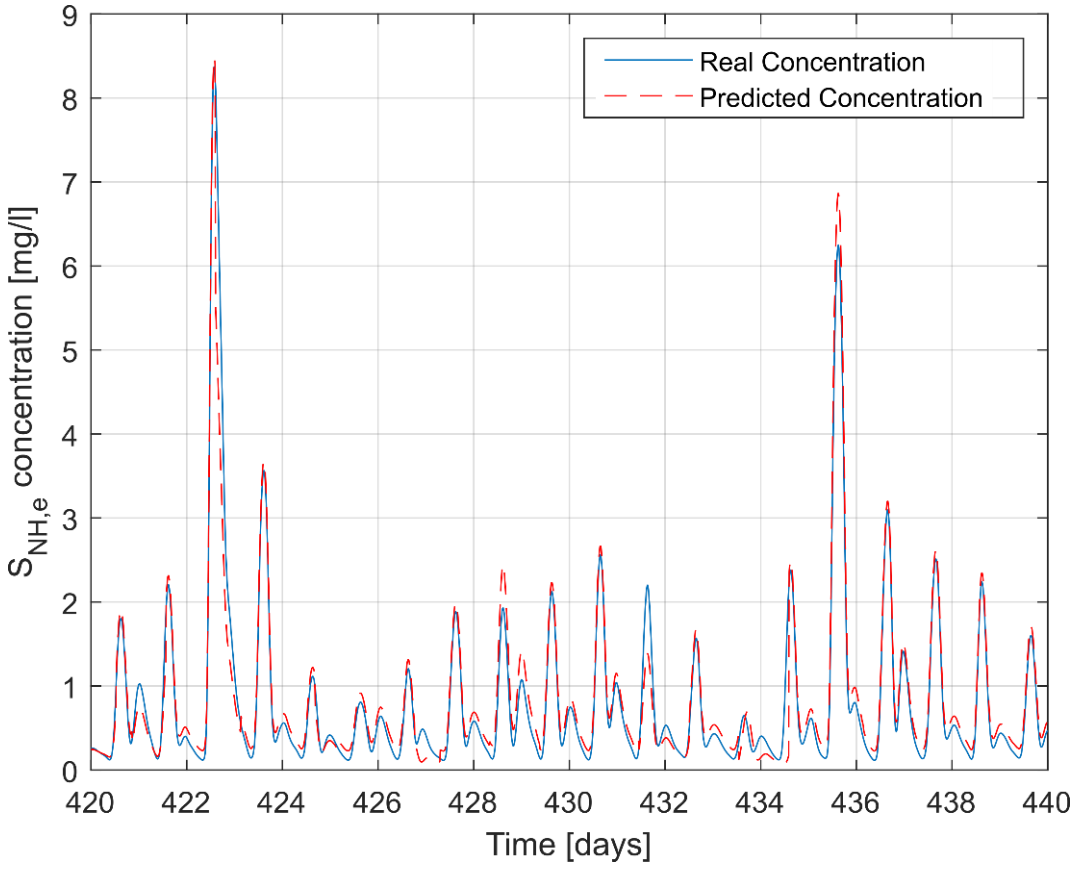


Figure 2.26 – The NN validation – The real and predicted evolution of $S_{NH,e}$

2.3.3. Estimating effluent quality using Neural Networks

Implementing model-based optimal control algorithms for WWTP, requires multiple numerical integration of WWTP models, which can pose time-related challenges, especially when dealing with real-time and high-complexity models. For this reason, this section explores the use of NN for predicting effluent variables based on influent variables, but also control actions [196].

$$EQI = \frac{1}{T \cdot 1000} \cdot \int_{t=245}^{t=609} \begin{pmatrix} B_{TSS} \cdot TSS_e(t) + B_{COD} \cdot COD_e(t) + \\ B_{NKj} \cdot S_{NKj,e}(t) + B_{NO} \cdot S_{NO,e}(t) + \\ B_{BOD5} \cdot BOD_e(t) \end{pmatrix} \cdot Q_e(t) \cdot dt \tag{2.17}$$

Equation (2.19) [133] shows that EQI is defined based on average values of specific quality variables of the effluent weighted with the factors B_X over the entire observation period T. These quality variables are:

- TSS_e – Total Suspended Solids in effluent
- COD_e – Chemical Oxygen Demand in effluent
- $S_{NKj,e}$ – Total Kjeldahl Nitrogen in effluent
- $S_{NO,e}$ – The nitrate nitrogen concentration in effluent
- BOD_e – Biochemical Oxygen Demand in effluent

A good prediction of EQI means a good prediction of this quality variables. Thus, this section aims at predicting these quality variables based on the same variables measured on the influent (TSS_i, COD_i, $S_{NKj,i}$, $S_{NO,i}$ and BOD_i) and one control action: $K_L a_3$ – the oxygen transfer coefficient in WWTP bioreactor 3, using the architecture presented in Figure 2.27.

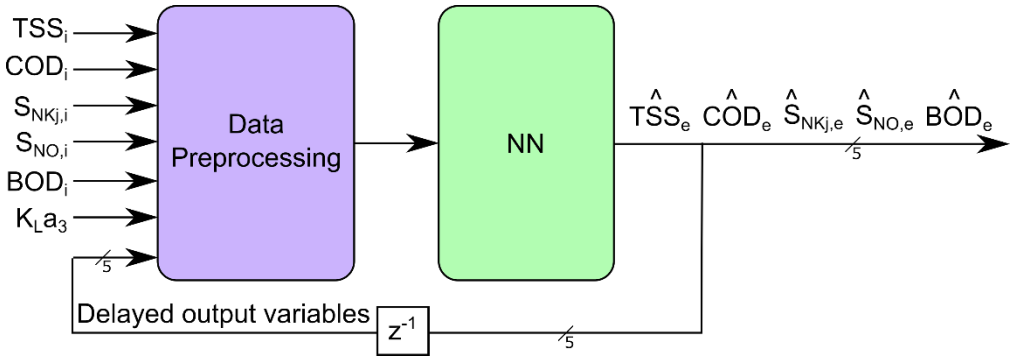


Figure 2.27 – NN-based effluent quality prediction architecture

The training and test data were obtained by integrating the BSM2 model and consists of measurements of influent and effluent quality variables collected under the influence of various values of $K_L a_3$ for the entire 609 days of the BSM2 influent, considering the following values for the oxygen transfer coefficients of WWTP bioreactors 4 and 5:

$$K_L a_4 = K_L a_3; \quad K_L a_5 = 0.5 \cdot K_L a_3 \tag{2.18}$$

During the simulation interval, $K_L a_3$ was varied using a deterministic approach: the value was increased from 0 to 250, in steps that were kept constant for an entire week before being incremented to the next value. Using this method ensures that the NN gets exposed to all scenarios that are probable regarding the value of $K_L a_3$. Further, the 609 days collected data was split as follows:

a) First 30 days were ignored, as it was considered the stabilisation period of the WWTP.
b) Next 450 days were selected as training dataset.
c) Last 129 days were selected as testing dataset.

Before being fed to the NN, the data goes throughout a preprocessing stage similar to the one implied in section 2.3.2 consisting of data normalisation using the Z-score normalisation method (see equation (2.13)) and a sliding window technique, as described in Figure 2.22, using the same window length ($WL = 10\ h$) and prediction horizon ($PH = 4\ h$). The NN is based on LSTM architecture being composed of two LSTM layers, 3 dense layers with decreasing number of neurons and one output layer, having the same structure as the one used in the previous section (see Figure 2.24), excepting that the two LSTM layers contain only 20 LSTM cells each. During the training process the K-Fold mechanism described in Figure 2.25 was used to rectify the imbalance effects posed by the available data.

The performances of the trained NN were assessed using the same metrics defined in the previous section by equations (2.14) and (2.16). The obtained values are:

1. $RMSE = 0.048$ – indicates high precision of the model
2. $R^2 = 0.99$ – the model is capable of accounting around 99% of the data variance

The values of the considered metrics proved the reliability and precision of predictions of the effluent quality variables using the implemented model, precision which is further demonstrated by using the model for predicting quality values for inputs that were not part of the training dataset (last 129 days of collected data). Figure 2.28 shows an example of real and predicted evolutions of one of the effluent quality variables: $S_{NO,e}$ for a part of the test dataset (that was considering a deterministic approach regarding $K_L a_3$ variation).

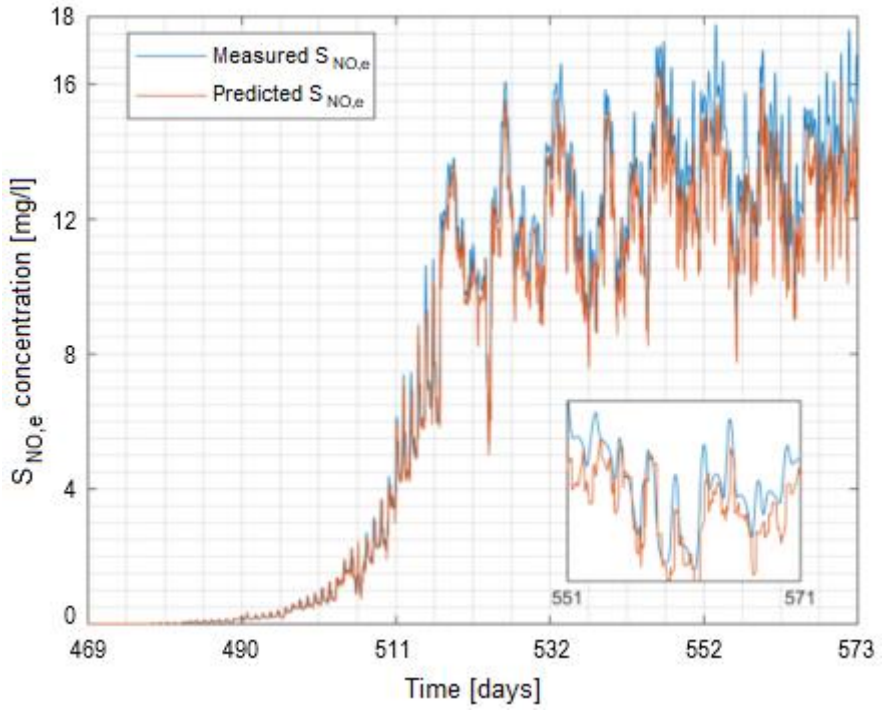


Figure 2.28 – The model validation – real and predicted evolution of $S_{NO,e}$ with deterministic $K_L a_3$

As the dataset used for training and testing the implemented NN used a deterministic method for varying $K_L a_3$, it is important to validate the obtained model under more real conditions. In this

sense, an additional testing dataset was generated using the same influent and a stochastic method for varying $K_L a_3$: values were randomly chosen from a realistic range of potential values (60 – 120). The new dataset was used to validate the trained NN, showing a 99% accuracy in predicting effluent quality variables. Figure 2.29 shows an example of real and predicted evolutions of two of the effluent quality variables: $S_{NO,e}$ and TSS_e for a part of the test dataset (that was considering a stochastic approach regarding $K_L a_3$ variation).

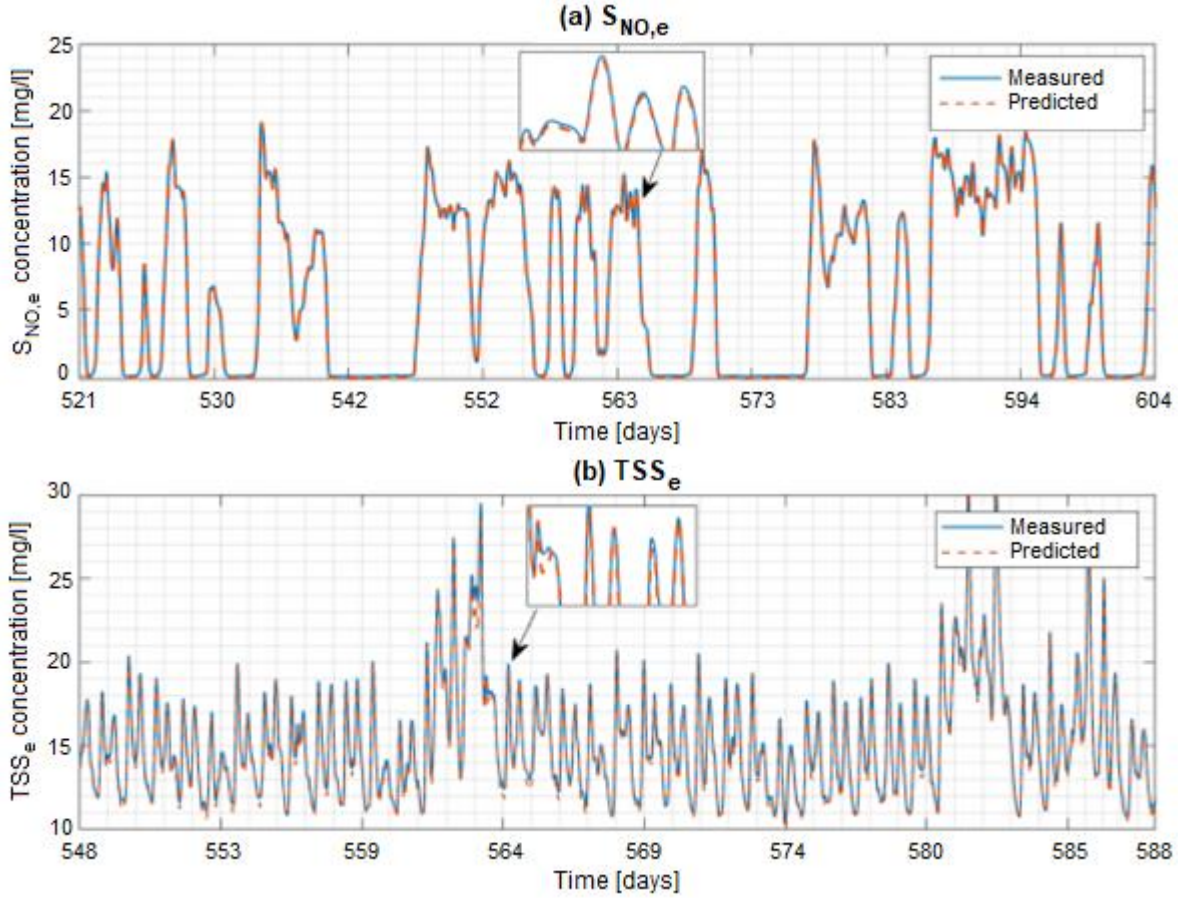


Figure 2.29 – The model validation – real and predicted evolution of effluent variables with stochastic $K_L a$ (a) $S_{NO,e}$; (b) TSS_e

2.4. Integrated Urban Wastewater System modelling

SNs and WWTPs are interconnected system, as the effluent of the first one is the influent of the other one. Consequently, the effluent of the SN is playing an important role in the WWTP performances, meaning that, when controlling SN, it is important to also consider the WWTP. On the other hand, the control strategies implied for WWTP operation should take into account if the SN is affected by considerable pluviometric events or not. Bearing in mind the presented reasons, it is important, when developing control strategies and optimization methods for wastewater transport and treatment, to consider the integrated system consisting of the SN and the WWTP. For this reason, IUWS models are required.

Consequently, this subchapter is focusing on developing two IUWS models by connecting SN models with WWTP models.

2.4.1. BSMSewer – ASM2d

The first IUWS model has been obtained by connecting a simple SN model with the WWTP model developed in [197], being scaled for serving a city with a population of about 250,000 inhabitants [198].

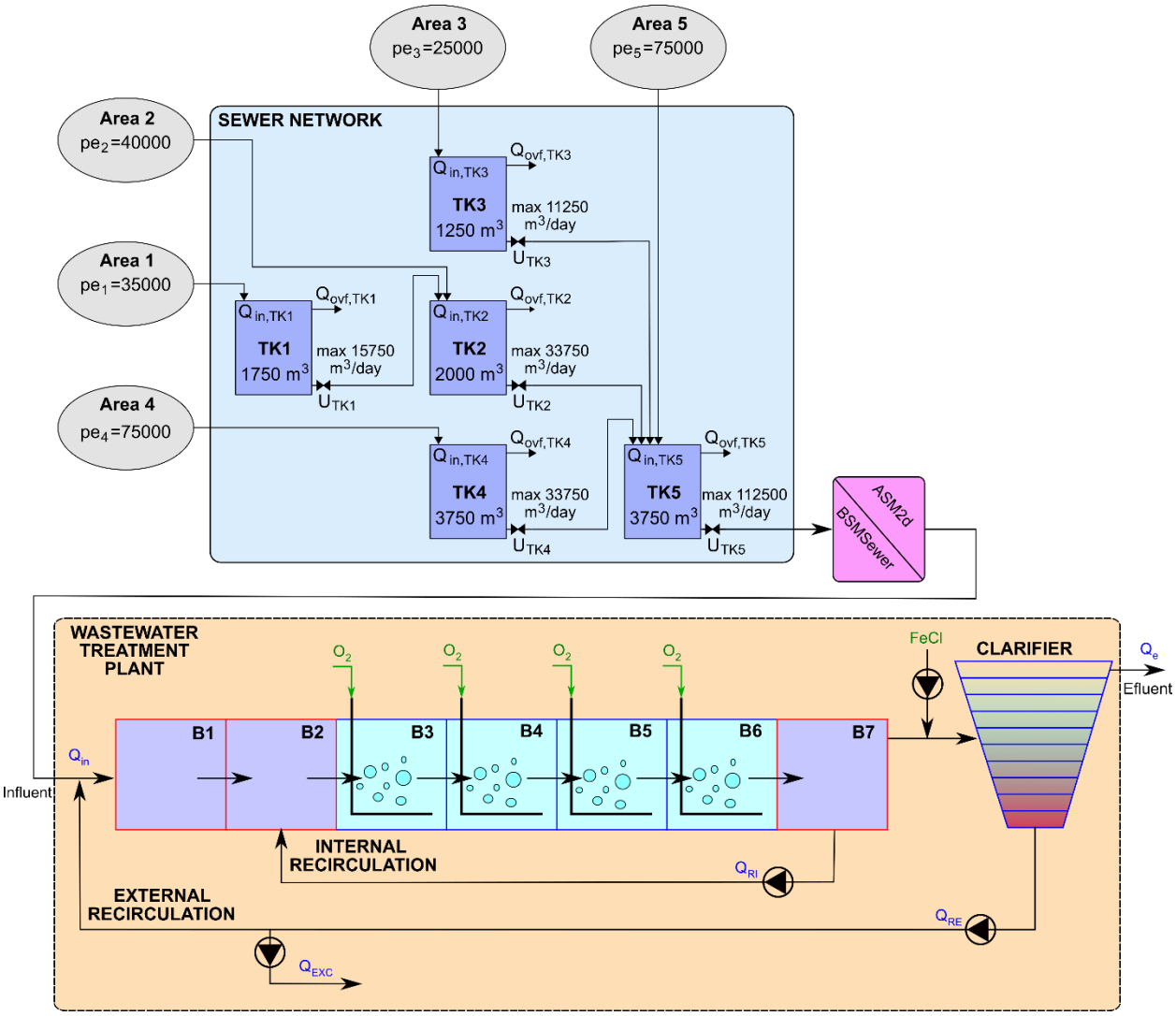


Figure 2.30 – The architecture of the IUWS (BSMSewer – ASM2d)

The architecture of the resulting IUWS is presented in Figure 2.30 and has three main components:

1. the SN model – a simple SN implemented in BSMSewer, with 5 storage tanks, each one related to a collecting area. The SN tanks parameters and the population equivalent of each of the collecting areas can be seen in Figure 2.30.
2. the WWTP – modelled using ASM2d model [197]. It contains seven bioreactors (two anoxic, four aerated and a deaeration one), a secondary clarifier, internal and external sludge recirculation circuits, an excess sludge removal system and a system for adding ferric chloride. The volumetric characteristics of the WWTP components are given in Table 2.9.
3. a coupling unit between the two subsystems.

Table 2.9 – The characteristics of the WWTP components

No.	Component	Volume [m^3]
1	B1 – Anoxic bioreactor with continuous mixing	1200
2	B2 – Anoxic bioreactor with continuous mixing	2200
3	B3 – Aerated bioreactor	2200
4	B4 – Aerated bioreactor	2200
5	B5 – Aerated bioreactor	3300
6	B6 – Aerated bioreactor	3300
7	B7 – Deaeration bioreactor	500
8	Secondary Clarifier	9000

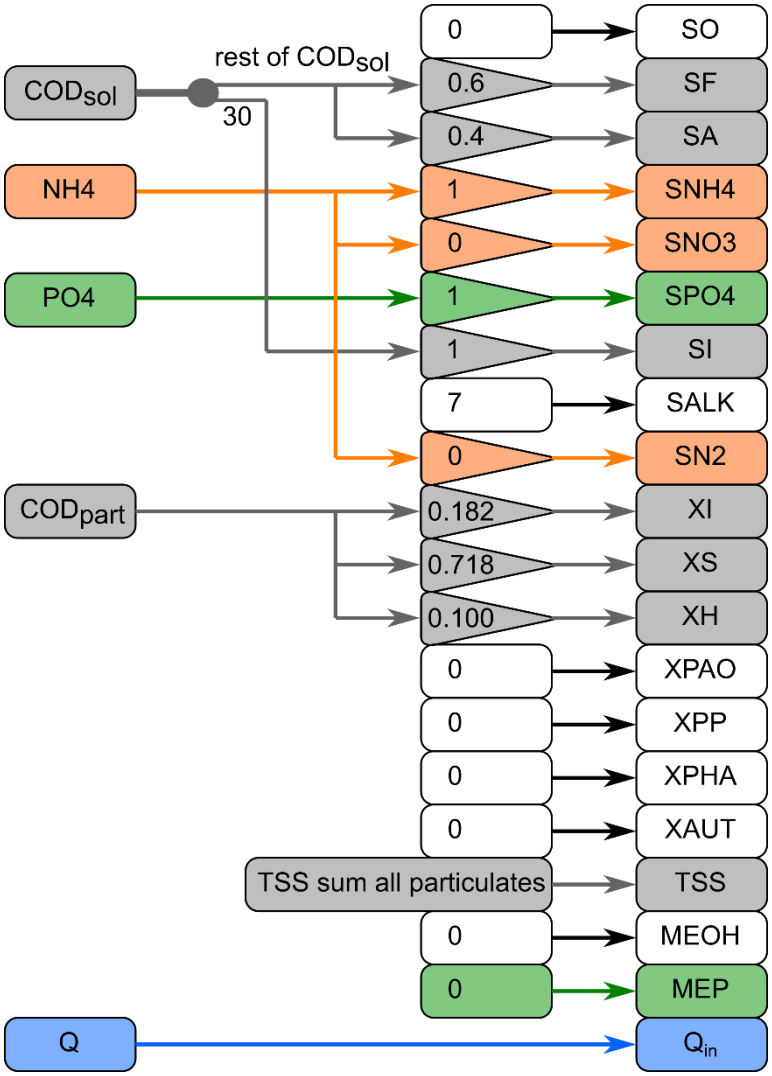


Figure 2.31 – The conversion from BSMSewer variables to ASM2d variables

As the SN is developed in BSMSewer, its effluent has 5 variables:

- COD_{sol} – Soluble Chemical Oxygen Demand
- COD_{part} – Particulate Chemical Oxygen Demand
- NH_4 – ammonia

- PO_4 – phosphate
- Q – outflow

On the other hand, as the WWTP is modelled using ASM2d model, its influent contains 20 variables, including the inflow, with their significance given in [128]. For this reason, a coupling unit between the two subsystems is necessary in order to make the variable conversion. This conversion has been performed according to the methodology proposed by [76] and is presented in Figure 2.31.

The IUWS model has been simulated for the forecasted influent presented in section 2.2.3, without taking into consideration any control system for neither the SN, nor the WWTP. The first set of results refers to the SN effluent (or the WWTP influent), resulted by aggregating the influents related to each of the collecting areas. The results are presented in Figure 2.32.

In Figure 2.32 (d) – (h), it can be seen that the SN effluent contains loads that are higher than those allowed to be discharged into natural receptors according to European legislation [5], limits that are marked with a red line. Moreover, the effects of the pluviometric events can be seen in all graphs, with higher flow and lower loads during them (marked in Figure 2.32 (a) with red and green circles for storm and rain event).

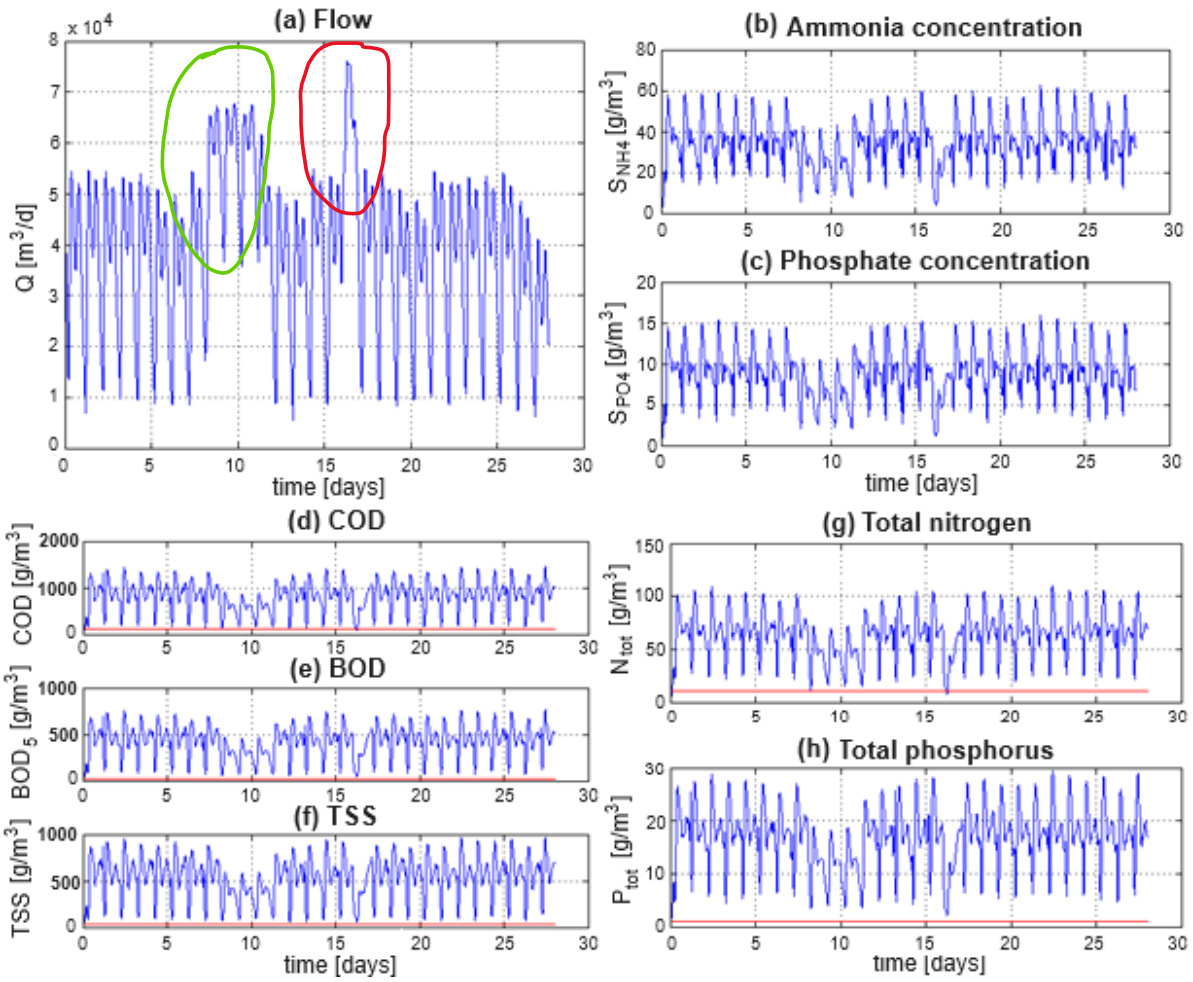


Figure 2.32 – SN effluent variables
(a) flow; (b) ammonia concentration; (c) phosphate concentration; (d) Chemical Oxygen Demand (COD); (e) Biochemical Oxygen Demand (BOD5); (f) Total Suspended Solids (TSS) concentrations; (g) total nitrogen concentration and (h) total phosphorus concentration

The second set of results refers to the WWTP effluent, considering the plant operating in two points differing by various values of aeration ($Q_{aeration}$), internal recirculation (Q_{RI}), external recirculation (Q_{RE}), excess sludge removal (Q_{EXC}) and addition of ferric chloride ($FeCl_3$) [197], according to Table 2.10.

Table 2.10 – The operating points of the WWTP

Operating point	$Q_{aeration}$ [m³/day]	Q_{RI} [m³/day]	Q_{RE} [m³/day]	Q_{EXC} [m³/day]	$FeCl_3$ [g/day]
A	75.600	57.600	20700	320	75.000
B	151.200	115.200	41400	720	150.000

The results obtained for both operating points are presented in Figure 2.33.

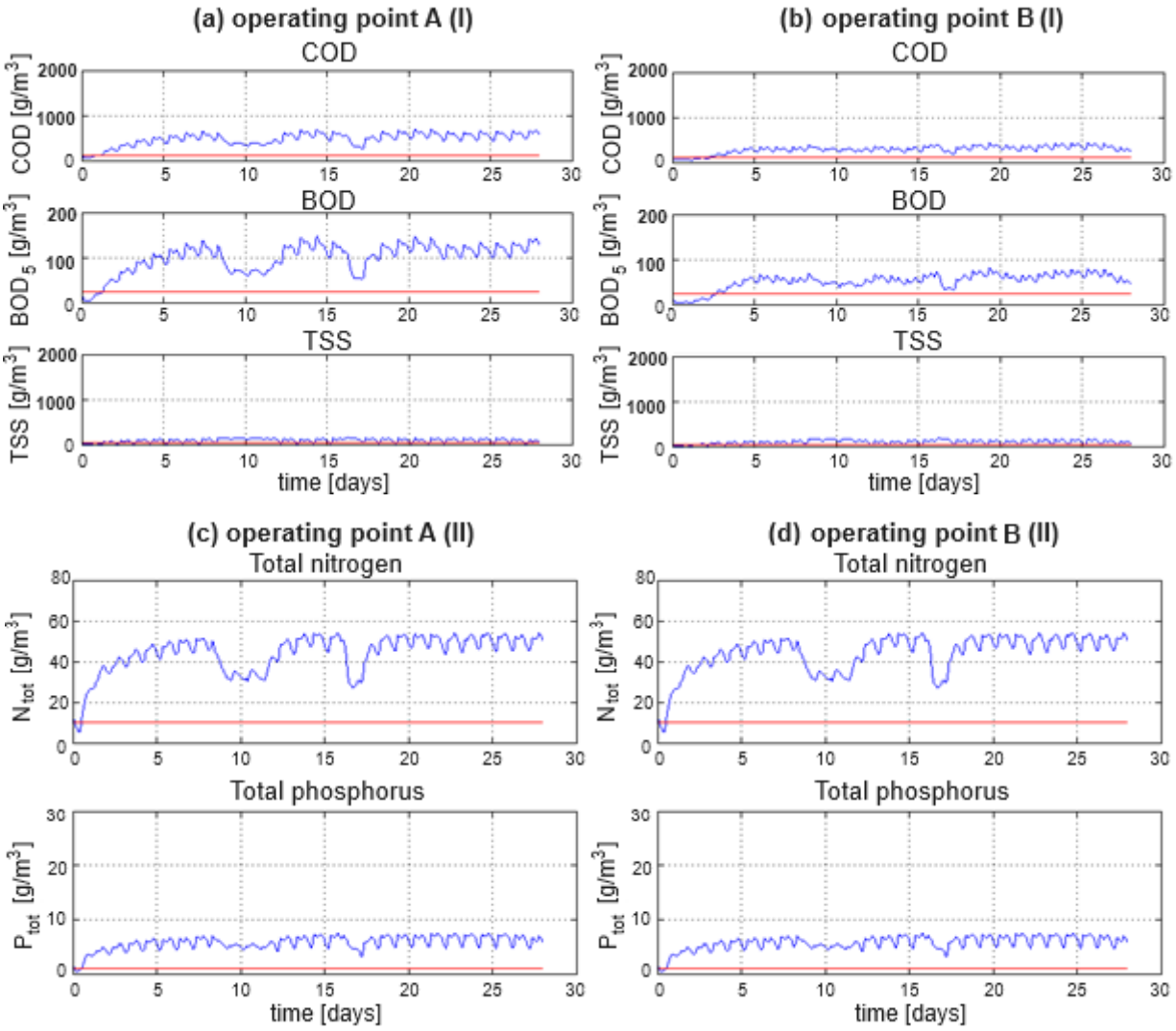


Figure 2.33 – WWTP effluent results
(a) and (c) loads in operating point A; (b) and (d) loads in operating point B

Decreases in all loads (COD, BOD5, TSS, total nitrogen and total phosphorus) can be observed in both operating points, however, not sufficient to comply with the legal limits (red lines). Of course, this implies further studies of the developed IUWS to develop integrated control algorithms such as the maximum efficiency of the integrated system is assured.

Regarding the two operating points, as expected, the treatment quality is better in operating point *B*, but with higher treatment costs, as presented in Table 2.11.

Table 2.11 – WWTP quality and cost indexes

Operating point	IQI [kg polluting units/day]	EQI [kg polluting units/day]	OCI
A	196059	109368	25511
B	196059	90528	41275

2.4.2. BSMSewer – BSM2G

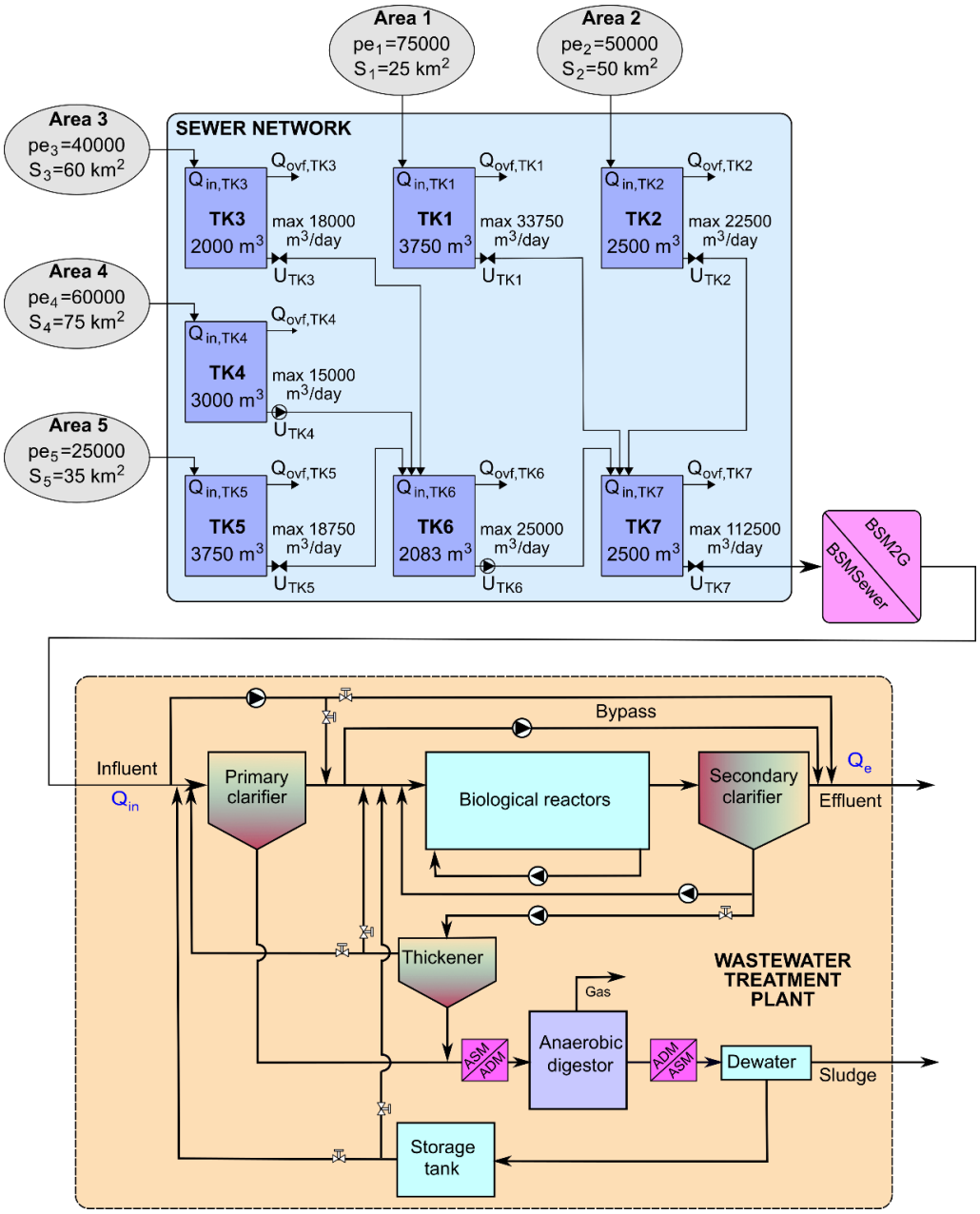


Figure 2.34 – The architecture of the IUWS (BSMSewer – BSM2G)

The second IUWS model has been developed also for serving a city with a population of about 250,000 inhabitants. The architecture of the resulting IUWS is presented in Figure 2.34 and has three main components:

1. the SN model – the model developed in subchapter 2.2
2. the WWTP – the BSM2G model [6]
3. a coupling unit between the two subsystems.

As in the case of the previously described IUWS model, the SN is developed in BSMSewer, so its effluent has 5 variables (COD_{sol}, COD_{part}, NH_4, PO_4 and Q). On the other hand, the BSM2G influent contains 21 variables:

- 14 variables defined by ASM1, including the inflow, with their significance given in [199].
- 7 additional variables which are related to GHG emissions, with their significance given in [6].

For this reason, a coupling unit between the two subsystem models is necessary in to make the variable conversion. This conversion is a modified version of the methodology proposed by [76] (from BSMSewer to ASM2d variables) and is presented in Figure 2.35.

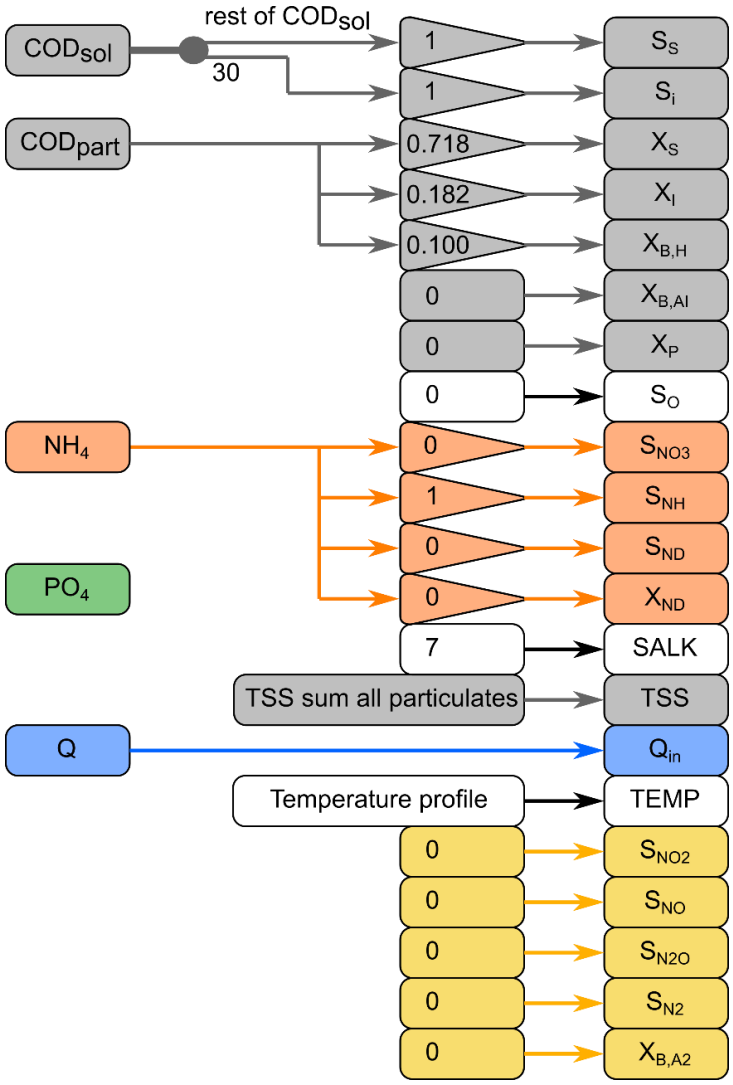


Figure 2.35 – The conversion from BSMSewer variables to BSM2G variables

2.4.2.1. Performance assessment

As this IUWS model has been developed for studying the interdependence of the SN and WWTP performances under various control schemes, it is important to have some indicators to measure the performance of each subsystem, but also of the integrated system.

For the SN, only two of the BSMSewer performance indicators described in Table 1.3 will be analysed when assessing the performance of the IUWS:

- the volume of overflow – V_{ovf} $[m^3/year]$
- the overflow quality index – OQI $[kg\ polluting-units\ /\ day]$

For the WWTP, the following performance indicators were considered:

- the effluent quality index – EQI $[kg\ polluting-units\ /\ day]$
- the operational cost index – OCI
- the total GHG emissions from biological treatment – GHG_{bio} $[kg\ CO_{2e}/day]$
- the total GHG emissions of the WWTP – GHG_{total} $[kg\ CO_{2e}/day]$

However, for the IUWS, there is no performance indicator defined in literature. Thus, in what follows, the basis for such an indicator will be defined. First, both subsystems can discharge pollutants in natural receptors, which are, separately, assessed by OQI (describing pollutants discharged by the SN) and EQI (describing pollutants discharged by the WWTP). However, OQI is calculated as defined in BSM1 [77] after converting the BSMSewer variables of the overflowed wastewater to ASM2d variables (as in Figure 2.30), while EQI is calculated as defined in BSM2 [133] based on ASM1 variables. Thus, OQI and EQI are not comparable, as OQI includes information about the phosphorus loads. For this reason, a new performance indicator is proposed for assessing the pollutants discharged by the SN: OQI_1 calculated in the same way as EQI, after converting the BSMSewer variables of the overflowed wastewater to ASM1 variables (as in Figure 2.34, excepting GHG related variables).

Now that both subsystems have quality indexes defined that are calculated in the same way and that have the same unit ($kg\ polluting-units\ /\ day$), an integrated Discharge Quality Index (DQI) can be defined, aiming at assessing the total quantity of pollutants discharged by the IUWS as the weighted sum of EQI and OQI_1.

$$DQI = w_{EQI} \cdot EQI + w_{OQI} \cdot OQI_1 \tag{2.19}$$

The two weights (w_{EQI} and w_{OQI}) must be chosen such as they are able to account for the severity of discharging from the corresponding subsystems. For example, if not all the SN overflow is properly directed to the same natural receptor as the effluent of the WWTP (i.e., part of the SN overflow floods the street) it is imperious to have a much higher value for w_{OQI}, than for w_{EQI}. On the other hand, if both the effluent of the WWTP and the overflow of the SN are discharged on the same point, w_{EQI} and w_{OQI} will have similar values.

In [200], the authors define a global performance indicator for the WWTP, indicator that accounts for EQI, OCI and GHG emissions. With the newly defined DQI, that global performance indicator could be modified in such way that it will also include information about the quantity of pollutants discharged by the SN, resulting an integrated performance indicator for the IUWS:

$$I(\lambda) = \lambda \cdot \overline{DQI} + \frac{1-\lambda}{2} \cdot \overline{OCI} + \frac{1-\lambda}{2} \cdot \overline{GHG_{total}} \tag{2.20}$$

with the following notation:

$$\bar{X} = \frac{X}{X_{BC}} \tag{2.21}$$

where X_{BC} is the value which was obtained for the indicator X in a base case. For example, a value of 0.64 for $\bar{X}$ means that the value of performance indicator X is only 64 % of the value of the same performance indicator in the base case. This approach provides a clear way to compare different scenarios relative to the base case. The factor $\lambda \in [0,1]$ is weighting the terms of the integrated indicator, allowing for assigning different degrees of importance to each of them.

The base case will be defined as the case in which the SN is not controlled (all valves and pumps are fully open or running at 100%), while the WWTP uses a PI controller manipulating the aeration flows in all the aerated bioreactors in order to regulate the DO concentration in the 2nd bioreactor (default control strategy in BSM2). Table 2.12 shows the values of the performance indicators in the base case.

Table 2.12 – The values of the IUWS performance indicators in the base case

Performance indicator	Value	Unit
$V_{ovf,BC}$	313942.26	$m^3/year$
$OQI_{1,BC}$	4007.44	$kg - polluting\ units/day$
EQI_{BC}	11958.81	$kg - polluting\ units/day$
OCI_{BC}	14436.05	-
$GHG_{total,BC}$	27159.32	$kg\ CO_{2e}/day$
DQI_{BC}	15966.25	$kg - polluting\ units/day$

It is important to mention that for calculating DQI in Table 2.12 with equation (2.19), the two weights involved were considered equal: $w_{EQI} = w_{OQI} = 0.5$ meaning that it was considered that the SN overflow is properly directed to the same natural receptor as the WWTP effluent.

Of course, the indicator defined in equation (2.20) needs some improvements in the sense that it should include information about the operational cost and the GHG gasses related to the SN. More exactly, a definition for an integrated operational cost index and a definition for the integrated GHG emissions of the IUWS are needed. This needs some extra research which will be done in subsequent research.

2.5. Chapter conclusions

This chapter delves into the modelling of wastewater collecting and treatment systems in a separate, but also integrate manner, presenting the development of a series of digital tools which will be helpful for simulating such systems during a control implementation stage.

Firstly, a SN mathematical model is implemented in BSMSewer, the model being fitted for a city the size of Galați, Romania (approximately 250,000 inhabitants on a total surface of 250 km^2).

The model is composed of seven storage tanks that are related to five collecting areas. Moreover, an influent scenario having a duration of 28 days is generated to be used for testing SN control strategies. The influent scenario is generated in two versions: forecasted and disturbed scenario, the last one containing a random component. This way, in the next chapter, when developing control strategies for SN, the forecasted influent will be used, while when testing the resulted control strategy, the disturbed one will be used. This will provide a way to validate the proposed control strategies under influent uncertainty conditions. The resulted SN model is simulated in various conditions: all valves fully opened and all pumps running at 100%, but also with some valves partially opened, and a series of 10 performance indicators are analysed for each simulation. It resulted that the values of the performance indicators of the storage tanks whose output control was diminished have increased, while the upstream tank indicators have decreased. This had a positive effect on some of the global performance indicators. Consequently, it has been proven that there are storage tank outlet controls combinations that could provide a better performance of the SN than the case when everything is running at 100% resulting the need for optimal control of the SN. On the other hand, implementing real-time optimal control of the SN will require numerical integration of the model multiple times in a short time interval. The integration of the implemented model over the 28 days horizon takes around 30 seconds when using a mid-range computer. This could pose a problem when the number of numerical integrations of the model is high during the optimization procedure resulting the need for a simplified model. Thus, a simplified model is proposed by keeping only the flow part of the model. The simplified model achieves a reduction of 90% of the integration time.

Regarding WWTP models, one of the main challenges model-based control is represented by the high complexity models that are available in the literature, leading to high numerical integration time. For this reason, a series of NN models is developed aiming at fitting various WWTP dynamics:

- firstly, a NN model aiming at fitting WWTP state variables dynamics is proposed. The proposed model has an MLP architecture, being implemented in two versions, one that can fit all the state variables and one that is able to fit only one of the state variables (the substrate). The two versions were trained using data obtained from a simplified 4-state mathematical model of a WWTP, the model validations showing that both versions can estimate the dynamics of the WWTP within an acceptable error.
- secondly, an LSTM NN is proposed for estimating a process variable. The NN model acts as a Soft Sensor, aiming at estimating the effluent ammonium concentration based on other easily measurable process values. A series of techniques are applied for enhancing the performances of the model: data normalization, sliding window technique and a K-Fold training method. The resulted model is validated on data that was not used for training showing a good accuracy of the model.
- Lastly, another LSTN NN is proposed for estimating the effluent variables that are involved in calculating EQI, based on the same quality variables of the influent and on the aeration rate in the aerated bioreactors. The resulted model is validated on data that was not used for training showing a good accuracy of the model. This model opens the way for implementing real-time optimal control of WWTPs that could minimize the pollutants discharged by the WWTP.

Regarding IUWS models, this chapter proposes two integrated models. One is obtained by combining a simple SN model developed in BSMSewer with a WWTP model previously developed based on ASM2d, while the second one is obtained by combining the SN model

described in the current chapter with the BSM2G model for WWTP. As the subsystems are implemented with different tools, in both cases the effluent variables of the SN are different from the influent variables of the WWTP. For this reason, both IUWS use a coupling unit between the two subsystems in order to make the variable conversions. As the second integrated model is intended to be used in the next chapter for exploring the possibility of enhancing the performances of the integrated systems, a methodology for assessing the performance of control strategies is proposed in terms of both subsystems' performance indicators.

In conclusion, this chapter introduces a series of tools to be used when developing optimal control strategies for wastewater collecting and treatment systems, demonstrates the need for optimal control of SN, proposes SN and WWTP models with low integration time, that could be used for developing online model-based control strategies and defines two IUWS systems alongside a methodology for assessing the performance of the control strategies of the integrated system.

Chapter 3. Optimal Control of Wastewater Collecting and Treatment Systems

3.1. Introduction

Optimal control strategies of wastewater collecting, and treatment systems is important as they assure that the wastewater resulted from human activities does not pollute the environment nor affect the human health in any way. Consequently, the main goal of SN optimal control is to assure the operational efficiency of the network under high inflow conditions, by directing as much wastewater and pollutants as possible to the WWTP. On the other hand, the control systems implied for the WWTP must assure that its effluent complies with the legal standards for water to be discharged into natural receptors in terms of the different pollutants loads, while maintaining, at the same time, a low operational cost. Additionally, GHG emissions resulted from wastewater treatment must be considered. All these goals can be achieved by manipulating various control variables from the systems, such as the outlet valves/pumps of the SN, or oxygen transfer coefficients from the WWTP aerated tanks, or by manipulating, in the top-level control structure, the setpoints of lower-level structure such as DO concentrations in the aerated tanks or the nitrogen concentration.

Consequently, the rest of this chapter is subdivided into four more subchapters. Subchapter 3.2 deals with developing optimal control strategies for SN, presenting two approaches: offline and online optimal control. In the first approach, five optimal control strategies are tested and compared, the one providing the best results being selected to be used for an analysis regarding which fitness function should be considered: quantity or quality of overflowed water. After the analysis, three more optimisation algorithms are tested and compared. After selecting the proper control strategy, the fitness function and the optimisation algorithm providing the best results, the implemented optimal control algorithm is used in a sliding window approach, being tested under influent uncertainties conditions. The second approach deals with online optimal control of SN. More specific, a MPC algorithm is imposed for controlling the SN. The implemented approach uses a simplified version of the SN model in order to reduce the optimisation time. It proposes a method for including pollutant information in the fitness function even if the used model if a flow one. Moreover, a computational effort test is conducted in order to check that the optimisation time is lower than the prediction horizon, demonstrating the usability of the proposed algorithm.

Subchapter 3.3 presents 3 optimal control strategies for WWTP. The first approach presents a MPC algorithm implied for minimising a cost function depending on treatment efficiency and treatment cost, while making use of the two NN models presented in section 2.3.1. In the second approach a Fuzzy-Optimal control strategy is implied. It is an extension of the existing control strategy of the WWTP in Galați, a city in Romania [197]. The extension of this strategy considers,

in addition to the optimal operating point regarding the dissolved oxygen concentration setpoint in the aerated bioreactors, applying a simple methodology to compute optimal values for the external recirculating rate based on the pluviometric regime using fuzzy techniques. After validating this approach, it is further extended in an Optimal-Setpoint-Based control strategy. More specific, for each pluviometric regime, the optimization algorithm will search for the optimal values of seven setpoints. The setpoints obtained for each regime are finally aggregated using the proposed fuzzy technique.

Subchapter 3.4 delves into considering the entire IUWS when developing control strategies of each subsystem (SN and WWTP), as both are interconnected. As the effluent of the SN represents the influent of the WWTP, it is important to also know the effects of the SN control strategies on the WWTP operation performances. It is expected that a higher flow from the SN, due to control strategies avoiding overflows, could lead to WWTP overloading, with considerable environmental effects. Therefore, SN control strategies should consider their effects on the WWTP operation efficiency in terms of pollution loads and wastewater flow. Consequently, the IUWS described in section 2.4.2 is further studied, following two directions for assessing the impact that SN has on the WWTP performances. In the first direction, the only control considered for the SN is in terms of SN outlet valve, while all other valves/pumps opened/running at 100%. The second direction considers using a MPC control algorithm described in section 3.2.2 for minimizing the environmental impact of SN. This strategy is further modified by integrating a constraint regarding the SN outlet valve opening into it. The last subchapter is dedicated to the conclusions of this chapter.

3.2. Sewer Network optimal control

The main goal on developing SN optimal control strategies is to reduce the environmental impact by decreasing the quantity of wastewater that overflows from the network in the natural receptors, alongside with the quantity of pollutants in the overflowed water, during heavy pluviometric events. This can be achieved by manipulating the SN storage tanks outlet commands (U_{TKi}).

Two approaches can be considered: offline optimal control and online optimal control, both having advantages and disadvantages. On one hand, offline optimal control does not depend on the model numerical integration time but is less robust when influent uncertainties are present. On the other hand, online optimal control requires a model that could be quickly integrated and can account differences between the forecasted influent and the real one.

The outflow of $TK7$ is the effluent of the SN (see Figure 2.1), thus keeping this tank's outlet command at 100% in the best solution with respect to SN performances. Moreover, analysing the results presented in Table 2.5 and obtained in simulation when no control was considered (all commands are kept at 100%) it can be observed that tank $TK7$ is not overflowing. Therefore, for the tanks whose outflow represents tank no. 7 inflow ($TK1$, $TK2$ and $TK6$), keeping the outlet command at 100% in also the best solution. Consequently, only manipulating the output controls of $TK3$, $TK4$ and $TK5$ can lead to improvements of the SN performances. Therefore, only these 3 tanks will be subject to optimization.

For all approaches, two of the SN performance indicators are computed and analysed: V_{ovf} and OQI. All the results are presented relatively scaled to the values of the same indicators in the "no control" case (see Table 2.5). The scaling is made according to equations (3.1) and (3.2):

$$\overline{V_{ovf}} = \frac{V_{ovf}}{V_{ovf,NC}} \tag{3.1}$$

$$\overline{OQI} = \frac{OQI}{OQI_{NC}} \tag{3.2}$$

where $V_{ovf,NC}$ and OQI_{NC} represents the values of the two performance indicators in the "no control" case. This approach provides a clear way to compare different scenarios relative to the base case. If the result is greater than 1, it indicates that the performance in the current scenario is worse than in the base case. If the result is less than 1, it indicates an improvement over the base case. Moreover, the scaled value gives a straightforward interpretation. For example, a value of 0.8 of $\overline{V_{ovf}}$ means the SN overflowed only 80% of the quantity overflowed in the base case, indicating a decrease with 20% of V_{ovf}.

3.2.1. Offline optimal control

Developing offline optimal control of SN will require a series of steps. Firstly, an optimal control strategy will be chosen, then it will be tested in various conditions minimizing either the volume of overflow or the overflow quality index or both in a MOO approach. After having the most suitable strategy and the best optimization objective, a series of optimization algorithms will be tested to see which one provides the best results. The identified optimization algorithm will be then used to implement the SN offline optimal control using a Sliding Window Technique.

3.2.1.1. Optimal control strategies

In the followings a series of 5 optimal control strategies [201] will be presented, tested for separately minimizing V_{ovf} and OQI and compared from the point of view of improvements in the SN efficiency in terms of the two indicators: V_{ovf} and OQI. For minimization, the use of GA was chosen.

GA is a metaheuristic algorithm which is commonly used to compute solutions for optimization problems. It is inspired from the natural selection process and uses a population of chromosomes. Each chromosome consists of genes and is a representation of the optimal problem solution. By using a series of biologically inspired operators (such as crossover, mutation or selection), the population evolves from the initial one to one that contains optimal problem solutions that minimizes a fitness function associated with a chromosome. At each generation, using the selection operator, a part of existing population is selected to breed a new generation. The breeding takes place by applying the crossover operator on a pair of parent chromosomes and by altering the resulting chromosome using the mutation operator [202].

The algorithm used in the followings for minimizing V_{ovf} or OQI has the following characteristics:

- the number of genes in the chromosomes will be chosen accordingly to each control strategy approach that will be presented.
- the population will consist of 20 individuals, the initial one being randomly generated from a uniform distribution.
- the selection operator chooses the parent chromosomes randomly from the population, for each candidate a probability directly proportional to its fitness function being used.
- the crossover operator generates an offspring chromosome (O) from the genes of two parent chromosomes ($P1$ and $P2$) using a randomly generated binary vector (S) with the same length as the chromosomes. For a randomly generated binary vector, each gene k of the offspring chromosome will inherit the value of gene k of the first parent if $S(k) = 0$, or of the second parent in the contrary case (Figure 3.1).

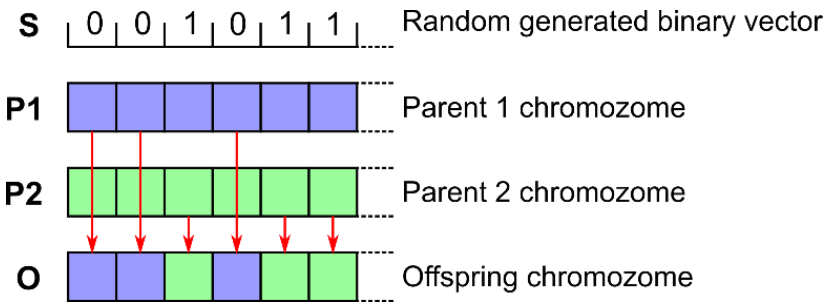


Figure 3.1 – The crossover operator of the GA

- the mutation operator adds to each gene of the offspring chromosome a value randomly chosen from a zero mean Gaussian distribution with a standard deviation calculated as:

$$\sigma_i = \sigma_{i-1} \cdot \left(1 - \frac{i}{G_{max}}\right) \tag{3.3}$$

  where i is the current generation number, G_{max} is the maximum number of generations and σ_i is the standard deviation at the generation i, with σ_1 being equal to the gene value range.
- stop conditions: the maximum number of generations reached or no improvements of the best function during the last 30 generations.

As stated before, 5 optimal control strategies will be implemented. In the first strategy, the output controls of $TK3$, $TK4$ and $TK5$ will be maintained constant at certain values that will be computed by the GA to minimize the fitness function [201]. This way, the chromosome will contain 3 genes, as shown in Figure 3.2:

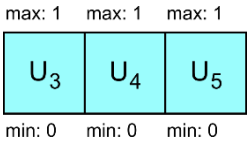


Figure 3.2 – The chromosome structure in Strategy #1

The next 3 strategies consider the output controls of $TK3$, $TK4$ and $TK5$ to vary in time, depending on the wastewater level in the corresponding tank [201], according to Figure 3.3.

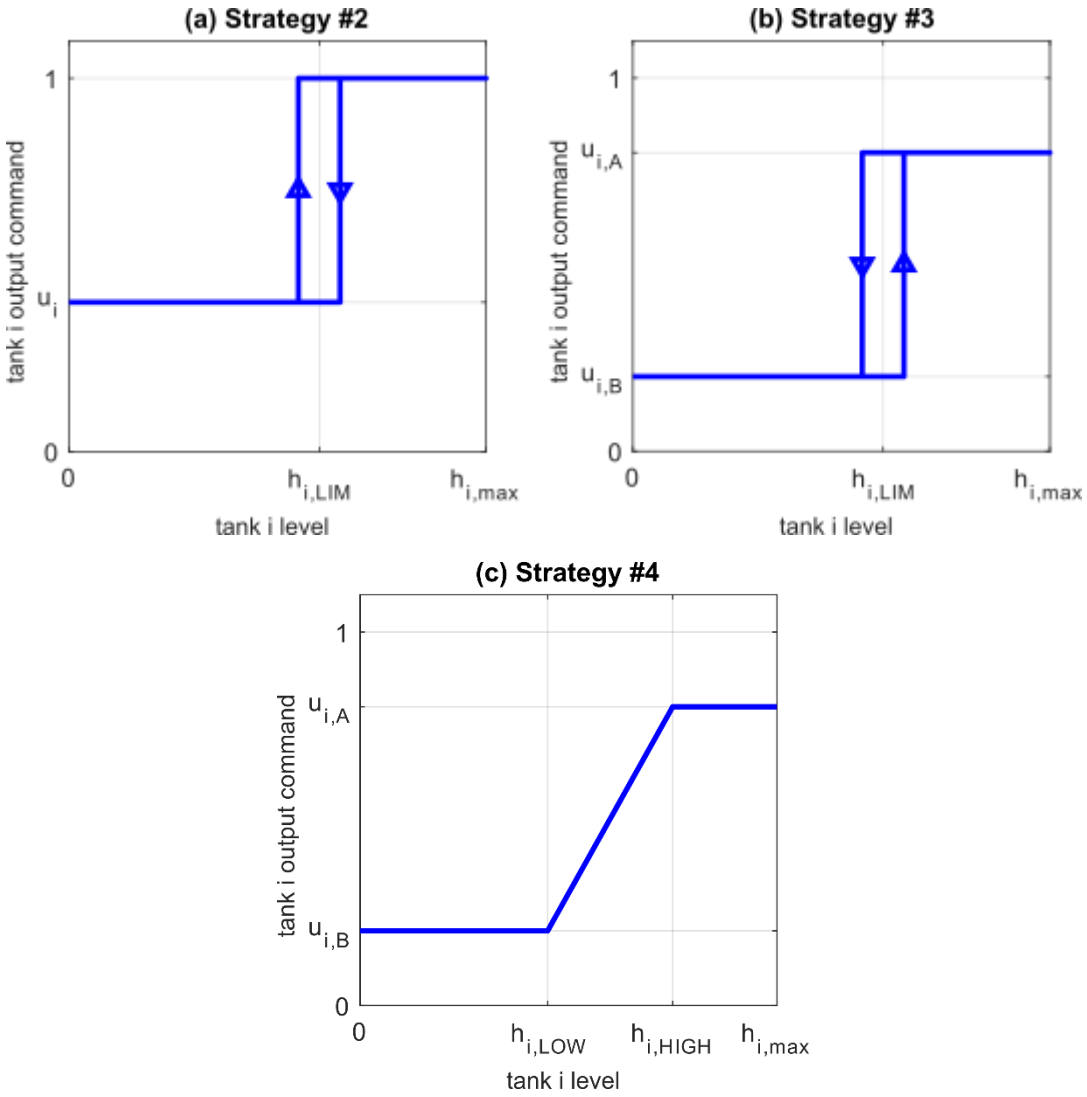


Figure 3.3 – Output command depending on liquid level in tank
(a) Strategy #2; (b) Strategy #3; (c) Strategy #4

In Strategy #2, the valve / pump control of tank i will be u_i if the wastewater level in that tank is below a certain limit $h_{i,LIM}$. In the contrary case, the valve / pump control of tank i will be 100% (see Figure 3.3a). This way, the overflow of the current tank will be as lowest as possible, as the output control is kept at maximum if the wastewater level is exceeding a certain limit. Moreover, a hysteresis has been considered around $h_{i,LIM}$ to prevent the quick change of the control when the wastewater level is around the limit. Thus, for each of the 3 tanks whose outputs are subject to optimization, the GA will determine the optimal values for $h_{i,LIM}$ and u_i ($i = \overline{1..3}$) that minimizes the fitness function. Figure 3.4 shows the chromosome structure for this strategy.

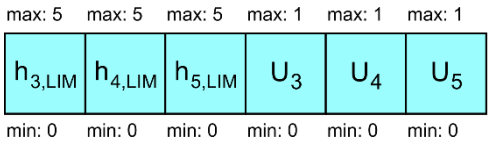


Figure 3.4 – The chromosome structure in Strategy #2

In Strategy #3, the valve / pump control of tank i will be $u_{i,A}$ if the wastewater level in that tank is above a certain limit $h_{i,LIM}$. In the contrary case, the valve / pump control of tank i will be $u_{i,B}$

(see Figure 3.3b). There are no inequality constraints between $u_{i,A}$ and $u_{i,B}$. This way, when the wastewater level exceeds the limit, the new control value can be either higher than the previous one, helping the current tank to overflow less, or smaller than the previous one, helping the downstream tanks to overflow less. Moreover, a hysteresis has been considered around $h_{i,LIM}$ to prevent the quick change of the control when the wastewater level is around the limit. Thus, for each of the 3 tanks whose outputs are subject to optimization, the GA will determine the optimal values for $h_{i,LIM}$, $u_{i,A}$ and $u_{i,B}$ ($i = \overline{1..3}$) that minimizes the fitness function. Figure 3.5 shows the chromosome structure for this strategy.

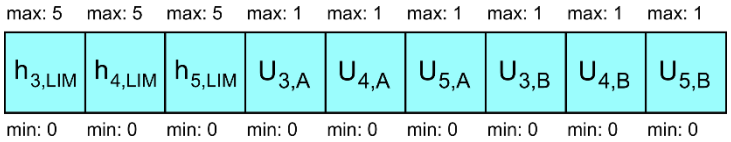


Figure 3.5 – The chromosome structure in Strategy #3

In Strategy #4, the valve / pump control of tank i will be $u_{i,A}$ if the wastewater level in that tank is above a certain limit $h_{i,HIGH}$, $u_{i,B}$ if the wastewater level in that tank is below a certain limit $h_{i,LOW}$ or a value scaled between $u_{i,A}$ and $u_{i,B}$ if the level is between $h_{i,LOW}$ and $h_{i,HIGH}$ (see Figure 3.6c). There are no inequality constraints between $u_{i,A}$ and $u_{i,B}$. Thus, for each of the 3 tanks whose outputs are subject to optimization, the GA will determine the optimal values for $h_{i,LOW}$, $h_{i,HIGH}$, $u_{i,A}$ and $u_{i,B}$ ($i = \overline{1..3}$) that minimizes the fitness function. However, $h_{i,LOW}$ must always be lower than $h_{i,HIGH}$, which will require at each step of the GA to validate the obtained solution. To avoid this, it will be considered that GA provides two values $h_{i,1}$ and $h_{i,2}$ which will be further used to determine $h_{i,LOW} = \min(h_{i,1}, h_{i,2})$ and $h_{i,HIGH} = \max(h_{i,1}, h_{i,2})$. Figure 3.6 shows the chromosome structure for this strategy.

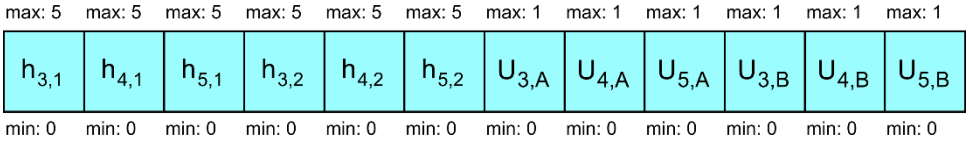


Figure 3.6 – The chromosome structure in Strategy #4

The last strategy is similar to Strategy #3, considering, this time, that the limit is at a fixed value $h_{i,LIM} = 3.5m$. This way the solution space dimension gets reduced by decreasing the number of genes in the chromosome, which should improve the convergence of the GA and will decrease the probability of getting stuck in a local minimum. Thus, for each of the 3 tanks whose outputs are subject to optimization, the GA will determine the optimal values for $u_{i,A}$ and $u_{i,B}$ ($i = \overline{1..3}$) that minimizes the fitness function. Figure 3.7 shows the chromosome structure for this strategy.

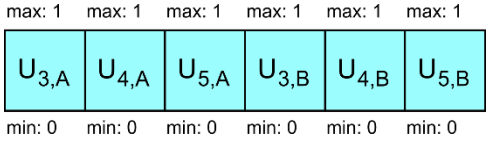


Figure 3.7 – The chromosome structure in Strategy #5

For each of the 5 strategies, the optimization algorithm has been run twice, the first time considering the fitness function to be V_{ovf} and the second time considering it to be OQI. Figure 3.8 shows the fitness function value evolutions for each of the strategies and fitness function.

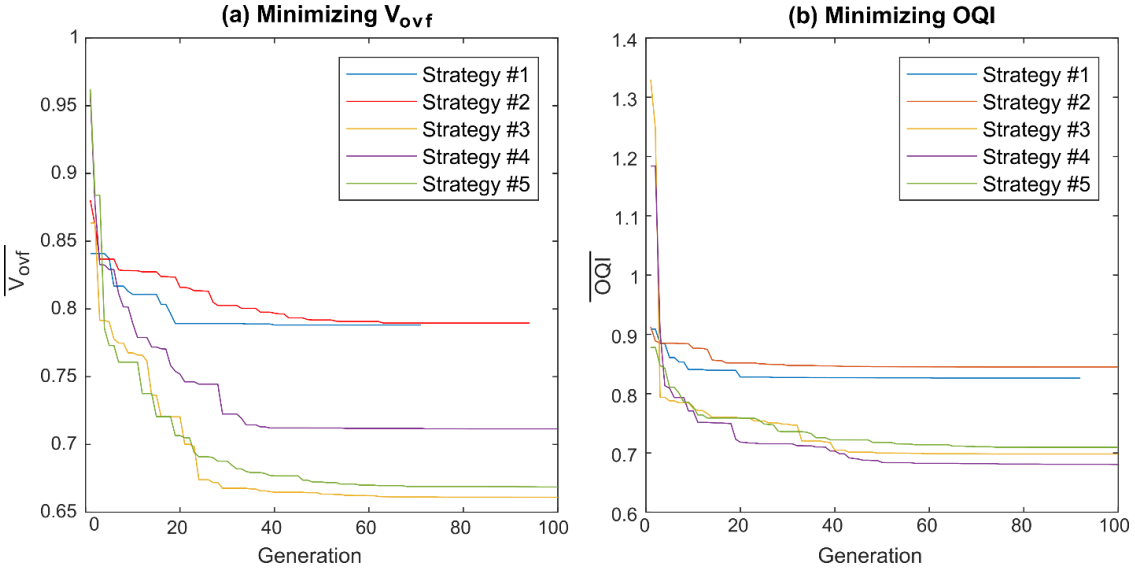


Figure 3.8 – Fitness function values evolutions
(a) when minimizing V_{ovf}; (b) when minimizing OQI

The solutions described in Table 3.1 and the performance indicators scaled with respect to their "no control" values and described in Table 3.2 have been obtained.

Table 3.1 – Solutions obtained with the five strategies

Strategy	Fitness function	Solution		
Strategy #1	V_{ovf}	$[u_3^* = 0.7$	$u_4^* = 0.8743$	$u_5^* = 0.6543]$
	OQI	$[u_3^* = 0.7062$	$u_4^* = 0.6872$	$u_5^* = 0.6742]$
Strategy #2	V_{ovf}	$\begin{bmatrix} h_{3,LIM}^* = 4.9192 \\ u_3^* = 0.7716 \end{bmatrix}$	$\begin{matrix} h_{4,LIM}^* = 0.2053 \\ u_4^* = 0.7983 \end{matrix}$	$\begin{bmatrix} h_{5,LIM}^* = 4.9896 \\ u_5^* = 0.6096 \end{bmatrix}$
	OQI	$\begin{bmatrix} h_{3,LIM}^* = 4.8716 \\ u_3^* = 0.6206 \end{bmatrix}$	$\begin{matrix} h_{4,LIM}^* = 4.7138 \\ u_4^* = 0.7312 \end{matrix}$	$\begin{bmatrix} h_{5,LIM}^* = 3.3904 \\ u_5^* = 0.9158 \end{bmatrix}$
Strategy #3	V_{ovf}	$\begin{bmatrix} h_{3,LIM}^* = 3.507 \\ u_{3,A}^* = 0.6997 \\ u_{3,B}^* = 0.8423 \end{bmatrix}$	$\begin{matrix} h_{4,LIM}^* = 4.3294 \\ u_{4,A}^* = 0.6910 \\ u_{4,B}^* = 0.8927 \end{matrix}$	$\begin{bmatrix} h_{4,LIM}^* = 2.0954 \\ u_{5,A}^* = 0.51 \\ u_{5,B}^* = 0.9836 \end{bmatrix}$
	OQI	$\begin{bmatrix} h_{3,LIM}^* = 3.3937 \\ u_{3,A}^* = 0.5510 \\ u_{3,B}^* = 0.9157 \end{bmatrix}$	$\begin{matrix} h_{4,LIM}^* = 0.8911 \\ u_{4,A}^* = 0.8598 \\ u_{4,B}^* = 0.8414 \end{matrix}$	$\begin{bmatrix} h_{5,LIM}^* = 3.9285 \\ u_{5,A}^* = 0.6190 \\ u_{5,B}^* = 0.9961 \end{bmatrix}$
Strategy #4	V_{ovf}	$\begin{bmatrix} h_{3,LOW}^* = 1.5247 \\ h_{3,HIGH}^* = 4.9168 \\ u_{3,A}^* = 0.6678 \\ u_{3,B}^* = 0.9829 \end{bmatrix}$	$\begin{matrix} h_{4,LOW}^* = 2.6187 \\ h_{4,HIGH}^* = 2.8814 \\ u_{4,A}^* = 0.6564 \\ u_{4,B}^* = 0.9976 \end{matrix}$	$\begin{bmatrix} h_{5,LOW}^* = 0.0654 \\ h_{5,HIGH}^* = 1.4234 \\ u_{5,A}^* = 0.6403 \\ u_{5,B}^* = 0.8426 \end{bmatrix}$
	OQI	$\begin{bmatrix} h_{3,LOW}^* = 2.265 \\ h_{3,HIGH}^* = 3.672 \\ u_{3,A}^* = 0.622 \\ u_{3,B}^* = 0.8871 \end{bmatrix}$	$\begin{matrix} h_{4,LOW}^* = 0.3715 \\ h_{4,HIGH}^* = 3.6782 \\ u_{4,A}^* = 0.8374 \\ u_{4,B}^* = 0.9323 \end{matrix}$	$\begin{bmatrix} h_{5,LOW}^* = 1.5886 \\ h_{5,HIGH}^* = 2.53 \\ u_{5,A}^* = 0.6492 \\ u_{5,B}^* = 0.9937 \end{bmatrix}$
Strategy #5	V_{ovf}	$\begin{bmatrix} u_{3,A}^* = 0.6085 \\ u_{3,B}^* = 0.9462 \end{bmatrix}$	$\begin{matrix} u_{4,A}^* = 0.8033 \\ u_{4,B}^* = 0.9008 \end{matrix}$	$\begin{bmatrix} u_{5,A}^* = 0.5609 \\ u_{5,B}^* = 0.7024 \end{bmatrix}$
	OQI	$\begin{bmatrix} u_{3,A}^* = 0.6626 \\ u_{3,B}^* = 0.9060 \end{bmatrix}$	$\begin{matrix} u_{4,A}^* = 0.4811 \\ u_{4,B}^* = 0.9955 \end{matrix}$	$\begin{bmatrix} u_{5,A}^* = 0.9417 \\ u_{5,B}^* = 0.9013 \end{bmatrix}$

Table 3.2 – Performances obtained with the five strategies

Strategy	Fitness function	$\overline{V_{ovf}}$	$\overline{OQI}$
Strategy #1	V_{ovf}	0.7882	0.8364
	OQI	0.8306	0.8263
Strategy #2	V_{ovf}	0.7896	0.8411
	OQI	0.8719	0.8449
Strategy #3	V_{ovf}	0.6611	0.6939
	OQI	0.7441	0.6981
Strategy #4	V_{ovf}	0.7116	0.7550
	OQI	0.6816	0.6806
Strategy #5	V_{ovf}	0.6686	0.7133
	OQI	0.7381	0.7094

The obtained results show that all optimal control strategies lead to significant improvements of the two performance indicators. The most efficient one in relation to V_{ovf} is Strategy #3 with a 33.89% reduction of the volume of overflow compared to the "no control" case ($\overline{V_{ovf}} = 0.6611$). The most efficient one in relation to OQI is Strategy #4 with a 31.94% reduction of OQI compared to the "no control" case ($\overline{OQI} = 0.6806$). However, the reduction of OQI when using Strategy #3 to minimize OQI is similar to the one obtained with Strategy #4, suggesting that Strategy #3 could be chosen as being the best one. For proving Strategy #3 reliability and robustness, the optimization procedure has been run 18 times for minimizing the volume of overflow resulting the statistical parameters described in Table 3.3.

Table 3.3 – Statistical parameters of Strategy #3 when minimizing V_{ovf}

	Maximum value	Minimum value	Mean value	Standard Deviation
$\overline{V_{ovf}}$	0.7890	0.6542	0.7015	0.0370
$\overline{OQI}$	0.8161	0.6939	0.7419	0.0386

Low values of the standard deviation have been obtained in relation to both performance indicators showing that the values of the two performance indicators are well grouped around the mean values. This proves that the strategy is robust and reliable.

3.2.1.2. Quantity vs. Quality

As observed in Table 3.2 and Table 3.3, minimizing V_{ovf} leads to decreased values of OQI and vice versa. Thus, it is important to understand the correlations between the two parameters to have the most suitable fitness function for the optimal control of the SN. This subsection aims at optimizing the efficiency of SN considering, this time, both performance indicators in the fitness function (MOO) and compare the results with the "no control" case, but also with the results obtained in the previous subsection when only SOO has been performed with respect to either V_{ovf} or OQI.

Two methods were approached for optimization, both being based on a controlled elitist GA [203]: a) **MOO** and b) **MOO in two steps** [204], [205]. For each of them, the values of the two performance indicators were scaled according to equations (3.1) and (3.2).

a) **the MOO algorithm** has the following characteristics:

1. the chromosome structure and number of genes according to Figure 3.5.
2. the population consists of 20 individuals, the initial one being randomly generated with a uniform distribution.
3. the selection operator chooses the parent chromosomes using a tournament mechanism. sets of 4 individuals are randomly chosen from the entire population. The best individual in each set becomes a parent.
4. the crossover operator: single point crossover.
5. the mutation operator: uniform mutation with a probability of 5%.
6. stop conditions: maximum number of generations reached or no improvements of the best function during the last 30 generations.

and, at each generation, follows the steps:

1. the parents are chosen from the current population using the tournament mechanism.
2. 16 offspring chromosomes are created using the two operators: crossover and mutation.
3. the fitness values for the offspring chromosomes are calculated.
4. an extended population is obtained by combining the offspring chromosomes with the current population.
5. a rank and a crowding distance [203] is calculated for each individual in the extended population.
6. the best 20 individuals from the extended population are selected to be in the next generation population.

The MOO algorithm has been run and the points on the Pareto Front that are graphically represented in Figure 3.9 has been obtained.

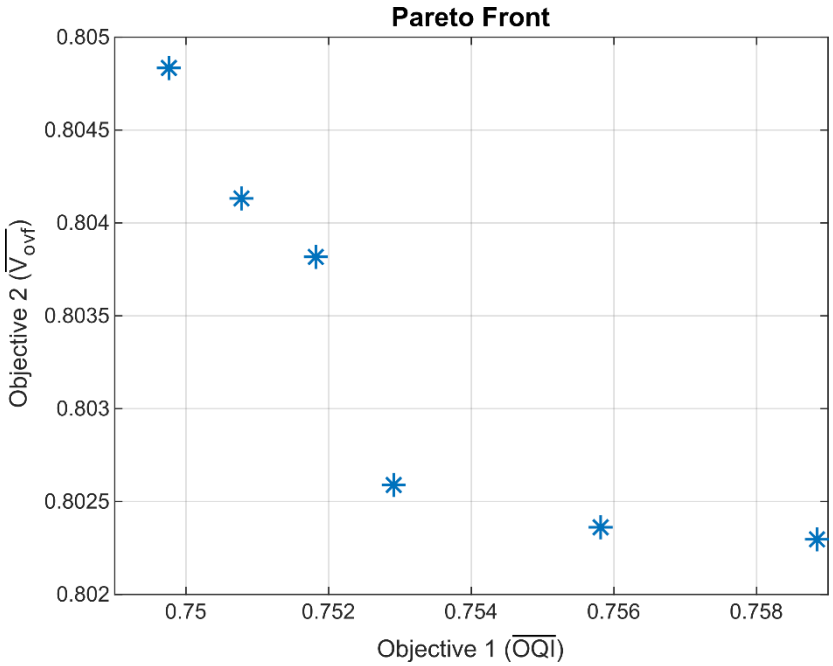


Figure 3.9 – The points on the Pareto Front

As noticed, the scaled values of V_{ovf} varies in the range $0.8023 - 0.8048$. This means that a reduction from the "no control" case ranging $19.52\% - 19.77\%$ have been obtained. On the other hand, the scaled values of OQI varies in the range $0.7498 - 0.7588$. This means that a reduction from the "no control" case ranging $24.12\% - 25.02\%$ have been also obtained.

The literature reports multiple methods that can be used for choosing the best compromise from the Pareto Front, all of them depending on the problem [206]: *Wald's criterion*, *Laplace's criterion*, *Hurwicz's criterion* etc. For the current problem, the *Nash Bargaining Solution* [207] will be used, as it is Pareto efficient and satisfies the monotonicity requirement (a principle of fair division). In this method, the chosen solution will be the one that maximizes the area of the rectangle defined by the point of disagreement (D) and the solution point, as represented in Figure 3.10.

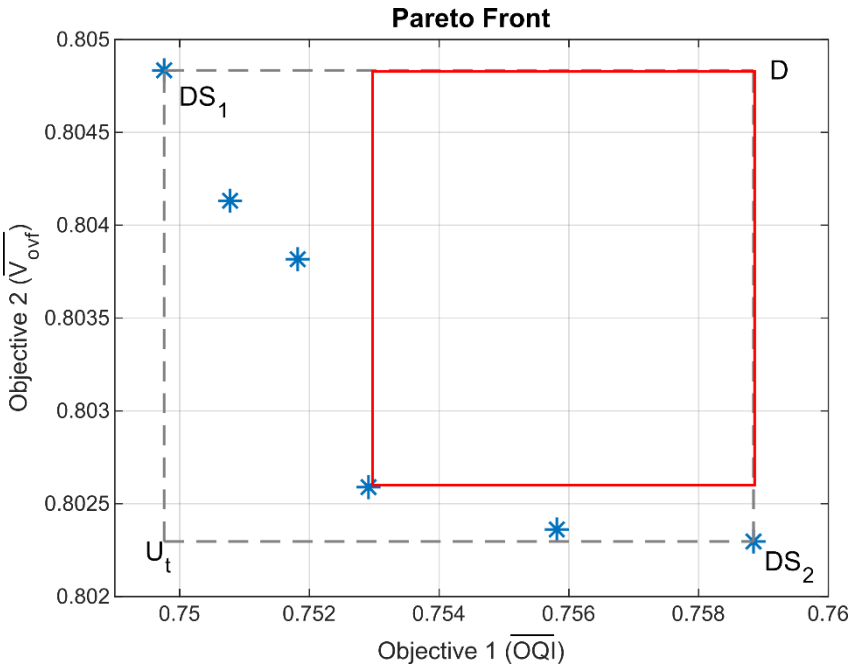


Figure 3.10 – Choosing the optimal solution using Nash Bargaining Solution

This way, the optimal solution described by Equation (3.4) has been obtained with a decrease of 19.74% of V_{ovf} and 24.71% of OQI, compared to the "no control" case.

$$\begin{bmatrix} h^*_{3,LIM} = 2.6064 & h^*_{4,LIM} = 1.6835 & h^*_{4,LIM} = 4.1865 \\ u^*_{3,A} = 0.6889 & u^*_{4,A} = 0.7109 & u^*_{5,A} = 0.9011 \\ u^*_{3,B} = 0.9927 & u^*_{4,B} = 0.7684 & u^*_{5,B} = 0.7793 \end{bmatrix} \tag{3.4}$$

Further, the MOO algorithm has been run 5 times obtaining the statistical parameters described in Table 3.4.

Table 3.4 – Statistical parameters of MOO algorithm solutions

	Maximum value	Minimum value	Mean value	Standard Deviation
$\overline{V_{ovf}}$	0.8053	0.7620	0.7874	0.0231
$\overline{OQI}$	0.8108	0.7529	0.7870	0.0245

Comparing the obtained results with the ones obtained when SOO has been separately performed for each of the performance indicators (see Table 3.2 and Table 3.3), it can be observed that the solution found using MOO is significantly worse than the solutions found when only one of the performance indicators was minimized. An explanation could be that the MOO algorithm tends to get trapped in local minimums and that it provides only a small portion of the Pareto Front, because the algorithm is an elitist one and the initial population is randomly chosen.

b) **the MOO in two steps algorithm** follows the procedure [208]:
   1. SOO is performed individually for both performance indicators.
   2. MOO is performed, including the SOO solutions in the initial population.

The SOO characteristics are the one presented in subsection 3.2.1.1 while the MOO characteristics are the one that were used for the MOO algorithm. The only differences on both algorithms' characteristics are the maximum number of generations that were chosen such as the total maximum number of fitness function evaluations (number of model numerical integrations) is the same, according to Figure 3.11.

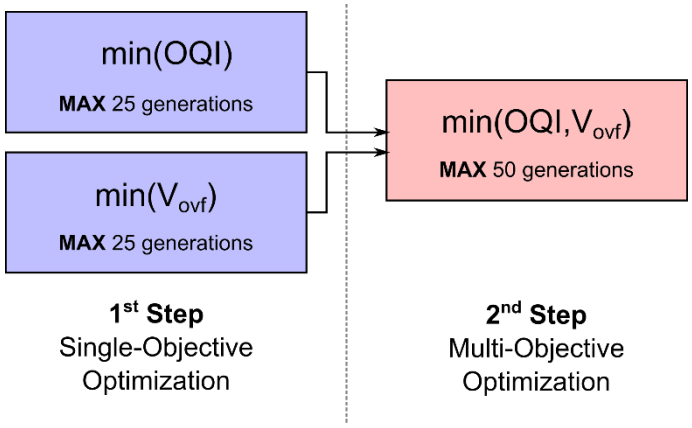


Figure 3.11 – The MOO in two steps algorithm

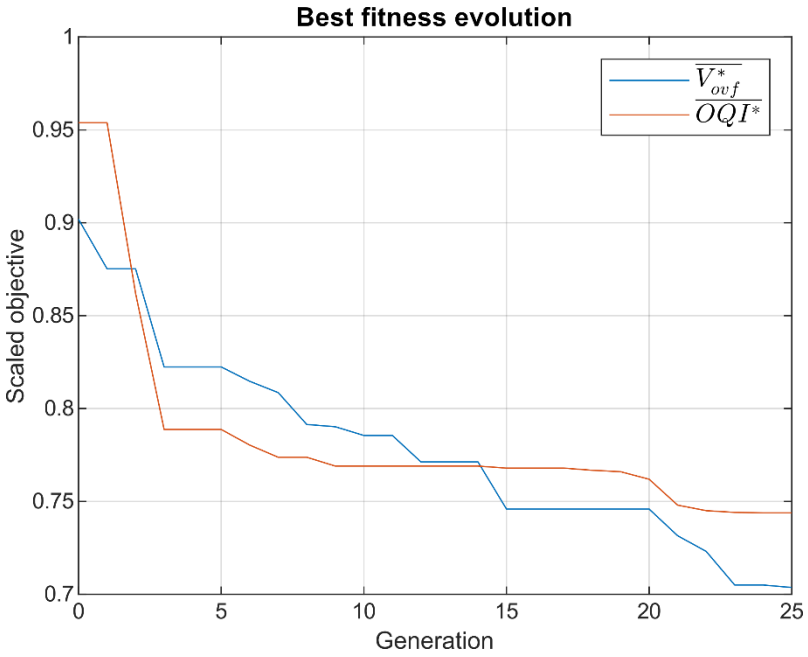


Figure 3.12 – The MOO in two steps algorithm – best fitness evolution during the SOO step

Firstly, OQI and V_{ovf} were separately minimized over 25 generations each obtaining the solutions with $\overline{OQI^*} = 0.7438$ and $\overline{V_{ovf}^*} = 0.7037$. Figure 3.12 shows the evolution of the best scaled fitness for each of the performance indicators.

After obtaining the SOO solutions, they were included in the MOO initial population, and the MOO algorithm has been run for 50 generations. The other 18 individuals in the MOO initial population were randomly generated. Figure 3.13 shows the SOO solutions alongside with the seven points on the Pareto Front obtained by running the MOO. All seven points on the Pareto Front are overlapping.

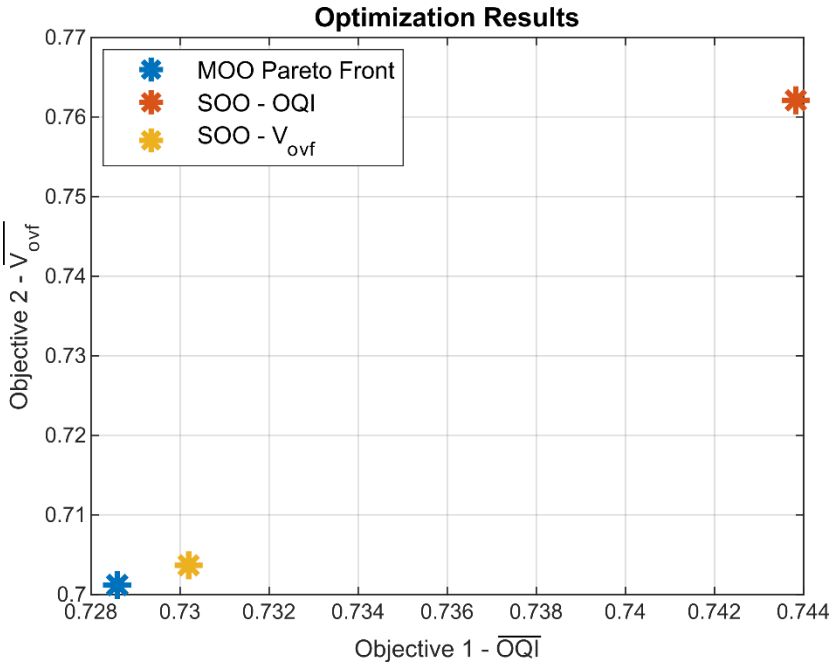


Figure 3.13 – The MOO in two steps algorithm – the optimisation results

This way, the optimal solution described by Equation (3.5) has been obtained with a decrease of 29.88% of V_{ovf} and 27.14% of OQI, compared to the "no control" case.

$$\begin{bmatrix} h_{3,LIM}^* = 1.3735 & h_{4,LIM}^* = 3.7458 & h_{4,LIM}^* = 1.9283 \\ u_{3,A}^* = 0.7775 & u_{4,A}^* = 0.5634 & u_{5,A}^* = 0.6545 \\ u_{3,B}^* = 0.9264 & u_{4,B}^* = 0.9993 & u_{5,B}^* = 0.9807 \end{bmatrix} \quad (3.5)$$

As observed, the obtained optimal solution is similar to the one obtained with SOO when minimizing V_{ovf}. Moreover, MOO in two steps provides only a small part of the Pareto Front, the points overlapping. This could be explained by the fact that there is a strong correlation between the two performance indicators, meaning that minimizing one of them, leads to minimizing the other one. However, SOO minimizing V_{ovf} is performing substantially better in terms of both performance indicators than SOO minimizing OQI. This is because of the geometry of the objective space. Thus, the analysis showed that V_{ovf} and OQI are strongly correlated, consequently, performing SOO minimizing V_{ovf} is the simplest solution to minimize the environmental impact of SN overflows.

3.2.1.3. Optimization algorithms

Proven that the best control strategy is Strategy #3 presented in subsection 3.2.1.1 and that the most suitable fitness function to be used for minimizing the environmental impact of SN overflows is V_{ovf}, the next step is to decide which optimization method would lead to the better results. For this reason, three more optimization methods where implemented [209]: 1. PSO, 2. Random generating the solution and 3. *FminSearch* algorithm. The results obtained with these three algorithms will be compared with the ones obtained when the GA was used as an optimization method (subsection 3.2.1.1).

1. The PSO algorithm is a metaheuristic one which is commonly used, in the same way as the GA, to find solutions for optimization problems. It is a swarm intelligence-based algorithm which defines a swarm of particles, each particle being a solution of the optimization problem that is moving in the search space. Each particle's velocity and position are updated using simple mathematical formulas [210]. In the implemented PSO algorithm, each particles movement depends on the best-known position of the particle and the best solution in the particle's neighbourhood [211], [212].

Thus, at every iteration, each particle velocity gets updated by summing to its inertia a cognitive and a social term:

$$v_{i+1} = w \cdot v_i + c_1 \cdot r_1 \cdot (p - x_i) + c_2 \cdot r_2 \cdot (g - x_i) \tag{3.6}$$

and each particle position is updated by:

$$x_{i+1} = x_i + v_{i+1} \tag{3.7}$$

where:

- x_i is the particle position at iteration i of the PSO algorithm.
- v_i is the particle velocity at iteration i of the PSO algorithm.
- p is the best-known position of the particle.
- g is the best solution in the particle neighborhood (a set of particles randomly chosen at each iteration and consisting of one quarter of the swarm).
- w is the particle adaptive inertia (it modifies itself between 0.1 and 1.1 to prevent getting stuck in local minimums).
- c_1 is the self-adjustment weight and has a value of 1.49.
- c_2 is the social-adjustment weight and has a value of 1.49.
- r_1 and r_2 are two uniformly distributed random vectors with values between 0 and 1.

The implemented PSO algorithm has the following characteristics:

- swarm size: 20 particles.
- maximum number of iterations: 100.
- random generated initial population.
- stop conditions: maximum number of iterations reached or no improvements of the best fitness during the last 30 iterations.

The optimization algorithm was run for 18 times. Table 3.5 shows the statistical results of the 18 runs.

Table 3.5 – Statistical parameters of PSO algorithm solutions

	Maximum value	Minimum value	Mean value	Standard Deviation
$\overline{V_{ovf}}$	0.7486	0.6257	0.6757	0.0386
$\overline{OQI}$	0.7901	0.6678	0.7220	0.0386

As observed, a mean reduction of 32.43% for V_{ovf} and 27.80% for OQI has been obtained, which are better that the mean values obtained with the GA algorithm (29.85% for V_{ovf} and 25.81% for OQI – see Table 3.3). The standard deviation values obtained with GA and PSO are similar, proving that PSO method provides better results than GA.

2. Random generating the solution – In order to validate that PSO and GA algorithms are indeed converging to minimum, a number of solutions equal to the number of fitness evaluations for the two metaheuristic algorithms (2000 evaluations) were randomly generated and evaluated. Thus, the solution providing the best results led to a decrease of 21.20% for V_{ovf} and 17.47% for OQI which is far worse than the results obtained with GA and PSO. Figure 3.14 shows the probability distribution of the fitness evaluations of the 2000 randomly generated solution.

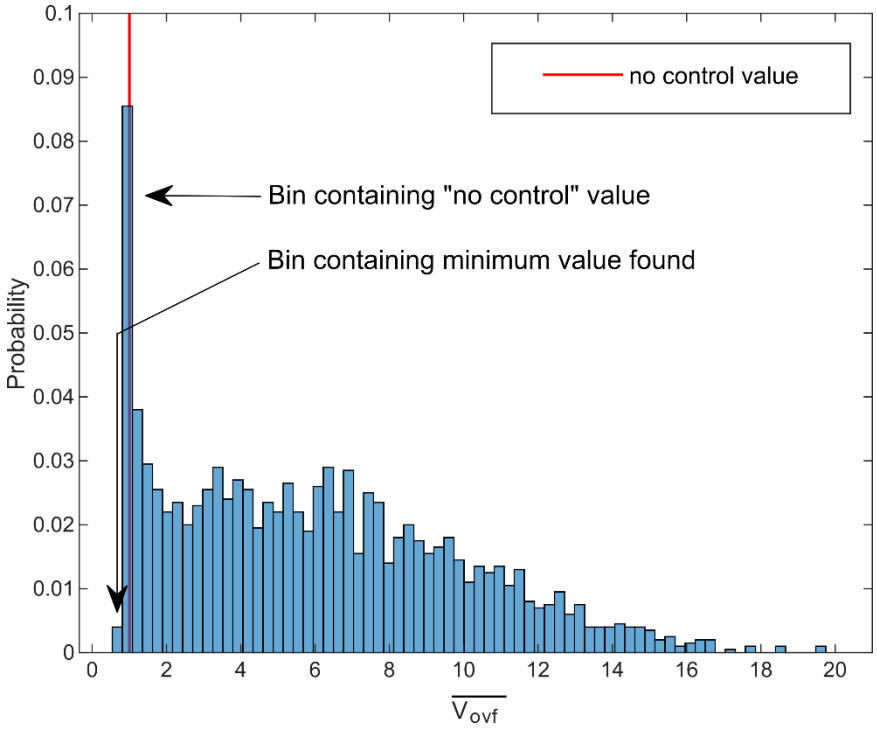


Figure 3.14 – The obtained probability distribution when randomly generating solutions

As observed, the bin with the highest probability (approximatively 9%) is the one that contains the values obtained in the “no control” case. The probability to obtain smaller values is under 1% (the bin containing the minimum values found). Consequently, in over 90% of cases, the random generated solution is worse than the “no control” case (all pumps running at 100% and all valves fully open).

3. FminSearch is a non-derivative heuristic optimization method which is using the Nelder-Mead simplex algorithm. It requires an initial point x_0 in the search space from where to start the objective function minimization [213]. The algorithm has been run from a series of initial points described in Table 3.6, the first one corresponding to the “no control” case, the second

corresponding to the situation in which all commands are at 50% and the last starting points are variants of the case when U_{TK3} and U_{TK4} are kept at 70% (see Table 2.7). The minimum fitness function found for each of the initial points can be seen in the last two columns of Table 3.6.

Table 3.6 – Initial points for FminSearch

Initial point no.	Initial point	$\overline{V_{ovf}}$	$\overline{OQI}$
1	$x_{0,1} = [5.0\ 5.0\ 5.0\ 1.0\ 1.0\ 1.0\ 1.0\ 1.0\ 1.0]$	0.7890	0.8405
2	$x_{0,2} = [2.5\ 2.5\ 2.5\ 0.5\ 0.5\ 0.5\ 0.5\ 0.5\ 0.5]$	0.8168	0.7951
3	$x_{0,3} = [5.0\ 5.0\ 5.0\ 0.7\ 0.7\ 1.0\ 0.7\ 0.7\ 1.0]$	0.8422	0.7508
4	$x_{0,4} = [5.0\ 5.0\ 5.0\ 1.0\ 1.0\ 1.0\ 0.7\ 0.7\ 1.0]$	0.8447	0.6317
5	$x_{0,5} = [5.0\ 5.0\ 5.0\ 0.7\ 0.7\ 1.0\ 1.0\ 1.0\ 1.0]$	0.8909	0.8310

As observed, FminSearch provided the worse results, even worse than the previous case where the solutions were randomly generated.

Concluding, the evolutionary algorithms (GA and PSO) provided the best results (significant reduction of both performance indicators compared to the “no control” case), with the ones provided by PSO being slightly better. For this reason, in what follows, PSO will be considered as the optimization method.

3.2.1.4. Optimization using Sliding Window Technique

The forecasted influent is not 100% accurate for long time periods, differences being possible in all 3 influent components: domestic, pluviometric and industrial. For this reason, performing the optimization for the entire time horizon of 28 days (finding one set of optimal controls to be used for the entire period) is susceptible to disturbances induced by influent uncertainties. Thus, in this subsection, the previously described optimal control algorithm will be modified by including it in a Sliding Window-based algorithm [214]. This way, instead of finding the optimal controls for the entire 28 days period, the algorithm will look only for optimal controls to be applied for just one day. The optimization algorithm will be run considering the forecasted influent and will be validated on the disturbed influent scenario.

Considering that $CMDS(i)$ represents the control action of day *i* and that the optimization algorithm is the one that previously provided the best results on minimizing V_{ovf} (PSO), Figure 3.15 describes the implemented algorithm.

Using this strategy comes with a series of advantages compared to the previously performed optimizations (only one day at a time is needed for influent forecast and, because days with 0 overflow when all controls are at 100% will not be subject to optimization, a lower computational effort will be assured).

The Sliding-Window based optimization algorithm has been run for 20 times. Each of the 20 sets of optimal control actions were used for the entire time horizon of 28 days for the forecasted influent and for the disturbed influent, obtaining the statistical parameters presented in Table 3.7

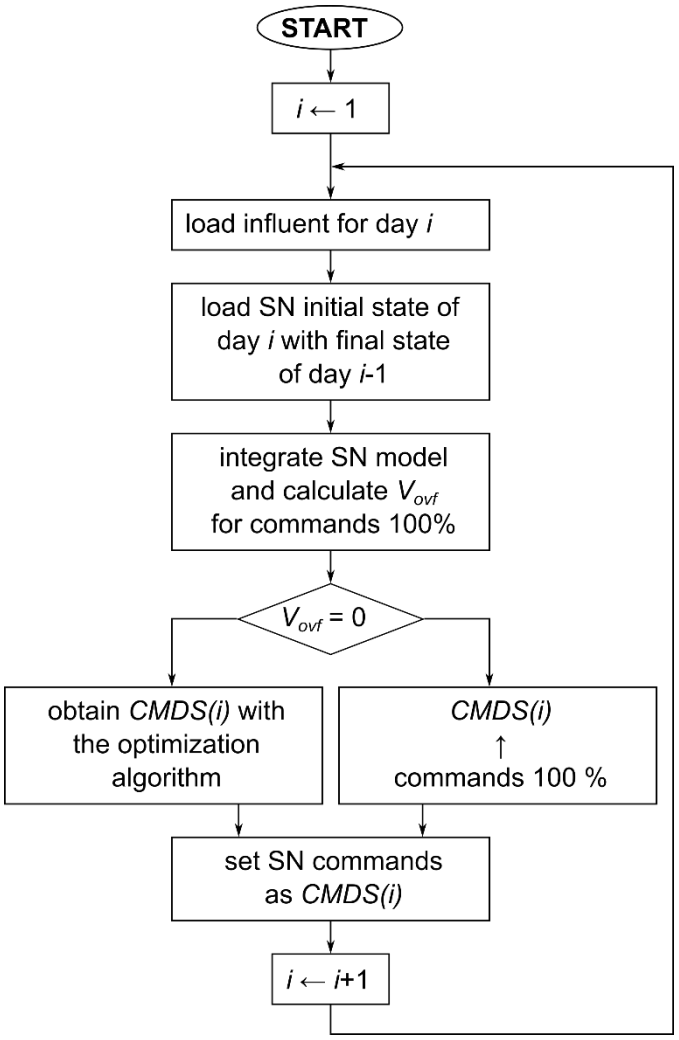


Figure 3.15 – The Sliding-Window based algorithm

Table 3.7 – Statistical parameters of Sliding-Window based PSO when minimizing V_{ovf}

Scenario		Maximum value	Minimum value	Mean value	Standard Deviation
Forecasted Influent	$\overline{V_{ovf}}$	0.4416	0.4137	0.4159	0.0064
	$\overline{OQI}$	0.4271	0.4042	0.4062	0.0054
Disturbed Influent	$\overline{V_{ovf}}$	0.4055	0.3480	0.3606	0.0160
	$\overline{OQI}$	0.4940	0.3755	0.3903	0.0270

As observed, a mean reduction of 58.41% for V_{ovf} and 59.38% for OQI has been obtained in the forecasted influent scenario and a mean reduction of 63.94% for V_{ovf} and 60.97% for OQI has been obtained in the disturbed influent scenario. This, alongside the low values of the standard deviations, prove that the Sliding-Window technique provides better results that running the optimization algorithm for the entire time horizon.

However, improvements in the results can be made by considering that at each 1-day time window, besides minimizing V_{ovf}, it is important to leave the SN in a state that could be helpful for future time windows. This could be achieved by trying to keep the wastewater level in the storage tanks at the end of the optimization window as low as possible. For this, a penalty term has been added into the fitness function to account for the wastewater levels in tanks. However,

acknowledging the fact that not all tanks are overflowing or subject to optimization, two variants of penalty have been implemented: one that uses only the wastewater levels in the tanks that are subject to optimization and one that uses the wastewater levels in all the tanks:

$$fitness_1 = V_{ovf} + w_p \cdot \sum_{i=3}^{5} h_i \tag{3.8}$$

$$fitness_2 = V_{ovf} + w_p \cdot \sum_{i=1}^{7} h_i \tag{3.9}$$

where w_p is the penalty weight.

For each of the two variants of penalty, the Sliding-Window based optimization algorithm has been run 20 times for $w_p = 1$ and for another 20 times for $w_p = 10$. Each of the obtained sets of optimal control actions were used for the entire time horizon of 28 days for the forecasted influent and for the disturbed influent, obtaining the statistical parameters presented in Table 3.8.

Table 3.8 – Statistical parameters of Sliding-Window based PSO with penalty term

Fitness function	w_p	Scenario		Maximum value	Minimum value	Mean value	Standard Deviation
$fitness_1$	1	Forecasted Influent	$\overline{V_{ovf}}$	0.4288	0.4135	0.4152	0.0038
			$\overline{OQI}$	0.4177	0.4036	0.4057	0.0036
		Disturbed Influent	$\overline{V_{ovf}}$	0.4652	0.3480	0.3676	0.0264
			$\overline{OQI}$	0.5441	0.3755	0.3982	0.0372
	10	Forecasted Influent	$\overline{V_{ovf}}$	0.4298	0.4137	0.4175	0.0063
			$\overline{OQI}$	0.4213	0.4042	0.4078	0.0066
		Disturbed Influent	$\overline{V_{ovf}}$	0.3900	0.3477	0.3618	0.0127
			$\overline{OQI}$	0.4168	0.3755	0.3895	0.0131
$fitness_2$	1	Forecasted Influent	$\overline{V_{ovf}}$	0.4271	0.4137	0.4151	0.0031
			$\overline{OQI}$	0.4186	0.4042	0.4051	0.0032
		Disturbed Influent	$\overline{V_{ovf}}$	0.3542	0.3478	0.3489	0.0018
			$\overline{OQI}$	0.3805	0.3755	0.3765	0.0018
	10	Forecasted Influent	$\overline{V_{ovf}}$	0.4176	0.4133	0.4144	0.0014
			$\overline{OQI}$	0.4046	0.4036	0.4044	0.0004
		Disturbed Influent	$\overline{V_{ovf}}$	0.4624	0.3478	0.3586	0.0311
			$\overline{OQI}$	0.5455	0.3755	0.3872	0.0397

The results shows that the algorithm performed better for the forecasted influent when $fitness_2$ was minimized using a penalty weight of $w_p = 10$. Analyzing the mean reductions, the differences compared to the other cases are small (under 0.5%). However, for the disturbed influent, the best results were obtained with the same penalty variant, but with $w_p = 1$. For this scenario, the differences in the mean reduction, compared to the other results, are still small (around 1 – 2 %), but the lower values of the standard deviations shows that this case provides results that are tighter around the average value.

Acknowledging the fact that all cases provided mean values of reduction that are close, it must be proven that the result obtained with $fitness_2$ and $w_p = 1$ are statistically different from the results obtained when no penalty was considered. For this, the two sets of results (V_{ovf} under

disturbed influent scenario) were subject to Wilcoxon's rank sum test [215] for a significance level of 5%. The null hypothesis was rejected (the obtain *p*-value being $p = 0.00016$) proving that the two set are statistically different, therefore, $fitness_2$ with $w_p = 1$ provides the best result under the disturbed influent scenario).

3.2.2. Online optimal control

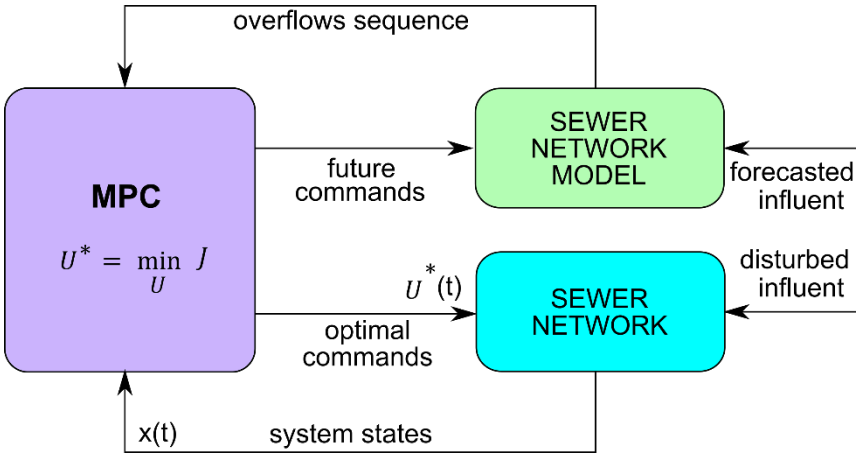


Figure 3.16 – The MPC structure

Further, the previously developed SN offline algorithm will be modified in an online optimal control algorithm [216] by including it in a MPC structure. MPC [217] is an advanced method that is used for controlling systems with higher complexity under the influence of a set of constraints. The algorithm requires an iterative optimization procedure to be applied on a system model over a finite time horizon (T_H – prediction horizon) that is continuously shifted forward with a certain step (T_S chosen such as $T_H = n_T \cdot T_S$ and $n_T \in \mathbb{N}$ is the number of steps in the prediction horizon). At any time t, the system state is sampled and set as the model initial state. After this, a fitness function is minimized over a time horizon ($[t, t + T_H]$), resulting a set of optimal controls $U^* = [u^*(t),\ u^*(t + T_S), u^*(t + 2 \cdot T_S), \dots, u^*(t + (n_T - 1) \cdot T_S)\ ]$. The first step from the computed optimal controls is applied to the real system ($u^*(t)$) and the procedures gets repeated starting from the moment $t + T_S$. Figure 3.16 shows the architecture of the MPC.

3.2.2.1. Model Predictive Control formulation

MPC usually requires three essential components:

1. a dynamic model of the system – as the optimization requires multiple numerical integrations of the process model, it must be assured that the model can be quickly integrated such as the optimization finishes within one step of the MPC. For this reason, the simplified model described in section 2.2.5 will be used as the process model.
2. a fitness function defined over the prediction horizon – the global yearly overflow volume:

$$J = V_{ovf} = \sum_{i=1}^{N} V_{ovf,TKi} \tag{3.10}$$

3. an optimization algorithm to be used for minimizing the fitness function by computing the optimal control actions – PSO algorithm with the same characteristics as the ones used in subsection 3.2.1.3, excepting:
   - the initial population includes the solution found at the previous MPC step, a solution encoding the "no control" case (all valves and pumps at 100%) and 18 randomly generated solutions.
   - the particle position in the search space defined by Equation (3.11) subject to $U_{TKi} \in [0, 1]$.

$$x = \begin{bmatrix} U_{TK3}(t) & U_{TK3}(t+T_S) & U_{TK3}(t+2\cdot T_S) & \dots & U_{TK3}(t+(n_T-1)\cdot T_S) \\ U_{TK4}(t) & U_{TK4}(t+T_S) & U_{TK4}(t+2\cdot T_S) & \dots & U_{TK4}(t+(n_T-1)\cdot T_S) \\ U_{TK5}(t) & U_{TK5}(t+T_S) & U_{TK5}(t+2\cdot T_S) & \dots & U_{TK5}(t+(n_T-1)\cdot T_S) \end{bmatrix} \quad (3.11)$$

3.2.2.2. Model Predictive Control parameters

The algorithm's two parameters, namely the prediction horizon time (T_H) and the step size (T_S), should be carefully selected to ensure optimal controller performance. Several considerations must be considered when determining these parameters:

- The optimization time should be shorter than T_S. Given the characteristics of the PSO algorithm, the maximum number of fitness evaluations at each MPC step corresponds to the swarm size multiplied by the maximum iteration count, resulting in 2000 evaluations. Since each fitness evaluation involves numerical integration of the model, there will be 2000 integrations per MPC step. Consequently, T_S needs to be chosen so that the optimization time remains within this interval. As the simplified model integration takes approximately 3 seconds for the entire 28-day time horizon, and optimization involves integrating the model over the prediction horizon $[t, t+T_H]$, which is shorter than 28 days, a minimum step size of 1 hour should be enough to satisfy the optimization time constraint.
- T_S should be set at a sufficiently low value to ensure a fine resolution of the solution space.
- T_H should be a multiple of the step size T_S.
- T_H should be small enough to provide a reliable weather prediction interval.
- T_H should be large enough to provide a broader solution space.
- A trade-off between T_S and T_H needs to be struck to maintain a reduced number of solution dimensions during optimization. This balance ensures the algorithm converges towards the global minimum effectively.

3.2.2.3. Simulation results

The simulation results were obtained by using the simplified model (see section 2.2.5) as the dynamic model required by MPC and the model implemented in BSMSewer (see subchapter 2.2) as the process that have to be optimized, as presented in Figure 3.17. The simplified model uses the forecasted influent (see subsection 2.2.3.1), while the process uses the disturbed one (see subsection 2.2.3.2).

Three cases were considered: 1st case uses Equation (3.10) as the fitness function, 2nd case updates this fitness function by including weights related to pollutants quantity and 3rd case integrates a penalty function as presented in the previous subsection (3.2.1.4).

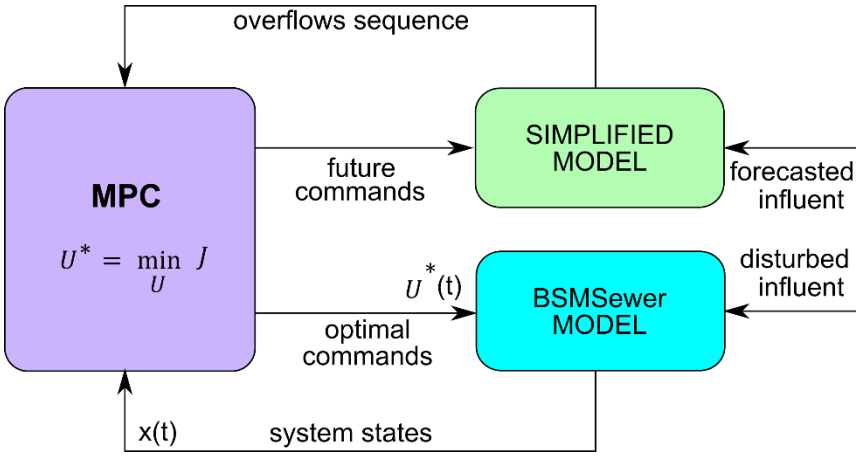


Figure 3.17 – The MPC simulation setup

1st case

In the first case, two sets of tests were considered: one set with $T_S = 1\ h$ and one set with $T_S = 2\ h$. For both sets, n_T was varied trough the values $\{3, 4, 6, 7, 12, 24\}$. Each of the 12 tests has been run 20 times resulting the statistical parameters presented in Table 3.9.

Table 3.9 – Statistical parameters of MPC (1st case)

T_S	n_T	T_H	Reduction of	Maximum value	Minimum value	Mean value	Standard Deviation
$1\ h$	3	$3\ h$	$\overline{V_{ovf}}$	0.5266	0.4664	0.7971	0.0135
			$\overline{OQI}$	0.7901	0.5434	0.5899	0.0513
	4	$4\ h$	$\overline{V_{ovf}}$	0.5278	0.4780	0.4996	0.0122
			$\overline{OQI}$	0.8801	0.5356	0.5970	0.0783
	6	$6\ h$	$\overline{V_{ovf}}$	0.5289	0.4692	0.4937	0.0174
			$\overline{OQI}$	0.8300	0.5330	0.6042	0.0723
	8	$8\ h$	$\overline{V_{ovf}}$	0.5329	0.4777	0.4987	0.0173
			$\overline{OQI}$	0.7871	0.5329	0.6025	0.0751
	12	$12\ h$	$\overline{V_{ovf}}$	0.5324	0.4619	0.4959	0.0177
			$\overline{OQI}$	0.7564	0.5067	0.5588	0.0531
	24	$24\ h$	$\overline{V_{ovf}}$	0.5298	0.4536	0.4946	0.0196
			$\overline{OQI}$	0.7180	0.4899	0.5713	0.0620
$2\ h$	3	$6\ h$	$\overline{V_{ovf}}$	0.5309	0.4644	0.5046	0.0206
			$\overline{OQI}$	0.7404	0.5228	0.6161	0.0615
	4	$8\ h$	$\overline{V_{ovf}}$	0.5573	0.4641	0.5095	0.0217
			$\overline{OQI}$	0.8064	0.5173	0.6010	0.0628
	6	$12\ h$	$\overline{V_{ovf}}$	0.5433	0.4403	0.4983	0.0250
			$\overline{OQI}$	0.6473	0.4788	0.5606	0.0460
	8	$16\ h$	$\overline{V_{ovf}}$	0.5429	0.4579	0.5032	0.0246
			$\overline{OQI}$	0.6517	0.4979	0.5820	0.0435
	12	$24\ h$	$\overline{V_{ovf}}$	0.5463	0.4735	0.5038	0.0270
			$\overline{OQI}$	0.6384	0.4735	0.5640	0.0453
	24	$48\ h$	$\overline{V_{ovf}}$	0.5394	0.4554	0.5067	0.0245
			$\overline{OQI}$	0.8070	0.4918	0.6113	0.0764

As observed, different values of the T_H do not significantly affect the average reduction of V_{ovf}. On the other hand, the standard deviation gets lower when T_H is smaller, which could be explained by the fact that the number of dimensions of the solution space increases with the increase of the value of T_H, therefore, the chance to get stuck in local minimums gets higher. Analyzing OQI, an average reduction of about 40 % can be observed. However, the standard deviation is higher, the reduction values ranging from 12% to 51%.

Concluding, T_H can be kept as low as possible in order not to increase the integration time of the model. Additionally, doubling T_S did not provide any significant improvements of neither the indicators. Moreover, a higher T_S value leads to the increase of the standard deviations of the V_{ovf} reduction (the obtained solutions are not so well grouped around the mean value).

The highest average reduction of V_{ovf} (50.63 %) has been obtained for $T_S = 1\ h$ with $T_H = 6\ h$ ($n_T = 6$), however, the differences between this and the other tests are not significant. On the other hand, the highest average reduction of OQI (44.12%) has been obtained for $T_S = 1\ h$ with $T_H = 12\ h$ ($n_T = 12$).

Figure 3.18 depicts the evolution of optimal commands during a pluviometric event. It highlights the filling levels of TK_3, TK_4, TK_5 and TK_6 when optimal commands are applied vs. the case of “no control”. The start of the pluviometric event is indicated by the green line, while the red marks an overflow event occurring in the absence of control measures. It is obvious that using the optimal commands effectively prevents this event by using the free space available in the other 3 tanks.

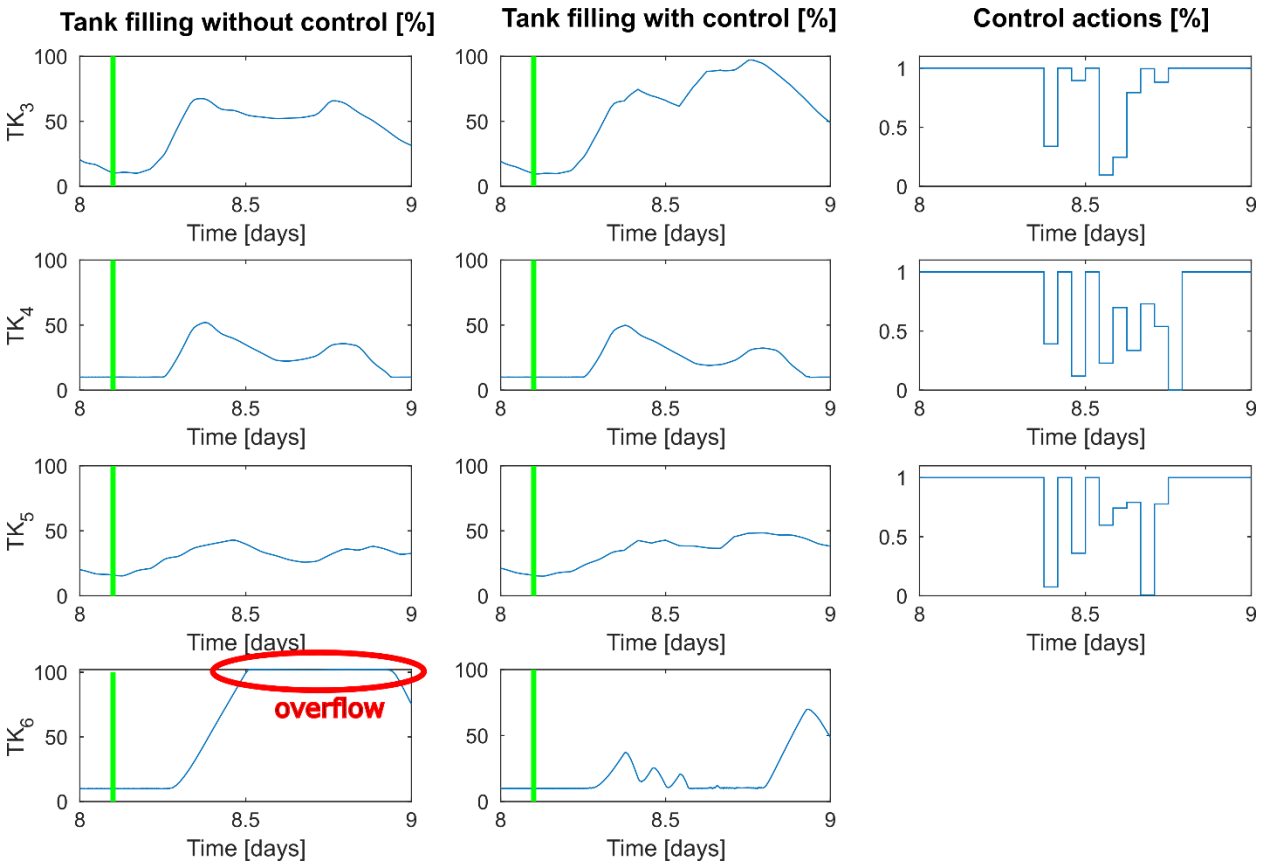


Figure 3.18 – Example MPC simulation result

2nd case

When analyzing Table 3.9, it could be observed that, for OQI, in all cases, the standard deviation is high (the reduction range from 12 % to 52 %), due to the fact that the solution space has many local minimums that provide similar reduction of V_{ovf}, but different reduction of OQI.

Because of this, it is necessary to differentiate between local minimums with similar reduction of V_{ovf}, but different reduction of OQI. Integrating OQI in the simplified model will lead to an increase in the model complexity and its integration time. Moreover, applying this solution in real-time control of SN will require expensive sensors to measure various loads in multiple points of the SN, leading to additional costs. In order to avoid this, another solution is proposed: offline measurement of pollutant concentrations from time to time and using these measurements to compute a set of weights w_{TKi}, one per storage tank, to be used in the fitness function to weight each tanks overflow volume:

$$J = \sum_{i=1}^{N} w_{TKi} \cdot V_{ovf,TKi} \tag{3.12}$$

For simulation and testing purposes, the weights w_{TKi} were determined using the medium loads in the storage tanks over 28 days. For each of the tanks, medium loads (without the weather component) were computed and converted to ASM2d variables [76]. Further, these variables were used to calculate a quality index QI_{TKi} for each storage tank in the same way that the effluent quality index gets calculated in BSM [77]. These quality indexes measured in $kg - polluting\ units/day$ are further divided by the medium flow, resulting quality indexes measured in $kg - polluting\ units/m^3$. Table 3.10 shows the obtained quality indexes.

Table 3.10 – Quality indexes for each tank

Quality Index QI_{TKi} $[kg - polluting\ units/m^3]$						
QI_{TK1}	QI_{TK2}	QI_{TK3}	QI_{TK4}	QI_{TK5}	QI_{TK6}	QI_{TK7}
5.2884	5.2884	5.2884	5.2884	6.1748	6.1074	6.3009

The quality indexes for the first four tanks share identical values due to their computation relying solely on the forecasted domestic influents from their respective collecting areas. As detailed in section 2.2.3, the forecasted domestic influent for each area is determined by multiplying the population equivalent with the average flow/loads per resident. This methodology results in a consistent pollutants concentration profile, independent of the population equivalent of the area, consequently leading to the uniformity of the quality index.

The resulted quality indexes were further scaled to the range $[1\ w_{max}]$ according to equation (3.13), resulting the weight w_{TKi}.

$$w_{TKi} = 1 + (w_{max} - 1) \cdot \frac{QI_{TKi} - \min(\{QI_{TKi} \mid i = \overline{1..7}\})}{\max(\{QI_{TKi} \mid i = \overline{1..7}\}) - \min(\{QI_{TKi} \mid i = \overline{1..7}\})} \tag{3.13}$$

Considering $T_S = 1\ h$ and $n_T = 6$ ($T_H = 6\ h$), 3 tests were carried out for 3 different values of w_{max}, each of them being run 20 times, obtaining the statistical parameters presented in Table 3.11. The results showed that weighting the overflow of each tank leads to small improvements in the mean reduction of V_{ovf} and substantial reduction (10 %) in the mean reduction of OQI

compared to the first case. The best V_{ovf} reduction occurs for $w_{max} = 2$, while the best reduction of OQI occurs for $w_{max} = 3$.

Table 3.11 – Statistical parameters of MPC (2nd case)

w_{max}	Reduction of	Maximum value	Minimum value	Mean value	Standard Deviation
2	$\overline{V_{ovf}}$	0.4929	0.4217	0.4661	0.0191
	$\overline{OQI}$	0.6964	0.4389	0.5051	0.0573
3	$\overline{V_{ovf}}$	0.5267	0.4234	0.4773	0.0275
	$\overline{OQI}$	0.6005	0.4316	0.4961	0.0415
4	$\overline{V_{ovf}}$	0.5199	0.4121	0.4779	0.0234
	$\overline{OQI}$	0.6373	0.4530	0.5137	0.0488

3rd case

The third case considers a penalty term related to the wastewater level in the storage tanks at the end of the prediction horizon, implemented in two variants, as presented in subsection 3.2.1.4. Thus, the following two fitness functions will be used:

$$J = \sum_{i=1}^{N} w_{TKi} \cdot V_{ovf,TKi} + w_p \cdot \sum_{i=3}^{5} h_i \tag{3.14}$$

$$J = \sum_{i=1}^{N} w_{TKi} \cdot V_{ovf,TKi} + w_p \cdot \sum_{i=1}^{7} h_i \tag{3.15}$$

For each of the two variants of penalty, the MPC has been run 20 times for $w_p = 1$ and 20 times for $w_p = 10$, obtaining the statistical parameters presented in Table 3.12.

Table 3.12 – Statistical parameters of MPC (3rd case)

J	w_p	Reduction of	Maximum value	Minimum value	Mean value	Standard Deviation
Equation (3.14)	1	$\overline{V_{ovf}}$	0.5256	0.4263	0.4719	0.0279
		$\overline{OQI}$	0.7609	0.4539	0.5017	0.0586
	10	$\overline{V_{ovf}}$	0.5064	0.4173	0.4749	0.0244
		$\overline{OQI}$	0.6987	0.4287	0.5078	0.0631
Equation (3.15)	1	$\overline{V_{ovf}}$	0.5075	0.4278	0.4719	0.0215
		$\overline{OQI}$	0.6760	0.4342	0.4961	0.0500
	10	$\overline{V_{ovf}}$	0.5250	0.4494	0.4888	0.0221
		$\overline{OQI}$	0.5880	0.4592	0.5182	0.0344

As observed, this time, the penalty term did not lead to any further improvements of the reduction of neither V_{ovf} nor OQI. Moreover, the penalty term just increased the computational effort of the PSO algorithm as the fitness function will never get 0, this stop condition of the optimization algorithm never being fulfilled).

3.2.2.4. Computational effort

An essential aspect in the implementation of MPC algorithms revolves around the integration time of the SN model. It becomes crucial to solve the optimization problem within a single MPC step. Moreover, a shorter integration enhances the adaptability of the MPC algorithm's parameterization which could lead to improved performances.

Hence, there exist three potential ways for reducing computational effort:

1. Using a simplified model with a briefer integration time, a topic which was explored in section 2.2.5 where SN model was simplified to diminish the integration effort. This simplification led to a reduction in integration time from 30 seconds to approximately 3 seconds over a 28-day time horizon.
2. Using parallel computing to integrate the model. The simplified model implementation in Simulink allows parallel execution, aiming at reducing the time of the metaheuristic optimization algorithm. However, the MATLAB Parallel Computing Toolbox requires additional time for pool initialization and cleanup. This added time must be outweighed by time savings from parallel computing. Hence, a computational machine equipped with more CPU cores is imperative to ensure the net reduction in optimization time surpasses the delays attributed to the MATLAB Parallel Computing Toolbox.
3. Using a more powerful computational machine to handle model integration.

To analyse the decrease of integration time when using a more powerful machine, experiments were conducted on four machines of varying specifications. The optimization algorithm was executed for a single prediction horizon ($T_S = 1\ h$ and $T_H = 6$) in both scenarios — with and without parallel computing — on each machine. Optimization times were recorded.

To ensure uniformity across all eight cases, the PSO algorithm retained only one stop criterion: reaching the maximum number of iterations (100). Consequently, each test requires precisely 2000 fitness evaluations, equivalent to 2000 integrations of the simplified model. Table 3.13 presents the outcomes of these computational effort tests.

As observed in the results, neither of the computational machines achieved a reduction in optimization time when using parallel computing due to the delays associated with loading and cleaning the parallel pool. Nevertheless, in scenarios without parallel computing, the optimization time is depending on the machine's capabilities, yielding times spanning from 32 minutes to 6 minutes, all of which provide to be enough for a MPC step. Opting for a more powerful computer yields a substantial reduction in optimization time. For instance, the most high-performance PC achieved a total optimization time of 6 minutes, translating to 3.479242 seconds per iteration of the PSO algorithm and a mere 173 milliseconds for each fitness function evaluation.

Clearly, using a high-performance computer for MPC holds the potential for significant optimization time reduction, enabling prospects for enhancing MPC performance by:

- decreasing the step size T_S to achieve enhanced solution space resolution.
- improving PSO algorithm performance through increasing the population size or increasing the maximum iteration count.

Table 3.13 – MPC computational effort tests results

Machine specifications	CPU cores	Optimization time without parallel computing [seconds]			Optimization time with parallel computing [seconds]	
		Total	Per iteration	Per fitness evaluation	Total	Per iteration
Intel® Core™ i5-6200U CPU @ 2.30GHz	2	1904.96	19.0496	0.95248	3729.46	37.2946
Intel® Core™ i5-10500T CPU @ 2.30GHz	6	653.51	6.5351	0.326755	2426.96	24.2696
Intel® Core™ i9-11900KF CPU @ 3.50GHz	8	416.68	4.1668	0.20834	1051.00	10.5100
Intel® Core™ i9-12900 CPU @ 3.40GHz	16	347.92	3.4792	0.17396	1072.03	10.7203

These enhancements can pave the way for further improvements in MPC performance, harnessing the advantages of a potent computing setup.

3.3. Wastewater Treatment Plant optimal control

The main goal on developing WWTP optimal control strategies is to reduce the environmental impact by optimizing the treatment efficiency of the plant while keeping at the same time a low operating cost. This can be achieved by manipulating a series of control values in the treatment process.

This subchapter will present three approaches regarding WWTP optimal control: a MPC strategy making use of the two NN models presented in the previous chapter (see section 2.3.1), a Fuzzy-Optimal control strategy and an Optimal-Setpoint-Based control strategy.

3.3.1. Model Predictive Control strategy based on Neural Network model

As the main goal of developing WWTP optimal control strategies is to reduce the environmental impact by optimizing the treatment efficiency of the plant while keeping at the same time a low operating cost, for the WWTP system presented in Figure 2.12 optimizing its efficiency can be achieved by controlling the aeration rate (W) in order to minimize the effluent substrate concentration (S). This will be achieved by using a MPC strategy.

MPC usually requires three essential components:

1. a dynamic model of the system – the two NN models described in section 2.3.1 will be used, resulting in two variants of the MPC.
2. a fitness function defined over the prediction horizon accounting for both efficiency and cost of treatment:

$$J = \int_{t}^{t+T_H} \left(\alpha \cdot W(\tau)^2 + (1-\alpha) \cdot \hat{S}(\tau)^2\right) d\tau \tag{3.16}$$

   where α is a weight that establishes the importance of each component.
3. an optimization algorithm to be used for minimizing the fitness function by computing the optimal control actions – *fmincon* algorithm [96] will be used to compute the optimal control actions:

$$W^* = \min_W J \tag{3.17}$$

   subject to $0 \leq W \leq 100$.

Figure 3.19 shows the structure of the MPC strategy involved in obtaining the following results [187]. As observed, some states are written in grey colour, meaning that they are available only for the 1st version of the NN model. Moreover, because the results were obtained in simulation, the mathematical model of the plant described by equations (2.8(2.8) – (2.11) has been used as the process to be controlled.

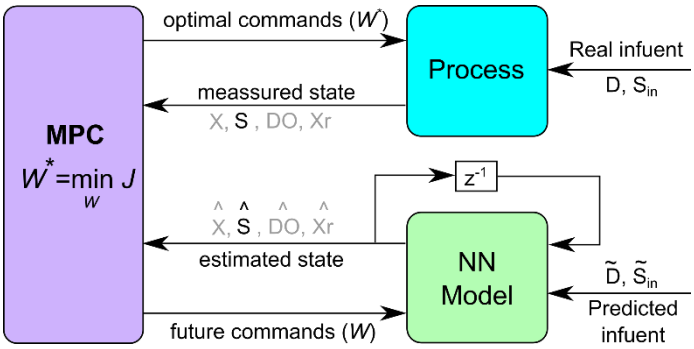


Figure 3.19 – The MPC control strategy

The obtained results were compared to a base case. The base case is represented by the value of the fitness function ($J^*_{base} = 5549862$) obtained when keeping the aeration rate at a constant value $W = 22.5522$ that assures minimum fitness function over the entire considered time horizon (609 days) when the generated influent described in the next subsection has been used.

3.3.1.1. The generated influent

The plant influent contains three variables:

1. D – the dilution rate
2. S_{in} – the substrate concentration
3. $DO_{in}(t)$ – the DO concentration – considered constant ($DO_{in}(t) = 2\ mg/l$)

D and S_{in} were generated for a time horizon of 609 days starting from the BSM2 dynamic influent [133] variables scaled to meet the plant specifications. More specific, D is inversely proportional to the flow of the BSM2 influent, while S_{in} is directly proportional to the readily biodegradable substrate (S_S) of BSM2 influent.

Figure 3.20 shows the dynamics of the generated influent for the first 30 days of the entire 609 days horizon.

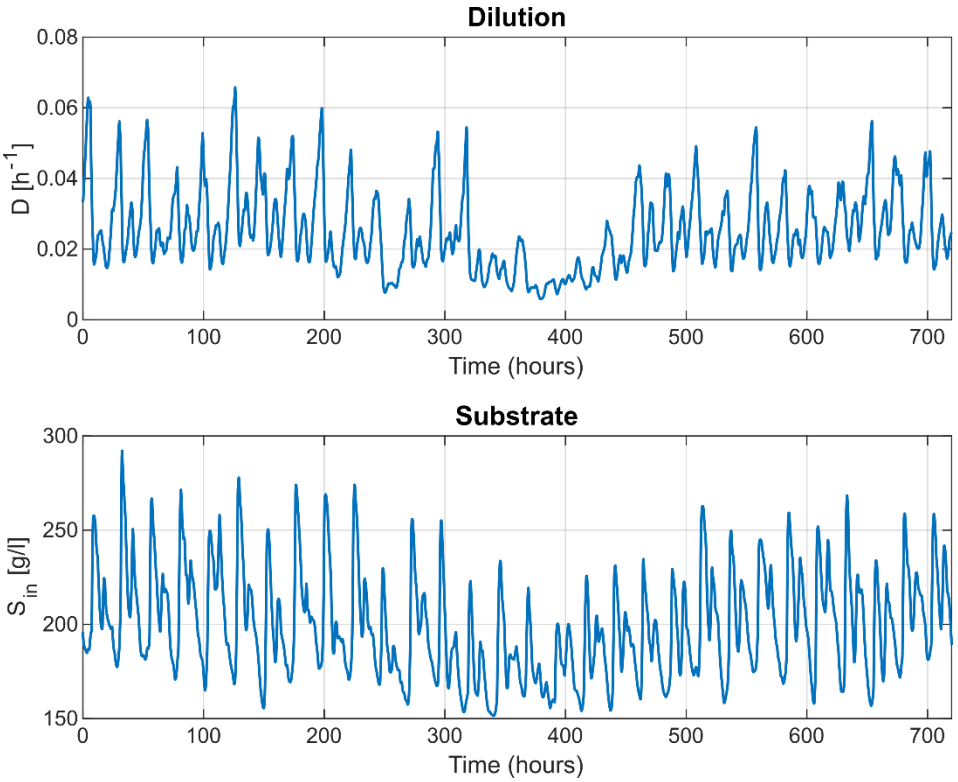


Figure 3.20 – The first 30 days of the generated influent

3.3.1.2. Model Predictive Control parameters

The algorithm's two parameters, namely the step size (T_S) and the prediction horizon time ($T_H = n_T \cdot T_S$), should be carefully selected to ensure optimal controller performance. This way, before obtaining results over the entire time horizon of 609 days, it is necessary to find the best values for the two MPC parameters. For this purpose, the following procedure is proposed [187]:

1. The MPC is run multiple times for the first 30 days of the influent considering all possible combinations of T_S and n_T with $T_S \in \{0.5, \overline{1 \dots 6}\}$ and $n_T \in \{\overline{1 \dots 24}\}$.
2. For each of the simulation results the following two indicators will be saved:
   - J_{30} – the value of the fitness function, calculated as in equation (3.16) for the entire 30 days horizon.
   - C_c – the computational cost being equal to the total number of NN model inferences.
3. Considering a factor $w_J \in [0, 1]$ meaning the importance of J_{30} over C_c, the best values of the two MPC parameters ($T_S{}^*$and $n_T{}^*$) can be determined as:

$$(T_S{}^*, n_T{}^*) = \min_{(T_S, n_T)} w_J \cdot J_{30} + (1 - w_J) \cdot C_c \tag{3.18}$$

For obtaining the following results a factor $w_J = 0.99$ has been considered.

3.3.1.3. Results obtained using the 1st version of NN model

This set of results was obtained while using the 1st version of the NN model described in subsection 2.3.1.1 as the process model in the MPC control structure described by Figure 3.19.

Before running the control algorithm for the entire time horizon of 609 days, the procedure described in the previous subsection has been used for determining the best values of the two MPC algorithm parameters. Thus, the best J_{30} value has been obtained for $T_S = 1\ h$ and $n_T = 10$ ($J_{30} = 186232$), however with a high computational cost ($C_c = 2158908$). In comparison, the best computational cost has been obtained for $T_S = 0.5\ h$ and $n_T = 1$ ($C_c = 44718$). Thus, for finding the MPC parameters that balances the performance and the computational effort, equation (3.18) has been involved. This way the best values of the MPC parameters were determined to be $T_S{}^* = 3\ h$ and $n_T{}^* = 3$. For these values, the two indicators have the following values: $J_{30} = 188508$ and $C_c = 309528$.

For the above determined MPC parameters, the algorithm has been run considering the entire time horizon of 609 days. Calculating the fitness value over the entire period, a value of $J_{v1}^* = 7106459$ has been obtained. Having in mind that this value is 28% higher than the value obtained in the base case $J_{base}^* = 5549862$, the implemented control structure is not proving its reliability when using the first version of the NN model.

Figure 3.21 shows an example of aeration rate and effluent substrate evolution during day no. 26 of the considered period. It should be noted that the substrate values are much higher in the MPC case than in the base case, while the aeration rate is continuously fluctuating putting stress on the controlled equipment.

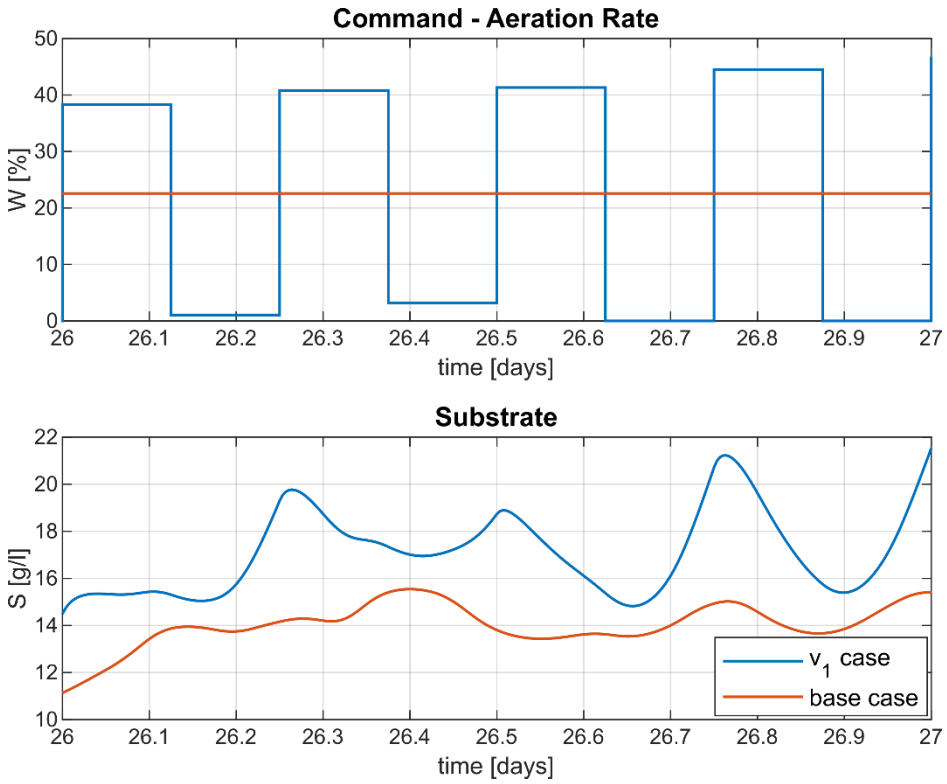


Figure 3.21 – Example of W and S evolution during day no. 26 (1st MPC version)

One explanation on obtaining worse results in this case than in the base case could be that the fitness space has multiple local minima and the optimization algorithm involved in the MPC control structure tends to get stuck in such a minimum.

3.3.1.4. Results obtained using the 2nd version of NN model

This set of results was obtained while using the 2nd version of the NN model described in subsection 2.3.1.2 as the process model in the MPC control structure described by Figure 3.19.

Before running the control algorithm for the entire time horizon of 609 days, the procedure described in subsection 3.3.1.2 has been used for determining the best values of the two MPC algorithm parameters. Thus, the best J_{30} value has been obtained for $T_S = 0.5\ h$ and $n_T = 20$ ($J_{30} = 184753$), however with a high computational cost ($C_c = 1924164$). In comparison, the best computational cost has been obtained for $T_S = 1\ h$ and $n_T = 1$ ($C_c = 80736$). Thus, for finding the MPC parameters that balances the performance and the computational effort, equation (3.18) has been involved. This way the best values of the MPC parameters were determined to be $T_S{}^* = 6\ h$ and $n_T{}^* = 2$. For these values, the two indicators have the following values: $J_{30} = 185389$ and $C_c = 239700$.

For the above determined MPC parameters, the algorithm has been run considering the entire time horizon of 609 days. Calculating the fitness value over the entire period, a value of $J_{v2}^* = 3735581$ has been obtained. Having in mind that this value is 32% lower than the value obtained in the base case $J_{base}^* = 5549862$, the implemented control structure is proving its reliability when using the 2nd version of the NN model.

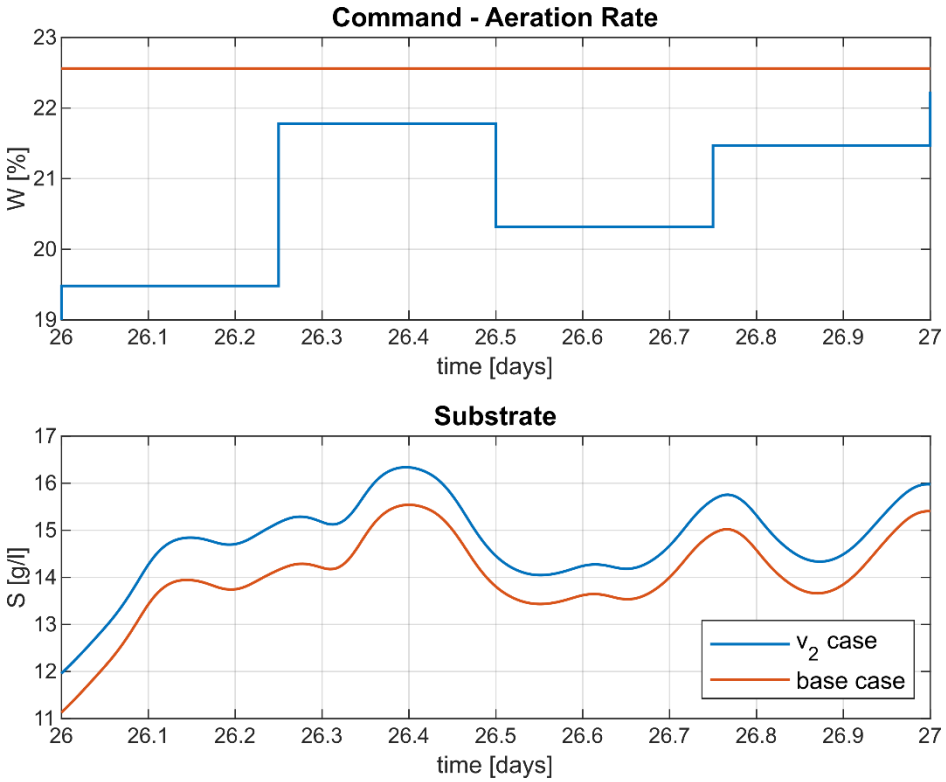


Figure 3.22 – Example of W and S evolution during day no. 26 (2nd MPC version)

Figure 3.22 shows an example of aeration rate and effluent substrate evolution during day no. 26 of the considered period. It should be noted that the substrate values are higher in the MPC case than in the base case, however, the fitness function value is lower because the treatment cost (the aeration rate) is lower than in the base case.

3.3.1.5. Results comparing

Both algorithm versions were tested in simulation considering an influent based on the BSM2 influent scenario. The obtained results were compared to a base case (aeration rate kept at a constant value). Figure 3.23 shows the evolution the fitness function for all the three considered cases, throughout the entire horizon of time.

As shown as in the above subsections, but also in the figure, the 1st version of the MPC algorithm (the one that is using the 1st version of the NN model) provides worse results than the base case. On the other hand, the 2nd version of the MPC algorithm (the one that is using the 2nd version of the NN model) provides better results than the base case. This is proving the reliability of the proposed control algorithm.

One explanation of the fact that the 1st version is worse than the base case, while the 2nd version is better, could be the fact that, in the 1st case, because all the state variables of the process are considered measurable, the NN model is able to correctly estimate even small variations in the organic substrate dynamics, leading to a complex geometry of the fitness space. This complex geometry of the fitness space implies a lot of local minima, increasing the chance that the optimization algorithm gets stuck in one of them, leading to the control algorithm performing worse.

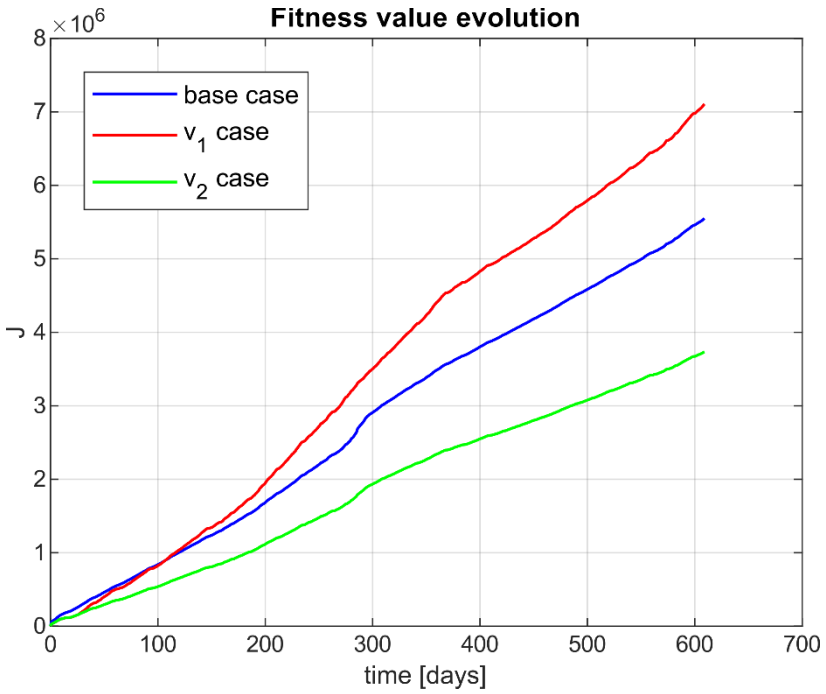


Figure 3.23 – The evolution of the fitness function in the three cases

Of course, in future research, the results could be even further improved by

- using an optimization algorithm that provides mechanisms for avoiding local minima.

- using more complex NN (i.e., LSTM, Temporal Fusion Transformer etc.) for estimating more process dynamics.
- considering more control variables (i.e., the recirculation rate, the excess sludge rate etc.).

3.3.2. Fuzzy-Optimal control strategy

This section describes an extension of the existing control strategy of the WWTP in Galați, a city in Romania, having approximatively 250,000 inhabitants, control strategy that is presented in [197]. The extension of this strategy considers, in addition to the optimal operating point regarding the dissolved oxygen concentration setpoint in the aerated bioreactors, applying a simple methodology to compute optimal values for the external recirculating rate based on the pluviometric regime using fuzzy techniques [218]. Moreover, the existing control strategy implies constant values for the sludge extraction rates from both clarifiers.

The results were obtained in simulation, using a model of the WWTP developed in SIMBA, which is similar to the BSM2 model [197]. Figure 3.24 shows, with red colour, the proposed control scheme, the fuzzy block being designed to determine the external recirculation flow by recognizing the pluviometric regime.

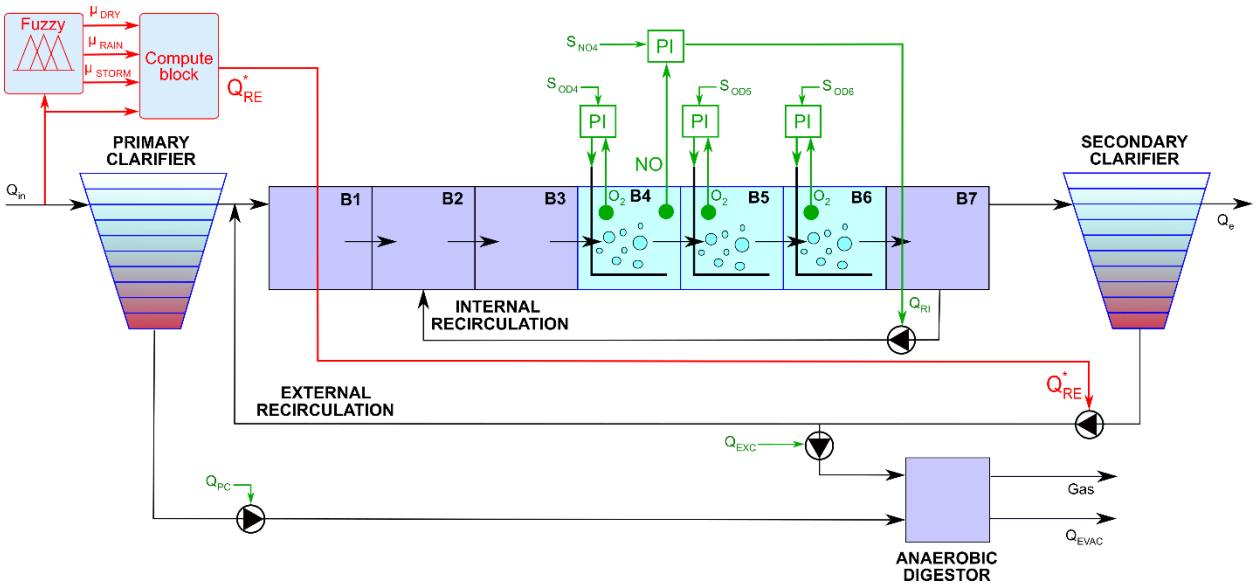


Figure 3.24 – The simplified scheme of the WWTP with the control strategy green lines denote existing control strategy, while the red line denotes the proposed extension

For evaluating the efficiency of the WWTP the following performance indicators were used:

- EQI – effluent quality index
- OCI – overall cost index
- J_3 – exceedances index, defined as:

$$J_3 = Ex\,[N_{tot} + NH_4 + TSS + COD + BOD_5] \tag{3.19}$$

where Ex represents the percentage time when the effluent of the WWTP exceeds the legal limits for: N_{tot} – total nitrogen, NH_4 – ammonium, TSS, COD and BOD_5.

- J – aggregated performance indicator, defined as:

$$J = 0.5 \cdot EQI + OCI + 100 \cdot J_3 \tag{3.20}$$

For simulation purposes, an WWTP influent with a time span of 210 days has been generated based on the BSM2 influent scenario [133] scaled to meet the plant specifications and combining three operating regimes of the WWTP: *DRY*, *RAIN* and *STORM*. The influent contains six *DRY* regimes with six *RAIN* ones and six *STORM* ones.

Figure 3.25 shows the influent flow for the first 70 days, with the rain and storm events highlighted. The loads related for each of the pluviometric regimes can be found, alongside an extensive description of the regimes in [197].

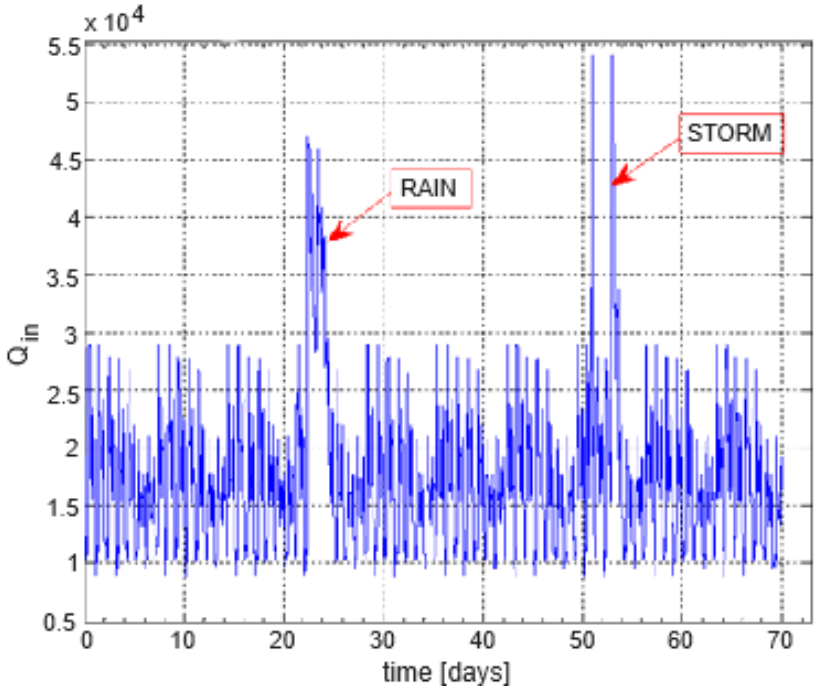


Figure 3.25 – First 70 days of the influent used for testing the fuzzy-optimal control strategy

Given the dependence of external recirculation flow on the influent flow in the form of:

$$Q_{RE,i} = k_i \cdot Q_{in}, \qquad i \in \{DRY, RAIN, STORM\} \tag{3.21}$$

for each of the pluviometric regime, calculating the optimal value of the external recirculation flow is done by solving the following optimal problem:

$$J_i^* = \min_{k_i} J \tag{3.22}$$

3.3.2.1. External recirculation flow rate optimal values in DRY regime

To obtain results in the DRY regime, k_{DRY} has been varied between 0.6 and 1.4, and the indicators EQI, OCI, J_3 (equation (3.19)) and J (equation (3.20)) were calculated, resulting in the values in Table 3.14.

Table 3.14 – Results obtained in the DRY regime

k_{DRY}	**0.6**	**0.7**	**0.8**	**0.9**	**1.0**	**1.2**	**1.4**
EQI	5369	5190	5163	5139	5156	5235	5354
OCI	2791	2930	3036	3131	3210	3343	3447
$Ex\,[N_{tot}]$	0	0	0	0	0	0	0
$Ex\,[NH_4]$	16	2	0	0	0	0	0
$Ex\,[NO]$	0	0	0	0	0	0	0
$Ex\,[TSS]$	0	0	0	0	0	0	0
$Ex\,[COD]$	0	0	0	0	0	0	0
$Ex\,[BOD]$	0	0	0	0	0	0	0
J_3	1552	215	0	0	0	0	0
J	7028	5739	5618	5700	5788	5960	6124

Figure 3.26 (a), (b) and (c) show the dependence of the three terms involved in the computation of the integrated performance indicator J (equation (3.20)) on k_{DRY}. It can be observed that the EQI indicator presents a minimum around the value of 0.9. OCI has a slow persistent increase, explained by the fact that the treatment cost increases when the external recirculation flow increases, due to pumping energy. On the other hand, J_3 decreases while k_{DRY} increases, reaching a value of 0 when k_{DRY} = 0.8. Figure 3.26 (d) shows the evolution of the integrated performance indicator as k_{DRY} increases. It can be observed that the minimum is reached for $k^*_{DRY} = 0.8$ ($J^*_{DRY} = 5618$), this value being selected for calculating the external recirculation flow during the DRY regime, according to equation (3.21).

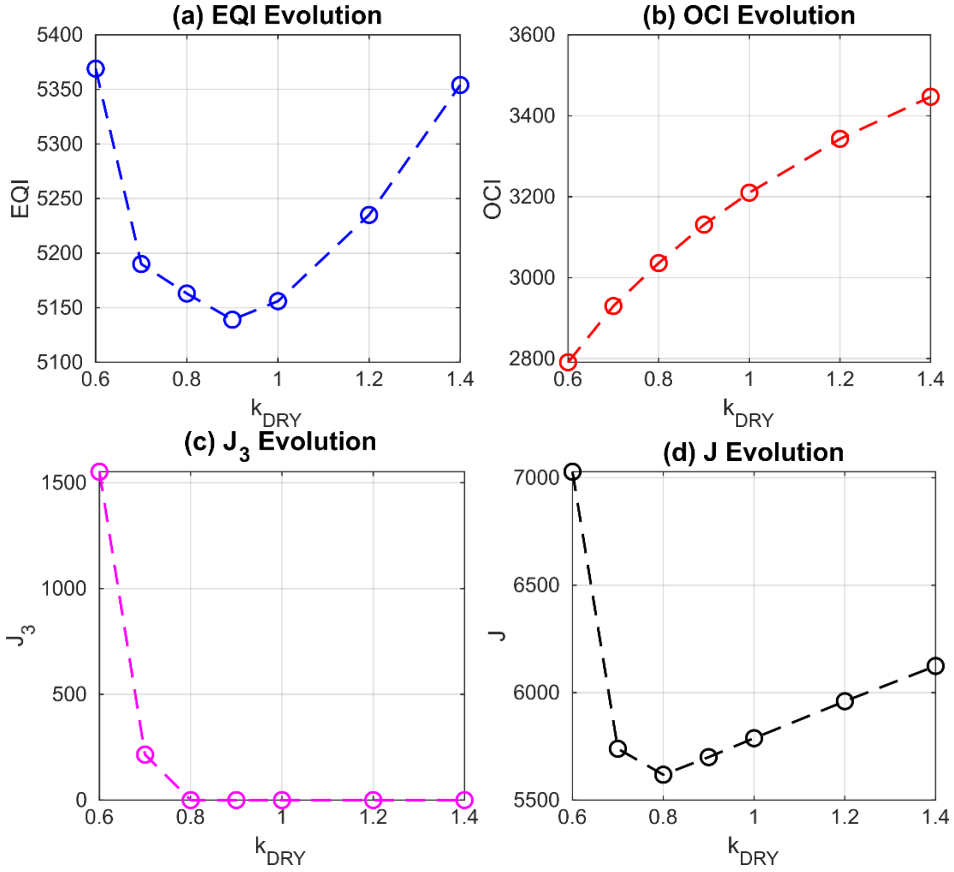


Figure 3.26 – The evolution of performance indicators as a function of k_{DRY}

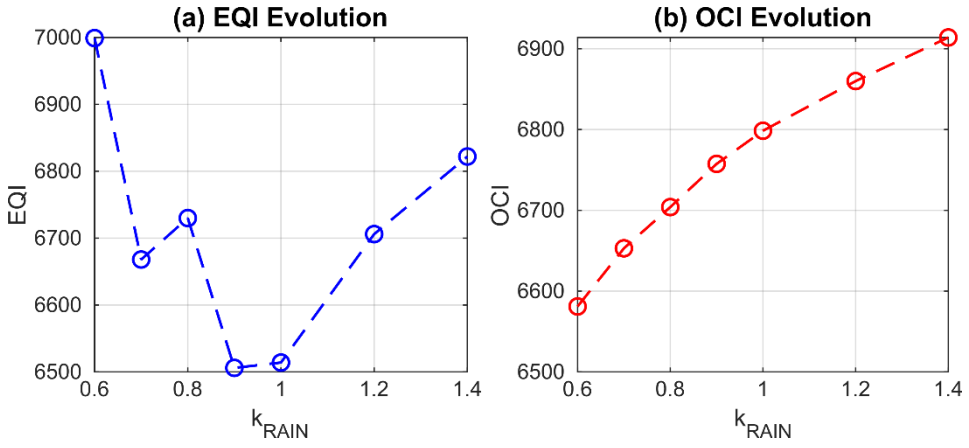
3.3.2.2. External recirculation flow rate optimal values in RAIN regime

To obtain results in the RAIN regime, k_{RAIN} has been varied between 0.6 and 1.4, and the indicators EQI, OCI, J_3 (equation (3.19)) and J (equation (3.20)) were calculated, resulting in the values in Table 3.15.

Table 3.15 – Results obtained in the RAIN regime

k_{RAIN}	0.6	0.7	0.8	0.9	1.0	1.2	1.4
EQI	6999	6668	6730	6506	6514	6706	6822
OCI	2762	2906	3008	3115	3197	3320	3428
$Ex\,[N_{tot}]$	0	0	0	0	0	0	0
$Ex\,[NH_4]$	53	31	22	8	3	1	0
$Ex\,[NO]$	0	0	0	0	0	0	0
$Ex\,[TS]$	0	0	0	0	1	7	9
$Ex\,[COD]$	0	1	3	4	5	6	8
$Ex\,[BOD]$	0	0	0	0	0	0	0
J_3	5277	3222	2532	1273	936	1432	1789
J	11538	9461	8905	7641	7390	8105	8628

Figure 3.27 (a), (b) and (c) show the dependence of the three terms involved in the computation of the integrated performance indicator J (equation (3.20)) on k_{RAIN}. It can be observed that the EQI indicator presents a minimum for $k_{RAIN} = 1$. OCI presents a similar behaviour as in the case of the DRY regime, however the increase rate is smaller. J_3 indicator presents a minimum value (936) for $k_{RAIN} = 1$. Figure 3.27 (d) shows the evolution of the integrated performance indicator as k_{AIN} increases. It can be observed that the minimum is reached for $k^*_{RAIN} = 1$ ($J^*_{RAIN} = 7390$), this value being selected for calculating the external recirculation flow during the RAIN regime, according to equation (3.21).



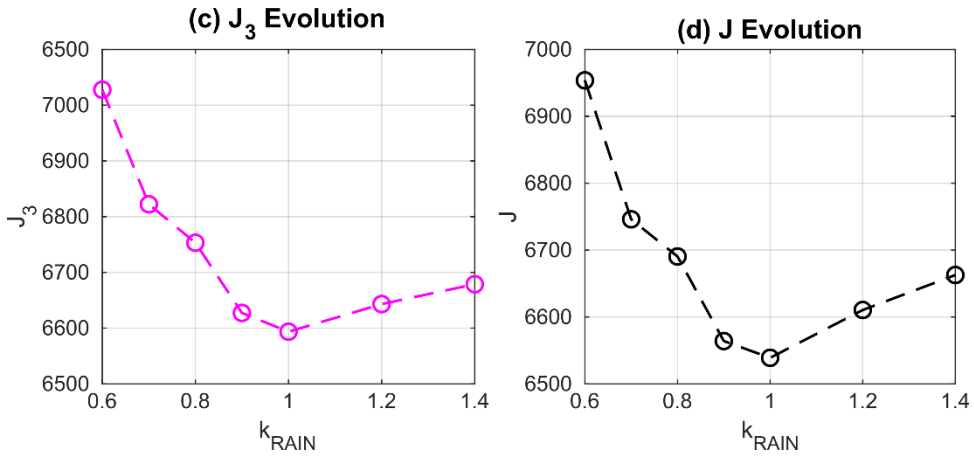


Figure 3.27 – The evolution of performance indicators as a function of k_{RAIN}

3.3.2.3. External recirculation flow rate optimal values in STORM regime

In the STORM regime, the results are presented in Table 3.16.

Table 3.16 – Results obtained in the STORM regime

k_{STORM}	**0.6**	**0.7**	**0.8**	**0.9**	**1.0**	**1.2**	**1.4**
EQI	6625	6265	6288	6156	6175	6305	6432
OCI	2830	2978	3080	3183	3263	3386	3492
$Ex\,[N_{tot}]$	0	0	0	0	0	0	0
$Ex\,[NH_4]$	50	27	20	9	4	0	0
$Ex\,[NO]$	0	0	0	0	0	0	0
$Ex\,[TSS]$	1	2	2	3	3	3	4
$Ex\,[COD]$	3	4	5	5	5	5	6
$Ex\,[BOD]$	0	0	0	0	0	0	0
J_3	5469	3239	2693	1608	1194	846	980
J	11612	9349	8918	7869	7544	7384	7688

Figure 3.28 (a), (b) and (c) show the dependence of the three terms involved in the computation of the integrated performance indicator J (equation (3.20)) on k_{STORM}. It can be observed that the EQI indicator presents a minimum (6156) around $k_{STORM} = 0.9$. OCI is increasing as k_{STORM} increases. On the other hand, J_3 decreases while k_{STORM} increases, reaching a minimum value of 846 when $k_{STORM} = 1.2$. Figure 3.28 (d) shows the evolution of the integrated performance indicator as k_{STOM} increases. It can be observed that the minimum is reached for $k^*_{STORM} = 1.2$ ($J^*_{STORM} = 7384$), this value being selected for calculating the external recirculation flow during the STORM regime, according to equation (3.21).

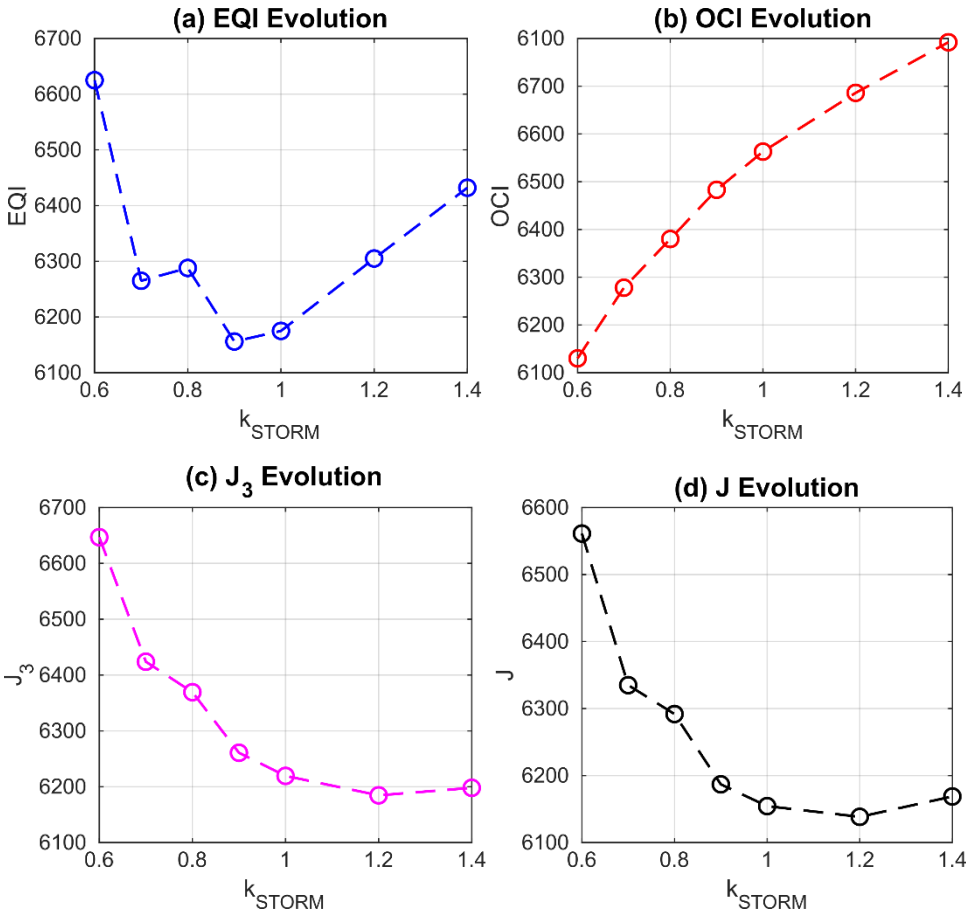


Figure 3.28 – The evolution of performance indicators as a function of k_{STORM}

3.3.2.4. Transitioning between pluviometric regimes

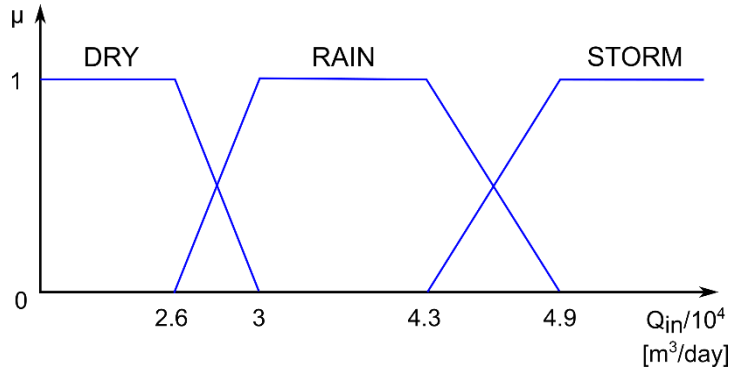


Figure 3.29 – Membership functions of Q_{in} to the operating regime

However, in reality, transitions between pluviometric regimes are not sudden, but gradual. Thus, it is important, in a transition between two regimes, to consider the optimal values of both regimes weighted with some membership degrees to the regimes. Determining some membership degree to the regimes can be made using fuzzy techniques. Hence, a fuzzy block described by the membership functions presented in Figure 3.29 has been implemented to determine the membership of Q_{in} to the pluviometric regimes.

Considering μ_i with $i \in \{DRY, RAIN, STORM\}$ the membership degree of Q_{in} to the pluviometric regime i, the optimal value of the external recirculation rate can be calculated according to:

$$Q_{RE}^* = k \cdot Q_{in} \tag{3.23}$$

where:

$$k = \sum_i \mu_i \cdot k_i^* \qquad i \in \{DRY, RAIN, STORM\} \tag{3.24}$$

Table 3.17 shows the values of the performance indicators obtained for all three pluviometric regimes (with their corresponding optimal value of k), together with the values obtained in the aggregated regime. As observed, the best values of the performance indicators are obtained in the DRY regime.

Table 3.17 – Results obtained in each regime and in the aggregate regime

Regime	DRY	RAIN	STORM	Aggregate regime
$\boldsymbol{k}$	0.8	1	1.2	according to equation (3.24)
$\boldsymbol{EQI}$	5163	6514	6305	5632
$\boldsymbol{OCI}$	3036	3197	3386	3070
$\boldsymbol{Ex\,[N_{tot}]}$	0	0	0	0
$\boldsymbol{Ex\,[NH_4]}$	0	3	0	7
$\boldsymbol{Ex\,[NO]}$	0	0	0	0
$\boldsymbol{Ex\,[TSS]}$	0	1	3	1
$\boldsymbol{Ex\,[COD]}$	0	5	5	2
$\boldsymbol{Ex\,[BOD]}$	0	0	0	0
$\boldsymbol{J_3}$	0	936	846	1000
$\boldsymbol{J}$	5618	7390	7384	6886

3.3.3. Optimal-Setpoint-Based control strategy

This section presents an optimal-setpoint-based control strategy [219], an extension of the fuzzy-optimal control strategy presented in the previous section. More specific, in this strategy, for each pluviometric regime $i \in \{DRY, RAIN, STORM\}$, the optimization algorithm will search for the optimal values of the following setpoints:

- $S_{OD4,i}^*$ – dissolved oxygen in bioreactor 4
- $S_{OD5,i}^*$ – dissolved oxygen in bioreactor 5
- $S_{OD6,i}^*$ – dissolved oxygen in bioreactor 6
- $S_{NO4,i}^*$ – nitrate concentration
- $Q_{RE,i}^*$ – external recirculation flow
- $Q_{PC,i}^*$ – sludge flow extracted from the primary clarifier
- $Q_{EXC,i}^*$ – excess sludge flow from the secondary clarifier

The obtained optimal values will be used for the current operating regime of the WWTP, or, in the case of regime transition, a fuzzy block (presented in Figure 3.29) will be used to account to the membership degree of the operating regimes. Figure 3.30 shows the schematic representation of the proposes control strategy.

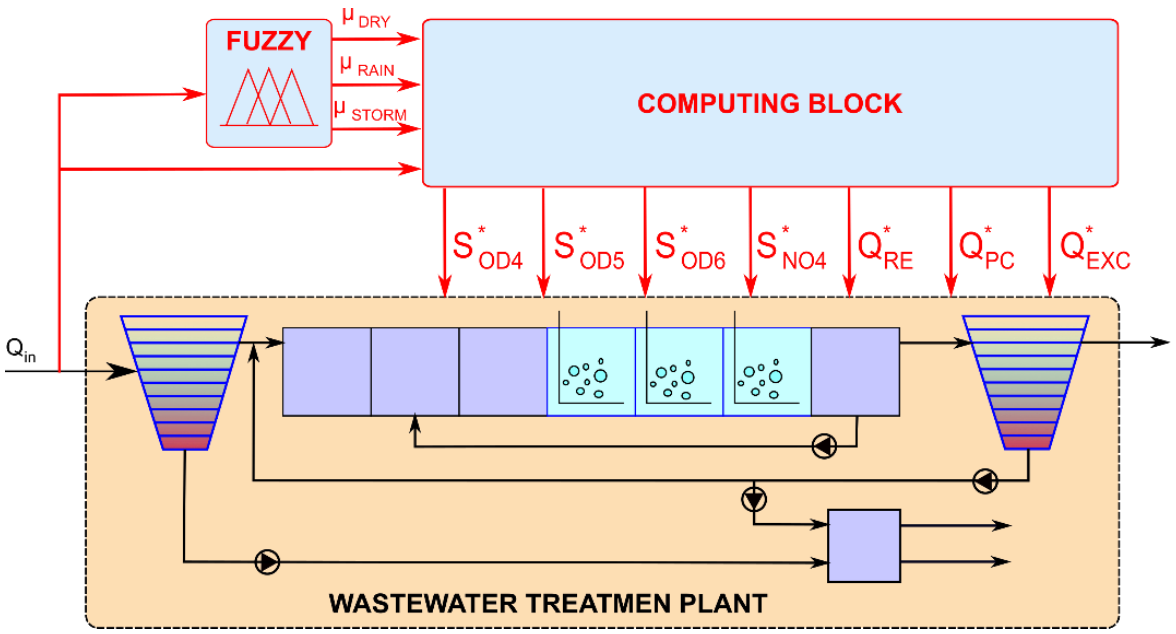


Figure 3.30 – The optimal-setpoint-based control strategy

For testing purposes, starting from the influent of BSM1 model [77], three influent scenarios were created, calibrated to the loads specific to the WWTP of Galați. Table 3.18 shows the WWTP design values and the measured average values over 2007 [197].

Table 3.18 – Average concentrations of the three influent scenarios

		WWTP Design Values			Measured Average Values		
No.	**Parameter**	**DRY**	**RAIN**	**STORM**	**DRY**	**RAIN**	**STORM**
1	$NH_4\ [g/m^3]$	36.77	34.09	35.20	31.65	29.34	30.80
2	$N_{tot}\ [g/m^3]$	60.65	56.17	58.74	40.39	37.43	39.42
3	$TSS\ [g/m^3]$	401.61	370.93	395.63	132	121.91	130.07
4	$BOD_5\ [g/m^3]$	342.96	316.91	336.89	133.66	123.60	131.10
5	$COD\ [g/m^3]$	637.89	593.92	628.87	236.93	219.95	233.12

The three influent scenarios were generated over a period of 16 weeks (112 days), of which the first 12 are used for getting the WWTP in a steady state regime, while the last 4 are used for assessing the control strategy performance. For testing the global operation of the WWTP, a fourth scenario has been generated by aggregating the 3 previously described scenarios. Figure 3.31 shows the four considered influent scenarios.

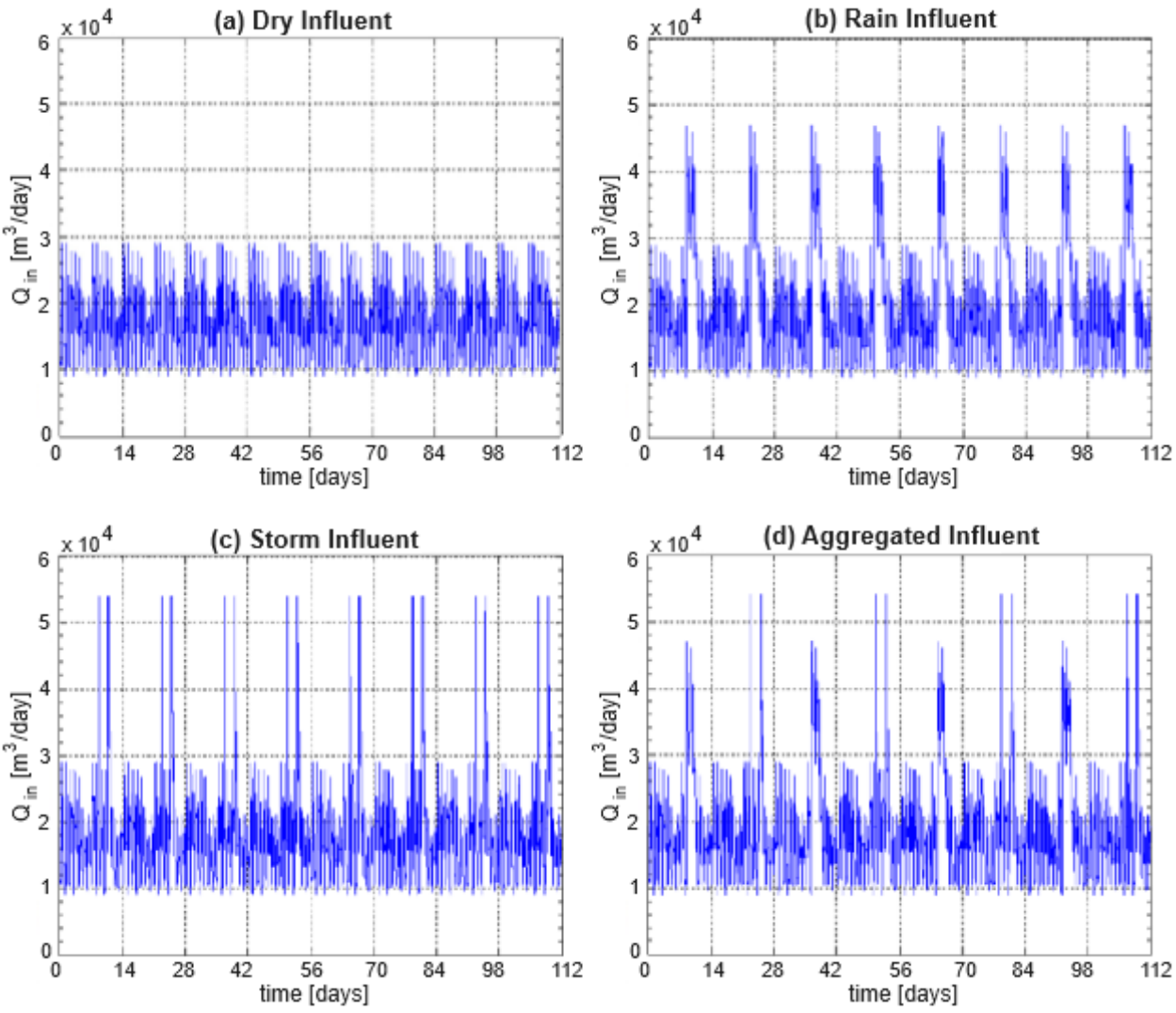


Figure 3.31 – Influent flow variations corresponding to the operating regimes (a) DRY, (b) RAIN, (c) STORM, (d) Aggregated

3.3.3.1. Computing the optimal setpoints

For each pluviometric regime $i \in \{DRY, RAIN, STORM\}$, the following vector of optimal setpoints will be calculated:

$$V_i^* = [S_{OD4,i}^* \quad S_{OD5,i}^* \quad S_{OD6,i}^* \quad S_{NO4,i}^* \quad Q_{RE,i}^* \quad Q_{PC,i}^* \quad Q_{EXT,i}^*] \tag{3.25}$$

However, having in mind the proportionality presented in equation (3.21) of the recirculation flow on the inflow (Q_{in}), the vector of optimal setpoints becomes:

$$V_i^* = [S_{OD4,i}^* \quad S_{OD5,i}^* \quad S_{OD6,i}^* \quad S_{NO4,i}^* \quad k_{RE,i}^* \quad Q_{PC,i}^* \quad Q_{EXT,i}^*] \tag{3.26}$$

with the limits of the vector components described in Table 3.19 and imposed for technological reasons.

This vector will be obtained by minimizing J, the integrated performance indicator defined by equation (3.20). Thus, for each of the pluviometric regime i, obtaining V_i^* is done by solving the following optimal problem:

$$V_i^* = \underset{V_i}{\operatorname{argmin}} J \tag{3.27}$$

Table 3.19 – Limits of the components of the optimal setpoints vector

Component	Unit	MIN	MAX
$S_{OD4,i}^*$	mg/l	0.3	4
$S_{OD5,i}^*$	mg/l	0.3	4
$S_{OD6,i}^*$	mg/l	0.4	4
$S_{NO4,i}^*$	mg/l	1	8
$k_{RE,i}^*$	–	0.5	4
$Q_{PC,i}^*$	m^3/day	200	720
$Q_{EXT,i}^*$	m^3/day	60	240

For solving this optimal problem, a GA has been involved. The algorithm used in the followings for minimizing J has the following characteristics:

- the number of genes in the chromosomes will be seven genes, as the expected solution contains seven dimensions (calculating seven setpoints), the structure of a chromosome being presented in Figure 3.32 with the gene bounds imposed by Table 3.19.

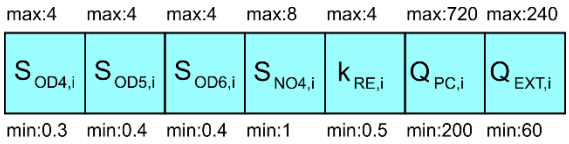


Figure 3.32 – The chromosome structure

- the population will consist of 10 individuals, the initial one being randomly generated with a uniform distribution.
- the selection operator chooses the parent chromosomes randomly from the population, for each candidate a probability directly proportional to its fitness function being used.
- the crossover operator generates an offspring chromosome (O) from the genes of two parent chromosomes ($P1$ and $P2$) using a randomly generated binary vector (S) with the same length as the chromosomes. For a randomly generated binary vector, each gene k of the offspring chromosome will inherit the value of gene k of the first parent if $S(k) = 0$, or of the second parent in the contrary case as presented in Figure 3.1.
- the mutation operator adds to each gene of the offspring chromosome a value randomly chosen from a zero mean Gaussian distribution with a standard deviation calculated as in equation (3.3).

The optimization algorithm has been run for each of the pluviometric regimes, each time using the corresponding influent scenario. Figure 3.33 shows the evolution of the fitness function when running the genetic algorithm in the case of the three considered pluviometric regimes.

The optimal setpoint vectors are presented in Table 3.20 and were used, together with the influent described in Figure 3.31 (a), (b) and (c) to simulate the system over the 16-week time

horizon and to evaluate the performance of the WWTP on the last 4 weeks. The obtained performance can be seen in Table 3.21.

Comparing the results presented in Table 3.21 with the results obtained with the previous proposed control strategy (see Table 3.17), it can be observed that, even if in the DRY regime the results are slightly worse, in the other two regimes there are substantial improvements of the integrated performance indicator.

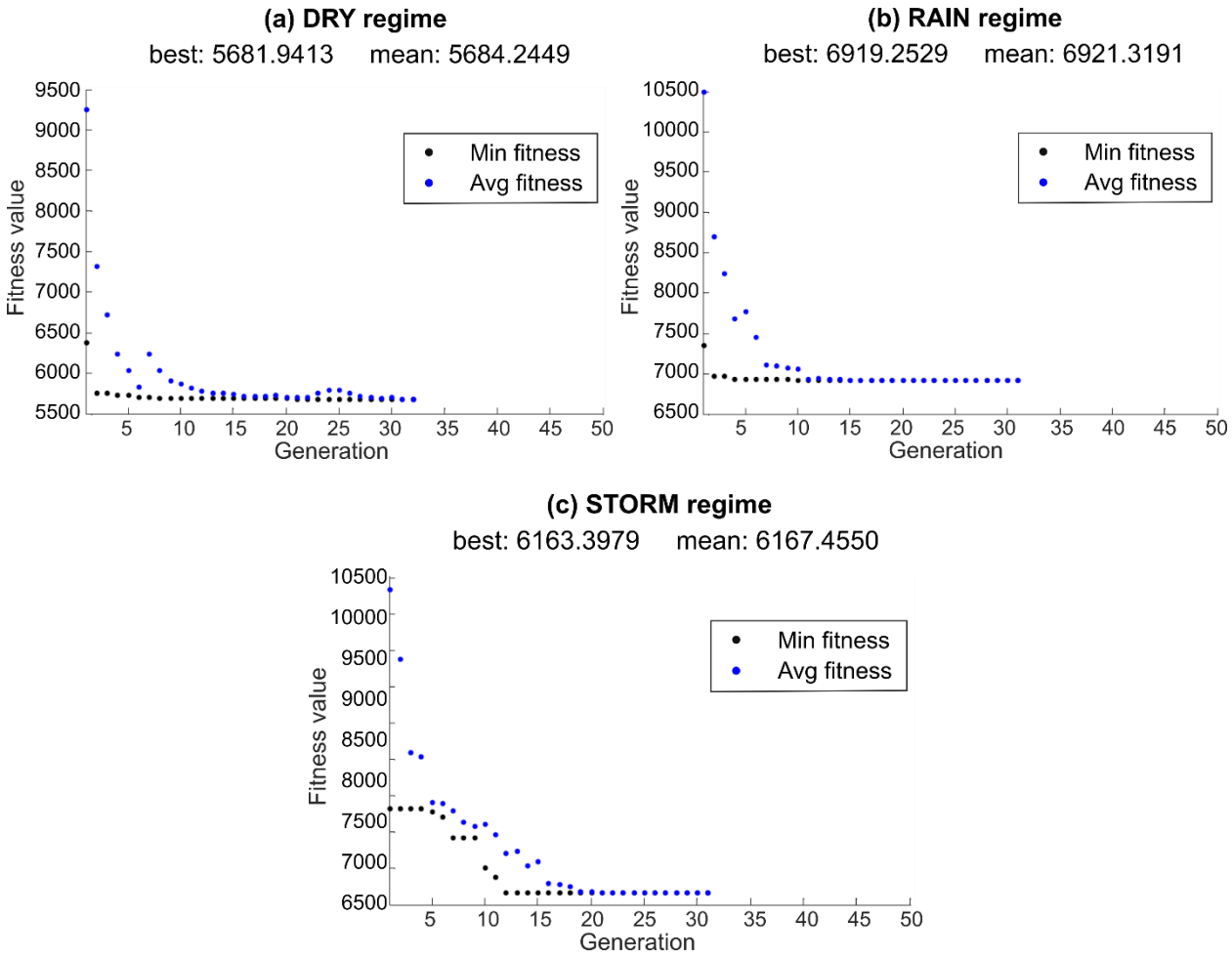


Figure 3.33 – Fitness function evolution in the three operating regimes (a) DRY, (b) RAIN, (c) STORM

Table 3.20 – The values of the optimal setpoints obtained for each regime

Regime	$S^*_{OD4,i}$	$S^*_{OD5,i}$	$S^*_{OD6,i}$	$S^*_{NO4,i}$	$k^*_{RE,i}$	$Q^*_{PC,i}$	$Q^*_{EXT,i}$
DRY	0.38	3.07	1.37	4.28	1.84	488.10	98.97
RAIN	0.67	1.25	1.95	1.52	1.71	349.52	100.05
STORM	0.84	1.51	2.34	6.28	1.68	470.10	99.78

Table 3.21 – Results obtained in each regime

	DRY	RAIN	STORM
$\boldsymbol{EQI}$	5591	6958	5989
$\boldsymbol{OCI}$	2886	3047	2809
$\boldsymbol{Ex\,[N_{tot}]}$	0	0	0
$\boldsymbol{Ex\,[NH_4]}$	0	1.52	1.85
$\boldsymbol{Ex\,[NO]}$	0	0	0
$\boldsymbol{Ex\,[TSS]}$	0	0.2	0
$\boldsymbol{Ex\,[COD]}$	0	2.21	1.74
$\boldsymbol{Ex\,[BOD]}$	0	0	0
$\boldsymbol{J_3}$	0	393	360
$\boldsymbol{J}$	5682	6919	6163

3.3.3.2. Transitioning between pluviometric regimes

Transitions between pluviometric regimes are not sudden, but gradual. Thus, it is important, in a transition between two regimes, to consider the optimal values of both regimes weighted with membership degrees to the regimes. Determining the membership degrees to the regimes will be done with a fuzzy block, the same as the one described in section 3.3.2 (see Figure 3.29).

Considering μ_i with $i \in \{DRY, RAIN, STORM\}$ the membership degree of Q_{in} to the pluviometric regime i, the optimal setpoint vector is given by:

$$V^*[j] = \sum_i \mu_i \cdot V_i^*[j] \qquad j \in \{1 \dots 7\}, \qquad i \in \{DRY, RAIN, STORM\} \tag{3.28}$$

meaning that:

$$S_{OD4}^* = \sum_i \mu_i \cdot S_{OD4,i}^* \tag{3.29}$$

$$S_{OD5}^* = \sum_i \mu_i \cdot S_{OD5,i}^* \tag{3.30}$$

$$S_{OD6}^* = \sum_i \mu_i \cdot S_{OD6,i}^* \tag{3.31}$$

$$S_{NO4}^* = \sum_i \mu_i \cdot S_{NO4,i}^* \tag{3.32}$$

$$k_{RE}^* = \sum_i \mu_i \cdot k_{RE,i}^* \tag{3.33}$$

$$Q_{PC}^* = \sum_i \mu_i \cdot Q_{PC,i}^* \tag{3.34}$$

$$Q_{EXC}^{*} = \sum_{i} \mu_i \cdot Q_{EXC,i}^{*} \tag{3.35}$$

Table 3.22 shows the values of the performance indicators obtained in the aggregated regime when using, as influent, the scenario described in Figure 3.31 (d).

Table 3.22 – Results obtained in the aggregate regime

	Aggregate regime
$\boldsymbol{EQI}$	6151
$\boldsymbol{OCI}$	3176
$\boldsymbol{Ex\,[N_{tot}]}$	0
$\boldsymbol{Ex\,[NH_4]}$	1.75
$\boldsymbol{Ex\,[NO]}$	0
$\boldsymbol{Ex\,[TSS]}$	0
$\boldsymbol{Ex\,[COD]}$	1.29
$\boldsymbol{Ex\,[BOD]}$	0
$\boldsymbol{J_3}$	303
$\boldsymbol{J}$	6555

As observed, comparing with the results obtained with the previous proposed control strategy (see Table 3.17), it can be concluded that the actual control strategy is providing better results in the aggregate regime.

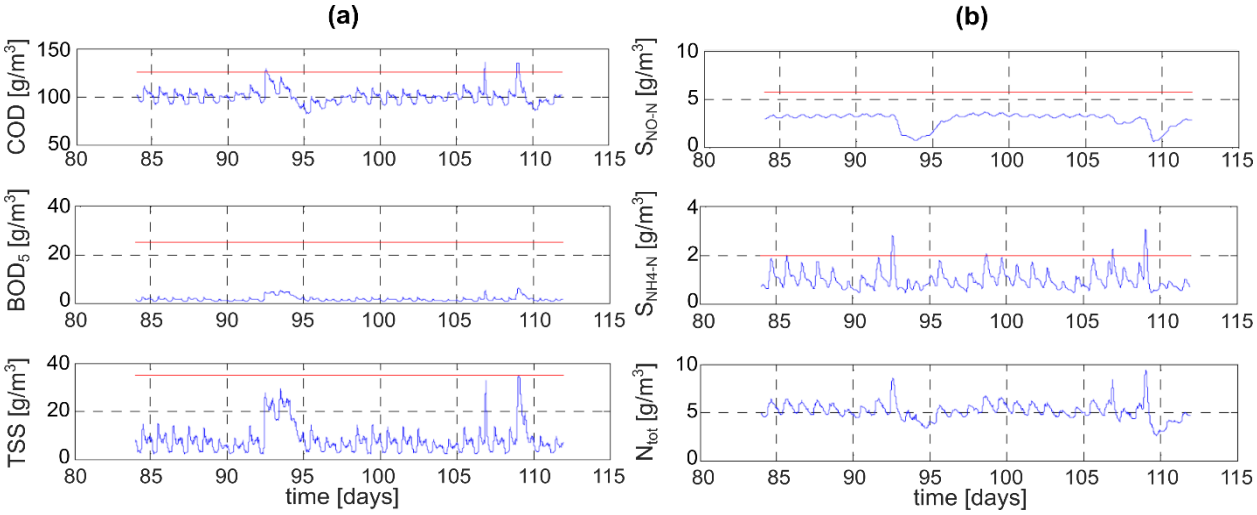


Figure 3.34 – Effluent loads in the aggregated regime
(a) COD, BOD5 and TSS, (b) $S_{NO\text{-}N}$, $S_{NH4\text{-}N}$ and N_{tot}

Figure 3.34 shows the main parameters assessing the quality of the WWTP effluent for the last 4 weeks of the simulation, considering the aggregate regime. The red line indicates the legal limits stipulated by the Romanian legislation [30]. As observed, ammonium and COD limits are exceeded for short periods of time (as also observed in Table 3.22, the exceeding moment corresponding to the maximum peaks in the influent flow.

3.4. Integrated Urban Wastewater System optimal control

The two systems, SN and WWTP are interconnected, and because the effluent of the SN represents the influent of the WWTP, it is important to also know the effects of the SN control strategies on the WWTP operation performances. A higher flow from the SN, due to control strategies avoiding overflows, could lead to WWTP overloading, with considerable environmental effects. Therefore, SN control strategies should consider their effects on the WWTP operation efficiency in terms of pollution loads and wastewater flow.

Thus, this subchapter studies the IUWS described in section 2.4.2, following two directions for assessing the impact that SN operation has on the WWTP performances:

- controlling only the SN outlet valve, without considering any other control strategy for the SN – all other valves/pumps opened/running at 100% [220].
- using the MPC control algorithm described in section 3.2.2 for the SN to minimize its environmental impact [216] and integrating a constraint regarding the SN outlet valve opening into this strategy.

It is important to mention that in both cases a simple PI controller has been considered for the WWTP. It is the A1 strategy defined by BSM2 [133] – manipulating the aeration flow of all the aerated WWTP tanks aiming at regulating the dissolved oxygen in the 4th bioreactor.

For calculating DQI with equation (2.19), the two weights involved were considered equal: $w_{EQI} = w_{OQI} = 0.5$ meaning that it was considered that the SN overflow is properly directed to the same natural receptor as the WWTP effluent.

3.4.1. Controlling Sewer Network outlet valve

As presented above, the first approach considers controlling the SN outlet valve opening ($U_{TK7} \in [0,1]$), while all the other valves of the SN are open 100% and all the SN pumps are running at full capacity. Considering the influent described in section 2.2.3, a series of simulations were performed for various SN outlet control actions. For each of the simulations, the performance indicators described in 2.4.2.1 were calculated and scaled using equation (2.21) with respect to the values obtained in the base case (see Table 2.12). Various control actions were considered for the outlet valve of the SN. These control actions were grouped in two categories: constant valve opening and limited outflow.

3.4.1.1. Constant valve opening

This case considers that the SN outlet valve control (U_{TK7}) is kept constant. With this assumption, multiple simulations have been made for various constant values of the outlet valve opening. These values were ranging from 5% (0.05) to 100% (1). The obtained results are graphically represented in Figure 3.35.

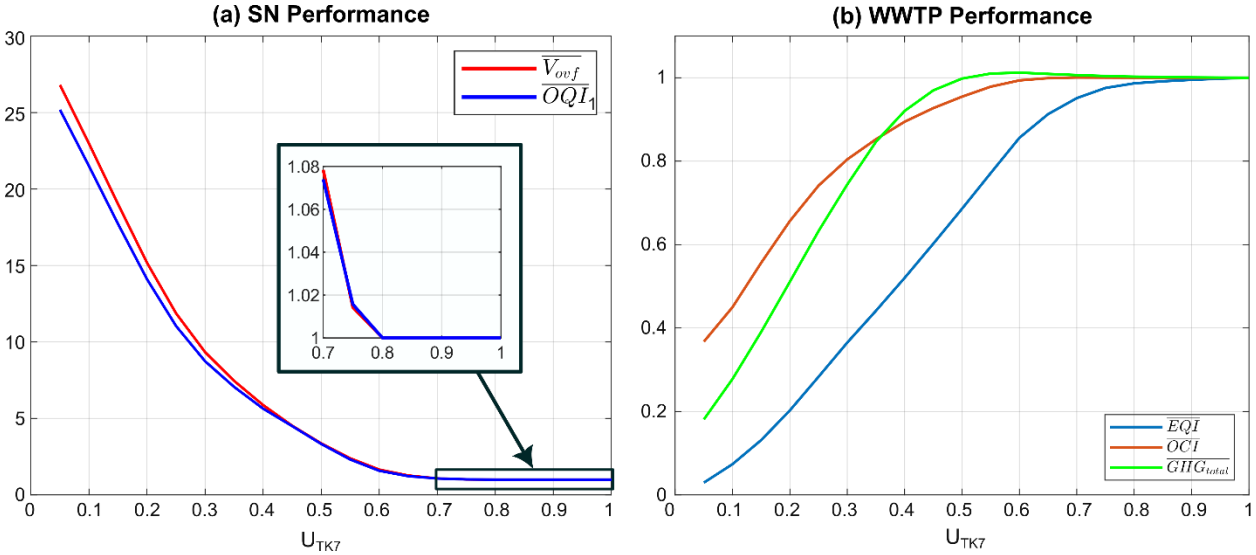


Figure 3.35 – Results obtained with constant outlet valve opening (a) SN performances (b) WWTP performances

Firstly, as seen in Figure 3.35 (a), U_{TK7} can be lowered to as much as 80% without impacting in any way the performances of the SN. Lowering it further leads to degrading SN performances, with dramatic effects (double quantity of wastewater and pollutants discharged compared to the base case) for $U_{TK7} < 0.65$. Secondly, as Figure 3.35 (b) shows the performances of the WWTP, it could be observed that the WWTP performances are improving with lower values of U_{TK7}. $\overline{EQI}$ consistently decreases with U_{TK7}, however, showing only small improvements when $U_{TK7} > 0.7$. $\overline{OCI}$ gets unchanged for $U_{TK7} > 0.7$, then it decreases with the decrease of the SN outlet valve opening. $\overline{GHG_{total}}$ shows a small increase (1%) while U_{TK7} lowers to 0.5, followed by consistent decrease for $U_{TK7} < 0.5$.

As the effects that SN outlet valve opening has on the two subsystems are opposing, it is important to see the effects on the overall IUWS in order to check if there are values of U_{TK7} for which the integrated system shows improvements, or the performance gains of one of the subsystems cancels out with the performance losses of the other one. Figure 3.36 shows the scaled values of the IUWS performance indicators (DQI – see equation (2.19), and $I(\lambda)$ – see equation (2.20)) for each constant value of the SN outlet valve opening.

As observed in Figure 3.36 (a), the minimum quantity of pollutants (DQI – a measure of the total pollutants that are discharged into the environment by the IUWS) is obtained when $U_{TK7} = 0.7$. However, it is only 2% less pollutants than in the base case. Moreover, usually the objective of minimizing the quantity of pollutants discharged is associated with other objectives such as minimizing the operational cost of the system, but also minimizing the GHG emissions. For this reason, Figure 3.36 (b) shows the integrated performance indicator $I(\lambda)$ for various values of U_{TK7} and λ. The red line shows the value of U_{TK7} that assures the minimum $I(\lambda)$ for each λ. While $\lambda > 0.3$ the best value of U_{TK7} remains constant at 0.7, however the overall improvement is under 2% compared to the base case. For $\lambda < 0.3$, as the importance of the pollutants discharged decreases and the importance of the other two performance indicators increases, the best value of U_{TK7} starts decreasing.

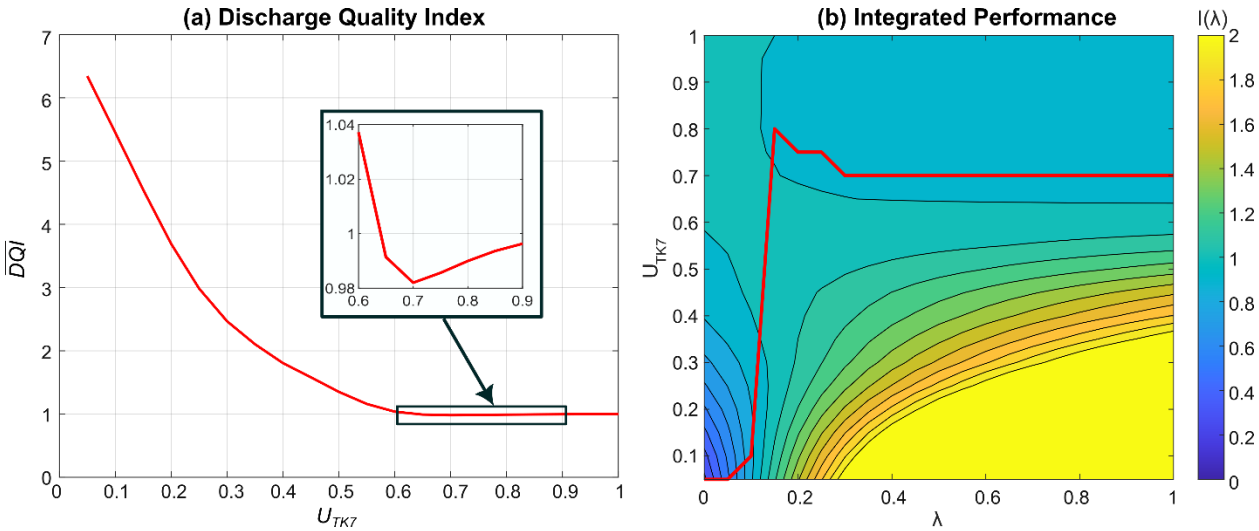


Figure 3.36 – Results obtained with constant outlet valve opening
(a) Discharge Quality Index (b) integrated performance indicator $I(\lambda)$ – red line shows the minimum obtained for each λ

Consequently, is has been proven that the SN outlet valve opening has an important effect on both subsystems, however, the effects are in antithesis, meaning that using a value of U_{TK7} that improves the performances of one of the subsystems leads to decreasing performances of the other one. Combining the effects, the best overall performance improvement is marginal (under 2%), thus, more control is needed at the SN level.

3.4.1.2. Limited outflow

This case considers that the SN outlet valve control is kept at the highest possible value that will keep the SN outflow ($Q_{out,TK7}$) limited to a certain constant value Q_{max}. The SN is modelled in BSMSewer, which models the tank outflow as [75]:

$$Q_{out,TK7} = U_{TK7} \cdot Q_{max,TK7} \cdot \frac{h_{TK7}}{h_{o,TK7} + h_{TK7}} \tag{3.36}$$

where $Q_{max,TK7}$ is the maximum possible outflow (the tank is full and the valve 100% open), h_{TK7} is the wastewater height in $TK7$, while $h_{o,TK7}$ is the wastewater height in $TK7$ that will assure $Q_{out,TK7} = Q_{max,TK7}/2$ when the valve is fully open. Hence, for determining the maximum valve opening that will limit the outflow to Q_{max}, the following control law has been considered:

$$U_{TK7} = \min\left(1, \quad \frac{Q_{max}}{Q_{max,TK7}} \cdot \frac{h_{o,TK7} + h_{TK7}}{h_{TK7}}\right) \tag{3.37}$$

With this control law, multiple simulations have been made for various values of Q_{max}. These values were ranging from 32000 m^3/day to 57000 m^3/day. The obtained results are graphically represented in Figure 3.37.

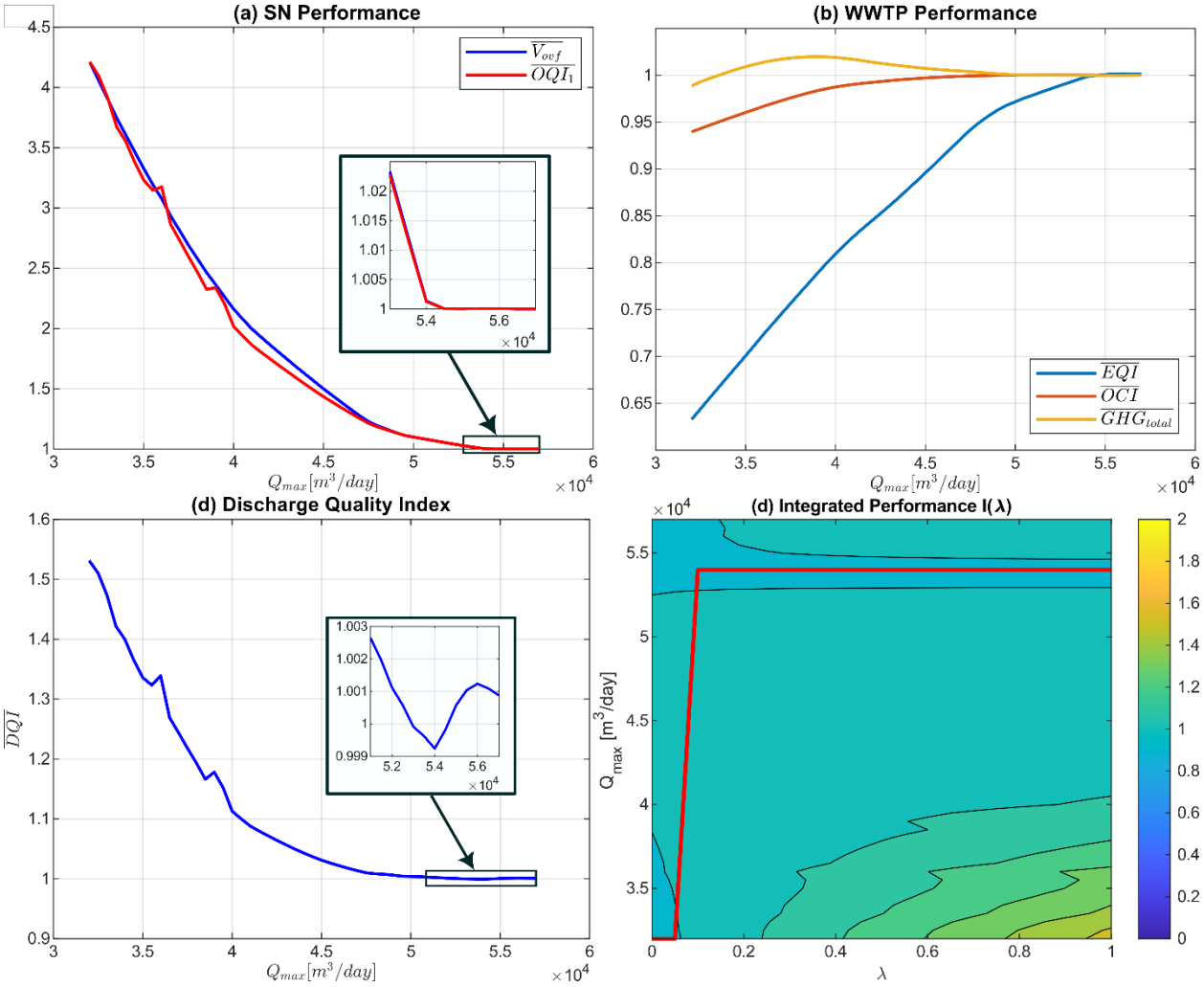


Figure 3.37 – Results obtained with limited outflow
(a) SN performances; (b) WWTP performances; (c) Discharge Quality Index; (d) integrated performance indicator $I(\lambda)$ – red line shows the minimum obtained for each λ

Firstly, as seen in Figure 3.37 (a), Q_{max} can be lowered to as much as 54500 m^3/day without impacting in any way the performances of the SN. Lowering it further leads to degrading SN performances, with dramatic effects (double quantity of wastewater and pollutants discharged compared to the base case) for $Q_{max} < 40000$ m^3/day. Secondly, as Figure 3.37 (b) shows the performances of the WWTP, it could be observed that the WWTP performances, excepting GHG emissions, are improving with lower values of Q_{max}. As the effects that SN outflow limiting has on the two subsystems are opposing, it is important to see the effects on the overall IUWS to check if there are values of Q_{max} for which the integrated system shows improvements. Figure 3.37 (c) and (d) show the scaled values of the IUWS performance indicators (DQI – see equation (2.19), and $I(\lambda)$ – see equation (2.20)) for each constant value of the SN outflow limit. As observed, the minimum quantity of pollutants is obtained when $Q_{max} = 54000$. However, it is improving less than 0.1%, which is negligible. Moreover, usually the objective of minimizing the quantity of pollutants discharged is associated with other objectives such as minimizing the operational cost of the system, but also minimizing the GHG emissions. For this reason, Figure 3.37 (d) shows the integrated performance indicator $I(\lambda)$ for various values of Q_{max} and λ. The red line shows the value of Q_{max} that assures the minimum $I(\lambda)$ for each λ. Unfortunately, no notable improvements (less than 0.1%) of the IUWS performances can be achieved no matter the value of λ.

Consequently, trying to limit the outflow of the SN to constant values is not useful in terms of the IUWS performance.

3.4.2. Model Predictive Control for the Sewer Network

This section considers that the SN is controlled by the MPC algorithm described in section 3.2.2 and analyses the effects posed on the overall IUWS. The tests were performed using the influent described in subsection 2.2.3.2. For each of the simulations, the performance indicators described in 2.4.2.1 were calculated and scaled using equation (2.21) with respect their base-case values (see Table 2.12). Two approaches were made: using the MPC algorithm as it is (unconstrained case) and constraining the MPC algorithm in terms of SN outlet valve opening (constrained case). The version of MPC used in this section considers:

- MPC step size – $T_S = 1\ h$
- MPC prediction horizon – $T_H = 6\ h$
- Fitness function – equation (3.12)

3.4.2.1. Unconstrained case

Table 3.23 shows the scaled values of the performance indicators in the unconstrained case.

Table 3.23 – IUWS performance indicators when SN is controlled by unconstrained MPC

Performance indicator	Scaled value
$\overline{V_{ovf}}$	0.4773
$\overline{OQI_1}$	0.4961
$\overline{EQI}$	0.9643
$\overline{OCI}$	0.9976
$\overline{GHG_{total}}$	1.0024
$\overline{DQI}$	0.8457

As expected, controlling the SN has positive effects only on the SN performances, without negatively impacting the WWTP performances. This leads to improvements of the overall IUWS in terms of decreasing the total quantity of pollutants discharged by the integrated system by 15.43 % ($\overline{DQI} = 0.8457$).

3.4.2.2. Constrained case

As it has been proved that it is possible to operate the SN using a MPC algorithm without negatively impacting the WWTP performances and that lowering the SN outlet valve opening can lead to improved WWTP performances, the following hypothesis arises: operating the SN using the same MPC algorithm but constrained in terms of SN valve opening should lead to further improvements of the IUWS performances. The MPC algorithm [216] considers only the performance of the SN, thus it is searching only for the optimal controls of the tanks that are relevant for improving this performance: U_{TK3}, U_{TK4} and U_{TK5}. However, adding a constraint related to SN outlet valve opening to this control algorithm, will lead to an increase in the

complexity of the optimization problem, in terms of that, this time, all tank's output controls play a role in the SN performance and implicitly in the IUWS performance.

The following results are obtained in simulation using the control structure presented in Figure 3.38. In that control structure, a simplified model of the SN (presented in section 2.2.5) is used as the model required by MPC, and the integrated model described in section 2.4.2 is used as the process.

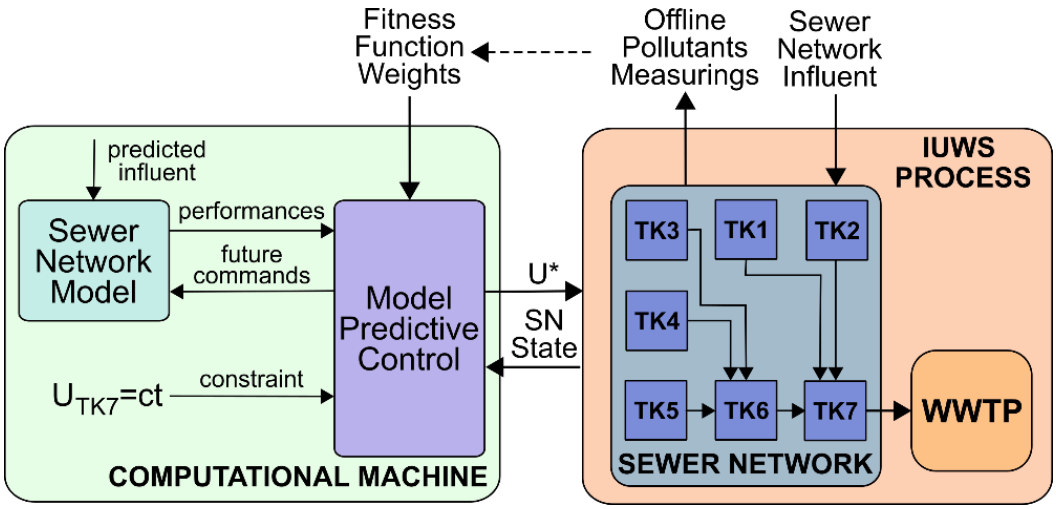


Figure 3.38 – The schematic representation of the constrained MPC control structure

The results were obtained considering various constant values for U_{TK7} ranging from 0.25 (25% valve opening) to 1.00 (full valve opening). For each constant value of U_{TK7}, a series of 10 simulations were made, and, for each of them, the performance indicators described in subsection 2.4.2.1 were calculated and scaled with respect to the values obtained in the base case. The statistics of the results can be seen in Figure 3.39.

It can be observed that having a low value for U_{TK7} leads to improvements in WWTP operation efficiency, but in deterioration of the SN performances. However, U_{TK7} can be lowered as much as 0.65 (65% valve opening) without any negative impact on the SN, and as much as 0.35 (35% valve opening) with just small loss of SN performances, loss that could be compensated by the gains of WWTP efficiency. Of course, having values lower than 0.35 will have massive negative impact on the SN. On the other hand, for $U_{TK7} > 0.7$ there are no changes in the WWTP performances comparatively to the base case, while lowering the constraint bellow this value provides a consistent decrease of all the WWTP performance indicators that were analysed.

Consequently, $U_{TK7} \in [0.3, 0.7]$ looks like an interval that could provide improvements of the integrated system performances. This could be further reinforced by analysing the DQI performance indicator, which measures the total pollutants discharged into the environment by the IUWS. As expected, improved performances of the IUWS can be observed for $U_{TK7} \in [0.3, 0.7]$ with a minimum plateau value of approximatively 0.5 (50% reduction of the total pollutants discharged) for $U_{TK7} \in [0.3\ 0.55]$.

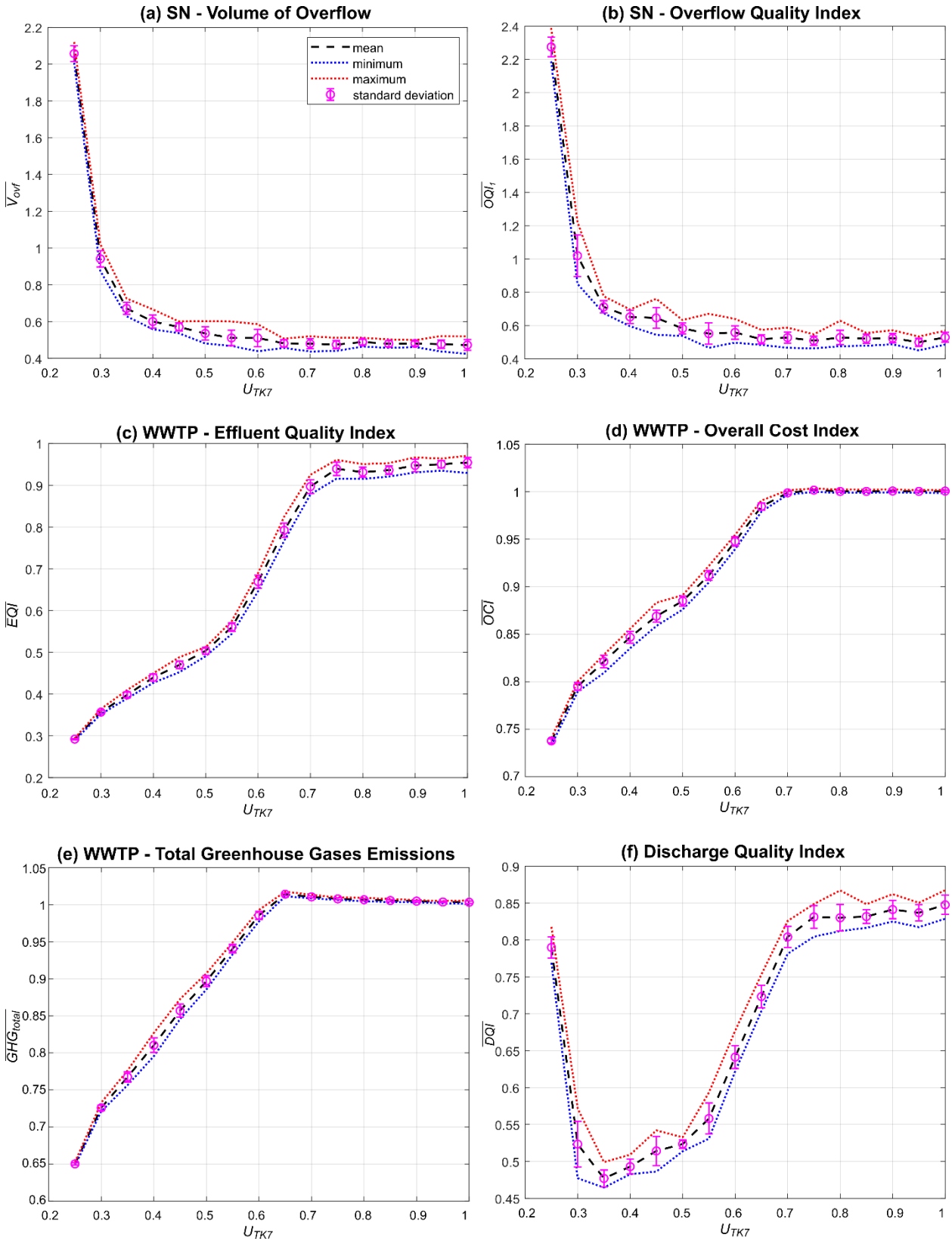


Figure 3.39 – Statistics of the resulted scaled values of the performance indicators (a) $\overline{V_{ovf}}$, (b) $\overline{OQI_1}$, (c) $\overline{EQI}$, (d) $\overline{OCI}$, (e) $\overline{GHG}$, (f) $\overline{DQI}$

Moreover, it could be observed that the standard deviation values are small enough for each performance indicator, demonstrating, this way, that the MPC algorithm keeps its reliability under U_{TK7} constraint conditions.

As seen in Figure 3.39, if minimizing the quantity of pollutants discharged is the only objective of controlling the IUWS, then using U_{TK7} in the plateau region of DQI will provide the best results. $U_{TK7} = 0.35$ is the best solution in this case, achieving a 52% reduction in the total quantity of pollutants discharged in the environment. Moreover, this solution also provides about 20-25% reduction of OCI and of GHG_{total}. On the other hand, usually the previously mentioned objective is coupled with reducing the cost of treatment and the GHG gases emitted by the WWTP. Thus, choosing the best value for U_{TK7} should be done by considering the integrated performance indicator $I(\lambda)$ described by equation (2.20). Figure 3.40 shows the mean values of $I(\lambda)$ with respect to U_{TK7} and λ.

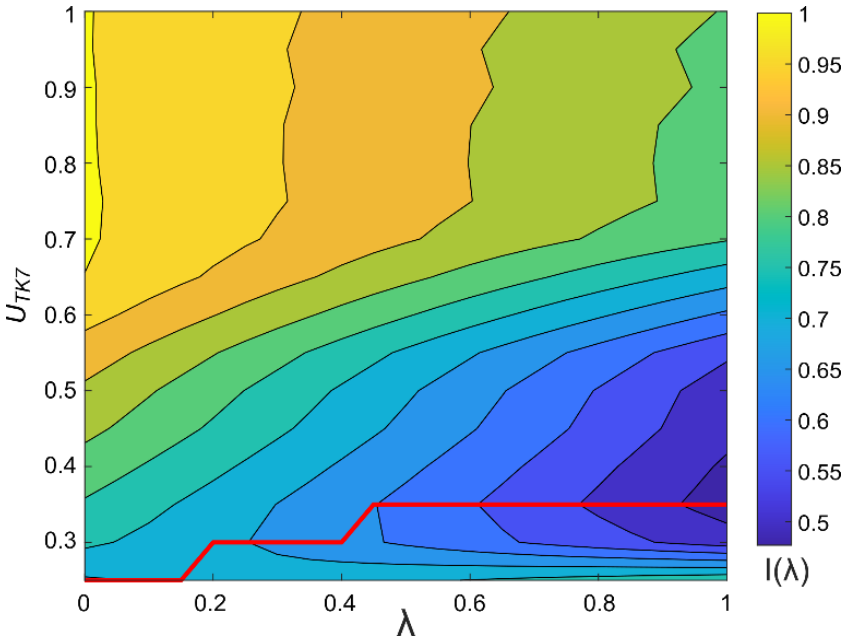


Figure 3.40 – The mean values of the integrated performance indicator with respect to U_{TK7} and λ
The red line means the minimum value obtained for each λ

As observed, the best value of U_{TK7} remains at 0.35 as long as λ is greater or equal with 0.4. On the contrary, as λ decreases under 0.4, the best value of U_{TK7} also decreases, as the importance of DQI is diminished over the importance of OCI and GHG_{total}.

One way to obtain further improvements is by considering a dynamic value for U_{TK7} which depends on the free space in the SN outlet tank. In this case, U_{TK7} will stay at its best value (0.35 as determined above) only when the free space in TK7 is medium. When the free space gets lower, the SN performances could be helped by opening the SN outlet valve a little bit more. On the other hand, when the TK7 free space gets higher, it means that it could store more wastewater, thus the valve can be closed more, helping this way the WWTP performances. This is achieved by using the fuzzy block described by Figure 3.41 to compute the MPC constraint related to U_{TK7}, resulting the control structure presented in Figure 3.42.

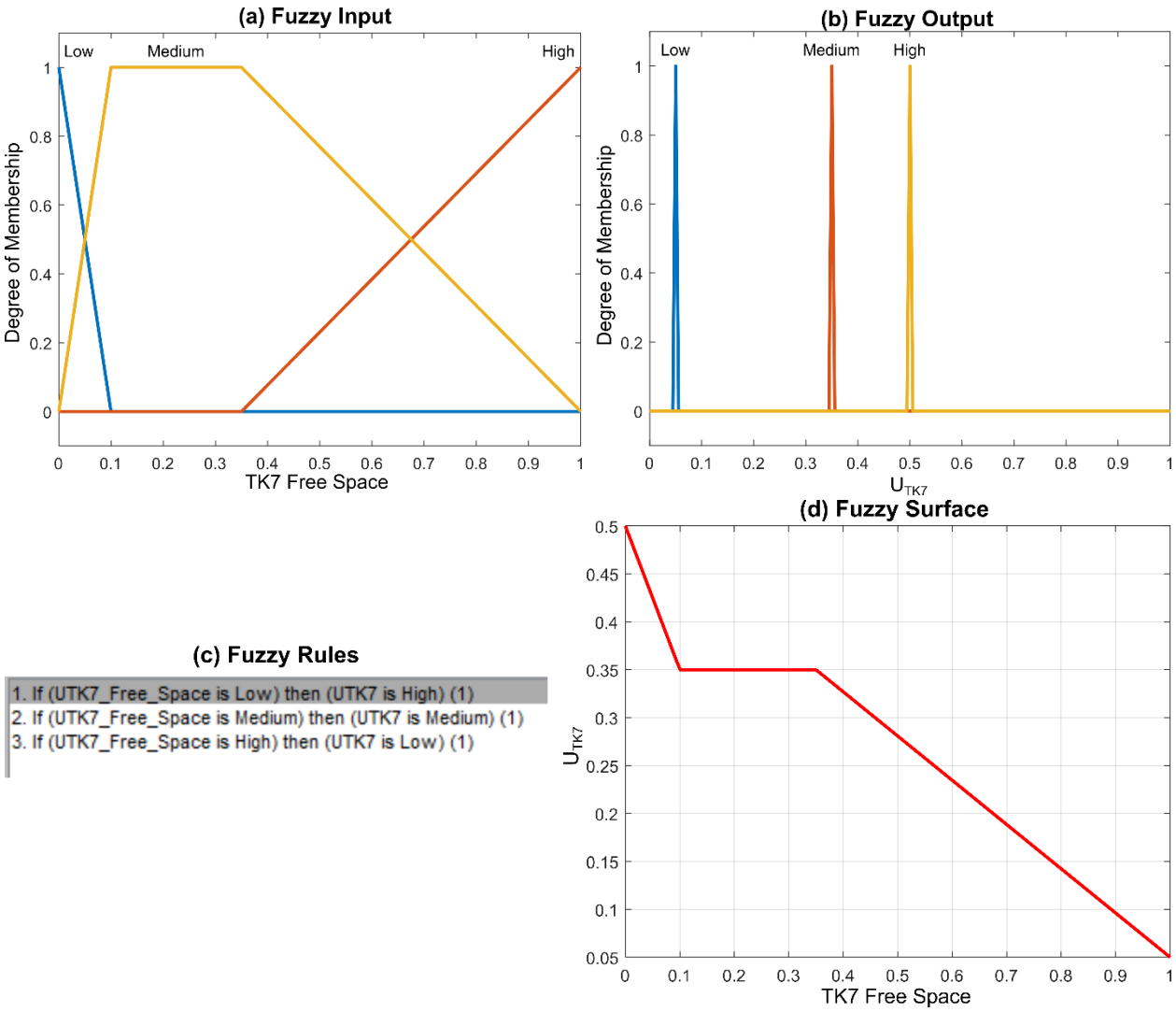


Figure 3.41 – Fuzzy block used to compute the MPC constraint
(a) Fuzzy input membership functions; (b) Fuzzy output membership functions; (c) Fuzzy rules; (d) Fuzzy surface

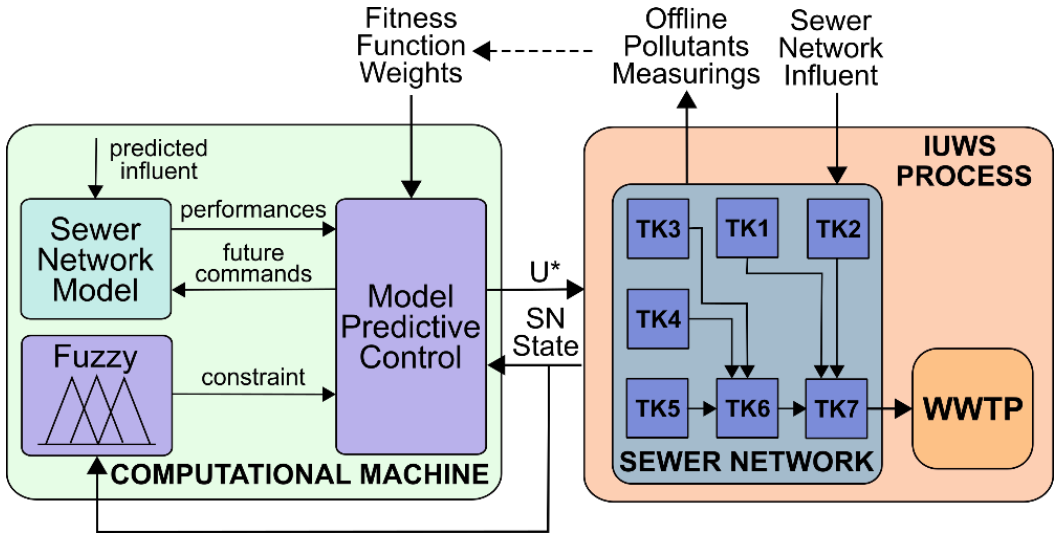


Figure 3.42 – The constrained MPC control structure with dynamic constraint

The obtained results shown comparatively with the ones obtained with the constant constraint case (the best ones) are presented in Table 3.24.

Table 3.24 – IUWS performance indicators when SN is controlled by the constrained MPC with the constraint dynamically computed

Performance indicator	Scaled values obtained with constant constraint $U_{TK7} = 0.35$				Scaled values obtained with dynamic constraint			
	MIN	MEAN	MAX	STD	MIN	MEAN	MAX	STD
$\overline{V_{ovf}}$	0.65	0.67	0.73	0.0312	0.54	0.59	0.69	0.0408
$\overline{OQI_1}$	0.67	0.71	0.78	0.0357	0.62	0.67	0.80	0.0638
$\overline{EQI}$	0.39	0.40	0.41	0.0067	0.37	0.38	0.39	0.0050
$\overline{OCI}$	0.81	0.81	0.83	0.0063	0.80	0.80	0.81	0.0050
$\overline{GHG_{total}}$	0.76	0.77	0.78	0.0066	0.74	0.75	0.76	0.0062
$\overline{DQI}$	0.46	0.48	0.50	0.0108	0.44	0.45	0.49	0.0173

As observed, dynamically computing the constraint leads to an additional 8% reduction of the wastewater discharged by the SN and an additional 4% reduction of the quantity of pollutants in the discharged wastewater. Moreover, the WWTP performances are decreasing with 1-2%. The total quantity of pollutants discharged by the IUWS (DQI) gets decreases by an additional 3%. The reliability of the new approach is demonstrated by the small values of the standard deviations. The next figure shows the difference between the two approaches looks in terms of the integrated performance indicator $I(\lambda)$ for various values of λ. It can be concluded that the new approach provides a consistent 2-3% improvement for all values of λ.

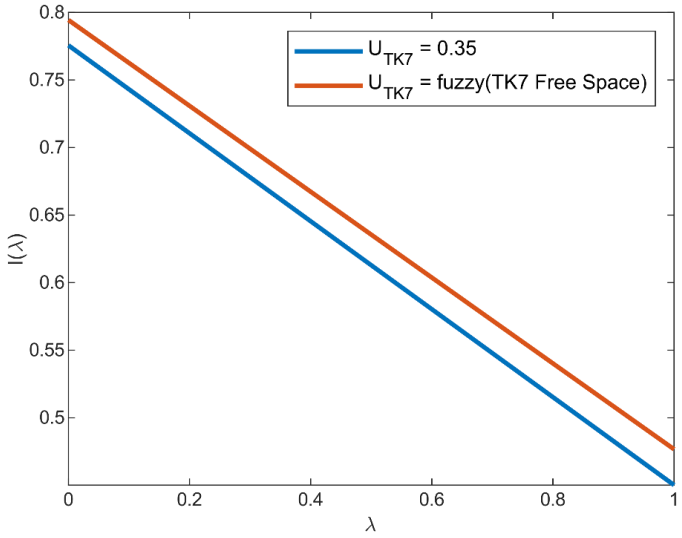


Figure 3.43 – Mean values of $I(\lambda)$ for various values of λ in both considered constrained cases

3.5. Chapter conclusions

This chapter delves into the optimal control of wastewater collecting and treatment systems in a separate, but also integrated manner, presenting the development of a series of control strategies that make use of the models developed in the previous chapter. Firstly, the optimal

control strategies for the SN described in subchapter 2.2 are developed, following two approaches: offline and online optimal control.

The development of SN offline optimal control followed the steps:

1. 5 optimal control strategies are defined, all of them controlling the output commands of 3 of the SN storage tanks, determining the values of the controls based on the wastewater level in the tanks. The optimisation is performed using GA. The five control strategies are tested for minimizing the quantity of wastewater overflowed, but also the quantity of pollutants in that wastewater, and the results are compared. The obtained results show that all optimal control strategies lead to significant improvements of the two performance indicators. The most efficient one in relation to V_{ovf} is Strategy #3 with a 33.89% reduction of the volume of overflow compared to the case when no control is performed. The most efficient one in relation to OQI is Strategy #4 with a 31.94% reduction of OQI compared to the case when no control is performed. However, the reduction of OQI when using Strategy #3 to minimize OQI is similar to the one obtained with Strategy #4, suggesting that Strategy #3 could be chosen as being the best one. The reliability and robustness of Strategy #3 when minimizing the volume of overflow is proved by running the optimization procedure 18 times and analysing the results from a statistical point of view.
2. As it was observed the minimizing V_{ovf} leads to decreased values of OQI and vice versa, the next step aims to understand the correlations between the two parameters to have the most suitable fitness function for the optimal control of the SN. Thus, the optimisation procedure is run again, considering, this time, as fitness function, the value of both indicators, resulting a MOO approach. Two methods were tested for optimization, both being based on a controlled elitist GA: a) MOO and b) MOO in two steps. The results obtained with the first method show that the performances are significantly worse than the solutions found when only one of the performance indicators was minimized. An explanation could be that the MOO algorithm tends to get trapped in local minimums and that it provides only a small portion of the Pareto Front, because the algorithm is an elitist one and the initial population is randomly chosen. For the second method, the MOO algorithm is preceded by a SOO stage, when the optimisation algorithm is run to minimize the two performance indicators separately. This approach shows that the obtained optimal solution is similar to the one obtained with SOO when minimizing V_{ovf}. Moreover, MOO in two steps provides only a small part of the Pareto Front, the points overlapping. This could be explained by the fact that there is a strong correlation between the two performance indicators, meaning that minimizing one of them, leads to minimizing the other one. However, SOO minimizing V_{ovf} is performing substantially better in terms of both performance indicators than SOO minimizing OQI. This is because of the geometry of the objective space. Thus, the analysis showed that V_{ovf} and OQI are strongly correlated, consequently, performing SOO minimizing V_{ovf} is the simplest solution to minimize the environmental impact of SN overflows.
3. The third step deals with choosing the best optimisation algorithm. 4 algorithms are tested: GA, PSO, FMinSearch and random generating the solution. It resulted that the evolutionary algorithms (GA and PSO) provide the best results (significant reduction of both performance indicators compared to the “no control” case), with the ones provided by PSO being slightly better.
4. The last step of SN offline optimal control integrates all the findings in the previous steps in a Sliding Window-based algorithm. This way, instead of finding the optimal controls for

the entire 28 days period, the algorithm will look only for optimal controls to be applied for just one day. This strategy has the main advantages that only one day at a time is needed for influent forecast and, that, because days with 0 overflow when all controls are at 100% will not be subject to optimization, a lower computational effort will be assured. Improvements are made by considering that at each 1-day time window, besides minimizing V_{ovf}, it is important to leave the SN in a state that could be helpful for future time windows. This is achieved by trying to keep the wastewater level in the storage tanks at the end of the optimization window as low as possible by adding a penalty term into the fitness function. The statistical results proved the reliability of the algorithm, showing an average reduction of approximatively 60% for both performance indicators.

For SN online optimal control, the use of a MPC approach is considered. For solving integration time related issues, the simplified model described in section 2.2.5 is used as the model required by the MPC. However, in this approach, it was observed that minimising V_{ovf} is not always providing minimum values for OQI. Solving this required to integrate information about pollutant quantities into the fitness function. As the simplified model contains only information about wastewater flow, an offline method is proposed: weighting the SN tanks volumes of overflows with weights that are calculated offline based on measurement of pollutant concentrations from time to time. The obtained results show an improvement of approximately 55% for both performance indicators.

Regarding optimal control of WWTP 3 approaches are made. The first approach is a MPC control strategy that makes use of the two NN models developed in section 2.3.1, resulting two versions of the MPC. Both algorithm versions were tested in simulation considering an influent based on the BSM2 influent scenario. The obtained results were compared to a base case (aeration rate kept at a constant value). The 1st version of the MPC algorithm (the one that is using the 1st version of the NN model) provides worse results than the base case. On the other hand, the 2nd version of the MPC algorithm (the one that uses the 2nd version of the NN model) provides better results than the base case. This is proving the reliability of the proposed control algorithm. One explanation for the fact that the 1st version is worse than the base case, while the 2nd version is better, could be the fact that, in the 1st case, because all the state variables of the process are considered measurable, the NN model is able to correctly estimate even small variations in the organic substrate dynamics, leading to a complex geometry of the fitness space. This complex geometry of the fitness space implies a lot of local minima, increasing the chance that the optimization algorithm gets stuck in one of them, leading to the control algorithm performing worse. The second approach considers extending an already existing control strategy developed for the WWTP in Galați, Romania. The extension consists of applying a simple methodology to compute optimal values for the external recirculating rate based on the pluviometric regime using fuzzy techniques. The optimal values for the external recirculating rate are computed separately for each pluviometric regime, then they are aggregated in a single value using a fuzzy block that sets the membership degree of the plants influent to one of the three regimes: dry, rain and storm. The results prove the improvements brought by the proposed strategy. The last approach extends this fuzzy-optimal control strategy such as the procedure is made for more setpoints involved in the WWTP control.

Lastly, the IUWS is studied. More specific, it is shown how the performances of the integrated systems can be improved by controlling the SN. This is achieved following two directions for assessing the impact that SN operation has on the WWTP performances. The first direction considers controlling only the SN outlet valve, without considering any other control strategy for

the SN and shows that the SN outlet valve opening has an important effect on both subsystems, however, the effects are opposing, meaning that using a value of the outlet valve opening that improves the performances of one of the subsystems leads to decreasing performances of the other one. Combining the effects, the best overall performance improvement is marginal (under 2%), thus, more control is needed at the SN level. The second direction considers using the MPC control algorithm described in section 3.2.2 for the SN to minimize its environmental impact. The first set of results considers the MPC as it is and demonstrates that it is possible to operate the SN without negatively impacting the WWTP. The second set of results consider a modified version of the MPC by constraining it in terms of SN outlet valve opening. It has been proved that for certain values of the constraint, the performance losses on the SN are not so dramatic, while the performance gains on the WWTP are major. Combining this, it resulted a reduction of 55% of the total pollutants discharged by the integrated system. Moreover, an additional small improvement can be achieved by dynamically computing the constraint using fuzzy techniques.

In conclusion, this chapter presented a series of control strategies for SN and WWTP, but also an analysis regarding the improvement of the performances of the IUWS by applying a control strategy to the SN.

Chapter 4. Final Conclusions and Future Work

Wastewater management is an essential topic in our society as water is a vital resource for all the life on Earth. Water pollution can have serious consequences for human health, environment and economy. In this context, wastewater management not only helps preventing further water pollution, but also contributes to the efforts of conserving the water resources by reusing the treated water. With the growth of the world's population, accelerated urbanization and the industry development, the amount of wastewater that requires treatment has increased. This led to the need of developing new wastewater management technologies and of improving the existing infrastructure.

One of the main reasons for wastewater management is protecting the human health. Wastewater can contain a wide range of contaminants, including pathogens, viruses, parasites and dangerous chemical substances. Drinking contaminated water can lead to various illnesses. Effective wastewater management removes, or at least significantly reduces, these contaminants ensuring that the water that is released is safe for humans. Moreover, water pollution poses a threat for the environment. Untreated wastewater can lead to massively polluted water bodies (such as rivers, lakes or even oceans). The excessive nutrients can lead to water eutrophication, a process in which the algae are proliferating which can further lead to oxygen depletion affecting the aquatic life.

In the actual geopolitical context, water plays a crucial role as a political stabilisation factor. The access to clean water and proper management of water resources are essential for maintaining peace and stability in many regions of the world. When water resources are limited or polluted, conflicts can arise between communities and countries, that can escalate into political tensions. Wastewater management and assuring an equitable access to water resources reduce the conflict risks and promote international cooperation.

Thus, this PhD thesis has explored the field of modelling and optimal control of wastewater collecting and treatment systems, by developing a model for a Sewer Network (SN) – full and simplified versions –, various Wastewater Treatment Plant (WWTP) models using Artificial Intelligence techniques and two Integrated Urban Wastewater Systems (IUWS). These models were further used in developing various optimal control strategies for both subsystems. For the SN, a series of optimal control strategies have been developed and tested using various optimization algorithms. The setup providing the best results was integrated into a sliding-window based approach resulting in an offline optimal control strategy. Further, online optimal control has been implemented for the SN using a Model Predictive Control (MPC) approach and various MPC hyperparameters and fitness functions being tested and compared. For the WWTP, a series of optimal control strategies ranging from MPC to fuzzy logic-base strategies were implemented. Finally, the effects that controlling the SN has on the WWTP and on the overall IUWS has been studied. From all these studied aspects, a series of important conclusions can be highlighted:

- The field of wastewater management is an important one and there is place for a lot of scientific research that could help to further reduce the wastewater effects on the environment and public health. This can be achieved when implementing SN and WWTP control strategies by considering the effects of these strategies on the entire IUWS and the current world problems: water quality, cost consumption, global warming, extreme pluvial events, floods, GHG emissions of WWTPs etc.
- Testing the SN model implemented in subchapter 2.2 showed that there are storage tank outlet controls combinations that could provide a better performance of the SN than the case when everything is running at 100% resulting the need for optimal control of the SN in order to find the optimal control combination.
- One of the main challenges related to WWTP models is represented by their high complexity, leading to high numerical integration time. This can be solved by using Machine Learning techniques, methods that are able to accurately estimate the dynamics of the state variables, process values and effluent variables.
- As SN models and WWTP models are created using different tools, usually, the effluent variables of the SN are different than the influent variables of the WWTP. For this reason, it can be concluded that for implementing IUWS models, the models of the two subsystems must be coupled using a conversion block between the two sets of variables.
- When dealing with SN optimal control, Particle Swarm Optimisation algorithm proves to be the best choice, as, statistically, it provides the best results.
- Using a Neural Network model of a WWTP in a MPC strategy showed that if the model is able to correctly estimate even small variations in the organic substrate dynamics, this can lead to complex geometry of the fitness space, which implies a lot of local minima, increasing the chance that the optimization algorithm gets stuck in one of them, leading to the control algorithm performing worse.
- It is possible to operate the SN without negatively impacting the WWTP. Moreover, by integrating a constraint regarding SN outlet valve opening into the SN MPC algorithm, the performance losses on the SN are not so dramatic, while the performance gains on the WWTP are major. Combining this, it resulted in a reduction of 55% of the total pollutants discharged by the integrated system. Additional improvement can be achieved by dynamically computing the constrain using fuzzy techniques.

In conclusion, wastewater management is a crucial and complex challenge that requires innovative approaches in order to protect the public health and the environment, and to ensure political stability. The research results presented in this PhD thesis regarding the modelling and optimal control of wastewater collecting and treatment systems demonstrate the importance of an integrated approach of these systems, but also the importance of developing efficient and flexible control strategies. Throughout the developed strategies, this thesis contributes to the improvement of the field of wastewater management. The use of an integrated approach and advanced strategies can enhance the performances of such systems protecting life on Earth, paving the way for building a safer and more sustainable future.

4.1. Original contributions

The main original contributions brought by the work presented in this PhD thesis are:

Subchapter 2.1 – SN modelling:

1. Designing a SN model for a mid-sized city having approximately 250,000 inhabitants spread over 250 ha split into five collecting areas. The model was implemented in two variants: a quality model developed in BSMSewer software package and a simplified flow model. The simplified model shows a 90 % reduction of the simulation time compared to the quality model, being an important puzzle piece when developing SN optimal control.

Subchapter 2.2 – WWTP modelling:

2. Designing and developing two Neural Network (NN) models for estimating the dynamics of a WWTP.
3. Designing and implementing a NN based Soft Sensor for estimating the effluent ammonia concentration of a WWTP based on other easily measured variables. The implemented NN model uses a Long-Short Term Memory (LSTM) architecture.
4. Designing and implementing a NN model for estimating the effluent quality variables of a WWTP based on influent quality variables and a control variable. The implemented NN model uses a Long-Short Term Memory (LSTM) architecture.

Subchapter 2.3 – IUWS modelling:

5. Designing and implementing two IUWS models obtained by combining a SN model implemented in BSMSewer with a WWTP model based on ASM2d and BSM2G models. For both IUWS models, a coupling unit between the two subsystems has been implemented in order to convert between the two sets of variables.
6. Defining a methodology for assessing the performance of IUWS control in terms of performances of both subsystems. Firstly, the quality of the SN overflowed wastewater has been defined in the same way that the WWTP effluent quality is defined. Secondly, combining the two previously mentioned quality metrics, a “Discharge Quality Index” has been defined, representing a measure the overall pollutants discharged by the IUWS. Finally, an integrated performance indicator has been defined for the WWTP, accounting, besides the quality of discharged water, for the treatment cost and greenhouse gases emissions.

Subchapter 3.1 – SN optimal control:

7. Designing and implementing an offline optimal control strategy for the SN. Firstly, a study has been conducted by implementing and testing a series of 5 optimal control strategies. Secondly, using the best control strategy identified at the previous step, an analysis regarding the quantity vs. quality of the overflowed water has been performed by implementing two versions of a multi-objective optimization algorithm. Thirdly, a series of four optimization algorithms were implemented and tested showing that Particle Swarm Optimization provides the best results. All the findings at these three steps were finally compiled in a Sliding-Window based optimization algorithm for offline optimal control of SNs. For this algorithm, a method for leaving the SN at the end of each step in a state that

could be advantageous for the next one is proposed, implemented, and proven to lead to further improvements of the SN performances.

8. Designing and implementing an online optimal control strategy for the SN based on a MPC approach. A method for integrating information about quantity of pollutants in the minimization criteria when the simplified model is used in the optimization procedure is proposed. The statistical analysis of the results shows the reliability of the proposed method, while the computational effort test proved its necessity. Moreover, the proposed method eliminates the need for expensive sensors to be mounted in multiple points of the network.

Subchapter 3.2 – WWTP optimal control:

9. Designing and implementing a MPC control strategy for a WWTP that uses the NN models mentioned at point 2 as the process model for improving the plant's effluent quality while maintaining a low treatment cost. For setting the values of the control algorithm hyperparameters, a methodology is defined such as the algorithm provides the best results with a low computational effort.
10. Designing and implementing a Fuzzy-Optimal control strategy and an Optimal-Setpoint-Based Control strategy for WWTP.

Subchapter 3.3 – IUWS optimal control:

11. Performing an analysis that the effects that SN control has on the WWTP and IUWS performances, demonstrating the advantages of considering the integrated system when developing SN control strategies.
12. Designing a methodology to constrain a SN MPC control strategy in terms of outlet valve opening in order to improve the performance of the IUWS. The results proven that even if the constrained control strategy provides a little bit worse in terms of SN performances, it leads to major improvements in the integrated system. Moreover, it has been proven that the methodology can be further improved by considering a dynamic way of calculating the SN outlet valve opening constraint based on the system state.

4.2. Future work

The work presented in this PhD thesis can be further extended in subsequent research as follows:

- Validate the results that were obtained in simulation in real IUWS environments, under uncertainty conditions.
- Extend the WWTP neural model presented in section 2.3.1 to capture more complex dynamics of the WWTP state variables, but also to capture the effects of other control variables than the aeration rate (such as recirculation or excess sludge rates) – a more complex type of NN could be used.

- Extend the neural model that can estimate WWTP effluent quality variables and that was presented in section 2.3.3 to capture the effects of other control variables than the aeration rate (such as internal/external recirculation or excess sludge rates).
- Use the neural model presented in section 2.3.3 in a mode-based control strategy (such as MPC).
- Develop a simplified IUWS model by combining the simplified SN model (presented in 2.2.5) with a neural model of a WWTP. This will require implementing an estimator for the SN effluent quality variables. The resulting simplified IUWS model could be used in a model-based control strategy that is able to minimize the environmental effects of the entire IUWS.
- Include information about GHG emissions in the SN model and update the integrated performance indicator defined in equation (2.20) by including information about the operational cost and the GHG gasses related to the SN.
- Extend the MPC used in section 3.3.1 with more complex neural models of the WWTP, but also improve its performance by using an optimization algorithm that has mechanisms for avoiding local minima.
- Improve the performances of the IUWS when the SN is controlled by the MPC algorithm constrained in terms of outlet valve opening by dynamically computing the constraint based not only on the SN state, but also on the actual quality of the WWTP effluent – fuzzy techniques might be implied.
- Redo the experiments presented in subchapter 3.4 related to the effects of SN control on the WWTP and IUWS performances, by considering various control strategies for the WWTP. This way it could be studies how the WWTP control strategy accentuates or diminishes the effects of SN control on the WWTP and overall IUWS performances.

4.3. Results dissemination

The work presented in this thesis has been disseminated in a series of journal articles and conference papers. The resulted journal articles, in chronological order, are:

1. S. Caraman, L. Luca, **I. Vasiliev**, and M. Barbu, “Optimal-Setpoint-Based Control Strategy of a Wastewater Treatment Process,” *Processes*, vol. 8, no. 10, p. 1203, 2020, doi: 10.3390/pr8101203, **ISI Indexed, IF 2.8, Q2**
2. **I. Vasiliev**, L. Luca, M. Barbu, R. Vilanova, and S. Caraman, “Optimal Control Strategy of a Sewer Network,” *Water*, vol. 14, no. 7, p. 1062, Mar. 2022, doi: 10.3390/w14071062, **ISI Indexed, IF 3, Q2**
3. **I. Vasiliev**, L. Luca, M. Barbu, R. Vilanova, and S. Caraman, “Sewer Network Multi-Objective Optimization using Genetic Algorithms,” *System Theory, Control and Computing Journal*, Jun. 2023, doi: 0.52846/stccj.2023.3.1.49
4. **I. Vasiliev**, L. Luca, M. Barbu, R. Vilanova, and S. Caraman, “Reducing the environmental impact of sewer network overflows using Model Predictive Control strategy,” *Water*

Resources Research, vol. 60, no. 1, p. e2023WR035448, 2024, doi: 10.1029/2023WR035448, **ISI Indexed, IF 4.6, Q1**

5. **I. Vasiliev**, L. Luca, M. Barbu, R. Vilanova, S. Caraman, and M. Meneses Benitez, "Integrated Urban Wastewater System operation: Performance evaluation and Sewer Network's operation implications," Water Science and Technology, 2024, **under review**

The resulted conference papers, in chronological order, are:

1. L. Luca, A. Pricopie, **I. Vasiliev**, M. Barbu and S. Caraman, "Fuzzy-Optimal Control Strategies for a Wastewater Treatment Plant," *24th International Conference on System Theory, Control and Computing (ICSTCC)*, Sinaia, 2020, doi: 10.1109/ICSTCC50638.2020.9259792, **IEEE, ISI Proceedings**
2. **I. Vasiliev**, L. Luca, M. Barbu, A. Pricopie, and S. Caraman, "Mathematical Model of a Collecting and Wastewater Treatment Integrated System," *25th International Conference on System Theory, Control and Computing (ICSTCC)*, Iași, 2021, doi: 10.1109/ICSTCC52150.2021.9607086, **IEEE, ISI Proceedings**
3. **I. Vasiliev**, L. Luca, M. Barbu, R. Vilanova, and S. Caraman, "Sewer Network Model of a City with a Medium Sized Population," *23rd International Carpathian Control Conference*, Sinaia, 2022, doi: 10.1109/ICCC54292.2022.9805864, **IEEE, ISI Proceedings**
4. **I. Vasiliev**, L. Luca, M. Barbu, R. Vilanova, and S. Caraman, "Multi-objective Optimization of a Sewer Network," *the 10th Edition of the Scientific Conference of the Doctoral Schools from the "Dunărea de Jos" University of Galati*, Galati, Romania, Jun. 2022
5. **I. Vasiliev**, L. Luca, R. Vilanova, and S. Caraman, "Sewer Network Modelling and Control – A Literature Review," in *2022 26th IEEE International Conference on System Theory, Control and Computing (ICSTCC)*, 2022, pp. 58–63. doi: 10.1109/ICSTCC55426.2022.9931870, **IEEE, ISI Proceedings**
6. **I. Vasiliev**, L. Luca, R. Vilanova, and S. Caraman, "Optimal Control of a Sewer Network," *in 2022 26th IEEE International Conference on System Theory, Control and Computing (ICSTCC)*, 2022, pp. 58–63. doi: 10.1109/ICSTCC55426.2022.9931810, **IEEE, ISI Proceedings**
7. **I. Vasiliev**, L. Luca, M. Barbu, R. Vilanova, and S. Caraman, "Sliding Window-based Particle Swarm Optimization Algorithm for a Sewer Network," *in 21st IFAC European Control Conference*, Jun. 2023, doi: 10.23919/ECC57647.2023.10178171, **IFAC, ISI Proceedings**
8. **I. Vasiliev**, L. Luca, M. Barbu, R. Vilanova, and S. Caraman, "An analysis towards integrated control of wastewater collecting and treatment systems," in *2023 27th International Conference on System Theory, Control and Computing (ICSTCC)*, 2023, pp. 233–238. doi: 10.1109/ICSTCC59206.2023.10308495, **IEEE**
9. A. E. Țîru, **I. Vasiliev**, L. Diaconu, R. Vilanova, D. Voipan, and H. Ratnaweera, "Integration of ANN for Accurate Estimation and Control in Wastewater Treatment," in *2023 IEEE 28th International Conference on Emerging Technologies and Factory Automation (ETFA)*, Sep. 2023, pp. 1–4. doi: 10.1109/ETFA54631.2023.10275569, **IEEE**

10. **I. Vasiliev**, I. Luca, L. Condrachi, L. Luca, M. Barbu, R. Vilanova, and S. Caraman, “Model Predictive Control of a wastewater treatment process using neural networks,” *in 2023 IEEE 28th International Conference on Emerging Technologies and Factory Automation (ETFA)*, Sep. 2023, pp. 1–7. doi: 10.1109/ETFA54631.2023.10275488, **IEEE**
11. D. Voipan, **I. Vasiliev**, L. Condrachi, A.-E. Voipan, and M. Barbu, “Enhancing effluent quality predictions in wastewater treatement with LSTM neural network,” *in 2024 28th International Conference on System Theory, Control and Computing (ICSTCC)*, 2024, **accepted**

Besides the papers disseminating the work presented in this thesis, two more conference papers were published in the field of system engineering:

1. **I. Vasiliev,** L. Frangu, and M. L. Cristea, “Pump Fault Detection Using Autoencoding Neural Network,” *23rd International Carpathian Control Conference*, Sinaia, 2022, doi: 10.1109/ICSTCC55426.2022.9931848, **IEEE, ISI Proceedings**
2. **I. Vasiliev**, L. Frangu, M. L. Cristea, and M. Cristian Costea, “Pump Fault Classification based on Autoencoding Convolutional Neural Network Residuum,” *in 2023 IEEE 28th International Conference on Emerging Technologies and Factory Automation (ETFA)*, Sep. 2023, pp. 1–7. doi: 10.1109/ETFA54631.2023.10275399, **IEEE**

References

[1] United Nations Department of Economic and Social Affairs, Population Division, *World Population Prospects 2022: Summary of Results*. United Nations, 2022.

[2] United Nations, *The United Nations World Water Development Report 2023: partnerships and cooperation for water*. UNESCO, 2023.

[3] United Nations General Assembly, *Transforming our world: the 2030 Agenda for Sustainable Development*. 2015.

[4] United Nations, *Blueprint for Acceleration: Sustainable Development Goal 6 Synthesis Report on Water and Sanitation*. 2023.

[5] European Parliament, "Directive 2000/60/EC of the European Parliament and of the Council of 23 October 2000 establishing a framework for Community action in the field of water policy," *Off. J. L*, vol. 327, Dec. 2000.

[6] X. Flores-Alsina, L. Corominas, L. Snip, and P. A. Vanrolleghem, "Including greenhouse gas emissions during benchmarking of wastewater treatment plant control strategies," *Water Res.*, vol. 45, no. 16, pp. 4700–4710, Oct. 2011, doi: 10.1016/j.watres.2011.04.040.

[7] Intergovernmental Panel on Climate Change, *IPCC Guidelines for National Greenhouse Gas Inventories*. Japan, 2006.

[8] Intergovernmental Panel on Climate Change, *Refinement to the 2006 IPCC Guidelines for National Greenhouse Gas Inventories*. Japan, 2019.

[9] United Nations, *The United Nations World Water Development Report 2024: water for prosperity and peace*. UNESCO, 2024.

[10] "Freshwater crisis," National Geographic. Accessed: Apr. 15, 2024. [Online]. Available: https://www.nationalgeographic.com/environment/article/freshwater-crisis

[11] J. S. Dueso, "Water as the first principle: Thales of Miletus' reasons," *Convivium*, no. 22, pp. 5–23, 2009.

[12] G. De Feo, P. Laureano, R. Drusiani, and A. N. Angelakis, "Water and wastewater management technologies through the centuries," *Water Supply*, vol. 10, no. 3, pp. 337–349, Jul. 2010, doi: 10.2166/ws.2010.102.

[13] D. Butler, C. Digman, C. Makropoulos, and J. W. Davies, *Urban Drainage*, 4th ed. Boca Raton: CRC Press, 2018. doi: 10.1201/9781351174305.

[14] A. T. Hodge, *Roman aqueducts and water supply*. Bloomsbury Academic, 2002.

[15] A. N. Angelakis and D. S. Spyridakis, “A brief history of water supply and wastewater management in ancient Greece,” *Water Supply*, vol. 10, no. 4, pp. 618–628, Sep. 2010, doi: 10.2166/ws.2010.105.

[16] S. J. Burian and F. G. Edwards, “Historical perspectives of urban drainage,” pp. 1–16, Apr. 2012, doi: 10.1061/40644(2002)284.

[17] E. C. Casella, “The archaeology of improvement in Britain, 1750–1850,” *Hist. Archaeol.*, vol. 42, no. 4, pp. 204–205, Dec. 2008, doi: 10.1007/BF03377171.

[18] G. Lofrano and J. Brown, “Wastewater management through the ages: A history of mankind,” *Sci. Total Environ.*, vol. 408, no. 22, pp. 5254–5264, Oct. 2010, doi: 10.1016/j.scitotenv.2010.07.062.

[19] N. S. Shifrin, “Pollution management in the twentieth century,” *J. Environ. Eng.*, vol. 131, no. 5, pp. 676–691, May 2005, doi: 10.1061/(ASCE)0733-9372(2005)131:5(676).

[20] Great Britain Parliament House of Commons, “The eighth report of the Royal Commission on sewage disposal,” *The Lancet*, vol. 180, no. 4657, pp. 1530–1531, Nov. 1912, doi: 10.1016/S0140-6736(01)41378-X.

[21] V. E. Shelford, “An experimental study of the effects of gas waste upon fishes with especial reference to stream pollution,” *Ill. Nat. Hist. Surv. Bull.*, vol. 011, no. 04, Mar. 1917.

[22] M. B. Ettinger, “Developments in detection of trace organic contaminants,” *J. Am. Water Works Assoc.*, vol. 57, no. 4, pp. 453–457, Apr. 1965, doi: https://doi.org/10.1002/j.1551-8833.1965.tb01424.x.

[23] P. Glibert and M. Burford, “Globally changing nutrient loads and harmful algal blooms: Recent advances, new paradigms, and continuing challenges,” *Oceanography*, vol. 30, no. 1, pp. 58–69, Mar. 2017, doi: 10.5670/oceanog.2017.110.

[24] M. M. Osiemo, G. M. Ogendi, and C. M’Erimba, “Microbial quality of drinking water and prevalence of water-related diseases in Marigat Urban Centre, Kenya,” *Environ. Health Insights*, vol. 13, p. 117863021983698, Jan. 2019, doi: 10.1177/1178630219836988.

[25] PricewaterhouseCoopers, “Rapid urbanisation,” PwC. Accessed: Apr. 11, 2024. [Online]. Available: https://www.pwc.nl/en/topics/megatrends/urbanisation.html

[26] Y. Liu, Y. Huang, Y. Liu, K. Li, and M. Li, “The impact of rainfall movement direction on urban runoff cannot be ignored in urban hydrologic management,” *Water*, vol. 13, no. 20, Art. no. 20, Jan. 2021, doi: 10.3390/w13202923.

[27] S. M. Papalexiou and A. Montanari, “Global and regional increase of precipitation extremes under global warming,” *Water Resour. Res.*, vol. 55, no. 6, pp. 4901–4914, Jun. 2019, doi: 10.1029/2018WR024067.

[28] European Council, “Council Directive 91/271/EEC of 21 May 1991 concerning urban waste-water treatment,” *Off. J. L*, vol. 330, May 1998, [Online]. Available: http://data.europa.eu/eli/dir/1998/83/oj

[29] European Council, “Consolidated text: Council Directive of 21 May 1991 concerning urban wastewater treatment (91/271/EEC)”, [Online]. Available: http://data.europa.eu/eli/dir/1991/271/2014-01-01

[30] Romanian Gouvernment, “Norme tehnice din 28 februarie 2002 (*actualizate*) privind colectarea, epurarea și evacuarea apelor uzate urbane, NTPA-011,” *Monit. Of.*, vol. 187, Mar. 2002, [Online]. Available: https://legislatie.just.ro/Public/DetaliiDocumentAfis/98309

[31] Romanian Gouvernment, “Normativ NTPA-002 din 28 februarie 2002 (*actualizat*) privind condițiile de evacuare a apelor uzate în rețelele de canalizare ale localităților și direct în stațiile de epurare,” *Monit. Of.*, vol. 187, Mar. 2002, [Online]. Available: https://legislatie.just.ro/Public/DetaliiDocumentAfis/98310

[32] J. Marsalek, T. O. Barnwell, W. Geiger, M. Grottker, W. C. Huber, A. J. Saul, W. Schilling, and H. C. Torno, “Urban Drainage Systems: Design and Operation,” *Water Sci. Technol.*, vol. 27, no. 12, pp. 31–70, Jun. 1993, doi: 10.2166/wst.1993.0291.

[33] H. Wang, G. Han, L. Zhang, Y. Qiu, J. Li, and H. Jia, “Integrated and control-oriented simulation tool for optimizing Urban Drainage System operation,” *Water*, vol. 14, no. 1, Art. no. 1, Jan. 2022, doi: 10.3390/w14010025.

[34] F. Zakizadeh, A. Moghaddam Nia, A. Salajegheh, L. A. Sañudo-Fontaneda, and N. Alamdari, “Efficient urban runoff quantity and quality modelling using SWMM model and field data in an urban watershed of Tehran Metropolis,” *Sustainability*, vol. 14, no. 3, Art. no. 3, Jan. 2022, doi: 10.3390/su14031086.

[35] Z. Zeng, X. Yuan, J. Liang, and Y. Li, “Designing and implementing an SWMM-based web service framework to provide decision support for real-time urban stormwater management,” *Environ. Model. Softw.*, vol. 135, p. 104887, Jan. 2021, doi: 10.1016/j.envsoft.2020.104887.

[36] M. Niazi, C. Nietch, M. Maghrebi, N. Jackson, B. R. Bennett, M. Tryby, and A. Massoudieh, “Storm Water Management Model: Performance review and gap analysis,” *J. Sustain. Water Built Environ.*, vol. 3, no. 2, p. 10.1061/jswbay.0000817, Jan. 2017, doi: 10.1061/jswbay.0000817.

[37] F. E. Å. Parnas, E. M. H. Abdalla, and T. M. Muthanna, “Evaluating three commonly used infiltration methods for permeable surfaces in urban areas using the SWMM and STORM,” *Hydrol. Res.*, vol. 52, no. 1, pp. 160–175, Jan. 2021, doi: 10.2166/nh.2021.048.

[38] R. E. Horton, “An approach towards a physical interpretation of infiltration capacity,” in *Proc. Soil Sci. Am.*, pp. 399–417.

[39] P. G. Holland, “Manning formula,” in *Hydrology and Lakes*, Dordrecht: Springer Netherlands, 1998, pp. 475–475. doi: 10.1007/1-4020-4513-1_149.

[40] L. Rossman and M. Simon, “Storm Water Management Model User’s Manual Version 5.2,” U.S. Environmental Protection Agency, Washington, DC, EPA/600/R-22/030, 2022.

[41] N. Marleni, K. Park, T. Lee, D. Navaratna, L. Shu, V. Jegatheesan, N. Pham, and A. Feliciano, “A methodology for simulating hydrogen sulphide generation in sewer network using EPA SWMM,” *Desalination Water Treat.*, vol. 54, no. 4–5, pp. 1308–1317, May 2015, doi: 10.1080/19443994.2014.922899.

[42] A.-K. McCall, R. Palmitessa, F. Blumensaat, E. Morgenroth, and C. Ort, “Modeling in-sewer transformations at catchment scale - implications on drug consumption estimates in wastewater-based epidemiology,” *Water Res.*, vol. 122, pp. 655–668, Oct. 2017, doi: 10.1016/j.watres.2017.05.034.

[43] B. K. Banik, C. Di Cristo, and A. Leopardi, “SWMM5 toolkit development for pollution surce identification in sewer systems,” *Procedia Eng.*, vol. 89, pp. 750–757, Jan. 2014, doi: 10.1016/j.proeng.2014.11.503.

[44] I. Vasiliev, L. Luca, R. Vilanova, and S. Caraman, “Sewer Network modelling and control – A literature review,” in *2022 26th International Conference on System Theory, Control and Computing (ICSTCC)*, Oct. 2022, pp. 58–63. doi: 10.1109/ICSTCC55426.2022.9931870.

[45] B. Joseph-Duran, C. Ocampo-Martinez, and G. Cembrano, “A control-oriented hybrid modelling approach for sewer networks: Barcelona case study,” 2013.

[46] A. Sleigh and I. Goodwill, “The St Venant Equations,” Jan. 2000.

[47] M. Marinaki and M. Papageorgiou, *Optimal real-time control of sewer networks*. in Advances in Industrial Control. London: Springer-Verlag, 2005. doi: 10.1007/b138719.

[48] S. Bagheri and A. Kabiri-Samani, “Overflow characteristics of streamlined weirs based on model experimentation,” *Flow Meas. Instrum.*, vol. 73, p. 101720, Jun. 2020, doi: 10.1016/j.flowmeasinst.2020.101720.

[49] V. Mînzu and I. Arama, “Nonlinear discrete model for the control of a sewer network,” *Ann. Dunarea Jos Univ. Galati*, vol. 38, Dec. 2015.

[50] C. Shen, H. Xia, X. Fu, X. Wang, and W. Wang, “Identifying risk components using a sewer-road integrated urban stormwater model,” *Water Resour. Manag.*, vol. 38, no. 8, pp. 3049–3070, Jun. 2024, doi: 10.1007/s11269-024-03804-0.

[51] C. Sun, L. Romero, B. Joseph-Duran, J. Meseguer, R. G. Palma, M. M. Puentes, V. Puig, and G. Cembrano, “Control-oriented quality modelling approach of sewer networks,” *J. Environ. Manage.*, vol. 294, p. 113031, Sep. 2021, doi: 10.1016/j.jenvman.2021.113031.

[52] C. C. Obropta and J. S. Kardos, “Review of urban stormwater quality models: Deterministic, stochastic, and hybrid approaches,” *JAWRA J. Am. Water Resour. Assoc.*, vol. 43, no. 6, pp. 1508–1523, 2007, doi: 10.1111/j.1752-1688.2007.00124.x.

[53] M. J. S. Safari and A. Danandeh Mehr, “Multigene genetic programming for sediment transport modeling in sewers for conditions of non-deposition with a bed deposit,” *Int. J. Sediment Res.*, vol. 33, no. 3, pp. 262–270, Sep. 2018, doi: 10.1016/j.ijsrc.2018.04.007.

[54] M. Najafzadeh, D. B. Laucelli, and A. Zahiri, “Application of model tree and Evolutionary Polynomial Regression for evaluation of sediment transport in pipes,” *KSCE J. Civ. Eng.*, vol. 21, no. 5, pp. 1956–1963, 2017, doi: http://dx.doi.org/10.1007/s12205-016-1784-7.

[55] O. Bailey, T. C. Arnot, E. J. M. Blokker, Z. Kapelan, and J. a. M. H. Hofman, “Predicting impacts of water conservation with a stochastic sewer model,” *Water Sci. Technol.*, vol. 80, no. 11, pp. 2148–2157, Dec. 2019, doi: 10.2166/wst.2020.031.

[56] O. Bailey, L. Zlatanovic, J. P. van der Hoek, Z. Kapelan, M. Blokker, T. Arnot, and J. Hofman, “A stochastic model to predict flow, nutrient and temperature changes in a sewer under water conservation scenarios,” *Water*, vol. 12, no. 4, p. 1187, Apr. 2020, doi: 10.3390/w12041187.

[57] J. Vollertsen, T. Hvitved-Jacobsen, and A. H. Nielsen, “Stochastic modeling of chemical oxygen demand transformations in gravity sewers,” *Water Environ. Res.*, vol. 77, no. 4, pp. 331–339, Aug. 2005, doi: 10.2175/106143005X51914.

[58] S. Coutu, T. Pouchon, P. Queloz, and N. Vernaz, “Integrated stochastic modeling of pharmaceuticals in sewage networks,” *Stoch. Environ. Res. Risk Assess.*, vol. 30, no. 4, pp. 1087–1097, Apr. 2016, doi: 10.1007/s00477-015-1118-1.

[59] V. Vijayashanthar, J. Qiao, Z. Zhu, P. Entwistle, and G. Yu, “Modeling fecal indicator bacteria in urban waterways using artificial neural networks,” *J. Environ. Eng.*, vol. 144, no. 6, p. 05018003, Jun. 2018, doi: 10.1061/(ASCE)EE.1943-7870.0001377.

[60] R. Penn, M. Maurer, F.-G. Michalec, A. Scheidegger, J. Zhou, and M. Holzner, “Quantifying physical disintegration of faeces in sewers: Stochastic model and flow reactor experiments,” *Water Res.*, vol. 152, pp. 159–170, Apr. 2019, doi: 10.1016/j.watres.2018.12.037.

[61] A. Campisano, C. Modica, E. Creaco, and G. Shahsavari, “A model for non-uniform sediment transport induced by flushing in sewer channels,” *Water Res.*, vol. 163, p. 114903, Oct. 2019, doi: 10.1016/j.watres.2019.114903.

[62] Y. H. Song, R. Yun, E. H. Lee, and J. H. Lee, “Predicting sedimentation in urban sewer conduits,” *Water*, vol. 10, no. 4, Art. no. 4, Apr. 2018, doi: 10.3390/w10040462.

[63] J. J. Ota and G. S. Perrusquía, “Particle velocity and sediment transport at the limit of deposition in sewers,” *Water Sci. Technol. J. Int. Assoc. Water Pollut. Res.*, vol. 67, no. 5, pp. 959–967, 2013, doi: 10.2166/wst.2013.646.

[64] I. Seco, A. Schellart, M. Gómez-Valentín, and S. Tait, “Prediction of organic combined sewer sediment release and transport,” *J. Hydraul. Eng.*, vol. 144, no. 3, p. 04018003, Mar. 2018, doi: 10.1061/(ASCE)HY.1943-7900.0001422.

[65] M. J. S. Safari, A. Shirzad, and M. Mohammadi, “Sediment transport modeling in deposited bed sewers: unified form of May’s equations using the particle swarm optimization algorithm,” *Water Sci. Technol. J. Int. Assoc. Water Pollut. Res.*, vol. 76, no. 3–4, pp. 992–1000, Aug. 2017, doi: 10.2166/wst.2017.267.

[66] J. A. Torres-Matallana, U. Leopold, K. Klepiszewski, and G. B. M. Heuvelink, “EmiStatR: A simplified and scalable urban water quality model for simulation of combined sewer overflows,” *Water*, vol. 10, no. 6, Art. no. 6, Jun. 2018, doi: 10.3390/w10060782.

[67] A. Brzezińska, G. Sakson, and M. Zawilski, “Predictive model of pollutant loads discharged by combined sewer overflows,” *Water Sci. Technol.*, vol. 77, no. 7, pp. 1819–1828, Feb. 2018, doi: 10.2166/wst.2018.050.

[68] G. Jiang, O. Gutierrez, K. R. Sharma, J. Keller, and Z. Yuan, “Optimization of intermittent, simultaneous dosage of nitrite and hydrochloric acid to control sulfide and methane productions in sewers,” *Water Res.*, vol. 45, no. 18, pp. 6163–6172, Nov. 2011, doi: 10.1016/j.watres.2011.09.009.

[69] T. Chaosakul, T. Koottatep, and C. Polprasert, “A model for methane production in sewers,” *J. Environ. Sci. Health Part A*, vol. 49, no. 11, pp. 1316–1321, Sep. 2014, doi: 10.1080/10934529.2014.910071.

[70] J. Sun, B.-J. Ni, K. R. Sharma, Q. Wang, S. Hu, and Z. Yuan, “Modelling the long-term effect of wastewater compositions on maximum sulfide and methane production rates of sewer biofilm,” *Water Res.*, vol. 129, pp. 58–65, Feb. 2018, doi: 10.1016/j.watres.2017.11.007.

[71] R. V. Matos, F. Ferreira, C. Gil, and J. S. Matos, “Understanding the effect of ventilation, intermittent pumping and seasonality in hydrogen sulfide and methane concentrations in a coastal sewerage system,” *Environ. Sci. Pollut. Res.*, vol. 26, no. 4, pp. 3404–3414, Feb. 2019, doi: 10.1007/s11356-018-3856-3.

[72] D. Jung, L. Hatrait, J. Gouello, A. Ponthieux, V. Parez, and C. Renner, “Emission of hydrogen sulfide (H2S) at a waterfall in a sewer: study of main factors affecting H2S emission and modeling approaches,” *Water Sci. Technol.*, vol. 76, no. 10, pp. 2753–2763, Aug. 2017, doi: 10.2166/wst.2017.428.

[73] N. Matias, R. Matos, F. Ferreira, J. Vollertsen, and J. S. Matos, “Release of hydrogen sulfide under intermittent flow conditions – the potential of simulation models,” *Water Sci. Technol.*, vol. 77, no. 3, pp. 777–787, Nov. 2017, doi: 10.2166/wst.2017.595.

[74] Z. Zuo, J. Chang, Z. Lu, M. Wang, Y. Lin, M. Zheng, D. Z. Zhu, T. Yu, X. Huang, and Y. Liu, “Hydrogen sulfide generation and emission in urban sanitary sewer in China: what factor plays the critical role?,” *Environ. Sci. Water Res. Technol.*, vol. 5, no. 5, pp. 839–848, Apr. 2019, doi: 10.1039/C8EW00617B.

[75] R. Saagi, X. Flores-Alsina, G. Fu, D. Butler, K. V. Gernaey, and U. Jeppsson, “Catchment & sewer network simulation model to benchmark control strategies within urban wastewater systems,” *Environ. Model. Softw.*, vol. 78, pp. 16–30, Apr. 2016, doi: 10.1016/j.envsoft.2015.12.013.

[76] K. V. Gernaey, X. Flores-Alsina, C. Rosen, L. Benedetti, and U. Jeppsson, “Dynamic influent pollutant disturbance scenario generation using a phenomenological modelling approach,” *Environ. Model. Softw.*, vol. 26, no. 11, pp. 1255–1267, 2011, doi: 10.1016/j.envsoft.2011.06.001.

[77] J. Alex, L. Benedetti, J. Copp, K. Gernaey, U. Jeppsson, I. Nopens, M. Pons, L. Rieger, C. Rosen, and J.-P. Steyer, “Benchmark Simulation Model no. 1 (BSM1),” *Rep. IWA Taskgroup Benchmarking Control Strateg. WWTPs*, Jan. 2008.

[78] J. Li, K. Sharma, W. Li, and Z. Yuan, “Swift hydraulic models for real-time control applications in sewer networks,” *Water Res.*, vol. 213, p. 118141, 2022, doi: 10.1016/j.watres.2022.118141.

[79] J. Li, W. Li, X. Chang, K. Sharma, and Z. Yuan, “Real-time predictive control for chemical distribution in sewer networks using improved elephant herding optimization,” *IEEE Trans. Ind. Inform.*, vol. 18, no. 1, pp. 571–581, 2022, doi: 10.1109/TII.2020.3028429.

[80] T. R. Rosin, Z. Kapelan, E. Keedwell, and M. Romano, “Near real-time detection of blockages in the proximity of combined sewer overflows using evolutionary ANNs and statistical process control,” *J. Hydroinformatics*, vol. 24, no. 2, pp. 259–273, 2022, doi: 10.2166/hydro.2022.036.

[81] P. K. Navin and Y. P. Mathur, “Layout and component size optimization of sewer network using spanning tree and modified PSO algorithm,” *Water Resour. Manag.*, vol. 30, no. 10, pp. 3627–3643, Aug. 2016, doi: 10.1007/s11269-016-1378-7.

[82] W. H. Hassan, Z. H. Attea, and S. S. Mohammed, “Optimum layout design of sewer networks by hybrid genetic algorithm,” *J. Appl. Water Eng. Res.*, vol. 8, no. 2, pp. 108–124, Apr. 2020, doi: 10.1080/23249676.2020.1761897.

[83] A. Haghighi and A. E. Bakhshipour, “Optimization of sewer networks using an adaptive genetic algorithm,” *Water Resour. Manag.*, vol. 26, no. 12, pp. 3441–3456, Sep. 2012, doi: 10.1007/s11269-012-0084-3.

[84] A. Haghighi and A. E. Bakhshipour, “Deterministic integrated optimization model for sewage collection networks using Tabu Search,” *J. Water Resour. Plan. Manag.*, vol. 141, no. 1, p. 04014045, Jan. 2015, doi: 10.1061/(ASCE)WR.1943-5452.0000435.

[85] P. K. Navin and Y. P. Mathur, “Design optimization of sewer system using particle swarm optimization,” in *Proceedings of Fifth International Conference on Soft Computing for Problem Solving*, vol. 437, Singapore: Springer Singapore, 2016, pp. 173–182. doi: 10.1007/978-981-10-0451-3_17.

[86] N. de Villiers, G. C. van Rooyen, and M. Middendorf, “Sewer network design layout optimisation using ant colony algorithms,” *J. South Afr. Inst. Civ. Eng.*, vol. 60, no. 3, pp. 2–15, Sep. 2018, doi: 10.17159/2309-8775/2018/v60n3a1.

[87] H. Safavi and M. A. Geranmehr, “Optimization of sewer networks using the mixed-integer linear programming,” *Urban Water J.*, vol. 14, no. 5, pp. 452–459, 2017, doi: 10.1080/1573062X.2016.1176222.

[88] R. Moeini, “Arc based ant colony optimization algorithm for solving sewer network design optimization problem,” *Sci. Iran.*, vol. 24, no. 3, pp. 953–965, Jun. 2017, doi: 10.24200/sci.2017.4079.

[89] M. Mauricio-Iglesias, I. Montero-Castro, A. L. Mollerup, and G. Sin, “A generic methodology for the optimisation of sewer systems using stochastic programming and self-optimizing control,” *J. Environ. Manage.*, vol. 155, pp. 193–203, May 2015, doi: 10.1016/j.jenvman.2015.03.034.

[90] V. Minzu, M. Barbu, and C. Nichita, “A Binary Hybrid Topology Particle Swarm Optimization algorithm for sewer network discharge,” in *2015 19th International Conference on System Theory, Control and Computing (ICSTCC)*, 2015, pp. 627–634. doi: 10.1109/ICSTCC.2015.7321363.

[91] V. Minzu and A. Serbencu, “Control structure for the optimal sewer network discharge,” in *2016 20th International Conference on System Theory, Control and Computing (ICSTCC)*, Oct. 2016, pp. 61–66. doi: 10.1109/ICSTCC.2016.7790641.

[92] M. Barbu, R. Vilanova, and I. Santin, “Fuzzy control applied on a Benchmark Simulation Model for sewer networks,” in *2016 20th International Conference on System Theory, Control and Computing (ICSTCC)*, 2016, pp. 180–185.

[93] S. R. Mounce, W. Shepherd, S. Ostojin, M. Abdel-Aal, A. N. A. Schellart, J. D. Shucksmith, and S. J. Tait, “Optimisation of a fuzzy logic-based local real-time control system for mitigation of sewer flooding using genetic algorithms,” *J. Hydroinformatics*, vol. 22, no. 2, pp. 281–295, Dec. 2019, doi: 10.2166/hydro.2019.058.

[94] B. Joseph-Duran, C. Ocampo-Martinez, and G. Cembrano, “Output-feedback control of combined sewer networks through receding horizon control with moving horizon estimation,” *Water Resour. Res.*, vol. 51, no. 10, pp. 8129–8145, 2015, doi: 10.1002/2014WR016696.

[95] M. Mahmoodian, O. Delmont, and G. Schutz, “Pollution-based model predictive control of combined sewer networks, considering uncertainty propagation,” *Int. J. Sustain. Dev. Plan.*, vol. 12, no. 01, pp. 98–111, Jan. 2017, doi: 10.2495/SDP-V12-N1-98-111.

[96] R. H. Byrd, J. C. Gilbert, and J. Nocedal, “A trust region method based on interior point techniques for nonlinear programming,” *Math. Program.*, vol. 89, no. 1, pp. 149–185, Nov. 2000, doi: 10.1007/PL00011391.

[97] E. B. Pedersen, H. R. Herbertsson, H. Niemann, N. K. Poulsen, and A. K. V. Falk, “Model Predictive Control of sewer networks,” *J. Phys. Conf. Ser.*, vol. 783, no. 1, p. 012026, Jan. 2017, doi: 10.1088/1742-6596/783/1/012026.

[98] L. R. Ben, C. Sun, R. G. Palma, B. J. Duran, J. Meseguer, G. Cembrano, and V. Puig, “A feedback simulation procedure for real-time control of urban drainage systems,” *IFAC-Pap.*, vol. 52, no. 23, pp. 101–106, Jan. 2019, doi: 10.1016/j.ifacol.2019.11.016.

[99] J. L. Svensen, H. H. Niemann, and N. K. Poulsen, “Model Predictive Control of overflow in sewer networks: A comparison of two methods,” in *2019 4th Conference on Control and Fault Tolerant Systems (SysTol)*, Sep. 2019, pp. 412–417. doi: 10.1109/SYSTOL.2019.8864755.

[100] A. Cembellín, M. Francisco, and P. Vega, “Distributed Model Predictive Control applied to a sewer system,” *Processes*, vol. 8, no. 12, Art. no. 12, Dec. 2020, doi: 10.3390/pr8121595.

[101] A. Cembellín, M. Francisco, and P. Vega, “Optimal operation of a benchmark simulation model for sewer networks using a qualitative distributed Model Predictive Control algorithm,” *Processes*, vol. 11, no. 5, Art. no. 5, May 2023, doi: 10.3390/pr11051528.

[102] K. El Ghazouli, J. El Khatabi, A. Soulhi, and I. Shahrour, “Model predictive control based on artificial intelligence and EPA-SWMM model to reduce CSOs impacts in sewer systems,” *Water Sci. Technol.*, vol. 85, no. 1, pp. 398–408, Jan. 2022, doi: 10.2166/wst.2021.511.

[103] S. C. Troutman, N. G. Love, and B. Kerkez, “Balancing water quality and flows in combined sewer systems using real-time control,” *Environ. Sci. Water Res. Technol.*, vol. 6, no. 5, pp. 1357–1369, 2020, doi: 10.1039/C9EW00882A.

[104] C. Brepols, H. Dahmen, M. Lange, A. Sohr, R. Kiesewski, and R. Rohlfing, “Model-based sewer network control - practical experiences,” in *New Trends in Urban Drainage Modelling*, G. Mannina, Ed., in Green Energy and Technology. Cham: Springer International Publishing, 2019, pp. 20–24. doi: 10.1007/978-3-319-99867-1_3.

[105] U. Rathnayake and A. H. M. Faisal Anwar, “Dynamic control of urban sewer systems to reduce combined sewer overflows and their adverse impacts,” *J. Hydrol.*, vol. 579, p. 124150, Dec. 2019, doi: 10.1016/j.jhydrol.2019.124150.

[106] D. Ochoa, G. Riaño-Briceño, N. Quijano, and C. Ocampo-Martinez, “Control of urban drainage systems: optimal flow control and deep learning in action,” in *2019 American Control Conference (ACC)*, Jul. 2019, pp. 4826–4831. doi: 10.23919/ACC.2019.8814958.

[107] S. Pei, L. Hoang, G. Fu, and D. Butler, “Real-time control of urban drainage systems using neuro-evolution,” *J. Environ. Manage.*, vol. 360, p. 121133, Jun. 2024, doi: 10.1016/j.jenvman.2024.121133.

[108] D. Zhang, N. Martinez, G. Lindholm, and H. Ratnaweera, “Manage sewer in-line storage control using hydraulic model and Recurrent Neural Network,” *Water Resour. Manag.*, vol. 32, no. 6, pp. 2079–2098, Apr. 2018, doi: 10.1007/s11269-018-1919-3.

[109] D. Zhang, G. Lindholm, and H. Ratnaweera, “Use long short-term memory to enhance Internet of Things for combined sewer overflow monitoring,” *J. Hydrol.*, vol. 556, pp. 409–418, Jan. 2018, doi: 10.1016/j.jhydrol.2017.11.018.

[110] D. Zhang, E. S. Hølland, G. Lindholm, and H. Ratnaweera, “Hydraulic modeling and deep learning based flow forecasting for optimizing inter catchment wastewater transfer,” *J. Hydrol.*, vol. 567, pp. 792–802, Dec. 2018, doi: 10.1016/j.jhydrol.2017.11.029.

[111] H. D. Monteith, H. R. Sahely, H. L. MacLean, and D. M. Bagley, “A rational procedure for estimation of Greenhouse-Gas emissions from municipal Wastewater Treatment Plants,” *Water Environ. Res.*, vol. 77, no. 4, pp. 390–403, 2005, doi: 10.1002/j.1554-7531.2005.tb00298.x.

[112] Y. Shen, J. L. Linville, M. Urgun-Demirtas, M. M. Mintz, and S. W. Snyder, “An overview of biogas production and utilization at full-scale wastewater treatment plants (WWTPs) in the United States: Challenges and opportunities towards energy-neutral WWTPs,” *Renew. Sustain. Energy Rev.*, vol. 50, pp. 346–362, Oct. 2015, doi: 10.1016/j.rser.2015.04.129.

[113] E. Yakamercan, A. Ari, and A. Aygün, “Land application of municipal sewage sludge: Human health risk assessment of heavy metals,” *J. Clean. Prod.*, vol. 319, p. 128568, Oct. 2021, doi: 10.1016/j.jclepro.2021.128568.

[114] *Advances in Wastewater Treatment I*, 1st ed., vol. 1. in Materials Research Foundations, vol. 1. Materials Research Forum LLC, 2021. doi: 10.21741/9781644901144.

[115] *About water treatment*. Helsinki: Kemira Oyj, 2020.

[116] S. Periyasamy, I. A. Kumar, and N. Viswanathan, “Activated carbon from different waste materials for the removal of toxic metals,” in *Green Materials for Wastewater Treatment*, Mu. Naushad and E. Lichtfouse, Eds., in Environmental Chemistry for a Sustainable World. , Cham: Springer International Publishing, 2020, pp. 47–68. doi: 10.1007/978-3-030-17724-9_3.

[117] J. N. Sahu, R. R. Karri, H. M. Zabed, S. Shams, and X. Qi, “Current perspectives and future prospects of nano-biotechnology in wastewater treatment,” *Sep. Purif. Rev.*, vol. 50, no. 2, pp. 139–158, Apr. 2021, doi: 10.1080/15422119.2019.1630430.

[118] E. Hu, “Catalytic ozonation for textile dyeing wastewater treatment and reuse,” 2016.

[119] G. B. Dirisu, U. C. Okonkwo, I. P. Okokpujie, and O. S. Fayomi, “Comparative analysis of the effectiveness of reverse osmosis and ultraviolet radiation of water treatment,” *J. Ecol. Eng.*, vol. 20, no. 1, pp. 61–75, Jan. 2019, doi: 10.12911/22998993/93978.

[120] M. Muloiwa, S. Nyende-Byakika, and M. Dinka, “Comparison of unstructured kinetic bacterial growth models.,” *South Afr. J. Chem. Eng.*, vol. 33, pp. 141–150, Jul. 2020, doi: 10.1016/j.sajce.2020.07.006.

[121] J. Monod, “The growth of bacterial cultures,” *Annu. Rev. Microbiol.*, vol. 3, no. 1, pp. 371–394, Oct. 1949, doi: 10.1146/annurev.mi.03.100149.002103.

[122] E. Maleki, A. Bokhary, and B. Q. Liao, “A review of anaerobic digestion bio-kinetics,” *Rev. Environ. Sci. Biotechnol.*, vol. 17, no. 4, pp. 691–705, Dec. 2018, doi: 10.1007/s11157-018-9484-z.

[123] D. E. Y. 1959 Contois, “Kinetics of bacterial growth: Relationship between population density and specific growth rate of continuous cultures,” *Microbiology*, vol. 21, no. 1, pp. 40–50, doi: 10.1099/00221287-21-1-40.

[124] M. C. M. Van Loosdrecht, C. M. Lopez-Vazquez, S. C. F. Meijer, C. M. Hooijmans, and D. Brdjanovic, “Twenty-five years of ASM1: past, present and future of wastewater treatment modelling,” *J. Hydroinformatics*, vol. 17, no. 5, pp. 697–718, Jun. 2015, doi: 10.2166/hydro.2015.006.

[125] M. Henze, C. Grady, W. Gujer, G. Marais, and T. Matsuo, “Activated Sludge Model 1,” *IAWQ Sci. Tech. Rep.*, vol. 1, 1987.

[126] H. Hauduc, L. Rieger, A. Oehmen, M. C. M. van Loosdrecht, Y. Comeau, A. Héduit, P. A. Vanrolleghem, and S. Gillot, “Critical review of activated sludge modeling: state of process knowledge, modeling concepts, and limitations,” *Biotechnol. Bioeng.*, vol. 110, no. 1, pp. 24–46, Jan. 2013, doi: 10.1002/bit.24624.

[127] W. Gujer, M. Henze, T. Mino, T. Matsuo, M. C. Wentzel, and G. v. R. Marais, “The Activated Sludge Model No. 2: Biological phosphorus removal,” *Water Sci. Technol.*, vol. 31, no. 2, pp. 1–11, Jan. 1995, doi: 10.1016/0273-1223(95)00175-M.

[128] M. Henze, W. Gujer, T. Mino, T. Matsuo, M. C. Wentzel, G. v. R. Marais, and M. C. M. Van Loosdrecht, “Activated Sludge Model No.2d, ASM2D,” *Water Sci. Technol.*, vol. 39, no. 1, pp. 165–182, Jan. 1999, doi: 10.2166/wst.1999.0036.

[129] G. J. F. Smolders, J. van der Meij, M. C. M. van Loosdrecht, and J. J. Heijnen, “Model of the anaerobic metabolism of the biological phosphorus removal process: Stoichiometry and pH influence,” *Biotechnol. Bioeng.*, vol. 43, no. 6, pp. 461–470, 1994, doi: 10.1002/bit.260430605.

[130] S. C. F. Meijer, “Theoretical and practical aspects of modelling activated sludge processes,” PhD Thesis, Delft University of Technology, 2004.

[131] W. Gujer, M. Henze, T. Mino, and M. van Loosdrecht, “Activated Sludge Model No. 3,” *Water Sci. Technol.*, vol. 39, no. 1, pp. 183–193, Jan. 1999, doi: 10.1016/S0273-1223(98)00785-9.

[132] C. Rosen, U. Jeppsson, and P. Vanrolleghem, “Towards a common benchmark for long-term process control and monitoring performance evaluation,” *Water Sci. Technol. J. Int. Assoc. Water Pollut. Res.*, vol. 50, pp. 41–9, Feb. 2004, doi: 10.2166/wst.2004.0669.

[133] K. Gernaey, U. Jeppsson, P. Vanrolleghem, and J. B. Copp, *Benchmarking of control strategies for wastewater treatment plants*. in Scientific and Technical Report Series. IWA Publishing, 2014.

[134] D. J. Batstone, J. Keller, I. Angelidaki, S. V. Kalyuzhnyi, S. G. Pavlostathis, A. Rozzi, W. T. M. Sanders, H. Siegrist, and V. A. Vavilin, “The IWA Anaerobic Digestion Model No 1 (ADM1),” *Water Sci. Technol.*, vol. 45, no. 10, pp. 65–73, May 2002, doi: 10.2166/wst.2002.0292.

[135] B.-J. Ni, M. Ruscalleda, C. Pellicer-Nàcher, and B. F. Smets, “Modeling nitrous oxide production during biological nitrogen removal via nitrification and denitrification: Extensions to the general ASM models,” *Environ. Sci. Technol.*, vol. 45, no. 18, pp. 7768–7776, Sep. 2011, doi: 10.1021/es201489n.

[136] K. E. Mampaey, B. Beuckels, M. J. Kampschreur, R. Kleerebezem, M. C. M. van Loosdrecht, and E. I. P. Volcke, “Modelling nitrous and nitric oxide emissions by autotrophic ammonia-oxidizing bacteria,” *Environ. Technol.*, vol. 34, no. 12, pp. 1555–1566, Jun. 2013, doi: 10.1080/09593330.2012.758666.

[137] W. C. Hiatt and C. P. L. Grady, “An updated process model for carbon oxidation, nitrification, and denitrification,” *Water Environ. Res.*, vol. 80, no. 11, pp. 2145–2156, 2008, doi: 10.2175/106143008X304776.

[138] L. Guo and P. A. Vanrolleghem, “Calibration and validation of an activated sludge model for greenhouse gases no. 1 (ASMG1): prediction of temperature-dependent N2O emission dynamics,” *Bioprocess Biosyst. Eng.*, vol. 37, no. 2, pp. 151–163, Feb. 2014, doi: 10.1007/s00449-013-0978-3.

[139] K. Blomberg, P. Kosse, A. Mikola, A. Kuokkanen, T. Fred, M. Heinonen, M. Mulas, M. Lübken, M. Wichern, and R. Vahala, “Development of an extended ASM3 model for predicting the nitrous oxide emissions in a full-scale wastewater treatment plant,” *Environ. Sci. Technol.*, vol. 52, no. 10, pp. 5803–5811, May 2018, doi: 10.1021/acs.est.8b00386.

[140] D. Kyung, M. Kim, J. Chang, and W. Lee, “Estimation of greenhouse gas emissions from a hybrid wastewater treatment plant,” *J. Clean. Prod.*, vol. 95, pp. 117–123, May 2015, doi: 10.1016/j.jclepro.2015.02.032.

[141] G. Mannina, T. F. Rebouças, A. Cosenza, and K. Chandran, “A plant-wide wastewater treatment plant model for carbon and energy footprint: Model application and scenario analysis,” *J. Clean. Prod.*, vol. 217, pp. 244–256, Apr. 2019, doi: 10.1016/j.jclepro.2019.01.255.

[142] K. Li, H. Duan, L. Liu, R. Qiu, B. van den Akker, B.-J. Ni, T. Chen, H. Yin, Z. Yuan, and L. Ye, “An integrated first principal and deep learning approach for modeling nitrous oxide emissions from wastewater treatment plants,” *Environ. Sci. Technol.*, vol. 56, no. 4, pp. 2816–2826, Feb. 2022, doi: 10.1021/acs.est.1c05020.

[143] W. Zhang, J. Zhang, and R. Bai, “Direct adaptive neural network control for dissolved oxygen concentration,” in *2018 13th World Congress on Intelligent Control and Automation (WCICA)*, Changsha, China: IEEE, Jul. 2018, pp. 1494–1499. doi: 10.1109/WCICA.2018.8630484.

[144] G. Han, H. Han, and J. Qiao, “A GPRFNN-based control system for wastewater treatment process,” in *2016 35th Chinese Control Conference (CCC)*, Chengdu: IEEE, Jul. 2016, pp. 891–896. doi: 10.1109/ChiCC.2016.7553199.

[145] A. Nair, V.-M. Cristea, P. Ş. Agachi, and M. Brehar, “Model calibration and feed-forward control of the wastewater treatment plant - case study for CLUJ-Napoca WWTP,” *Water Environ. J.*, vol. 32, no. 2, pp. 164–172, May 2018, doi: 10.1111/wej.12310.

[146] I. Pisa, A. Morell, J. L. Vicario, and R. Vilanova, “ANN-based internal model control strategy applied in the WWTP industry,” in *2019 24th IEEE International Conference on Emerging*

Technologies and Factory Automation (ETFA), Zaragoza, Spain: IEEE, Sep. 2019, pp. 1477–1480. doi: 10.1109/ETFA.2019.8868241.

[147] J. Pascual-Pañach, M. À. Cugueró-Escofet, M. Sànchez-Marrè, and P. Aguiló-Martos, “Application of CBR for intelligent process control of a WWTP,” *Artif. Intell. Res. Dev.*, pp. 160–169, 2019, doi: 10.3233/FAIA190119.

[148] J. Drewnowski, “Advanced supervisory control system implemented at full-scale WWTP—A case study of optimization and energy balance improvement,” *Water*, vol. 11, no. 6, p. 1218, Jun. 2019, doi: 10.3390/w11061218.

[149] J. Qiao, G. Han, H. Han, C. Yang, and W. Li, “Decoupling control for wastewater treatment process based on recurrent fuzzy neural network,” *Asian J. Control*, vol. 21, no. 3, pp. 1270–1280, May 2019, doi: 10.1002/asjc.1844.

[150] W. Zhang and J. Qiao, “Multi-variable direct self-organizing fuzzy neural network control for wastewater treatment process,” *Asian J. Control*, vol. 22, no. 2, pp. 716–728, Mar. 2020, doi: 10.1002/asjc.1919.

[151] M. Simon-Várhelyi, V. M. Cristea, A. V. Luca, and M. A. Brehar, “Optimization and control of aeration distribution in the WWTP nitrification reactor,” *Rev. Roum. Chim.*, vol. 65, no. 6, pp. 601–609, 2020, doi: 10.33224/rrch.2020.65.6.11.

[152] R. Piotrowski, H. Sawicki, and K. Żuk, “Novel hierarchical nonlinear control algorithm to improve dissolved oxygen control in biological WWTP,” *J. Process Control*, vol. 105, pp. 78–87, Sep. 2021, doi: 10.1016/j.jprocont.2021.07.009.

[153] Q. Yang, W. Cao, W. Meng, and J. Si, “Reinforcement-Learning-based tracking control of waste water treatment process under realistic system conditions and control performance requirements,” *IEEE Trans. Syst. Man Cybern. Syst.*, pp. 1–11, 2021, doi: 10.1109/TSMC.2021.3122802.

[154] A. G. Shiek, V. R. K. Machavolu, M. M. Seepana, and S. R. Ambati, “Design of control strategies for nutrient removal in a biological wastewater treatment process,” *Environ. Sci. Pollut. Res.*, vol. 28, no. 10, pp. 12092–12106, Mar. 2021, doi: 10.1007/s11356-020-09347-2.

[155] B. Ying-Chun and Q. Jun-Fei, “Heuristic dynamic programming using echo state network for multivariable tracking control of wastewater treatment process: E-HDP controller for multivariable tracking control of WWTP,” *Asian J. Control*, vol. 17, no. 5, pp. 1654–1666, Sep. 2015, doi: 10.1002/asjc.994.

[156] G. Harja, G. Vlad, and I. Nascu, “MPC advanced control of dissolved oxygen in an activated sludge wastewater treatment plant,” in *2016 IEEE International Conference on Automation, Quality and Testing, Robotics (AQTR)*, Cluj-Napoca, Romania: IEEE, May 2016, pp. 1–6. doi: 10.1109/AQTR.2016.7501329.

[157] Y.-C. Bo and X. Zhang, “Online adaptive dynamic programming based on echo state networks for dissolved oxygen control,” *Appl. Soft Comput.*, vol. 62, pp. 830–839, Jan. 2018, doi: 10.1016/j.asoc.2017.09.015.

[158] J. Qiao, G. Han, H. Han, C. Yang, and W. Li, “A hybrid intelligent optimal control system design for wastewater treatment process,” *Inf. Technol. Control*, vol. 46, no. 3, pp. 382–394, Sep. 2017, doi: 10.5755/j01.itc.46.3.16061.

[159] J. Pang, S. Yang, L. He, Y. Chen, and N. Ren, “Intelligent control/operational strategies in WWTPs through an integrated Q-Learning algorithm with ASM2d-guided reward,” *Water*, vol. 11, no. 5, p. 927, May 2019, doi: 10.3390/w11050927.

[160] H. Han, J. Zhang, S. Du, H. Sun, and J. Qiao, “Robust optimal control for anaerobic-anoxic-oxic reactors,” *Sci. China Technol. Sci.*, vol. 64, no. 7, pp. 1485–1499, Jul. 2021, doi: 10.1007/s11431-020-1821-2.

[161] J.-F. Qiao, Y. Hou, L. Zhang, and H.-G. Han, “Adaptive fuzzy neural network control of wastewater treatment process with multiobjective operation,” *Neurocomputing*, vol. 275, pp. 383–393, Jan. 2018, doi: 10.1016/j.neucom.2017.08.059.

[162] H.-G. Han, L. Zhang, H.-X. Liu, and J.-F. Qiao, “Multiobjective design of fuzzy neural network controller for wastewater treatment process,” *Appl. Soft Comput.*, vol. 67, pp. 467–478, Jun. 2018, doi: 10.1016/j.asoc.2018.03.020.

[163] J. Qiao and W. Zhang, “Dynamic multi-objective optimization control for wastewater treatment process,” *Neural Comput. Appl.*, vol. 29, no. 11, pp. 1261–1271, Jun. 2018, doi: 10.1007/s00521-016-2642-8.

[164] H. Zhou and J. Qiao, “Multiobjective optimal control for wastewater treatment process using adaptive MOEA/D,” *Appl. Intell.*, vol. 49, no. 3, pp. 1098–1126, Mar. 2019, doi: 10.1007/s10489-018-1319-7.

[165] H. Han, Z. Liu, Y. Hou, and J. Qiao, “Data-driven multiobjective predictive control for wastewater treatment process,” *IEEE Trans. Ind. Inform.*, vol. 16, no. 4, pp. 2767–2775, Apr. 2020, doi: 10.1109/TII.2019.2940663.

[166] E. S. S. Tejaswini, S. Panjwani, U. B. B. Gara, and S. R. Ambati, “Multi-objective optimization based controller design for improved wastewater treatment plant operation,” *Environ. Technol. Innov.*, vol. 23, p. 101591, Aug. 2021, doi: 10.1016/j.eti.2021.101591.

[167] H.-G. Han, Z. Liu, W. Lu, Y. Hou, and J.-F. Qiao, “Dynamic MOPSO-based optimal control for wastewater treatment process,” *IEEE Trans. Cybern.*, vol. 51, no. 5, pp. 2518–2528, May 2021, doi: 10.1109/TCYB.2019.2925534.

[168] S. Heo, K. Nam, S. Tariq, J. Y. Lim, J. Park, and C. Yoo, “A hybrid machine learning–based multi-objective supervisory control strategy of a full-scale wastewater treatment for cost-effective and sustainable operation under varying influent conditions,” *J. Clean. Prod.*, vol. 291, p. 125853, Apr. 2021, doi: 10.1016/j.jclepro.2021.125853.

[169] H. Han, L. Zhang, H.-X. Liu, C. Yang, and J. Qiao, “Intelligent optimal control system with flexible objective functions and its applications in wastewater treatment process,” *IEEE Trans. Syst. Man Cybern. Syst.*, vol. 51, no. 6, pp. 3464–3476, Jun. 2021, doi: 10.1109/TSMC.2019.2927631.

[170] Y. Xie, D. Wang, and J. Qiao, “Dynamic multi-objective intelligent optimal control toward wastewater treatment processes,” *Sci. China Technol. Sci.*, vol. 65, no. 3, pp. 569–580, Mar. 2022, doi: 10.1007/s11431-021-1960-7.

[171] C. Chen, H. Han, H. Sun, H. Yang, and J. Qiao, “Multi-objective integrated robust optimal control for wastewater treatment processes,” *IEEE Trans. Autom. Sci. Eng.*, vol. 21, no. 2, pp. 1380–1391, Apr. 2024, doi: 10.1109/TASE.2023.3240497.

[172] D. Kim, J. D. Bowen, and E. C. Ozelkan, “Optimization of wastewater treatment plant operation for greenhouse gas mitigation,” *J. Environ. Manage.*, vol. 163, pp. 39–48, Nov. 2015, doi: 10.1016/j.jenvman.2015.07.005.

[173] P. Yapıcıoğlu and Ö. Demir, “Minimizing greenhouse gas emissions of an industrial wastewater treatment plant in terms of water–energy nexus,” *Appl. Water Sci.*, vol. 11, no. 12, p. 180, Dec. 2021, doi: 10.1007/s13201-021-01484-4.

[174] D. Butler and M. Schutze, “Integrating simulation models with a view to optimal control of urban wastewater systems,” *Environ. Model. Softw.*, vol. 20, no. 4, pp. 415–426, Apr. 2005, doi: 10.1016/j.envsoft.2004.02.003.

[175] K. R. Sharma, S. Corrie, and Z. Yuan, “Integrated modelling of sewer system and wastewater treatment plant for investigating the impacts of chemical dosing in sewers,” *Water Sci. Technol.*, vol. 65, no. 8, pp. 1399–1405, Apr. 2012, doi: 10.2166/wst.2012.019.

[176] M. Barbu, R. Vilanova, I. Santin, and M. Meneses, “Decentralized control strategies evaluation for an Integrated Urban Wastewater System,” in *2017 18th International Carpathian Control Conference (ICCC)*, Sinaia, Romania: IEEE, May 2017, pp. 46–51. doi: 10.1109/CarpathianCC.2017.7970369.

[177] L. Guo, S. Tik, J. M. Ledergerber, D. Santoro, E. Elbeshbishy, and P. A. Vanrolleghem, “Conceptualizing the sewage collection system for integrated sewer-WWTP modelling and optimization,” in *New Trends in Urban Drainage Modelling*, G. Mannina, Ed., in Green Energy and Technology. , Cham: Springer International Publishing, 2019, pp. 842–847. doi: 10.1007/978-3-319-99867-1_145.

[178] R. Saagi, X. Flores-Alsina, S. Kroll, K. V. Gernaey, and U. Jeppsson, “A model library for simulation and benchmarking of integrated urban wastewater systems,” *Environ. Model. Softw.*, vol. 93, pp. 282–295, Jul. 2017, doi: 10.1016/j.envsoft.2017.03.026.

[179] P. Shanahan, D. Borchardt, M. Henze, W. Rauch, P. Reichert, L. Somlyódy, and P. Vanrolleghem, “River Water Quality Model no. 1 (RWQM1): I. Modelling approach,” *Water Sci. Technol.*, vol. 43, no. 5, pp. 1–9, Mar. 2001, doi: 10.2166/wst.2001.0238.

[180] K. Seggelke, R. Löwe, T. Beeneken, and L. Fuchs, “Implementation of an integrated real-time control system of sewer system and waste water treatment plant in the city of Wilhelmshaven,” *Urban Water J.*, vol. 10, no. 5, pp. 330–341, Oct. 2013, doi: 10.1080/1573062X.2013.820331.

[181] S. Kroll, G. Dirckx, B. M. R. Donckels, M. Van Dorpe, M. Weemaes, and P. Willems, “Modelling real-time control of WWTP influent flow under data scarcity,” *Water Sci. Technol.*, vol. 73, no. 7, pp. 1637–1643, Dec. 2015, doi: 10.2166/wst.2015.641.

[182] S. Kroll, A. Fenu, T. Wambecq, M. Weemaes, J. Van Impe, and P. Willems, “Energy optimization of the urban drainage system by integrated real-time control during wet and dry weather conditions,” *Urban Water J.*, vol. 15, no. 4, pp. 362–370, Apr. 2018, doi: 10.1080/1573062X.2018.1480726.

[183] Z. Lu, M. Wang, M. Zhang, J. Li, Y. Xu, H. Shi, Y. Liu, and X. Huang, “Water-level based discrete integrated dynamic control to regulate the flow for sewer-WWTP operation,” *Front. Environ. Sci. Eng.*, vol. 14, no. 3, p. 45, Jun. 2020, doi: 10.1007/s11783-020-1222-4.

[184] C. Sun, L. Romero, B. Joseph-Duran, J. Meseguer, E. Muñoz, R. Guasch, M. Martinez, V. Puig, and G. Cembrano, “Integrated pollution-based real-time control of sanitation

systems," *J. Environ. Manage.*, vol. 269, p. 110798, Sep. 2020, doi: 10.1016/j.jenvman.2020.110798.

[185] I. Vasiliev, L. Luca, M. Barbu, R. Vilanova, and S. Caraman, "Sewer network model of a city with a medium sized population," in *23rd International Carpathian Control Conference*, Sinaia, 2022. doi: 10.1109/ICCC54292.2022.9805864.

[186] W. J. Ng, *Industrial wastewater treatment*. Imperial College Press, 2006.

[187] I. Vasiliev, I. Luca, L. Condrachi, L. Luca, M. Barbu, R. Vilanova, and S. Caraman, "Model Predictive Control of a wastewater treatment process using neural networks," in *2023 IEEE 28th International Conference on Emerging Technologies and Factory Automation (ETFA)*, Sep. 2023, pp. 1–7. doi: 10.1109/ETFA54631.2023.10275488.

[188] F. Nejjari, B. Dahhou, A. Benhammou, and G. Roux, "Non-linear multivariable adaptive control of an activated sludge wastewater treatment process," *Int. J. Adapt. Control Signal Process.*, vol. 13, no. 5, pp. 347–365, 1999, doi: 10.1002/(SICI)1099-1115(199908)13:5<347::AID-ACS543>3.0.CO;2-8.

[189] H. N. Koivo, "Neural Networks: Basics using MATLAB Neural Network Toolbox," 2008.

[190] A. E. Țîru, I. Vasiliev, L. Diaconu, R. Vilanova, D. Voipan, and H. Ratnaweera, "Integration of ANN for accurate estimation and control in wastewater treatment," in *2023 IEEE 28th International Conference on Emerging Technologies and Factory Automation (ETFA)*, Sep. 2023, pp. 1–4. doi: 10.1109/ETFA54631.2023.10275569.

[191] S. Naduvil-Vadukootu, R. A. Angryk, and P. Riley, "Evaluating preprocessing strategies for time series prediction using deep learning architectures," in *The Thirtieth International Flairs Conference*, 2017.

[192] I. Pisa, "Artificial Neural Networks in the wastewater industry. From conventional to data-based industrial control," PhD Thesis, Autonomous University of Barcelona, 2022.

[193] S. Hochreiter and J. Schmidhuber, "Long Short-Term Memory," *Neural Comput.*, vol. 9, no. 8, pp. 1735–1780, Nov. 1997, doi: 10.1162/neco.1997.9.8.1735.

[194] C. Bergmeir, R. J. Hyndman, and B. Koo, "A note on the validity of cross-validation for evaluating autoregressive time series prediction," *Comput. Stat. Data Anal.*, vol. 120, pp. 70–83, Apr. 2018, doi: 10.1016/j.csda.2017.11.003.

[195] I. N. Da Silva, D. Hernane Spatti, R. Andrade Flauzino, L. H. B. Liboni, and S. F. Dos Reis Alves, *Artificial Neural Networks*. Cham: Springer International Publishing, 2017. doi: 10.1007/978-3-319-43162-8.

[196] D. Voipan, I. Vasiliev, L. Condrachi, A.-E. Voipan, and M. Barbu, "Enhancing effluent quality predictions in wastewater treatement with LSTM neural network," in *2024 28th International Conference on System Theory, Control and Computing (ICSTCC)*, 2024.

[197] L. Luca, "Advanced control strategies for biological waste water treatment processes," Dunarea de Jos, Galati, Romania, 2018.

[198] I. Vasiliev, L. Luca, M. Barbu, A. Pricopie, and S. Caraman, "Mathematical model of a collecting and wastewater treatment integrated system," in *2021 25th International Conference on System Theory, Control and Computing (ICSTCC)*, IEEE, 2021, pp. 419–424. doi: 10.1109/ICSTCC52150.2021.9607086.

[199] K. V. Gernaey, M. C. M. van Loosdrecht, M. Henze, M. Lind, and S. B. Jørgensen, “Activated sludge wastewater treatment plant modelling and simulation: state of the art,” *Environ. Model. Softw.*, vol. 19, no. 9, pp. 763–783, Sep. 2004, doi: 10.1016/j.envsoft.2003.03.005.

[200] M. Barbu, R. Vilanova, M. Meneses, and I. Santin, “On the evaluation of the global impact of control strategies applied to wastewater treatment plants,” *J. Clean. Prod.*, vol. 149, pp. 396–405, Apr. 2017, doi: 10.1016/j.jclepro.2017.02.018.

[201] I. Vasiliev, L. Luca, M. Barbu, R. Vilanova, and S. Caraman, “Optimal control strategy of a sewer network,” *Water*, vol. 14, no. 7, p. 1062, Mar. 2022, doi: 10.3390/w14071062.

[202] M. Mitchell, *An introduction to genetic algorithms*. Cambridge, MA, US: MIT Press, 1996.

[203] K. Deb and T. Goel, “Controlled elitist Non-dominated Sorting Genetic Algorithms for better convergence,” in *Evolutionary Multi-Criterion Optimization*, vol. 1993, E. Zitzler, L. Thiele, K. Deb, C. A. Coello Coello, and D. Corne, Eds., in Lecture Notes in Computer Science, vol. 1993. , Berlin, Heidelberg: Springer Berlin Heidelberg, 2001, pp. 67–81. doi: 10.1007/3-540-44719-9_5.

[204] I. Vasiliev, L. Luca, M. Barbu, R. Vilanova, and S. Caraman, “Multi-objective optimization of a sewer network,” presented at the 10th Edition of the Scientific Conference of the Doctoral Schools from the “Dunărea de Jos” University of Galaţi, Galati, Romania, Jun. 2022.

[205] I. Vasiliev, L. Luca, M. Barbu, R. Vilanova, and S. Caraman, “Sewer network multi-objective optimization using genetic algorithms,” *Syst. Theory Control Comput. J.*, vol. 3, no. 1, Art. no. 1, Jun. 2023, doi: 10.52846/stccj.2023.3.1.49.

[206] C. C. Aldea and C. Olariu, “Selecting the optimal software solution under conditions of uncertainty,” *Procedia - Soc. Behav. Sci.*, vol. 109, pp. 333–337, Jan. 2014, doi: 10.1016/j.sbspro.2013.12.467.

[207] H. S. Sánchez, A. Visioli, and R. Vilanova, “Optimal Nash tuning rules for robust PID controllers,” *J. Frankl. Inst.*, vol. 354, no. 10, pp. 3945–3970, Jul. 2017, doi: 10.1016/j.jfranklin.2017.03.012.

[208] G. Guariso and M. Sangiorgio, “Improving the performance of multiobjective genetic algorithms: An elitism-based approach,” *Information*, vol. 11, no. 12, p. 587, Dec. 2020, doi: 10.3390/info11120587.

[209] I. Vasiliev, L. Luca, R. Vilanova, and S. Caraman, “Optimal control of a sewer network,” in *2022 26th International Conference on System Theory, Control and Computing (ICSTCC)*, Sinaia, Romania: IEEE, Oct. 2022, pp. 80–85. doi: 10.1109/ICSTCC55426.2022.9931810.

[210] M. R. Bonyadi and Z. Michalewicz, “Particle Swarm Optimization for single objective continuous space problems: A review,” *Evol. Comput.*, vol. 25, no. 1, pp. 1–54, Mar. 2017, doi: 10.1162/EVCO_r_00180.

[211] E. Mezura-Montes and C. A. Coello Coello, “Constraint-handling in nature-inspired numerical optimization: Past, present and future,” *Swarm Evol. Comput.*, vol. 1, no. 4, pp. 173–194, Dec. 2011, doi: 10.1016/j.swevo.2011.10.001.

[212] M. E. H. Pedersen, *Good parameters for particle swarm optimization*. Hvass Lab., Copenhagen, Denmark, Tech. Rep. HL1001, 2010.

[213] J. C. Lagarias, J. A. Reeds, M. H. Wright, and P. E. Wright, “Convergence properties of the Nelder-Mead simplex method in low dimensions,” *SIAM J. Optim.*, vol. 9, no. 1, pp. 112–147, Jan. 1998, doi: 10.1137/S1052623496303470.

[214] I. Vasiliev, L. Luca, M. Barbu, R. Vilanova, and S. Caraman, “Sliding window-based Particle Swarm Optimization algorithm for a sewer network,” in *2023 European Control Conference (ECC)*, Jun. 2023, pp. 1–6. doi: 10.23919/ECC57647.2023.10178171.

[215] M. P. Fay and M. A. Proschan, “Wilcoxon-Mann-Whitney or t-test? On assumptions for hypothesis tests and multiple interpretations of decision rules,” *Stat. Surv.*, vol. 4, pp. 1–39, 2010, doi: 10.1214/09-SS051.

[216] I. Vasiliev, L. Luca, M. Barbu, R. Vilanova, and S. Caraman, “Reducing the environmental impact of sewer network overflows using Model Predictive Control strategy,” *Water Resour. Res.*, vol. 60, no. 1, p. e2023WR035448, Jan. 2024, doi: 10.1029/2023WR035448.

[217] E. F. Camacho and C. Bordons, *Model Predictive Control*. in Advanced Textbooks in Control and Signal Processing. London: Springer, 2007. doi: 10.1007/978-0-85729-398-5.

[218] L. Luca, A. Pricopie, I. Vasiliev, M. Barbu, and S. Caraman, “Fuzzy-optimal control strategies for a wastewater treatment plant,” in *2020 24th International Conference on System Theory, Control and Computing (ICSTCC)*, IEEE, 2020, pp. 564–569.

[219] S. Caraman, L. Luca, I. Vasiliev, and M. Barbu, “Optimal-setpoint-based control strategy of a wastewater treatment process,” *Processes*, vol. 8, no. 10, p. 1203, Sep. 2020, doi: 10.3390/pr8101203.

[220] I. Vasiliev, L. Luca, M. Barbu, R. Vilanova, and S. Caraman, “An analysis towards integrated control of wastewater collecting and treatment systems,” presented at the 2023 27th International Conference on System Theory, Control and Computing (ICSTCC), IEEE, 2023.